TRANSIENT STABILITY ANALYSIS OF NIGERIA POWER SYSTEM: MULTIMACHINE APPROACH

BY

IZUEGBUNAM FABIAN IZUNDU: B.Eng, M.Eng
REG. NO: 20024587028

A THESIS SUBMITTED TO THE POSTGRADUATE SCHOOL
FEDERAL UNIVERSITY OF TECHNOLOGY, OWERRI

IN PARTIAL FULFILLMENT OF THE REQUIREMENTS FOR THE AWARD OF THE DOCTOR OF PHILOSOPHY, (Ph.D) IN POWER SYSTEM ENGINEERING.

NOVEMBER, 2010

CERTIFICATION

I certify that this work "Transient Stability Analysis of Nigeria Power System: Multimachine Approach" was carried out by MR. IZUEGBUNAM FABIAN IZUNDU (20024587028) in partial fulfillment for the award of the Doctor of Philosophy (Ph.D) in Power System Engineering in the Department of Electrical and Electronic Engineering, Federal University of Technology, Owerri.

……..…	…….
Engr. Prof. C.C. Okoro Principal Supervisor	Date
……..	…….
Engr. Prof. S.O.E. Ogbogu Co-Supervisor	Date
……..	…….
Engr. Dr. E.N.C. Okafor Co-Supervisor	Date
……..	…….
Engr. Dr. E.N.C. Okafor Head of Department	Date
…….	……..…
Dean of SEET	Date
…….	…….
Dean of PGS	Date
…….	…….
Engr. Prof. Frank N. Okafor External Examiner	Date

DEDICATION

This research is dedicated to THE HOLY TRINITY: GOD THE FATHER, THE SON, and THE HOLY SPIRIT.

ACKNOWLEDGEMENT

This work will not be complete without expressing my sincere thanks and appreciations to those who in one way or the other contributed to the success of this research. The immense contributions of my supervisors Engr. Prof. C.C. Okoro, Engr. Prof. S.O.E. Ogbogu and Engr. Dr. E.N.C. Okafor were unquantifiable. Their motivations, encouragement and sound academic inputs are well appreciated. A posthumous appreciation goes to late Engr. Prof. T.C. Nwodo who not only encouraged me to embark on this research, but also provided some resource materials which proved useful in the course of this work.

The unrestrained encouragement from Engr. Dr. (Mrs.) G.A. Chukwudebe deserves thanks and appreciation. I wish to also express my sincere thanks to Engr. Dr. M.C. Ndinechi and Engr. Dr. F.K. Okpara who gave me their thesis to use as a guide. I appreciate the entire EEE staff both teaching and non-teaching staff for being wonderful colleagues.

My special thanks are extended to my parents Chief Christopher Izuegbunam (posthumous) and Mrs. Josephine Izuegbunam for their prayers and encouragement, and to my elder brother Mr. Nelius Izuegbunam for his support and prayers.

I remain grateful to some wonderful PHCN staff for providing the National Grid data for this research through Miss Ijioma Ebere (ex-student of EEE) and to Miss Ijioma Ebere(my student) who remained an interface between me and these staff of PHCN.

Finally, I wish to express my unrestrained gratitude to my colleague and friend Engr. Paul E. Okon of Exxon-Mobil, Eket for procuring some requisite text books from United States for me; and to some of my students who assisted me in arranging the Grid data and software development (Ubah C.B.,Ichetaonye O.A.,Nwoko I.M. and Ogalue D.K.), I say thank you.

May God Almighty bless you all.

TABLE OF CONTENTS

Title page i
Certification ii
Dedication iii
Acknowledgment iv
Abstract v
Table of contents vi
List of tables ix
List of figures x
List of abbreviations and symbols xiv

CHAPTER ONE
1.0 Introduction 1
1.1 Background knowledge 3
1.2 Problem statement 5
1.3 Objectives 6
1.4 Justification of study 7
1.5 Scope of study 7
1.6 Structure of the thesis 8
CHAPTER TWO 9
2.0 Literature Review 9
2.1 Load flow study 11
2.2 Transient stability analysis 13
2.2.1 Coherent generator-based transient stability analysis 18
CHAPTER THREE
3.0 Methodology 22
3.1 Power system equipment and networks 22
3.2 The synchronous generator 22
3.2.1 Bulk power generation in power networks 27
3.2.2 abc – odq frame of reference 28

3.2.3 Transient parameters of the synchronous generator 34
3.2.4 The generator in the transient state 44
3.3 The transmission system 48
3.3.0 The transmission systems model 48
3.3.1 Transmission line model 49
3.3.2 The transformer model with complex ratio 51
3.3.3 The in-phase transformer model 51
3.3.4 Phase shifting transformer model 53
3.3.5 The unified power network model 54
3.3.6 The unified power flow equation 60
3.3.7 Substation controls 60
3.3.7.1 Load – break switches 60
3.3.7.2 Circuit breakers 61
3.4 Power system protection 61
3.4.1 Generator protection 62
3.4.2 Line protection 63
3.5 National grid data 64
3.5.1 Generation data 64
3.5.2 Transmission line data 65
3.6 Theory of power flow and stability computations 68
3.6.1 Single machine to infinite bus system 68
3.6.2 Method of solutions of power flow problems 74
3.6.3 Power flow equations 75
3.6.4 Gauss Seidel method 76
3.6.5 Newton Raphson method 79
3.7 Modelling of multimachine power system 85
3.8 Multimachine transient stability equations 88
3.8.1 The rotor swing equation 88
3.9 Step by step solution of swing equation 94

3.10 Data preparation for transient stability 99
3.11 Coherent generator identification 104
3.11.1 Mathematical formulation 104
3.11.2 Coherent generators dynamic equivalent Construction technique 109
3.11.2.1 Mathematical formulation 110
3.11.2.2 The algorithm for the coherent machines identification and dynamic equivalents construction 114

CHAPTER FOUR

4.0 Power flow and stability of the Existing and Proposed National grids 115
4.1 Derivation of Existing national grid injected current equation 115
4.2 Derivation of Proposed national grid injected current equation 119

CHAPTER FIVE

5.0 Result and Discussion 135
5.1 Existing network power flow results 135
5.2 Proposed network power flow results 136
5.3 Result of transient stability analysis of existing network under three-phase fault at some selected buses and lines. 138
5.4 Result of transient stability analysis of proposed network under three-phase fault at some selected buses and lines. 147
5.4.1 Results of generators-coherency check and aggregation for a three-phase fault at bus 3 line 3-44. 161

CHAPTER SIX

6.0 Conclusion and Recommendations 166
6.1 Conclusion 166
6.2 Recommendations 168

Contribution to knowledge 170

References 171

Appendix A: Existing 330KV National Grid bus data, power flow results, and line flow and losses.
A1: Existing 330KV National Grid bus data 183
A2: Existing 330KV National Grid power flow results 184
A3: Existing 330KV National Grid line flow and losses 185

Appendix B: Proposed 330KV National Grid bus data, power flow results and line flow and losses.
B1: Proposed 330KV National Grid bus data 188
B2: Proposed 330KV National Grid power flow results 190
B3: Proposed 330KV National Grid line flow and losses 192

Appendix C: Proposed 330KV National Grid bus data based on coherent generators aggregation application.
C1: Y_{bus} matrix for proposed 330KV Nigeria power system at faulted bus 3 198
C2: Proposed Grid generator fault-induced power variation 199
C3: Study and external systems generators classified based on fault-on percentage power variation 200
C4: γ- index data for proposed grid generators coherency check 201
C5: β - Index data for proposed grid generators coherency check 202
C6: Aggregated grid generator groups data 203
C7: New Grid Generators data for aggregation 203
C8: New Grid systems bus data after aggregation 204
C9: Line data for New Grid system after aggregation 206
Appendix D: MATLAB SOFTWARE PROGRAMS 209

LIST OF TABLES

Table 1.1:	Expected New Power Stations and their capacities	2
Table 3.1:	Generators data for Existing 330KV National Grid	64
Table 3.2:	Generators data for Proposed 330KV National Grid	64
Table 3.3:	Existing National grid transmission lines data	65/66
Table 3.4:	Proposed National grid transmission lines data	66
Table 5.1:	Lines with losses above 10MW in Existing Network	136
Table 5.2:	Buses with intolerable voltage profile violation in Proposed Network	137
Table 5.3:	Lines with losses above 10MW in Proposed Network	138
Table 5.4:	The summary of transient stability analysis of Existing Nigeria Power System	140
Table 5.5:	The summary of transient stability analysis of Proposed Nigeria Power System	149

LIST OF FIGURES

Figure 3.1 Synchronous machine schematic and circuit diagrams 23

Figure 3.2 Equivalent electric circuit of the synchronous machine after 0dq reference frame transformation. 34

Figure 3.3 Equivalent circuits for the determination of subtransient time constants 35

Figure 3.4 Equivalent circuits for transient and steady-state reactances 36

Figure 3.5 d – and q – axis circuits 38

Figure 3.6 d – and q – axis circuits for determining transient inductance 39

Figure 3.7 d – axis coupled circuit for transient time constants determination 41

Figure 3.8 Equivalent circuits of d – and q – axis coupled circuits 42

Figure 3.9 Equivalent circuits for d – and q – axis subtransient open – and short-circuits time constants 43

Figure 3.10 Synchronous generator classical model with pre-fault and post -fault voltage and current phasors 44/45

Figure 3.11 Equivalent π model of a transmission line 49

Figure 3.12 Transformer model with complex ratio 51

Figure 3.13 In – phase transformer equivalent π model 51/52

Figure 3.14 Phase-shifting transformer model 53

Figure 3.15 Transformer symmetrical model 54

Figure 3.16 Unified π model 55

Figure 3.17 Machine to infinite bus system schematic 68

Figure 3.18 Equivalent circuits for machine to infinite bus system 69

Figure 3.19 Machine energy changes after a disturbance 70

Figure 3.20 Influence of the fault distance in machine to infinite

bus system 73
Figure 3.21 Effect of faults on power angle characteristics 74
Figure 3.22 Generic power system network 75
Figure 3.23 Newton-Raphson power flow algorithm 84
Figure 3.24 Classical model of a large power network 85
Figure 3.25 Step-by-step method for solution of swing equation 97
Figure 3.26 Generator model 99
Figure 3.27 Transient stability analysis algorithm 103
Figure 3.28 Large power network with coherent generator groups 110
Figure 3.29 Algorithm for coherent machines identification and dynamic equivalents construction 114
Figure 4.1 Existing 330KV Nigeria power network 115
Figure 4.2 Proposed 330KV Nigeria power network 119
Figure 5.1 Swing curves for fault at bus 4, line 4-20 with clearing time of 0.16 sec. 141
Figure 5.2 Swing curves for fault at bus 20, line 4-20 with clearing time of 0.16 sec. 141
Figure 5.3 Swing curves for fault at bus 13, line 13-16 with clearing time of 0.16sec. 142
Figure 5.4 Swing curves for fault at bus 16, line 13-16 with clearing time of 0.16sec. 142
Figure 5.5 Swing curves for fault at bus 16, line 13-16 with clearing time of 0.20sec. 143
Figure 5.6 Swing curves for fault at bus 16, line 13-16 with clearing time of 0.22sec. 143
Figure 5.7 Swing curves for fault at bus 16, line 13-16 with critical clearing time of 0.21sec. 144
Figure 5.8 Swing curves for fault at bus 10, line 10-13 with clearing time of 0.16sec. 144

Figure 5.9 Swing curves for fault at bus 13, line 10-13 with clearing time of 0.16sec. 145
Figure 5.10 Swing curves for fault at bus 18, line 13-18 with clearing time of 0.3sec. 145
Figure 5.11 Swing curves for fault at bus 13, line 13-18 with clearing time of 0.3sec. 146
Figure 5.12 Swing curves for fault at bus 40, line 31-40 with clearing time of 0.16sec. 151
Figure 5.13 Swing curves for fault at bus 40, line 31-40 with clearing time of 0.3sec. 151
Figure 5.14 Swing curves for fault at bus 31, line 31-40 with clearing time of 0.16sec. 152
Figure 5.15 Swing curves for fault at bus 31, line 31-40 with clearing time of 0.3sec. 152
Figure 5.16 Swing curves for fault at bus 2, line 2-31 with clearing time of 0.16sec. 153
Figure 5.17 Swing curves for fault at bus 2, line 2-31 with clearing time of 0.17sec. 153
Figure 5.18 Swing curves for fault at bus 2, line 2-31 with clearing time of 0.18sec. 154
Figure 5.19 Swing curves for fault at bus 31, line 2-31 with clearing time of 0.16sec. 154
Figure 5.20 Swing curves for fault at bus 31, line 2-31 with critical clearing time of 0.29sec. 155
Figure 5.21 Swing curves for fault at bus 31, line 2-31 with clearing time of 0.3sec. 155
Figure 5.22 Swing curves for fault at bus 22, line 2-25 with clearing time of 0.16sec. 156

Figure 5.23 Swing curves for fault at bus 22, line 22-25 with clearing time of 0.2sec. 156
Figure 5.24 Swing curves for fault at bus 22, line 22-25 with clearing time of 0.3sec. 157
Figure 5.25 Swing curves for fault at bus 25, line 22-25 with clearing time of 0.16sec. 157
Figure 5.26 Swing curves for fault at bus 25, line 22-25 with clearing time of 0.2sec. 158
Figure 5.27 Swing curves for fault at bus 25, line 22-25 with clearing time of 0.3sec. 158
Figure 5.28 Swing curves for fault at bus 3, line 3-44 with clearing time of 0.16sec. 159
Figure 5.29 Swing curves for fault at bus 44, line 3-44 with clearing time of 0.16sec. 159
Figure 5.30 Swing curves for fault at bus 44, line 3-44 with critical clearing time of 0.21sec. 160
Figure 5.31 Swing curves for fault at bus 44, line 3-44 with clearing time of 0.22sec. 160
Figure 5.32 Swing curves for machines 2 and 6 for fault at bus 3, line 3-44 162
Figure 5.33 Equivalent swing curve for machines 2 and 6 162
Figure 5.34 Swing curves for machines 7 and 8 for fault at bus 3, line 3-44 163
Figure 5.35 Equivalent swing curve for machine 7 and 8 163
Figure 5.36 Swing curves for machines 10 and 11 for fault at bus 3, line 3-44 164
Figure 5.37 Equivalent swing curve for machines 10 and 11 164
Figure 5.38 Swing curves of new network after aggregation for fault at bus 3, 3-44/41 165

LIST OF ABBREVIATIONS AND SYMBOLS

Abbreviations:

AC	-	Alternating current
AVR	-	Automatic Voltage Regulator
EAC	-	Equal Area Criterion
EEAC	-	Extended Equal Area Criterion
COI	-	Centre of Inertia
CI	-	Coherency Index
ECN	-	Electricity Corporation of Nigeria
FG	-	Federal Government
IPP	-	Independent Power Producers
KE	-	Kinetic Energy
KV	-	Kilovolts
MSE	-	Mean Square Error
MW	-	Mega Watts
NEPA	-	National Electric Power Authority
NDA	-	Nigeria Dams Authority
NERC	-	National Electricity Regulatory Commission
NIPP	-	National Integrated Power Projects
PEBS	-	Potential Energy Boundary Surface
PWD	-	Public Works Development
RKE	-	Rate of Change of Kinetic Energy
SEP	-	Stable Equilibrium Point
SMIB	-	Single Machine to Infinite Bus
SPEF	-	Structure Preserving Energy Functions
SVC	-	Static Var Compensator
TEF	-	Transient Energy Function
UEPs	-	Unstable Equilibrium Points
a_{ij}	-	transformation ratio of transformer

a_i, a_j - accelerations of machines i and j

b_{ij} - the series susceptance between buses i and j

b^{sh}_{ij} - the shunt susceptance between buses i and j

D_d - the damping-torque coefficient in Nm

D_e - Coherent generator group equivalent damping coefficient

E' - Generator internal voltage behind transient reactance

g_{ij} - the series conductance between buses i and j

g_{ij}^{sh} - the shunt conductance between buses i and j

$e_i^{(k+1)}$ - the real component of the voltage, $v_i^{(k+1)}$

$f_i^{(k+1)}$ - the imaginary component of the voltage, $v_i^{(k+1)}$

H - Generator inertia constant

H_e - Coherent generator group equivalent inertia constant

I^o_d,I^o_q - Pre-fault direct- and quadrature-axis currents

I^f_d,I^f_q - Fault-on direct- and quadrature-axis currents

ΔI_d - change in direct-axis current due to fault

ΔI_q - change in quadrature-axis current due to fault

J - Moment of inertia

L_D - rotor director-axis damper winding self inductance

L_F - rotor field winding self inductance

L_Q - rotor quadrature-axis damper winding self inductance

L_a, L_b, L_c - stator windings self inductances for phases a, b, c

L_{fa}, L_{fb}, L_{fc} - mutual inductances between rotor field winding and stator phase windings a, b, c

L_{ab}, L_{ac}, L_{bc} - stator windings inter-phase mutual inductances

L_d, L_q, - inductances of the fictitious direct- and quadrature-axis armature windings.

L'_d, L'_q, $L''_q L''_q$ - direct- and quadrature- axis transient and subtransient inductances.

L_S - submatrix of the stator self inductance

L_R - submatrix of the rotor self indcutance

L_{SR} - submatrix of the stator-to-rotor mutual inductance

L^T_{SR} - transpose of submatrix of the stator-to-rotor mutual inductance.

M_D - amplitude of mutual inductance between direct-axis damper winding and fictitious direct-axis armature winding

M_f - amplitude of the mutual inductance between direct-axis windings and field winding

M_Q - amplitude of the mutual inductance between quadrature-axis damper winding and fictitious quadrature-axis armature winding

n - the number of generators

L_{Da}, L_{Db}, L_{Dc} - mutual inductances between rotor direct-axis damper winding and stator phases (a, b, c) windings

L_{Qa}, L_{Qb}, L_{Qc} - mutual inductances between quadrature-axis damper winding and stator phase (a, b, c) windings

P - Park's transformation matrix

P^{-1} - inverse of park's transformation matrix

P^T - transpose of park's transformation matrix

P_a - accelerating power

P_e - electrical power output of a generator

P_D - Damping power

P_m - mechanical power supplied by a prime mover to a generator

ΔP_{mi} - change in mechanical input power of generator i

ΔP_{ei} - change in electrical power output of generator i

P_{me} - coherent generator group equivalent mechanical power

M - inertia coefficient

M_R - amplitude of mutual inductance between rotor field winding and direct-axis damper winding

R_a, R_b, R_c - stator windings resistances for phases a, b, c

R_D - rotor direct-axis damper winding resistance

R_F - rotor field winding resistance

R_Q - rotor quadrature-axis damper winding resistance

S_n - rated apparent power of a generator

$S_i = P_i + Q_i$ - apparent power output of generator i

S_T - sum of apparent power received by p buses of the coherent generator group

t_{ij} - transformation ratio for transformer with complex ratio

T_e - the electromagnetic torque

T_t - the torque produced by the turbine in Nm

T'_{do},T''_{do} - open-circuit direct-axis transient and subtransient time constants

T'_d,T''_d - short-circuit direct-axis transient and subtransient time constants

T'_{qo}, T''_{qo} - open-circuit quadrature-axis transient and subtransient time constants

T'_q, T''_q - short-circuit quadrature-axis transient and subtransient time constants.

V^o_d, V^o_q - pre-fault direct-and quadrature-axis voltages

V^f_d, V^f_q - fault-on direct-and quadrature-axis voltages

ΔV_d - change in direct-axis voltage due to fault

ΔV_q - change in quadrature-axis voltage due to fault

V_e, V_e^* - equivalent terminal voltage of the coherent generator group and its conjugate

X'_{dpre}, X'_{df}, X'_{dpost} – pre-fault, fault-on and post-fault transient reactances

X_d, X'_d, X''_d	-	direct-axis synchronous, transient and subtransient reactances
X_q, X'_q, X''_q	-	quadrature-axis synchronous, transient and subtransient reactances
X'_{de}	-	equivalent machine transient reactance of the coherent generator group
Ybus	-	Bus admittance matrix
y_{ij}	-	admittance between buses i and j
y^{sh}_{ij}	-	the shunt admittance between buses i and j
$\hat{Y}$	-	reduced system admittance matrix
V_s	-	generator terminal voltage
ω	-	angular velocity of the generator in electrical radians
$\Delta\omega$	-	rotor speed deviation equivalent to (ω - ω_s)
ω_s	-	synchronous angular velocity in electrical radians equivalent to $2\pi f$
ω_m	-	the rotor shaft velocity in mechanical radians per second
$\Delta\omega_m$	-	speed deviation in mechanical radians per second
ω_{sm}	-	the mechanical angular velocity
ε	-	accuracy factor
α	-	synchronous generator rotor acceleration
α_{ij}	-	electrical proximity index for generators i and j
γ_{ij}	-	damping index for i^{th} and j^{th} machines
β_{ij}	-	inertia index for i^{th} and j^{th} machines
δ	-	rotor angle with respect to infinite busbar
δ_i	-	rotor angle of generator i with respect to infinite busbar
δ_{ij}	-	rotor angle of generator i with respect to generator j
δ_m	-	rotor angle expressed in mechanical radians
δ'	-	transient rotor angle between E' and V_s

λ_a, λ_b, λ_c - total flux linkages of phases a, b, c

λ_{aa}, λ_{bb}, λ_{cc}, - self-flux linkages of phases a, b, c

λ_{fa}, λ_{fb}, λ_{fc}, - field flux linkages with phases a, b, c

λ_{abc}, - matrix of phase flux linkages

λ_{FDQ}, - matrix of flux linkages of the field winding, and the direct- and quadrature-axis damper windings

λ_{odq}, - matrix of armature flux linkages in the rotor reference frame

λ_F, - total flux linkage of field winding

λ_D, - total flux linkage of rotor direct-axis damper winding

λ_Q, - total flux linkage of rotor quadrature-axis damper winding

ABSTRACT

The recent power sector reform in Nigeria has thrown up enormous challenges in this sector, ranging from the construction of more power stations, construction of new transmission lines and substations. The existing network of 8-plants and 26 bus-bars expanded to the proposed network of 16 generating plants with 49 bus-bars. This network expansion requires re-appraisal for power evacuation capabilities, relay systems setting and establishment of stability margins for adverse system fault conditions on the network. Power flow evaluations of the existing and proposed 330KV networks were done using the Newton-Raphson technique. The transient stability analysis of the two networks was also simulated by direct method using ode45 MATLAB programmed functions. The critical clearing time of 0.21second and stability margin of 0.238 were established for a three-phase fault at bus 16, line 13 – 16 of the existing Grid. In the proposed Grid, the critical clearing times and stability margins for three-phase faults at buses 3 (line 3 – 44) and 31 (line 2 – 31) were established as 0.21second, 0.238 and 0.29second, 0.448 respectively. The results provided a suite of specifications and standards for the proposed grid system. An algorithm for coherent generators was developed with which the 16 machines in proposed network were reduced to 13 machines system. The network reduction was carried out through coherent generators aggregation and construction of dynamic equivalents representing the aggregated generators.

Key words: existing network, proposed network, power flow, transient stability, coherent generators, dynamic equivalents, clearing time, stability margin, swing curve.

CHAPTER ONE

1.0 Introduction

Despite an installed capacity of about 5610MW in the Nigerian National Grid as at 2001, the available capacity dropped to below 2000MW. Electricity supply to private, commercial and industrial consumers became grossly inadequate and erratic. Many industries had to close down causing a downturn of the national economy, and the quality of life of the citizens reduced considerably. The general outcry of industry chieftains and the energy starved consumers kick-started a national debate on the problems of the power industry sector; it became obvious that a number of problems led to the near collapse of the sector. There was a dearth of generating capacity and its planners had not considered the pattern of the load demand and the rapid increase of national population. Besides the high dependence of the sector on foreign technology, the lack of skilled maintenance staff and lack of new investment over a long period had a negative impact on the industry. The Federal Government of Nigeria virtually declared an Energy Emergency and took a number of steps aimed at improving the fortunes of the sector.

The Power Sector Reform Act which was enacted in 2005, led to the unbundling of PHCN into eighteen companies (six generation, one transmission and eleven distribution companies) to reduce administrative bureaucracy and increase the speed of response of the companies to consumer complaints. The new legal framework also instituted the National Electricity Regulatory Commission (NERC) to license and regulate bodies engaged in electricity generation. The private sector obtained licenses to own power plants under the Independent Power Producers (IPPs) thereby opening the door to new investments in the power sector. The Transmission Company of Nigeria (TCN) became the backbone of the sector that can enter into power purchase agreements with the IPPs. The Federal Government also assisted the PHCN to build four new Gas fired power plants at Geregu,

Omotosho, Papalanto and Afam. The Government in addition set up the National Integrated Power Project (NIPP) to build seven new power plants in the oil producing areas of the country. The outlook for future installed power generation capacity in the country became much brighter as shown in table1.1 (Achibong, 2007).

Table 1.1: Expected new power stations and their capacities

Expected New Power Stations	**Expected Capacities(MW)**
7 NIPP Power Stations	2,556
4 FG Power Stations	1,434
2 State Owned IPPs	800
5 Joint Venture IPPs	2,780
10 Private IPPs	5,391.5
Total Capacity	**12,961.5**

The existing national grid was made up of 5000km of 330kV transmission lines and 6000km of 132KV transmission lines with twenty five (25) 330KV and eighty nine (89) 132KV substations. The distribution facilities included 55,143km of 33KV and 11KV distribution lines. The proposed grid system would have an increased installed generating capacity of about 18,571.5MW. About 7000km of transmission facility were planned under NIPP (Achibong, 2007). It is expected that the addition of new power plants and transmission facilities would alter considerably the performance criteria of the grid system. In the light of the above the system operators have to face the challenges of ensuring that the stability of the system is maintained using new criteria to be developed. These challenges arising from the rapidly expanding grid system have to be systematically appraised through research and operational experiences to identify areas of weaknesses and corrective measures to be imposed to ensure system stability. In order to meet the expectation of the

Nigerian economic planners to make the country one of the twenty most developed economies by the year 2020, the power industry must be pulled out of the present state to provide a stable and secure supply of electricity.

1.1 Background Knowledge

Through load flow studies, the solutions of the steady-state operating conditions of electric power transmission systems are provided, and these are most frequently performed in power system analysis (Ekwue et al., 1991). The essence of load flow is to find out the real and reactive powers flowing in each line along with the magnitude and phase angle of the voltage at each bus of the system for specific loading conditions (Okoro et al., 2007). In performing load flow studies, the network bus-bars are classified into three based on the direction of power flow in a particular bus and the specified variables. The three types of buses include load bus, voltage controlled bus, and reference or slack bus. In load bus, the real and reactive power are specified, while the voltage magnitude and phase angle of the voltage are unknown. In a voltage controlled bus, the real power and voltage magnitude are specified, while reactive power and phase angle of voltage are unknown. The last is known as the reference or slack bus because it takes up the slack in losses (Elgerd, 1979). It is also known as swing bus. In this bus, real and reactive power demands are unknown, while voltage magnitude and load angle are specified.

Power system stability concerns the power system's response to disturbances (Fouad et al., 1992), and a disturbance is a sudden change in an operating condition or an operating parameter of the power system (IEEE Task Force, 1982). When the linearization of the system equations for the purpose of analysis is justified after a disturbance, such disturbance is considered small; otherwise, it is regarded as large. In other words, a small disturbance is a disturbance for which the equations that describe the

dynamics of the power system may be linearized for analysis purposes (Machowski et al., 1997). Small disturbance include small variations in loads and generation. In power system stability studies, the period of interest is the transient period prior to the attainment of new steady state conditions. The power system is considered to operate at steady state when the operating parameters are assumed constant for the purpose of analysis. Under this condition, the peak-to-peak amplitude of the system current waveform is assumed time invariant (constant). When a disturbance occurs in a power system initially operating at steady state, the stability concern becomes whether an acceptable steady state condition could be reached as a fall out of the transient. If the disturbance is considered large, the stability concern is referred to as “transient stability”. Examples of large disturbances include: short-circuits on transmission line, loss of generation, loss of large load, loss of a tie between two subsystems etc. when the disturbance is small, it is referred to as “steady state stability”. Transient stability is thus, the ability of the power system to maintain synchronism when subjected to a severe transient disturbance. The resulting system response to such disturbance involves large excursions of generator rotor angle which is influenced by the non-linear power-angle relationship (Kundur, 1994). Stability is dependent on both the initial operating state of the system and the severity of the disturbance. In carrying out transient stability studies, particularly in problems involving electromechanical transients, slow varying phase is assumed and this assumption is justified considering the high moments of inertia exhibited by turbine – generator sets (Bergen et al., 2000). Transient stability as earlier defined concerns but not limited to the maintenance of synchronism between generators following a severe disturbance. The general purpose transient analysis involves quality investigation of the power system dynamic behaviour (Fouad et al., 1992). The equations describing the dynamic behaviour of a power system are highly nonlinear. These nonlinear equations

describe the dynamic behaviour of the synchronous generators in the system. In transient stability analysis, the generator parameters such as rotor angels, internal emfs, terminal voltages, currents, etc. are particularly of interest. These parameters in turn influence the behaviour of other network parameters such as voltage at key buses, real power and reactive power flow in transmission lines, etc. Also the operation of various stability controls is equally investigated.

In the event of a major fault like a short-circuit, the transient reactance X'_d is subjected to change, thus leading to change in the electric power output of the generator, P'_e and thereby altering the power balance within the system. The altered power balance results to energy transfer between the generators, leading to rotor oscillations. The three states associated with the system disturbance have various transient reactance values which include the pre-fault transient reactance, X'_{dpre}, the fault-on transient reactance, X'_{df}, and the post-fault transient reactance, $X'_{dpost.}$

1.2 Problem Statement

In the past two decades, the Nigeria power system has been characterized by incessant interruptions caused by inadequacies in power generation capacity, transmission and distribution facilities etc. These lapses have resulted in shutting down of industries, loss of jobs, downturn of national economy, drop in the quality of life of citizens, high cost of living occasioned by high cost of production and so on. In recognition of these challenges, the Federal Government through its power reform, has opened up the power sector by licensing independent power producers, and expanding the Nigeria power system through National Integrated Power Projects aimed at building more power generating stations to boost generation capacity as well as reinforcing the existing power transmission and distribution facilities through building new transmission lines across the country; and refurbishing,

replacing of aging facilities, and construction of more transmission and distribution substations. The anticipated positive changes in the Nigeria power system will obviously throw up stability challenges to the system operators. The challenges include:

- System protection coordination
- Stability of the grid system after specified faults
- Voltage profiles and utilization of transmission capacities of the power network
- Power Evacuation and reactive power management for system stability
- Identification of remedial actions such as FACTs placement to ensure system stability.

1.3 Objectives

The achievement of a secure and stable power system is not for operations alone; hence considerable planning and research are necessary for system performance development. The work should provide research inputs that are needed for secure operation of the national grid. These inputs include determination of the adequacy of the generation expansion schemes to meet the national power demand, accessment of the network configuration and operating conditions of the Nigeria power system vis-à-vis the reliability criteria. Others include to investigate and analyze system upsets when subjected to severe disturbances as well as ascertain the disturbance types the system can withstand, determination of the critical clearing time for superimposed operating condition and the adequacy of the transmission facilities for bulk power evacuation with the new generating stations.The result of these will enable the system managers to make informed decisions and take guided steps toward ensuring the security and stability of the Nigeria power system.

1.4 Justification of study

The proposed expanded National grid considered in this research consists of 16 power plants and 49 busbars interconnected by 330KV transmission lines. There is therefore need for a comprehensive investigation of the performance and stability analysis of the expanded grid. Transient stability study of the Nigeria power system is thus required to assess the system's response to the transient conditions following major disturbances. Such studies are fundamental when new generating and transmitting facilities are added to the system (Saadat, 2002). This research is very auspicious at this period when a lot of generating plants and transmission facilities are being constructed across the country through the National Integrated Power Projects. Through this research, the technical information on the system stability, voltage profile and transmission capabilities, types of disturbances the system can withstand, safe margins for system operating limits etc. can be provided. This information when managed properly will enhance efficient power system operation.

1.5 Scope of study

The research covered existing (8- machines, 26-bus system) and proposed (16- machines, 49 - bus system) Nigeria power system at 330KV voltage level. Separate load flow studies and transient stability studies are carried out for these two networks under specified fault conditions at various locations in both systems. The method adopted in this research is such that the structure of the network is preserved to such extent that the accuracy of the result is not compromised. The method involved identification of coherent machine groups, coherent machines aggregation, network reduction and construction of coherency-based dynamic machine equivalents, to represent different coherent generators groups; and integration of these subsystems to form a

new network comprising the study area machines, external area machines and the rest of system machines.

1.6 Structure of the thesis

The thesis has been arranged in such a manner as to facilitate understanding and promote coherency. In this regard, the introduction, background study, problem statements, objectives and the study scope are covered in chapter one; while chapter two dwelt on the literature review. Chapter three focused on the methodology which considered the power system equipment and networks, national grid data, theory of power flow and stability computations. Chapter four covers the power flow and stability evaluation of the existing and proposed national grids. Chapter five dwelt on the results and discussion, while chapter six covers recommendations and conclusion.

CHAPTER TWO

2.0 Literature Review

The incessant electric power interruptions prevalent in the Nigeria power system and the steps so far taken by the Federal Government of Nigeria through the construction of more new power generating stations and transmission lines further increased the complexity of the Nigeria 330KV power network. The proposed new 330KV grid system of installed capacity of about 10,000MW comprising 16 machines and 49 busbars as compared to the existing network of about 8 machines and 26 bus-bars requires innovative tools that will preserve the network structure during transient stability analysis. In view of the challenges and requirements of this task of complex power system network analysis, there is need to review the previous work done by various authors on Nigeria power system, examine their findings and recommendations as well as existing tools and principles adopted and proposed by various reputable researchers in power system transient analysis. This will enhance proper assessment of the proposed Nigeria 330KV power network expansion adequacy and the level of improvement achievable from the existing grid system based on generation capacity, transmission lines adequacy, network configuration and system stability.

Over the years, various authors have assessed the performance of the Nigeria power system and made informed technical input towards improving the efficiency of the network. Among these authors, a good number whose findings and recommendations are technically in line with most of the available literature are considered in this text.

Okoro and Achugbu, (2007), identified the deficiencies and problems of the National Grid to include weak transmission and distribution networks, weak grid control centres, and preponderance of obsolete equipment, lack of back-up technology base and inadequate local research and development input. The authors further opined that over population of single circuit

transmission lines and absence of redundancy in the Nigeria power system constitute weak grid configuration, and suggested placement of synchronous condensers as a good means of improving the voltage profile and system stability.

Okafor, (2009), identified the low generation capacity, radial nature of the network with the absence loops and alternative routes for power flow in the event of emergency as factors that contribute to high level of instability in the national grid system.

Onohaebi et al., (2007), identified the predominant radial, fragile and very long transmission lines to be responsible for the prevailing high risk of partial or total system collapse when ever a major fault occurs in the network and thus makes the control of voltage difficult. According to Onohaebi et al, (2007), the present network has only one major loop system involving Benin – Ikeja West – Ayede – Oshogbo and back to Benin. The authors suggested the construction of more lines and substations in the following transmission routes as a means of improving the existing network: additional Benin – Onitsha 330KV line and substation, Gombe – Yola – Jalingo 330KV single circuit line and substation, Alaoji – Calaber 330KV line, Gombe – Damaturu 330KV line and substation, Damaturu – Maiduguri 330KV and substation, Jos – Makurdi 330KV single circuit line, and Alaoji – Enugu 330KV single circuit line.

Onohaebi and Igbinovia, (2007), recommended the provision of more loops in the national grid system to improve its security. The suggested loops include: Makurdi – New Haven 330KV line, Abuja – Ajaokuta 330KV line, additional circuits on the Ayede – Oshogbo and Kaduna – Kano lines, additional line along Egbin – Ikeja West to ease the existing double circuit, and additional line between Shiroro – Kaduna to ease the existing double circuit.

Omoigui and Ojo, (2007), investigated the steady-state and transient stabilities of the restructured Nigeria 330KV Electric power network and likened the system structure to those of Taiwan and Brazil whose network topology is longitudinal with the generating stations located far from major load centres leading to prevalent low bus voltages and poor damping system. The authors recommended transmission network restructuring and introduction of flexible AC transmission system (FACTS) devices as panacea towards improving the voltage profile of the system buses and network stability.

2.1 Power flow study

The transient stability evaluation of any power system involves performing power flow study of the system, and power flow data forms the input data for transient stability analysis. In a well designed power system, the generated power and load demands of the consumers must be balanced such that there are no lines over load or abnormal system voltages. Under normal conditions, electric power transmission systems operate in their steady-state mode and the basic calculation required to determine the characteristics of this state is termed load flow or power flow (Arrillaga J. and Arnold C.P., 1990). The essence of power flow studies is to determine the steady-state operating characteristics of the power generation and transmission system for a given set of busbar loads (Arrillaga et al., 1990; Saadat, 2002; and Elgerd, 1979). In performing the power flow studies, the active power generation is usually specified according to economic dispatch practice, and the generator voltage magnitude is maintained at a specified level by the automatic voltage regulator acting on the machine excitation (Monticelli, 1999; Arrillaga et al., 1990 and Elgerd, 1979). Loads are usually specified by their constant active and reactive power requirement which is normally assumed unaffected by the small variations of voltage and

frequency anticipated during normal steady-state operation (Arrillaga et al., 1990). The power flow solution is expected to provide information of voltage magnitudes and angles, active and reactive power flows in the individual transmission units, losses and reactive power generated or absorbed at voltage-controlled buses (Arrillaga et al., 1990; Saadat, 2002). The complete definition of power flow requires knowledge of the following four variables at each bus i in the system (Arrillaga et al., 1990; Saadat, 2002; Elgerd, 1979): real or active power $P_{i,}$ reactive or quadrature power $Q_{i,}$ voltage magnitude $|V_i|$, and voltage phase angle θ_i. Out of these four variables, only two are known apriori to solve the problem, while the remaining two variables are determined through load flow at a given bus. Three different bus conditions are defined based on the steady-state assumptions of constant system frequency and constant voltages as follows (Arrillaga et al., 1990; Saadat, 2002):

(a) Voltage- controlled bus: In this bus, the total injected active power P_i is specified, and the voltage magnitude $|V_i|$ is maintained at a specified value by reactive power injection. This type of bus generally corresponds to either a generator whereby P_i is fixed through turbine governor setting, and V_i is fixed by automatic voltage regulators acting on the machine excitation, or a bus where the voltage is fixed by supplying reactive power from static shunt capacitors or rotating synchronous compensators as in substations.

(b) NonVoltage- controlled bus: In this bus, the total injected power, $P_i + jQ_i$ is specified. For a practical power system, this corresponds to a load centre where the consumers draw its power needs. P_i and Q_i in this bus are assumed unaffected by small variations in bus voltage.

(c) Slack or Swing bus: This bus arises because the system losses are not known prior to the computation of the power flow, hence the total injected power cannot be specified at every single system bus. It is a

normal practice to choose one of the available voltage controlled buses as slack, and to regard its active power as unknown. The slack bus voltage is usually assigned as the system phase reference.

Through power flow study, a set of simultaneous nonlinear algebraic power equations are solved for two unknown variables at each node in the power network. A second set of linear variable power equations are derived from the first set of nonlinear equations, and an iterative technique is applied to this new set for solution. The basic load flow program requires reading of the system data such as busbar power conditions, network connections and impedance, and formation of the admittance matrix (Arrillaga et al., 1990; Saadat, 2002). The initial voltages are specified for all the system buses. For base case power flows, PQ buses are set to 1 + j0, while PV busbars are set to V + j0 (Arrillaga et al., 1990). The iteration cycle is terminated when the busbar voltages and angles are such that the specified conditions of load and generation are satisfied. This condition is accepted when power mismatches for all buses are less than a small tolerance ε (with typical value of 0.001pu) (Saadat, 2002). Voltage accuracy in the range of 0.00001 to 0.00005pu is assumed satisfactory (Saadat, 2002). The sum of the square of the absolute values of power mismatches is a further criterion sometimes used (Arrillaga et al., 1990). When a solution has been reached, complete terminal conditions for all buses are computed as well as line power flows and losses.

2.2 Transient stability analysis

The stability of a power system following some predetermined operating condition is a dynamic problem and requires to some extent elaborate plant component models. Assumptions are usually that prior to the dynamic analysis, the system is operating in the steady-state and that a load flow solution is available. According to (Bergen and Vittal, 2000), transient

stability concerns the maintenance of synchronism between generators following a severe disturbance.

Elgerd, (1979) and Machowski et al., (1997), compared a single swinging rotor to a mechanical mass – spring – damper system, and thus likened a multimachine system to a number of masses (representing the generators) suspended from a "network" comprising of elastic strings (representing the transmission lines). In the steady-state each of the strings is loaded below its breaking point (steady-state stability limit). When one of the string suddenly breaks (representing a line tripping), the masses will experience coupled transient motion (swing of the rotors) with fluctuation in the forces in the strings (line powers). Such a sudden disturbance may result in the system reaching a new equilibrium state characterized by a new set of string forces (line powers) and string extensions (rotor angles) or due to the transient forces involved, one string may break so weakening the network and producing a chain reaction of broken strings and eventual total system collapse. The limitations of this mechanical analogue of the power system include:

(i) the stiffness of the string should be nonlinear so as to model correctly the nonlinear synchronizing power coefficients. (ii) the string stiffness should be different in the steady-state from the transient state in order to model correctly different steady-state and transient state models of the generators.

According to Machowski et al., (1997), in real power system, a disturbance may affect the stability of the network in one of the following four ways:

(i) The generator(s) nearest to the fault may loose synchronism without exhibiting any synchronous swings; other generators affected by the fault undergo a period of synchronous operation.

(ii) The generator(s) nearest to the fault loose synchronism after exhibiting synchronous oscillations.

(iii) The generator(s) nearest to the fault is the first to lose synchronism with the system.

Fouad and Vittal, (1992), described the principle of transient stability as analogous to a ball rolling on the inner surface of a bowl with the area inside the bowl representing the region of stability, while the outside is the region of instability. The rim of the bowl is irregular in shape so that different points on the rim have different heights. When the energy is applied to the ball, it gains kinetic energy (K.E) and rolls up the surface inside the bowl along a path determined by the direction of initial motion. The authors opined that the point where the ball will stop is governed by the amount of kinetic energy initially injected. If the ball converts all its kinetic energy (K.E) into potential energy (P.E) before reaching the rim, then it will roll back and eventually settle down at the stable equilibrium point again. But where the K.E injected is high enough to cause the ball to go over the rim, the ball will enter the region of instability and will not return to the stable equilibrium point. The surface inside the bowl represents the potential energy surface (PES), and the rim of the bowl represents the potential energy boundary surface (PEBS). Two quantities required to determine if the ball will enter the instability region include:

(i) initial kinetic energy injected, (ii) the height of the rim at the crossing point. The location of the crossing point depends on the direction of the initial motion. This description is comparable to the power system initially operating at the steady-state, but when a fault occurs, the system equilibrium will be disturbed and the synchronous machines accelerate. The power system thereby gains kinetic energy and potential energy during the fault-on period and system moves away from the stable equilibrium point (SEP). After fault clearing, the kinetic energy is converted into potential energy in the same manner as the ball rolling up the potential energy surface. In order to avoid instability, the system must be capable of absorbing the kinetic energy at a

time when the forces on the generators tend to bring them toward new equilibrium positions, and this is dependent on the potential energy-absorbing capability of the post disturbance system.

The available tools for transient stability analysis include the principle of equal area criterion (EAC) as explained by many authors (Okoro and Awosope, 1987; Saadat, 2002; Kundur, 1994; Fouad et al., 1992), determines the stability of the given system based mainly on the knowledge of the system state (load angle and velocity) at the time of fault clearing. This method is particularly adequate for transient analysis of a single machine to infinite bus (SMIB) system and machine to machine system. An extension of this approach to multimachine systems is formulated using energy functions, known as Lyapunov's functions, which is a generalization of energy functions (Gless, 1966). The conservativeness of results of Lyapunov's method when applied to practical systems constitutes its shortcomings. There were also barriers in extending the method to more complex systems with detailed models.

Fouad, and Vital, (1992) and Kundur, (1994), applied transient energy function (TEF) method which is comparable to equal area criterion. For any given post-disturbance network configuration, there is a maximum or critical amount of transient energy that the system can absorb. The application of TEF in the transient stability assessment requires the following:

- The functions that adequately describe the transient energy responsible for separation of one or more synchronous machines from the rest of the system.
- An estimate of the critical energy required for the machines to lose synchronism.

TEF analysis is equivalent to the equal area criterion, hence for a two-machine system, the critical energy is uniquely defined. The kinetic energy gained during the fault-on period is added to the potential energy at the

corresponding rotor angle, and the sum is compared to the critical potential energy to determine stability. The limitations of this method include:

- The presence of transfer conductance, resulting in the existence of unstable limit cycle around SEP, which reduces the region of attraction (stability) (Chiang, 1989).
- The number of unstable equilibrium points (UEPs) on the stability boundary increases considerably with system size.
- Inclusion of detailed generator models with AVR is not possible.

Sue et al., (1989 and 1992), applied the Extended Equal Area Criterion (EEAC) to transient stability analysis. This method is simple and reasonably reliable technique for direct stability evaluation. The approach is based on the conjecture that the loss of synchronism of a multi-machine system, whenever it occurs, is triggered off by the machine's irrevocable separation into two groups. Hence, the idea of subdividing the system machines into the 'critical group', generally comprising few machines, and the remaining group, comprising the majority of system machines. The conjecture further assumed that the system stability can be assessed by replacing the machines of each group by an equivalent and finally the two equivalent machines replaced by a single machine to infinite bus (SMIB) system. Subsequently, the equal area criterion is applied to the SMIB system for stability analysis. The limitations of EEAC include very tedious procedure in identifying the reliable critical-clusters and inability to accommodate detailed generator models. The benefits include classical model representation of generators as well as loads being represented as constant impedances. There is also no need for the use of centre of inertia (COI) reference frame.

The development of structure preserving energy functions (SPEF) made the inclusion of load models and network based controller models such as Static Var Compensator (SVC) feasible (Bergen et al., 1981; Padiyar et al., 1987, 1989 and 1995; Tsolas et al., 1985). This method of assessing the

transient stability of a multi machine system involves the determination of the stability boundary for a particular fault. This is equivalent to determining the critical energy, W_{CR} for that fault. The critical energy, W_{CR} can be determined through computation of the controlling Unstable Equilibrium Point (UEP), and the Potential Energy Boundary Surface (PEBS). The benefits of this method include its flexibility; that is, it works with both classical generator model and detailed model, and allows the inclusion of load models and network-based controller models (AVR). It also gives accurate prediction of critical clearing time and performs better with machine model (1.0) than model (1.1). The limitations include its inability to predict oscillatory instability caused by fast acting excitation systems, and can only predict 'first swing' stability.

2.2.1 Coherent generator-based transient stability analysis

Coherent generator-based transient stability analysis for sometime now has been attracting attention of various researchers in power industry because it enables the relevant system structure to be retained while assessing the system stability. It involves reducing the order of the large system's model as well as its complexity. The reduction is based on the impact of large disturbances in a particular area known as the study system. The system external to the study system is thus not of direct interest in stability analysis, and are therefore represented by dynamic equivalents in recognition that it affects the response of the study system to disturbances. The method involves constructing dynamic equivalents to represent each coherent generator group in the external system thereby reducing the total number of machines involved in a given fault condition. The two types of dynamic equivalents include: modal equivalents and coherency-based equivalents.

Modal equivalents (Undrill et al., 1971; Van Oirsouw, 1990; Geeves, 1988; Prince et al., 1978), produces linear equations that do not represent

models of physical devices. It uses a linearized model of the external system and reduces the order of the model by ignoring the contribution to the system responses due to slow varying modes. It also requires computation of eigenvalues and eigenvectors which can be tedious.

Coherency-based equivalents (Lee and Schweppe, 1973; Podmore, 1978; Germond and Podmore, 1978), involve two steps: (i) identification of coherent groups in the external system, and (ii) dynamic aggregation of a coherent group of generating units into an equivalent generating unit which exhibits the same speed, voltage, total mechanical and electrical power as the group, during any disturbance where the units in the group remain coherent. There are various ways of identifying coherent generators.

Lee and Schweppe, (1973), used the concepts of distance measure such as admittance distance, reflection distance and acceleration distance to identify coherent generators for construction of dynamic equivalents. The concept of power variation of the generators at the instant of initiated fault is also applied to classify the machines into inner circle (study area) machines and outer circle (external area) machines. The inner circle machines are machines located very close to the fault, whereas the outer circle machines are machines located far away from the fault. The machines with power variation of less than 30% of the pre-fault value are regarded as being in the outer circle zone, while the rest are in the inner circle area. The authors also established some coherency determining indices inequalities such as Admittance distance ($Y_d \geq 0.3$), Acceleration distance index ($A_d \leq 0.3$), and inertia index ($\beta \leq 0.9$) which must be satisfied before group of machines are deem coherent.

Spalding, Yee, and Goudie, (1977), applied the principle of singular points in coherency identification. The singular points include the post-fault Stable Equilibrium Point (SEP) and Unstable Equilibrium Point (UEP). This approach considers the change in relative machine angles from the stable

equilibrium point of the system differential equations to that of the unstable equilibrium point corresponding to the system instability expected to result from the fault condition under investigation. By comparing these equilibrium points of the dynamic system equations and the admittance distance from the network structure, the coherent groups are identified.

Podmore, (1978), suggested a method of coherency identification based on a simplified linear model of power system known as clustering Algorithm. By this method, the linearized network equations and the linearized dynamic equations are deemed clustered and hence solved in each time step of the desired time interval in order to determine the angular deviation of the machines.

Al-Fuhaid, (1987), applied the coherency identification method that uses the properties of exponential matrix and Cayley-Hamilton theorem. This method is known as the mean square error and uses the state transition matrix to determine the linearized system dynamic equations. The mean square error (MSE) of the change in rotor angle of the machines over a time period $T_,$ is taken as the coherency measure.

Rudmick, Patino, and Brameller, (1981), applied the concept of energy function for coherency identification in a large power system. The approach is based on rate of change of kinetic energy, relating the power system behaviour to its potential energy and kinetic energy. This method is anchored on the principle that when a fault occurs in a power network, the speeds of the machines close to the fault increase, thereby increasing their kinetic energy, while other machines in the network decelerate until the fault is cleared. The process of kinetic energy absorption commences when the fault is cleared. Therefore, the kinetic energy of each machine contributes reasonably to the state of the final system behaviour. It has been established that the rate of change of kinetic energy (RKE) at the critical fault clearing time has a maximum negative value.

Krishnaparandhama et al., (1981), proposed a method of coherency machines identification based on equal acceleration principle. The application of this technique does not require solving the system dynamic equation, rather the necessary information of the coherent machines is obtained from the system admittance matrix and the machines inertia constants. The authors adopted the principle that the coherency of generators is dependent of the magnitude of disturbance according to (Podmore, 1978) and hence used a linearized system model in the method.

Sankaranarayanan et al., (1983), applied a coherency machines identification method based on the principle of equal acceleration for the coherency machines. The approach which is similar to that deployed by Krishnaparandhama et al., (1981), used the linearized acceleration equation with the damping coefficient neglected.

According to Sankaranarayanan, et al., (1983), an increase in acceleration of the i^{th} machine due to the influence of other system machines will increase $\Delta\delta_i$. The increment of $\Delta\delta_i$ will in turn lead to a decrease in the acceleration of the i^{th} machine and at the same time increase the acceleration of j^{th} machine, leading to an increase in $\Delta\delta_j$. The resultant effect of the above scenario is that both machines i and j will attempt to swing together. The coherent generator-based transient stability analysis is attracting interest of many researchers globally due to its benefits anchored on simplifying the complex power network, reduction in computing time, and minimal memory space requirement for stability analysis.

Chapter Three

3.0 Methodology

3.1 Power System Equipment and Networks

Electric power system comprises of devices for generation, transmission, distribution and consumption of electric power (Stein and Hunt, 1979). Electric power generation means obtaining electric power through conversion from some other form of power (Izuegbunam, 2002). The synchronous generator also known as alternator is more the often used as power generating device for an ac power. The input power to synchronous generator is mechanical and is provided by prime movers. Examples of prime movers include steam turbine, which converts the heat power of steam into mechanical power, while steam could be produced through water heating in a boiler using fossil fuel such as coal, Oil or gas etc. Heat could also be obtained by nuclear fission in an atomic reactor and exchanger. Other prime movers include gas turbines, internal combustion engines (gasoline or diesel). They convert the chemical of the fuel directly into mechanical power. In hydroelectric power plants, the power of flowing water is usually harnessed and water wheels are used as prime movers. Nigeria bieng blessed with abundant energy resources have only harnessed an infinitesimal amount to construct her generating stations ranging from hydro, thermal and gas fired, to feed the national grid (Izuegbunam, 2002). The generating voltage is usually in the range of 16 to 25KV and can be stepped up to 132, 330KV and above via power transformers for long distance transmission.

3.2 The Synchronous Generator

A synchronous machine is an ac machine whose speed under steady-state conditions is proportional to the frequency of the current in its armature. The magnetic field created by the armature currents rotates at the same speed as that created by field current on the rotor (which is rotating at synchronous

speed) and steady torque results (Fitzgerald and Kingsley, 1961). Figure 3.1 shows the schematic and circuit diagram of a model (2.1) synchronous generator.

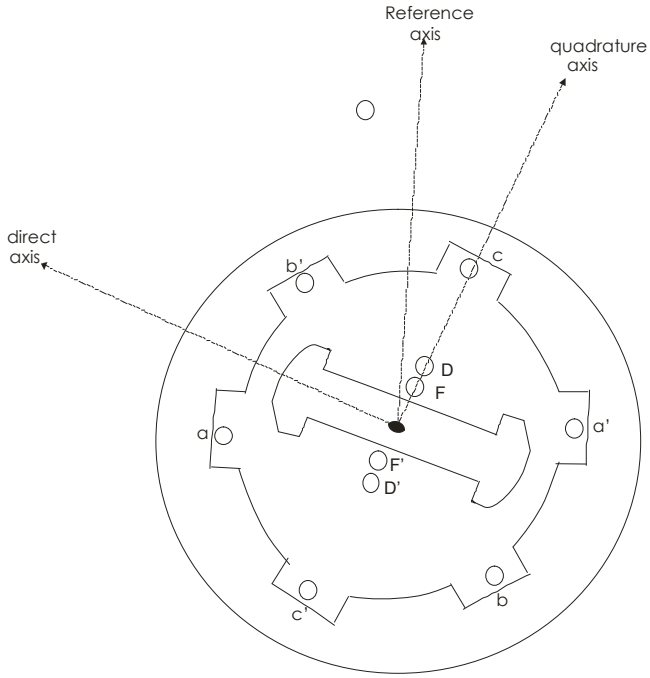

(a) Synchronous machine – abc reference frame

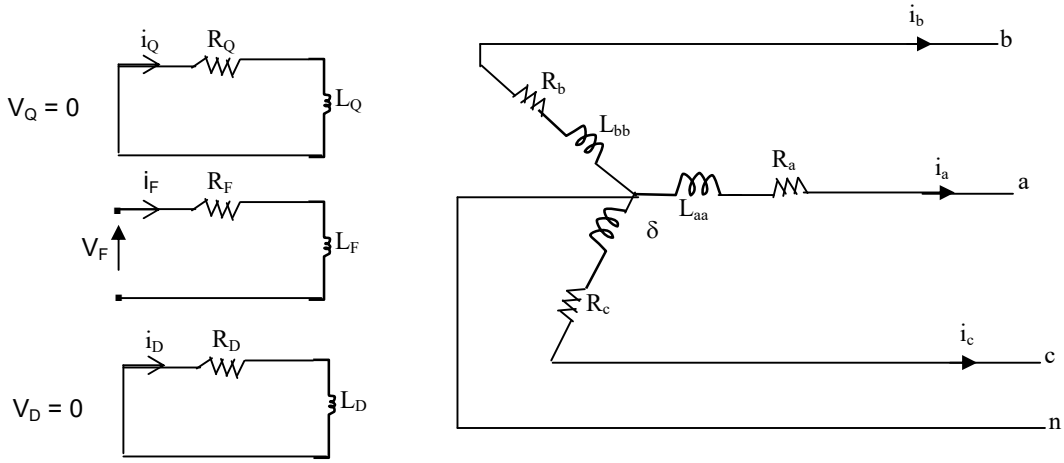

(b) Circuit diagram of a synchronous machine

Figure 3.1 synchronous machine schematic and circuit diagrams.

The voltage equations for above circuit diagram are written in matrix form as,

$$\begin{bmatrix} V_a \\ V_b \\ V_c \\ -V_F \\ 0 \\ 0 \end{bmatrix} = - \begin{bmatrix} R_a & 0 & 0 & 0 & 0 & 0 \\ 0 & R_b & 0 & 0 & 0 & 0 \\ 0 & 0 & R_c & 0 & 0 & 0 \\ 0 & 0 & 0 & R_F & 0 & 0 \\ 0 & 0 & 0 & 0 & R_D & 0 \\ 0 & 0 & 0 & 0 & 0 & R_Q \end{bmatrix} \begin{bmatrix} i_a \\ i_b \\ i_c \\ i_F \\ i_D \\ i_Q \end{bmatrix} - \frac{d}{dt} \begin{bmatrix} \lambda_a \\ \lambda_b \\ \lambda_c \\ \lambda_F \\ \lambda_D \\ \lambda_Q \end{bmatrix} \qquad (3.1)$$

Re-writing equation (3.1) in a compact and partitioned form gives,

$$\begin{bmatrix} V_{abc} \\ V_{FDQ} \end{bmatrix} = - \begin{bmatrix} R_{abc} & 0 \\ 0 & R_{FDQ} \end{bmatrix} \begin{bmatrix} i_{abc} \\ i_{FDQ} \end{bmatrix} - \frac{d}{dt} \begin{bmatrix} \lambda_{abc} \\ \lambda_{FDQ} \end{bmatrix} \qquad (3.2)$$

Where,

$$V_{FDQ} = - \begin{bmatrix} V_F \\ 0 \\ 0 \end{bmatrix}$$

$i_{FDQ} = \begin{bmatrix} i_F \\ i_D \\ i_Q \end{bmatrix}$, are rotor voltages, currents and flux linkages respectively.

$$\lambda_{FDQ} = \begin{bmatrix} \lambda_F \\ \lambda_D \\ \lambda_Q \end{bmatrix}$$

Also,

$V_{abc} = \begin{bmatrix} V_a \\ V_b \\ V_c \end{bmatrix}$, $i_{abc} = \begin{bmatrix} i_a \\ i_b \\ i_c \end{bmatrix}$, $\lambda_{abc} = \begin{bmatrix} \lambda_a \\ \lambda_b \\ \lambda_c \end{bmatrix}$, are stator voltages, currents and flues linkages respectively.

The flux linkages of the generator which are functions of self-and mutual inductances can be expressed in matrix formed as,

$$\begin{bmatrix}\lambda_a\\ \lambda_b\\ \lambda_c\\ \lambda_F\\ \lambda_D\\ \lambda_Q\end{bmatrix}=\begin{bmatrix} L_{aa} & L_{ab} & L_{ac} & L_{aF} & L_{aF} & L_{aQ}\\ L_{ba} & L_{bb} & L_{bc} & L_{bF} & L_{bD} & L_{bQ}\\ L_{ca} & L_{cb} & L_{cc} & L_{cF} & L_{cD} & L_{cQ}\\ L_{Fa} & L_{Fb} & L_{Fc} & L_{FF} & L_{FD} & L_{FQ}\\ L_{Da} & L_{DAb} & L_{Dc} & L_{DF} & L_{DD} & L_{DQ}\\ L_{Qa} & L_{Qb} & L_{Qc} & L_{QF} & L_{QD} & L_{QQ}\end{bmatrix}\begin{bmatrix}i_a\\ i_b\\ i_c\\ i_F\\ i_D\\ i_Q\end{bmatrix} \tag{3.3}$$

Putting equation (3.3) in compact form gives,

$$\begin{bmatrix}\lambda_{abc}\\ \lambda_{FDQ}\end{bmatrix}=\begin{bmatrix}L_S & L_{SR}\\ L_{ST}^{T} & L_R\end{bmatrix}\begin{bmatrix}i_{abc}\\ i_{FDQ}\end{bmatrix} \tag{3.4}$$

The stator self-inductances are gives as,

$$\begin{aligned} L_{aa} &= L_S + L_M \cos 2\theta\\ L_{bb} &= L_S + L_M \cos 2\left(\theta - \frac{2\pi}{3}\right)\\ L_{cc} &= L_S + L_M \cos 2\left(\theta + \frac{2\pi}{3}\right)\end{aligned} \tag{3.5}$$

where L_S and L_M are constant, and $L_S > L_M \geq 0$

The self-inductances of each stator phase winding reaches a maximum value each time the rotor direct-axis aligns with the axis of the phase winding. At that point, the rotor position is such that the reluctance of the flux path becomes minimum, and this occurs twice per complete cycle of rotor rotation for two-pole salient pole generator shown in figure 3.2

The stator mutual inductances are given as,

$$\begin{aligned} L_{ab} &= L_{ba} = -M_S - L_M \cos 2\left(\theta + \frac{\pi}{6}\right)\\ L_{bc} &= L_{cb} = -M_S - L_M \cos 2\left(\theta - \frac{\pi}{2}\right)\\ L_{ca} &= L_{ac} = -M_S - L_M \cos 2\left(\theta + \frac{5\pi}{6}\right)\end{aligned} \tag{3.6}$$

where $M_S > L_M \geq 0$

The mutual inductance between each of the stator windings is negative, and its magnitude is maximum at the point when the rotor direct-axis is midway between the axes of the two corresponding windings.

The stator to rotor mutual inductances are given as,

$$
\begin{aligned}
L_{aF} &= L_{Fa} = M_F \cos\theta \\
L_{bF} &= L_{Fb} = M_F \cos\left(\theta - \frac{2\pi}{3}\right) \\
L_{cF} &= L_{Fc} = M_F \cos\left(\theta + \frac{2\pi}{3}\right) \\
L_{aD} &= L_{Da} = M_D \cos\theta \\
L_{bD} &= L_{Db} = M_D \cos\left(\theta - \frac{2\pi}{3}\right) \\
L_{cD} &= L_{Dc} = M_D \cos\left(\theta + \frac{2\pi}{3}\right) \\
L_{aQ} &= L_{Qa} = M_Q \sin 0 \\
L_{bQ} &= L_{Qb} = M_Q \sin\left(\theta - \frac{2\pi}{3}\right) \\
L_{cQ} &= L_{Qc} = M_Q \sin\left(\theta + \frac{2\pi}{3}\right)
\end{aligned}
\qquad (3.7)
$$

The mutual inductances between the stator and rotor winding change with rotor position and assume a maximum positive value whenever the axes of a stator and the rotor windings align and have the same positive flux direction. The inductance however takes a negative minimum value when the flux directions are in opposition, and becomes zero when the axes are perpendicular.

The rotor self-and mutual inductances are given as,

$$L_{FF} = L_F,\ L_{DD} = L_D,\ L_{QQ} = L_Q \quad (3.8)$$

$$L_{FD} = L_{DF} = M_R,\ L_{FQ} = L_{QF} = 0,\ L_{DQ} = L_{QD} = 0 \quad (3.9)$$

The self and mutual inductances of the rotor windings are constant and are independent of rotor position. And because of the perpendicular arrangement of the direct-axis and quadrature-axis windings to each other, their mutual inductances are zero. The mutual inductance between any two circuits both in direct axis (or both in quadrature axis) is constant (Saadat, 2002).

3.2.1 Bulk Power Generation in Power Networks

Electric energy is generated in large hydro – electric, thermal and nuclear stations. Various types of electric power plants for bulk power generation include:

(a) Fossil – Fuel Plant: In this type of plant, coal, oil or natural gas is burned in a furnace. The combustion of the fuel produces heat which is utilized to heat up water to produce steam. The steam in turn drives a turbine which is mechanically coupled to an electric generator.

(b) Hydroelectric Power Plant: Hydroelectric power is obtained from conversion of potential energy stored in the heights of artificial lakes to generate electricity using water wheel turbines coupled to synchronous generators (Okoro, 2010). Hydraulic turbines derive power from the force exerted by water as it falls from an upper to a lower reservoir (Gupta, 1998). The vertical distance between the upper reservoir and the level of the turbines is referred to as the head. The size of the head is used in the classification of hydroelectric power plants as high – head, medium – head, and low- head. In pump storage scheme, water is pumped from a lower reservoir to a higher one during off – peak times, and the water allowed to flow down hill in the conventional hydroelectric mode during times of peak demand.

(c) Nuclear Power Plant: In a nuclear power plant, the controlled nuclear fission is the source of energy. During fission, heat is generated which is transferred to a coolant flowing through the reactor.

Other sources of energy include biomass, geothermal, photovoltaic, solar, wind power, tidal power, fuel cells etc

.

3.2.2 abc- odq Frame of Reference (Saadat, 2002; Machowski et al., 1997)

In recognition that most of the elements that constitute the Inductance Matrix, L in the flux linkage equations are dependent on the rotor angular position and hence are functions of time, abc reference frame also known as park's transformation helps in converting these elements into time-invariant terms. The park's transformation matrix P for this exercise is chosen such that there is power invariant after transformation; and such that inverse of the matrix must be equal to its transpose, hence the product of P and P^T must be equal to one; thus, the matrix is said to be orthogonal.

That is,

$$P^{-1} = P^T$$

and $PP^T - 1$ (3.10)

The transformation transforms the stator parameters from (abc) reference frame to (odq) reference frame using trigonometrical function of the angleθ.

The park's transformation for currents is given as,

$$\begin{bmatrix} i_o \\ i_d \\ i_q \end{bmatrix} = \sqrt{2}/3 \begin{bmatrix} 1/\sqrt{2} & 1/\sqrt{2} & 1/\sqrt{2} \\ cos\theta & \cos(\theta - \frac{2\pi}{3}) & \cos(\theta + \frac{2\pi}{3}) \\ sin\theta & \sin(\theta - \frac{2\pi}{3}) & \sin(\theta + \frac{2\pi}{3}) \end{bmatrix} \begin{bmatrix} i_a \\ i_b \\ i_c \end{bmatrix} \quad (3.11)$$

Equation (3.11) can be re-written in matrix notation as,

$$iodq = Piabc \quad (3.12)$$

where,

$$P = \sqrt{2/3}\begin{bmatrix} 1/\sqrt{2} & 1/\sqrt{2} & 1/\sqrt{2} \\ cos\theta & \cos(\theta - \frac{2\pi}{3}) & \cos(\theta + \frac{2\pi}{3}) \\ sin\theta & \sin(\theta - \frac{2\pi}{3}) & \sin(\theta + \frac{2\pi}{3}) \end{bmatrix} \quad (3.13)$$

stator voltages and flux linkages can also be transformed as,

$$V_{odq} = PV_{abc} \quad (3.14)$$

$$\lambda_{odq} = P\lambda_{abc} \quad (3.15)$$

The inverse park's transformation matrix is given as,

$$P^{-1} = \sqrt{2/3}\begin{bmatrix} 1/\sqrt{2} & cos\theta & sin\theta \\ 1/\sqrt{2} & \cos(\theta - \frac{2\pi}{3}) & \sin(\theta - \frac{2\pi}{3}) \\ 1/\sqrt{2} & \cos(\theta + \frac{2\pi}{3}) & \sin(\theta + \frac{2\pi}{3}) \end{bmatrix} \quad (3.16)$$

The transformation of time-varying inductances to rotor reference frame (odq) with the original rotor quantities unaffected give,

$$\begin{bmatrix} \lambda_{odq} \\ \lambda_{FDQ} \end{bmatrix} = \begin{bmatrix} P & 0 \\ 0 & I \end{bmatrix} \begin{bmatrix} \lambda_{abc} \\ \lambda_{FDQ} \end{bmatrix} \quad (3.17)$$

And conversely, the following relationship can also be derived from equation (3.17),

$$\begin{bmatrix} \lambda_{abc} \\ \lambda_{FDQ} \end{bmatrix} = \begin{bmatrix} P^{-1} & 0 \\ 0 & I \end{bmatrix} \begin{bmatrix} \lambda_{odq} \\ \lambda_{FDQ} \end{bmatrix} \quad (3.18)$$

Applying appropriate transformation relations into equation (3.4) give,

$$\begin{bmatrix} \lambda_{odq} \\ \lambda_{FDQ} \end{bmatrix} - \begin{bmatrix} P & 0 \\ 0 & I \end{bmatrix} \begin{bmatrix} L_S & L_{SR} \\ L_{SR}^T & L_R \end{bmatrix} \begin{bmatrix} P^{-1} & 0 \\ 0 & I \end{bmatrix} \begin{bmatrix} i_{odq} \\ i_{FDQ} \end{bmatrix} \quad (3.19)$$

Substituting the inductances in equations (3.5), (3.6), (3.7), (3.8) and (3.9) into equation (3.19) results to,

$$\begin{bmatrix}\lambda_0\\ \lambda_d\\ \lambda_q\\ \lambda_F\\ \lambda_D\\ \lambda_Q\end{bmatrix} = \begin{bmatrix}L_0 & 0 & 0 & 0 & 0 & 0\\ 0 & L_d & \omega L_d & KM_F & KM_D & 0\\ 0 & 0 & L_q & 0 & 0 & KM_Q\\ 0 & KM_F & 0 & L_F & 0 & 0\\ 0 & KM_D & 0 & M_R & L_D & 0\\ 0 & 0 & KM_Q & 0 & 0 & L_Q\end{bmatrix}\begin{bmatrix}i_0\\ i_d\\ i_q\\ i_F\\ i_D\\ i_Q\end{bmatrix} \quad (3.20)$$

where,

$$L_0 = L_S - 2M_S$$
$$L_d = L_S + M_S + \frac{3}{2}L_M \quad (3.21)$$
$$L_q = L_S + M_S - \frac{3}{2}L_M$$

and

K = $\sqrt{3}/2$

The transformation of the stator – based currents (i_{abc}) and voltages (V_{abc}) into rotor-based currents (i_{odq}) and voltages (V_{odq}) give,

$$\begin{bmatrix}i_{odq}\\ i_{FDQ}\end{bmatrix} = \begin{bmatrix}P & 0\\ 0 & I\end{bmatrix}\begin{bmatrix}i_{abc}\\ i_{FDQ}\end{bmatrix} \quad (3.22)$$

$$\begin{bmatrix}i_{abc}\\ i_{FDQ}\end{bmatrix} = \begin{bmatrix}P^{-1} & 0\\ 0 & I\end{bmatrix}\begin{bmatrix}i_{odq}\\ i_{FDQ}\end{bmatrix} \quad (3.23)$$

$$\begin{bmatrix}V_{abc}\\ V_{FDQ}\end{bmatrix} = \begin{bmatrix}P^{-1} & 0\\ 0 & I\end{bmatrix}\begin{bmatrix}V_{odq}\\ V_{FDQ}\end{bmatrix} \quad (3.24)$$

Putting equations (3.18), (3.23) and (3.24) into (3.2) gives,

$$\begin{bmatrix}V_{odq}\\ V_{FDQ}\end{bmatrix} = \begin{bmatrix}P & 0\\ 0 & I\end{bmatrix}\begin{bmatrix}R_{abc} & 0\\ 0 & R_{FDQ}\end{bmatrix}\begin{bmatrix}P^{-1} & 0\\ 0 & I\end{bmatrix}\begin{bmatrix}i_{odq}\\ i_{FDQ}\end{bmatrix} - \begin{bmatrix}P & 0\\ 0 & I\end{bmatrix}$$
$$\frac{d}{dt}\left\{\begin{bmatrix}P^{-1} & 0\\ 0 & I\end{bmatrix}\begin{bmatrix}\lambda_{odq}\\ \lambda_{FDQ}\end{bmatrix}\right\} \quad (3.25)$$

Equation (3.25) can be reduced to,

$$\begin{bmatrix} V_{odq} \\ V_{FDQ} \end{bmatrix} = \begin{bmatrix} R_{abc} & 0 \\ 0 & R_{FDQ} \end{bmatrix} \begin{bmatrix} i_{odq} \\ i_{FDQ} \end{bmatrix} - \begin{bmatrix} P\frac{dP^{-1}}{dt} & 0 \\ 0 & I \end{bmatrix} \begin{bmatrix} \lambda_{odq} \\ \lambda_{FDQ} \end{bmatrix} - \frac{d}{dt} \begin{bmatrix} \lambda_{odq} \\ \lambda_{FDQ} \end{bmatrix} \quad (3.26)$$

Evaluating $P\frac{dP^{-1}}{dt}$ gives,

$$P\frac{dP^{-1}}{dt} = P\frac{d\theta}{dt}\frac{dP^{-1}}{d\theta}$$

$$= P\omega\frac{dP^{-1}}{d\theta} \quad (3.27)$$

Therefore, by making appropriate substitution, equation (3.27) modifies to,

$$P\frac{dP^{-1}}{dt} = \sqrt{2}/3 \begin{bmatrix} 1/\sqrt{2} & 1/\sqrt{2} & 1/\sqrt{2} \\ cos\theta & \cos(\theta - \frac{2\pi}{3}) & \cos(\theta + \frac{2\pi}{3}) \\ sin\theta & \sin(\theta - \frac{2\pi}{3}) & \sin(\theta + \frac{2\pi}{3}) \end{bmatrix} \omega$$

$$\frac{d}{d\theta}\left\{\sqrt{2}/3 \begin{bmatrix} 1/\sqrt{2} & cos\theta & sin\theta \\ 1/\sqrt{2} & \cos(\theta - \frac{2\pi}{3}) & \sin(\theta - \frac{2\pi}{3}) \\ 1/\sqrt{2} & \cos(\theta + \frac{2\pi}{3}) & \sin(\theta + \frac{2\pi}{3}) \end{bmatrix}\right\}$$

$$2/3\,\omega \begin{bmatrix} 1/\sqrt{2} & 1/\sqrt{2} & 1/\sqrt{2} \\ cos\theta & \cos(\theta - \frac{2\pi}{3}) & \cos(\theta + \frac{2\pi}{3}) \\ sin\theta & \sin(\theta - \frac{2\pi}{3}) & \sin(\theta + \frac{2\pi}{3}) \end{bmatrix}$$

$$\begin{bmatrix} 0 & -sin\theta & cos\theta \\ 0 & -\sin(\theta-\frac{2\pi}{3}) & \cos(\theta-\frac{2\pi}{3}) \\ 0 & -\sin(\theta+\frac{2\pi}{3}) & \cos(\theta+\frac{2\pi}{3}) \end{bmatrix}$$

$$= 2/3\omega \begin{bmatrix} 0 & -1/\sqrt{2}\{sin\theta+\sin(\theta-\frac{2\pi}{3})+\sin(\theta+\frac{2\pi}{3})\} & 1/\sqrt{2}\{cos\theta+\cos(\theta-\frac{2\pi}{3})+\cos(\theta+\frac{2\pi}{3})\} \\ 0 & -\cos\theta\sin\theta-\cos(\theta-\frac{2\pi}{3})\sin(\theta-\frac{2\pi}{3})-\cos(\theta+\frac{2\pi}{3})\sin(\theta+\frac{2\pi}{3}) & \cos^2\theta+\cos^2(\theta-\frac{2\pi}{3})+\cos^2(\theta+2\cos(\theta+\frac{2\pi}{3}) \\ 0 & -\sin^2\theta-\sin^2(\theta-\frac{2\pi}{3})-\sin^2(\theta+\frac{2\pi}{3}) & \cos\theta\sin\theta+\cos(\theta-\frac{2\pi}{3})\sin(\theta-\frac{2\pi}{3})+\cos(\theta+\frac{2\pi}{3})\sin(\theta+\frac{2\pi}{3}) \end{bmatrix}$$

$$= 2/3\,\omega \begin{bmatrix} 0 & -1/\sqrt{2}\{0+(-0.8660)+0.8660\} & 1/\sqrt{2}\{1+(-0.5)+(-0.5)\} \\ 0 & 0-(-0.5)(-0.8660)-(-0.5)(0.8660) & 1+0.25+0.25 \\ 0 & 0+(-0.75)-(0.75) & 0+(-0.5)(-0.5)(-0.8660)+(-0.5)(0.8660) \end{bmatrix}$$

$$= \qquad 2/3\omega \begin{bmatrix} 0 & 0 & 0 \\ 0 & 0 & 3/2 \\ 0 & -3/2 & 0 \end{bmatrix}$$

$$= \qquad \omega \begin{bmatrix} 0 & 0 & 0 \\ 0 & 0 & 1 \\ 0 & -1 & 0 \end{bmatrix} \qquad (3.28)$$

Putting equations (3.20) and (3.28) into (3.26) gives

$$\begin{bmatrix} V_0 \\ V_d \\ V_q \\ -V_F \\ 0 \\ 0 \end{bmatrix} = \begin{bmatrix} R_a & 0 & 0 & 0 & 0 & 0 \\ 0 & R_b & \omega L_d & 0 & 0 & -\omega KM_Q \\ 0 & -\omega L_d & R_c & -\omega KM_F & -\omega KM_D & 0 \\ 0 & 0 & 0 & R_F & 0 & 0 \\ 0 & 0 & 0 & 0 & R_D & 0 \\ 0 & 0 & 0 & 0 & 0 & R_Q \end{bmatrix} \begin{bmatrix} i_0 \\ i_d \\ i_q \\ i_F \\ i_D \\ i_Q \end{bmatrix}$$

$$\begin{bmatrix} L_0 & 0 & 0 & 0 & 0 & 0 \\ 0 & L_d & \omega L_d & KM_F & KM_D & 0 \\ 0 & 0 & L_q & 0 & 0 & KM_Q \\ 0 & KM_F & 0 & L_F & 0 & 0 \\ 0 & KM_D & 0 & M_R & L_D & 0 \\ 0 & 0 & KM_Q & 0 & 0 & L_Q \end{bmatrix} \frac{d}{dt} \begin{bmatrix} i_0 \\ i_d \\ i_q \\ i_F \\ i_D \\ i_Q \end{bmatrix} \quad (3.29)$$

Equation (3.29) can be re-written in compact form as,

$$V = -Ri - L\frac{di}{dt} \quad (3.30)$$

Also, equation (3.30) can be put in the form,

$$\frac{di}{dt} = -L^{-1}Ri - L^{-1}V \quad (3.31)$$

Figure 3.2 shows the equivalent electric circuit of the system in figure 3.1 after odq refernce frame transformation.

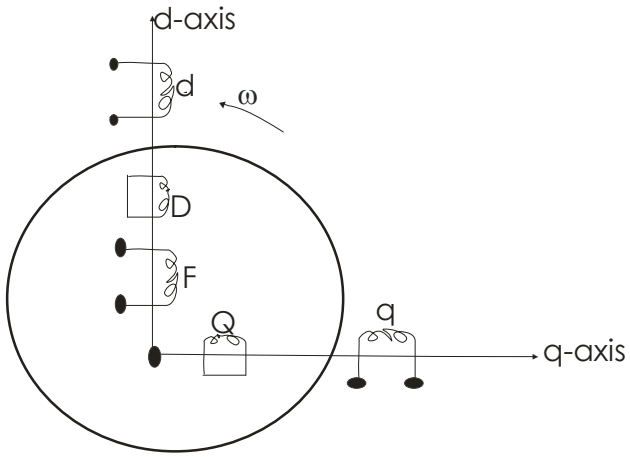

Figure 3.2 equivalent electric circuit of the system in figure 3.1 after odq refernce frame transformation.

The odq refernce frame transformation as seen from the transformed machine equations show the disappearance of the time dependence inductances, leading to a number of mutual inductances becoming zero in the transformed system. Furthermore, there are no couplings between equivalent circuits on different axes in figure 3.2, but only between those on the same axes (Anderson, 2003). A disturbance in the current in d-axis stator winding will lead to current changes in the D- and F- windings which in turn will decay with different time constants in the two circuits.

3.2.3 Transient Parameters of the Synchronous Generator

The pre-fault armature reactance and transient reactance (steady-state value) differs from the fault-on value due to the influence of the additionally induced currents in the rotor windings at fault period. This higher induced fault current on rotor windings oppose the armature flux, thereby preventing it from entering the rotor windings. The phenomenon is known as the screening of the rotor from the fault - induced changes in the armature flux (Machowski et al., 1997). As soon as the fault is cleared, the current in the rotor field winding and the damper windings force the armature reaction flux totally out of the rotor, thereby keeping the rotor flux linkages constant. Under this condition, the generator is said to be in subtransient state. As the energy is dissipated in the rotor winding resistances, the currents maintaining the constant rotor flux linkages decay with time thereby making way for the armature flux to penetrate the rotor windings. The comparative large size of rotor damper windings resistances to field winding resistance makes it possible for the damper current to decay first, thus permitting the armature flux to enter the rotor pole face without penetrating the field winding itself. The generator under this condition is said to be in transient state. The field

current subsequently decays with time to its steady-state value, thus allowing the armature reaction flux to penetrate the entire rotor and once again follows the minimum reluctance path (Fitzgerald and Kingsley, 1961; Anderson, 2003; Machowski et al., 1997).

Figure 3.3 shows the equivalent circuits for determining the open-circuit and short-circuit subtransient time constants.

(a) Open-circuit (b) Short -circuit

Figure 3.3: Equivalent circuits for the determination subtransient time constants.

From figure 3.3(a), neglecting the leakage reactions X_L, the open-circuit subtransient time constant is obtained as,

$$T_{d0}^{''} = X_D + \frac{X_a X_f}{\frac{X_a + X_f}{\omega R_D}} \approx \frac{X_D X_d'}{\omega R_D} \qquad (3.32)$$

From figure 3.3 (b), the short-circuit subtransient time constant is obtained as,

$$T_d^{''} = \frac{X_D}{\omega R_D} \qquad (3.33)$$

Figure 3.4 shows the equivalent circuits for determination of transient reactance and steady state reactance.

(a) Transient reactance (b) Steady- state reactance

Figure 3.4 Equivalent circuits for transient and steady-state reactances.

From figure 3.4 (a), neglecting the armature reaction leakage reactance, X_L,

$$X_d' \approx \frac{X_a X_f}{X_a + X_f} \tag{3.34}$$

Similarly,

$$X_d'' \approx \frac{1}{\frac{1}{X_D} + \frac{1}{X_d'}} \tag{3.35}$$

$$X_D \approx \frac{X_d' X_d''}{X_d' - X_d''} \tag{3.36}$$

Dividing equation (3.33) by equation (3.32), and substituting for X_D from equation (3.36) gives,

$$\frac{T_d''}{T_{d0}''} = \left(\frac{\omega R_D}{X_D \mid X_d'}\right) x \left(\frac{X_D}{\omega R_D}\right)$$

$$= \frac{\frac{X_d' X_d''}{X_d' - X_d''}}{\frac{X_d' X_d''}{X_d' - X_d''} + X_d'}$$

$$= \frac{X_d' X_d''}{\left(X_d' - X_d''\right)\left(\left(\frac{X_d' X_d''}{X_d' - X_d''}\right) + X_d'\right)}$$

$$= \frac{X_d' X_d''}{\left(X_d' X_d''\right) + (X_d')^2 - X_d' X_d''}$$

$$= \frac{X_d' X_d^{"}}{X_d' X_d^{"}} + \frac{X_d' X_d^{"}}{(X_d')^2} - \frac{X_d' X_d^{"}}{X_d' X_d^{"}}$$

hence,

$$\frac{T_d^{"}}{T_{d0}^{"}} = 1 + \frac{X_d^{"}}{X_d'} - 1$$

$$T_d^{"} \cong T_{d0}^{"} \frac{X_d^{"}}{X_d'} \tag{3.37}$$

Similarly,

$$T_q^{"} \cong T_{q0}^{"} \frac{X_q^{"}}{X_q'} \tag{3.38}$$

$$T_d' \cong T_{d0}' \frac{X_d'}{X_d} \tag{3.39}$$

$$T_q' \cong T_{q0}' \frac{X_q'}{X_q} \tag{3.40}$$

The open-circuit time constants are usually larger than the short-circuit values. In the absence of the manufacturers' specified values, the following assumptions are made (Mahowski et al., 1997),

$$X_q' = 2X_q^{"} \; and \; T_q^{"} = 10T_q^{"}$$

In terms of circuit elements, and magnetic coupling of the direct-axis circuits as well as the quadrate-axis circuits coupling, the steady-state, transient and subtransient inductances and time constants can also be determined.

When the synchronous generator operates in the steady-state, the armature flux permeates the entire rotor circuits, the field and damper winding currents are constant. The armature current only sees the synchronous inductance L_d

in the direct axis and L_q in the quadrature axis. Figure 3.5 shows direct-axis and quadrature-axis coupled circuits for stead-state operation.

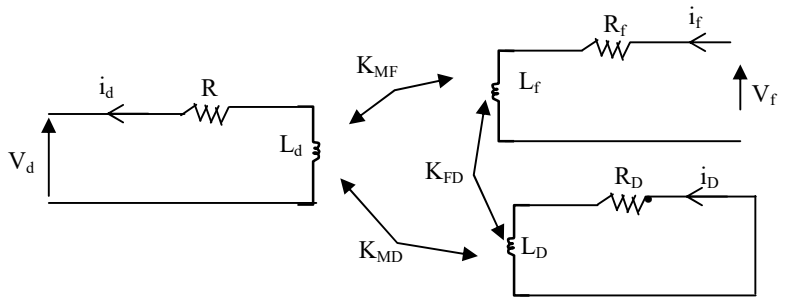

(a). Direct-axis coupled circuits

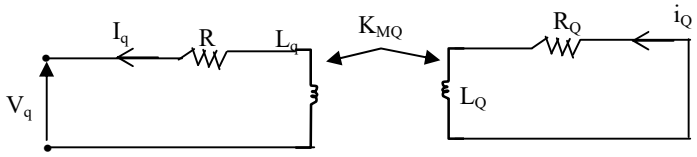

(b). Quadrate-axis coupled circuits

Figure 3.5: d- and q- axis circuits.

Under transient state operation, the armature flux permeates the damper circuits and the field winding screens the rotor body from the armature flux. The damper circuits become ineffective and could be removed from the model, while the screening behaviour of the field winding is modeled by short-circuiting the field winding and setting its resistance equal to zero as shown in figure 3.6. This arrangement effectively represents the current changes that would occur in the field winding in order to maintain the flux linkages of this winding constant.

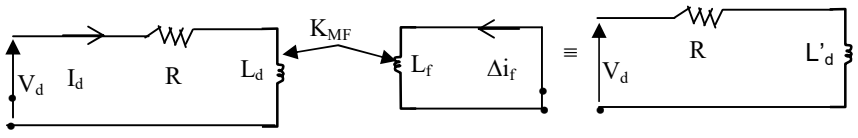

(a). Quadrate-axis coupled circuits

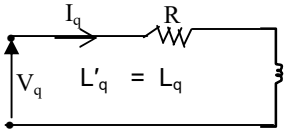

(b). Quadrate-axis circuits

Figure 3.6: d- and q- axes circuits for determining transient inductance.

From figure 3.6 (a), the voltage equations can be written as,

$$V_d = Ri_d + L_d \frac{di_d}{dt} + KM_F \frac{d\Delta i_f}{dt} \quad (3.41)$$

$$\Delta V_f = 0 = L_f \frac{d\Delta i_f}{dt} + KM_F \frac{di_d}{dt} \quad (3.42)$$

As the initial conditions are zero, putting equations (3.41) and (3.42) in Laplace transform by substituting s for $\frac{d}{dt}$ gives,

$$V_d = (R + sL_d)i_d + sKM_F\Delta i_f \quad (3.43)$$

$$0 = sKM_F i_d + sL_F\Delta i_f \quad (3.44)$$

putting equations (3.43) and (3.44) in matrix form gives,

$$\begin{bmatrix} V_d \\ 0 \end{bmatrix} = \begin{bmatrix} R + sL_d & sKM_F \\ sKM_F & sL_F \end{bmatrix} \begin{bmatrix} i_d \\ \Delta i_f \end{bmatrix} \quad (3.45)$$

From the standard matrix expression given by,

$$\begin{bmatrix} V_1 \\ 0 \end{bmatrix} = \begin{bmatrix} Z_{11} & Z_{12} \\ Z_{21} & Z_{22} \end{bmatrix} \begin{bmatrix} i_1 \\ i_2 \end{bmatrix} \quad (3.46)$$

$$V_1 = Z_{eq} i_1$$

Where,

$$z_{eq} = [Z_{11} \quad -Z_{12}Z_{22}^{-1} \quad Z_{21}]$$

Hence, from equation (3.45),

$$V_d = \left[(R + sL_d) - sKM_F \frac{1}{sL_F} sKM_F\right] i_d$$

$$= (R + sL_d) - \frac{K^2 M_F^2}{L_F}$$

$$= \left[R + s\left(L_d - \frac{K^2 M_F^2}{L_F}\right)\right] i_d$$

$$V_d = [R + sL'_d] i_d \quad (3.47)$$

Where,

$$L'_d = L_d - \frac{K^2 M_F^2}{L_F} \quad (3.48)$$

$$X'_d = \omega L'_d \quad (3.49)$$

Equation (3.49) is the direct-axis transient inductance. Because there is no field winding in the quadrate axis, the quadrature-axis transient inductance equals the steady-state q-axis inductance, hence,

$$L'_q = L_q \quad (3.50)$$

$$X'_q = \omega L'_q = X_q \quad (3.51)$$

However, the decay time constant of the induced field current is dependent on whether the d-axis armature winding is open-circuited or short-circuited.

Figure 3.7 show direct - axis coupled circuits for the determination of open- and short-circuit transient constants (T'_{do} and T'_{d}).

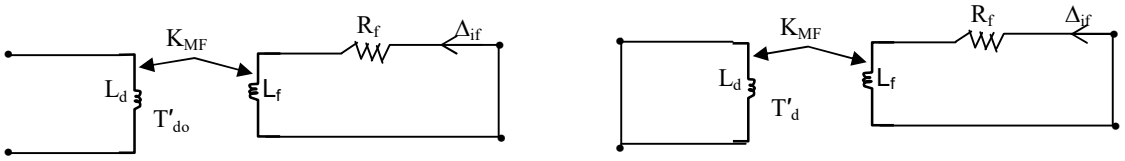

(a). Open-circuit d-axis armature circuit (b). Short-circuit d-axis armature circuit

Figure 3.7: d- axis coupled circuit for transient time constants determination.

From figure 3.7(a), when the direct axis armature circuit is open-circuited, the d-axis transient open-circuit time constant T'_{do} is obtained as,

$$T'_{d0} = \frac{L_F}{R_F} \tag{3.52}$$

From figure 3.7(b), when the armature is short circuited, the time constant becomes the d-axis transient short-circuit time constant T'_d, and can be obtained as,

$$T'_d = \left(L_F - \frac{K^2 M_F^2}{L_d}\right)\frac{1}{R} = T'_{d0}\frac{L''_d}{L_d} \tag{3.53}$$

And since there is no quadrate axis field circuit, there is also no q-axis transient time constant.

Finally, in the subtransient-state, the armature flux is deflected round the damper winding, thus screening the field winding from the armature flux. Under subtransient conditions, all the rotor circuits are represented by short-circuited windings with zero resistance.

Figure 3.8 shows the circuit arrangement for subtransient d-and q- axis coupled circuits.

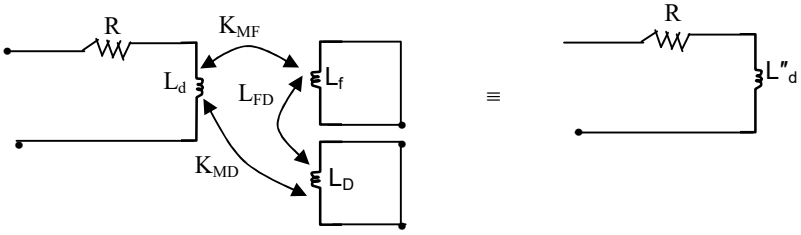

(a) d-axis coupled circuits

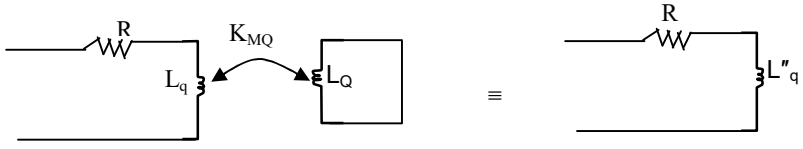

(b) q-axis coupled circuits

Figure 3.8: Equivalent circuits of d - and q- axis coupled circuits.

From figure 3.8(a), the voltage equations for the coupled circuits are,

$$V_d = Ri_d + L_d \frac{di_d}{dt} + K_{MF} \frac{d\Delta i_f}{dx} + K_{MD} \frac{di_D}{dt} \quad (3.54)$$

$$0 = K_{MF} \frac{di_d}{dt} + L_F \frac{d\Delta i_f}{dt} + L_{FD} \frac{di_D}{dt} \quad (3.55)$$

$$0 = K_{MD} \frac{di_d}{dt} + L_{FD} \frac{d\Delta i_f}{dt} + L_D \frac{di_D}{dt} \quad (3.56)$$

Taking the Laplace transform of equations (3.54), (3.55) and (3.56) give,

$$V_d = (R + sL_d)i_d + sK_{MF}\Delta i_f + sK_{MD} \quad (3.57)$$

$$0 = sK_{MF}i_d + sL_F\Delta i_f + sL_{FD}K_{MD} \quad (3.58)$$

$$0 = sK_{MD}i_d + sL_{FD}\Delta i_f + sL_D i_D \quad (3.59)$$

Putting equations (3.57), (3.58), and (3.59) in matrix form gives,

$$\begin{bmatrix} V_d \\ 0 \\ 0 \end{bmatrix} = \begin{bmatrix} R + sL_d & sL_{MF} & sK_{MD} \\ sK_{MF} & sL_F & sL_{FD} \\ sK_{MD} & sL_{FD} & sL_D \end{bmatrix} \begin{bmatrix} i_d \\ \Delta i_f \\ i_D \end{bmatrix} \quad (3.60)$$

Also, $V_d = (R + sL_d'')i_d$ (3.61)

Applying matrix procedure to equation (3.60), gives

$$L_d'' = L_d - \left[\frac{K^2M_F^2L_D + K^2M_D^2L_F - 2KM_FKM_DL_{FD}}{L_DL_F - L_{FD}^2}\right] \quad (3.62)$$

$$X_d' = \omega L_d'' \quad (3.63$$

In the quadrature – axis,

$$L''_q = L_q - \frac{K^2M^2_Q}{L_Q} \quad (3.64)$$

$$X''_q = \omega L''_q \quad (3.65)$$

The subtransient open-circuit and short-circuit time constants for the current decay in the damper winding can be determined by using figure 3.9.

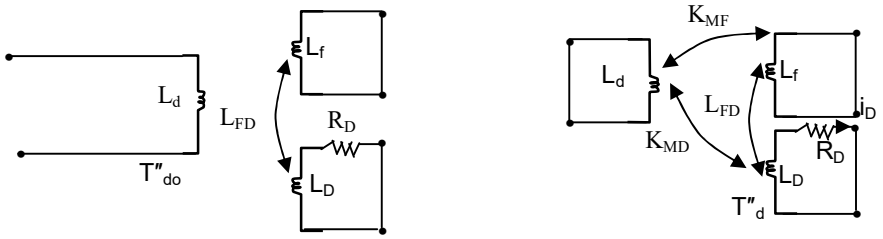

(a). d-axis coupled circuits for subtransient open-and short-circuits time constants.

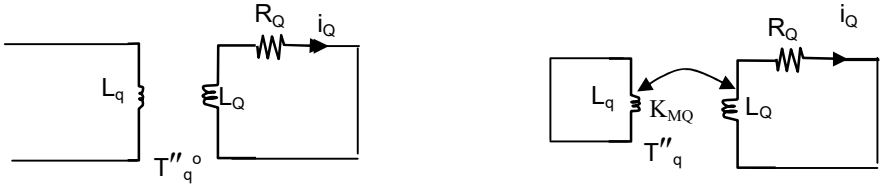

(b). q-axis equivalent circuits for subtransient open-and short-circuits time constants.

Figure 3.9: Equivalent circuits for d-and q- axis subtransient open- and short-circuits time constants.

From figure 3.9 (a), open-circuit and short-circuit d-axis subtransient time constants are expressed as,

$$T_{d0}^{''} = \left(L_D - \frac{L_{FD}^2}{L_F}\right)\frac{1}{R_D} \tag{3.66}$$

$$T_d^{''} = L_D - \left[\frac{(L_{FD}^2 L_d + K^2 M_D^2 L_F - 2 L_{FD} K M_D K M_F)}{L_d L_F - K^2 M_F^2}\right]\frac{1}{R_D}$$

$$= T_{d0}^{''}\frac{L_d^{''}}{L_d^{'}} \tag{3.67}$$

Where,

$T_{d0}^{''}$ = the d-axis subtransient open-circuit time constant.

$T_d^{''}$ = the d-axis subtransient short-circuit time constant.

From figure 3.9 (b), if there is no rotor body screening effects in q-axis, the open-circuit and short-circuit q-axis subtransient time constants are given as,

$$T_{q0}^{''} = \frac{L_Q}{R_Q} \tag{3.68}$$

$$T_q^{''} = \left(L_Q - \frac{K^2 M_Q^2}{L_q}\right)\frac{1}{R_Q} = T_{q0}^{''}\frac{L_q^{''}}{L_q'} \tag{3.69}$$

In principle, the effective reactance varies with time after the disturbance. For the period up to typically one second after the disturbance, the value X_d' is appropriate to be used for analysis, and after that X_d is valid. For really fast dynamic of the order of about few tens of milliseconds after a disturbance, the subtransient reactance $X_d^{''}$ becomes the effective reactance and hence should be used (Anderson, 2003).

3.2.4 The Generator in the Transient State

Figure 3.10 shows the classical generator model in transient state and its phasor diagrams.

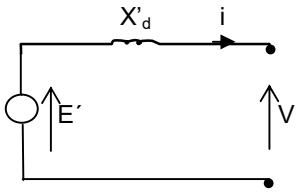

(a) Synchronous generator circuit model

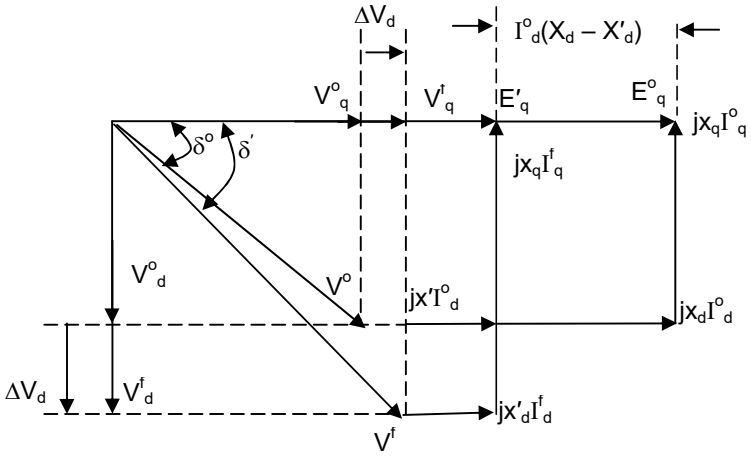

(b) Pre-fault and post fault voltage phasor

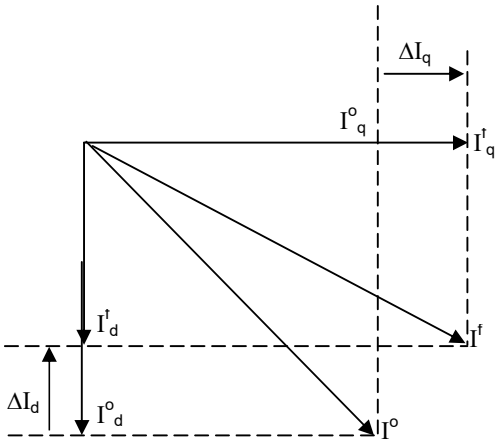

(c) Pre-fault and post fault current phasor

Figure 3.10 synchronous generator classical model with pre-fault and post fault voltage and current phasors.

From the phasors,

$$I_d^0 = \frac{E^0 - X_q^0}{X_d} \tag{3.70}$$

$$I_q^0 = \frac{V_d^0}{X_q} \tag{3.71}$$

$$V_d^0 = I_q^0 X_q \tag{3.72}$$

Equations (3.70), (3.71) and (3.72) are pre-fault direct- and quadrature axis currents and voltage components values.

The occurrence of fault leads to sudden change in voltage from pre-fault value of V^0 to post fault value V^f, thereby resulting to the change in the d- and q- axis voltage components with the amount ΔV_d and ΔV_q respectively. The d - and q - axis current components as measured immediately following the fault will change with the amounts,

$$\Delta I_d = -\frac{\Delta V_q}{X_d'} \tag{3.73}$$

OR

$$\Delta V_q = -\Delta I_d X_d' \tag{3.74}$$

$$\Delta I_q = \frac{\Delta V_d}{X_q} \tag{3.75}$$

OR

$$\Delta V_d = \Delta I_q X_q \tag{3.76}$$

Equation (3.74) implies that a positive change in q-axis voltage components causes a reduction in d-axis current component I_d, that is, a negative value ΔI_d.

$$V_d^f = V_d^0 \Delta V_d \tag{3.77}$$

Substituting equations (1.71) and (1.75) into (1.76) gives,

$$V_d^f = I_q^0 X_q + \Delta I_q X_q = \Delta I_q^f X_q \tag{3.78}$$

Similarly,

$$V_q^f = V_q^0 + \Delta V_q \tag{3.79}$$

Putting ΔV_q from equation (3.74) into (3.79) gives,

$$V_q^f = V_q^0 + (-\Delta I_d X_d')$$

Hence,

$$V_q^0 = V_q^f + \Delta I_d X_d' \tag{3.80}$$

From figure 3.10(b),

$$E' = V_q^f + X_d' I_d^f = V_q^0 + X_d' I_d^0 \tag{3.81}$$

Also,

$$E' = E^0 - (X_d - X_d') I_d^0 \tag{3.82}$$

Substituting equation (3.60) into (3.82) gives,

$$E' = \frac{X'_d E^0 + (X_d - X'_d)V_q^0}{X_d} \quad (3.83)$$

That transient electric power equation for a salient-pole synchronous generator is given by,

$$P'_e = \frac{|V^f||E'|}{X'_d}\sin\delta' + \frac{|V^f|^2}{2}\left(\frac{1}{X'_q} - \frac{1}{X'_d}\right)\sin\delta' \quad (3.84)$$

Where $\delta' = < E' - < V^f$

If the effect of transient saliency is neglected, $X'_q = X'_d$, then equation (3.84) reduces to,

$$P'_e = \frac{|V^f||E'|}{X'_d}\sin\delta' \quad (3.85)$$

The following assumptions are made for the classical generator mode:

(a). The emf E' behind transient reactance X'_d is constant during transient period.

(b). The angle of the emf is assumed to coincide with the rotor angle.

The swing equation is given by,

$$\frac{Md^2\delta'}{dt^2} = P_m - \frac{|E'||V^f|}{X'_d}\sin\delta' - \frac{Dd\delta'}{dt} \quad (3.86)$$

This model allows the generator reactance to be treated in a similar way to the reactance of the transmission lines and other network elements. The approach is very useful for multimachine systems when combining the algebraic equations describing the generator and the network. The algebraic equation describing the armature voltage is given by

$$V^f = E' - jX'_d I \quad (3.87)$$

The assumption of small changes in the direct-axis component of the generator current, and in the internal emf, means that only generators located far away from the point of disturbance should be represented by the classical model.

3.3 The Transmission System

Power transmission involves transferring bulk power from remote generating stations to various load centres or substations (Gupta, 1998). This is usually carried out at Extra – High voltage or High voltage levels depending on the distances involved and permissible operating voltage levels of the country concerned. The transmission system of an area or state is known as a grid, and is made up of primary transmission and secondary transmission systems.

In the primary transmission system, high voltage transmission lines transmit electrical power from the sending end substations to the receiving end substations. The transmission voltages in Nigeria are 132KV and 330KV. While the secondary transmission system forms the link between the main receiving end substations and the secondary substations. At the secondary substations, the voltage is stepped down to 33KV, 11KV, and power is thereafter fed into the primary distribution system.

3.3.0 The Transmission Systems Model

The primary function of a power system is to provide the real and reactive powers demand by the various loads connected to the system, and the transmission line provides a route for the surplus power on one bus to the surplus load on the other and/or to serve as an emergency link (Elgerd, 1979). Load flow is the basic calculation required to determine the characteristics of the electrical transmission systems operating in their steady-state model (Arrillaga and Arnold, 1990).

3.3.1 Transmission Line Model

The equivalent π model of a transmission line shown in figure 3.11 comprises the following complex parameters: series impedance, Z_{ij}, shunt **admittances** y^{sh}_{ij} and y^{sh}_{ji}.

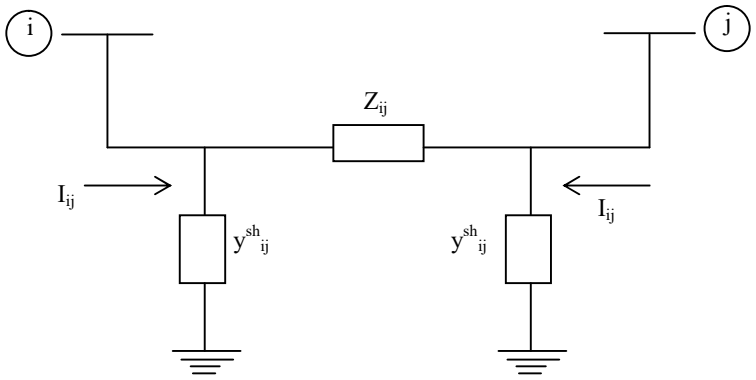

Figure 3.11: Equivalent π model of a transmission line.

From figure 3.11, series impedance and the caressing admittance are given as

$$Z_{ij} = r_{ij} + jx_{ij} \tag{3.88}$$

$$y_{ij} = Z_{ij}^{-1} = g_{ij} + jb_{ij} \tag{3.89}$$

where,

g_{ij} = the series conductance

b_{ij} = the series susceptance

and are given as,

$$g_{ij} = \frac{r_{ij}}{r_{ij}^2 + x_{ij}^2} \tag{3.90}$$

$$b_{ij} = -\frac{x_{ij}}{r_{ij}^2 + x_{ij}^2} \tag{3.91}$$

The shunt admittance y^{sh}_{ij} is expressed as,

$$y_{ij}^{sh} = g_{ij}^{sh} + jb_{ij}^{sh} \tag{3.92}$$

The complex currents I_{ij} and I_{ji} in figure 3.11 can b expressed as functions of the complex voltage at the terminal buses i and j as follows:

$$I_{ij} = y_{ij}(E_i - E_j) + y_{ij}^{sh} E_i \quad (3.93)$$

$$I_{ji} = y_{ji}(E_j - E_i) + y_{ji}^{sh} E_j \quad (3.94)$$

Where,

$$E_i = V_i e^{j\theta i}$$

$$E_j = V_j e^{j\theta j}$$

In a real transmission line, r_{ij} and x_{ij} have positive values, hence the g_{ij} is positive and b_{ij} is negative (inductive susceptance); the shunt susceptance b^{sh}_{ij} and the shunt conductance g^{sh}_{ij} are both positive (Monticelli, 1999). Also the x/r ratio in 330KV line is higher than that in 132KV line, and at the same time, a smaller $|b/b^{sh}|$ ratio. Higher x/r ratios generally imply better decoupling between active and reactive parts of the power flow problem, while smaller $|b/b^{sh}|$ may indicate the need for some form of compensation either of the series, the shunt, or both (Monticelli, 1999).

3.3.2 The Transformer Model with Complex Ratio

Figure 3.12 shows the transformer model with complex ratio

$$t_{ij} = e^{j\varphi ij} \; and \; (\bar{t}_{ij} = a_{ij}^{-1} e^{-j\varphi ij})$$

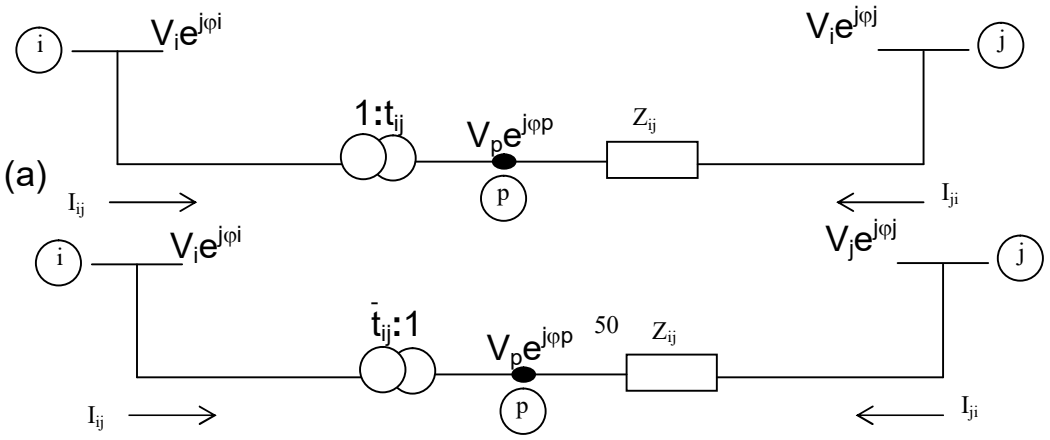

(b)

Where $t_{ij} = \frac{1}{\bar{t}_{ij}}$

Figure 3.12: Tranformer model with complex ratio

3.3.3 The In – Phase Transformer Model

Figure 3.13 show both in-phase transformer model and its equivalent π model.

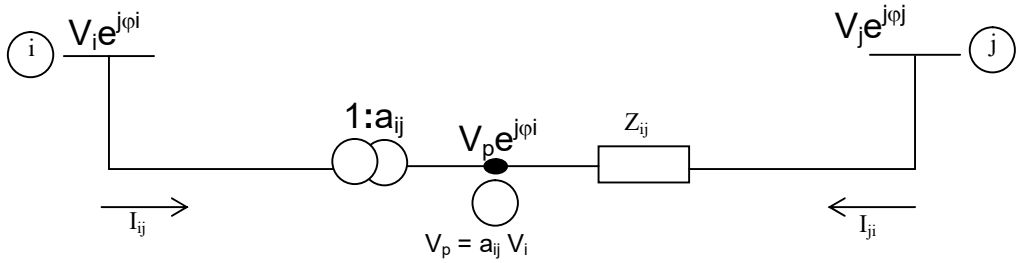

(a) In-phase transformer model

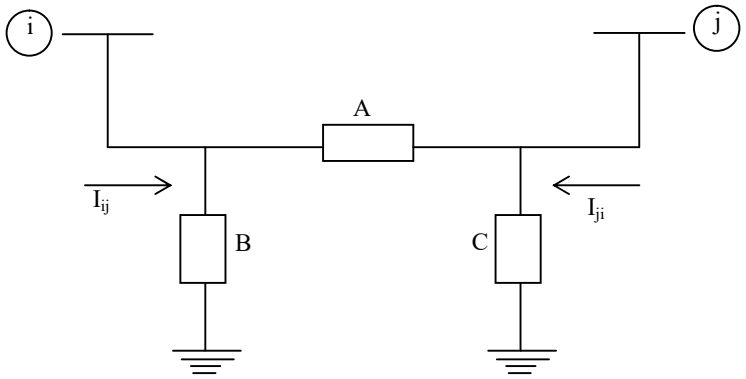

(b) In-phase transformer equivalent π model

Figure 3.13: In-phase transformer model and its equivalent π model.

From figure 3.13(a), the ideal voltage magnitude ratio is given as,

$$\frac{V_p}{V_i} = a_{ij}$$

And because $\theta_i = \theta_p$, therefore the ratio between the complex voltages at nodes i and p is given as,

$$\frac{E_p}{E_i} = \frac{V_p e^{j\theta p}}{V_i e^{j\theta i}} = a_{ij} \quad (3.95)$$

Since there are no losses in the ideal transformer (which is represented by the portion i-p of the transformer model), hence,

$$E_i I_{ij}^* - E_p I_{ji}^* - 0 \quad (3.96)$$

From equations (3.95) and (3.96), the current ratio gives,

$$\frac{I_{ij}^*}{I_{ji}^*} = -\frac{|I_{ij}|}{|I_{ji}|} = -a_{ij} \quad (3.97)$$

where , $I_{ij} = -I_{ji}$

Equation (3.97) shows that the complex currents I_{ij} and I_{ji} are out of phase by 180^o.

From figure 3.13(a), the current injection equations are given as,

$$I_{ij} = -a_{ij}y_{ij}(E_j - E_p) = (a_{ij}^2 y_{ij})E_i + (-a_{ij}y_{ij})E_j \quad (3.98)$$

$$I_{ji} = y_{ij}(E_j - E_p) = (-a_{ij}y_{ij})E_i + (y_{ij})E_j \quad (3.99)$$

From figure 3.13(b), the currents injection equations are given as,

$$I_{ij} = (A + B)E_i + (-A)E_j \quad (3.100)$$

$$I_{ji} = (-A)E_i + (A + C)E_j \quad (3.101)$$

Comparing equations (3.98), (3.99), and (3.100), (3.101),

Show that,

$$A = a_{ij}y_{ij}$$

$$B = a_{ij}(a_{ij} - 1)y_{ij}$$

$$C = (1 - a_{ij})y_{ij}$$

3.3.4 Phase Shifting Transformer Model

The phase-shifting transformers are used to control active power flows (Monticelli, 1999). The control variable is the phase angle, while the controlled variable is the active power flow in the branch where the shifter is placed. Figure 3.14 shows the phase-shifting transformer model.

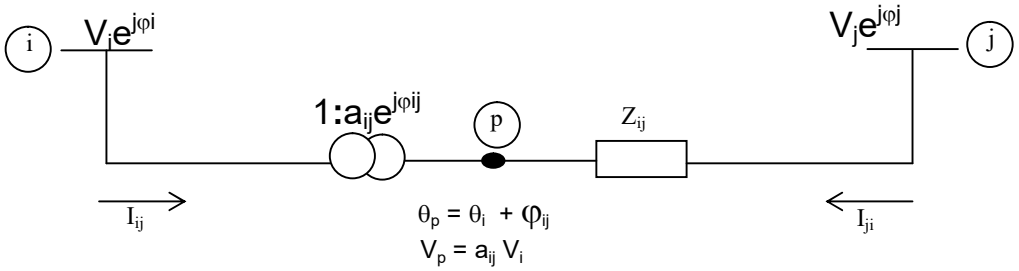

Figure3.14 Phase –shifting transformer model with ($t=ae^{j\varphi}$).

Phase-shifting transformer affects both phase and magnitudes of complex voltages E_i and E_p, without changing their ratio, in that,

$$\frac{E_p}{E_i} = t_{ij} = a_{ij}e^{j\varphi ij} \qquad (3.102)$$

From figure 3.14,

$$\theta_p = \theta_i + \varphi_{ij}$$

and,

$$V_p = a_{ij}V_i$$

Applying equations (1.95) and (1.101) gives,

$$\frac{I_{ij}}{I_{ji}} = -t_{ij}^* = -a_{ij}e^{-j\varphi ij} \qquad (3.103)$$

Expressing the complex currents I_{ij} and I_{ji} in terms complex voltages at the shifter terminal nodes gives,

$$I_{ij} = -t_{ij}^* y_{ij}(E_j - E_p) = (y_{ij})E_i + (-t_{ij}^* y_{ij})E_j \qquad (3.104)$$

$$I_{ji} = y_{ij}(E_j - E_p) = (-t_{ij}y_{ij})E_i + (y_{ij})E_j \quad (3.105)$$

The existence of nonzero phase shift in equation (3.104) and (3.105) make the determination of the A, B, and C parameters of the equivalent π model impossible since the coefficient $-t_{ij}^{*}y_{ij}$ of E_j in the I_{ij} equation differ from the coefficient $-t_{ij}y_{ij}$ of E_i in the I_{ji} equation (Monticelli, 1999).

3.3.5 The Unified Power Network Model

The dependence of the complex currents I_{ij} and I_{ji} equations on the side the tap is located for both transformers and shifters represent an asymmetrical arrangement. In the unified model, the unified complex current expressions are developed for lines, transformers and shifters irrespective of the side on which the tap is located, including a situation where there are taps on either sides of the model (Monticelli, 1999).

Figure 3.15 shows a transformer symmetrical model with shunt elements neglected.

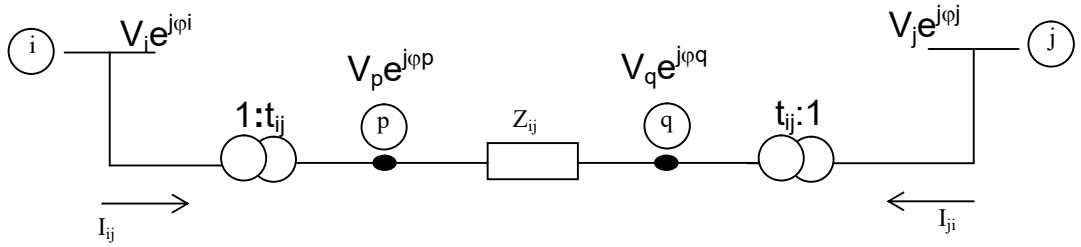

Figure 3.15: Transformer symmetrical model

Form figure 3.15,

$$I_{ij} = t_{ij}^{*}I_{pq} = t_{ij}^{*}(E_p - E_q)y_{ij} = t_{ij}^{*}(t_{ij}^{*}E_i - t_{ji}E_j)y_{ij} \quad (3.106)$$

$$I_{ji} = t_{ji}^{*}I_{qp} = t_{ji}^{*}(E_q - E_p)y_{ij} = t_{ji}^{*}(t_{ji}E_j - t_{ij}E_i)y_{ij} \quad (3.107)$$

Where,

$$t_{ij} = a_{ij}e^{j\varphi ij}$$

$$t_{ji} = a_{ji}e^{j\varphi ji}$$

Hence, equations (3.106) and (3.107) give,

$$I_{ij} = \left(a_{ij}^2 E_i - t_{ij}^* t_{ji} E_j\right) y_{ij} \quad (3.108)$$

$$I_{ji} = \left(a_{ji}^2 E_j - t_{ji}^* t_{ij} E_i\right) y_{ij} \quad (3.109)$$

Equations (3.108) and (3.109) are symmetrical because when i and j are interchanged as in the I_{ij}equation, it results to the I_{ji} equation and vice-versa.

Figure 3.16 shows a unified π model with appropriate definitions how π model of a transmission line as well as a phase-shifting transformer model can be derived.

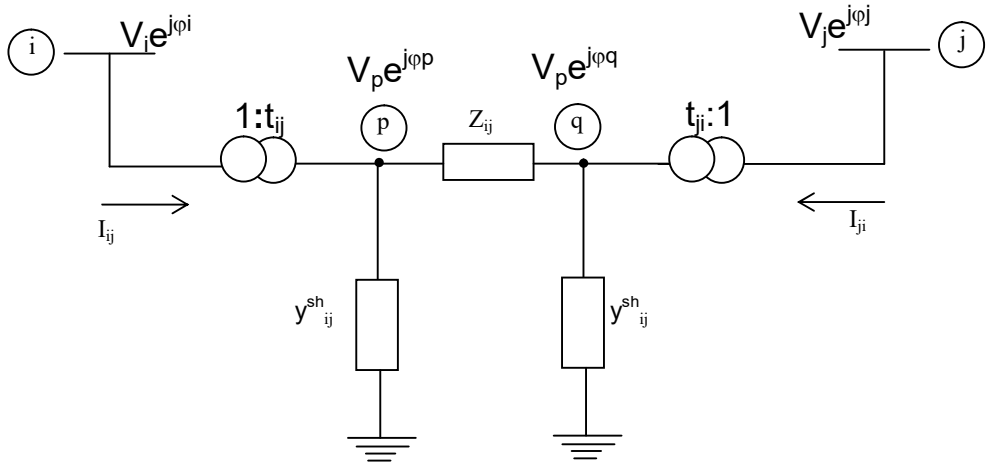

Figure 3.16: Unified πmodel

Transformation definitions / assumptions include,

i. If t_{ij} = t_{ji} = 1.0, the resulting equations become that of equivalent π model of a transmission line.

If the shunt elements are neglected, and t_{ij} = 1.0, and $t_{ji} = a_{ji}e^{j\varphi ji}$

ii. the resulting model becomes that of a phase-shifting transformer with tap located on the bus j side.

From figure 3.16, the general expressions for I_{ij} and I_{ji} are given as,

$$I_{ij} = \left(a_{ij}^2 E_i - t_{ij}^* t_{ji} E_j\right) y_{ij} + y_{ij}^{sh} a_{ij}^2 E_i \quad (3.110)$$

$$I_{ji} = \left(a_{ji}^2 E_j - t_{ji}^* t_{ij} E_i\right) y_{ij} + y_{ji}^{sh} a_{ji}^2 E_j \quad (3.111)$$

Active and Reactive power flows in transmission line, in-phase transformer and phase shifting transformer are derived as follows:-

i. **Transmission line**

The complex current I_{ij} in a transmission line is given by,

$$I_{ij} = y_{ij}\left(E_i - E_j\right) + jb_{ij}^{sh} E_i \quad (3.112)$$

The complex power flow $\left(S_{ij}^* = P_{ij} - Q_{ij}\right)$ gives,

$$S_{ij}^* - E_i^* I_{ij} - y_{ij} V_i e^{-j\theta i}\left(V_i e^{j\theta i} - V_j e^{j\theta j}\right) + jb_{ij}^{sh} V_i^2$$

$$= y_{ij} V_i e^{-j\theta i} V_i e^{j\theta i} - y_{ij} V_i e^{-j\theta i} V_j e^{j\theta j} + jb_{ij}^{sh} V_i^2$$

$$= y_{ij} V_i^2 e^{j(\theta_i - \theta_i)} - y_{ij} V_i V_j e^{-j\theta ij} + b_{ij}^{sh} V_i^2$$

$$= y_{ij} V_i^2 - y_{ij} V_i V_j \left(\cos\theta_{ij} - \mathrm{j}\sin\theta_{ij}\right) + b_{ij}^{sh} V_i^2$$

$$= y_{ij} V_i^2 - y_{ij} V_i V_j \cos\theta_{ij} + jy_{ij} V_i V_j \sin\theta_{ij} + jb_{ij}^{sh} V_i^2$$

but $y_{ij} = g_{ij} + jb_{ij}$

Therefore,

$$S_{ij}^* = E_i^* I_{ij} = \left(g_{ij} + jb_{ij}\right) V_i^2 - \left(g_{ij} + jb_{ij}\right) V_i V_j \cos\theta_{ij}$$

$$+ j\left(g_{ij} + jb_{ij}\right) V_i V_j \sin\theta_{ij} + jb_{ij}^{sh} V_i^2$$

$$= V_i^2 g_{ij} + jV_i^2 b_{ij} - V_i V_j g_{ij} \cos\theta_{ij} - jV_i V_j b_{ij} \cos\theta_{ij}$$

$$+jV_iV_jg_{ij}\sin\theta_{ij} - V_iV_jb_{ij}\sin\theta_{ij} + jb_{ij}^{sh}V_i^2$$

Separating real and reactive parts give,

$$P_{ij} = V_i^2 g_{ij} - V_iV_jg_{ij}\cos\theta_{ij} - V_iV_jb_{ij}\sin\theta_{ij} \quad (3.113)$$

$$Q_{ij} = -V_i^2\left(b_{ij} + b_{ij}^{sh}\right) + V_iV_jb_{ij}\cos\theta_{ij} - V_iV_jg_{ij}\sin\theta_{ij} \quad (3.114)$$

Similarly, the active and reactive power flowing in opposite direction are given as,

$$P_{ji} = V_j^2 g_{ij} - V_iV_jg_{ij}\cos\theta_{ij} + V_iV_jb_{ij}\sin\theta_{ij} \quad (3.115)$$

$$Q_{ji} = -V_j^2\left(b_{ij} + b_{ij}^{sh}\right) + V_iV_jb_{ij}\cos\theta_{ij} + V_iV_jg_{ij}\sin\theta_{ij} \quad (3.116)$$

The active and reactive power losses in the line are given as,

$$P_{ij} + P_{ji} = g_{ij}\left(V_i^2 + V_j^2 - 2V_iV_j\cos\theta_{ij}\right) = g_{ij}|E_i - E_j|^2 \quad (3.117)$$

$$\begin{aligned} Q_{ij} + Q_{ji} &= -b_{ij}^2\left(V_i^2 + V_j^2\right) - b_{ij}\left(V_i^2 + V_j^2 - 2V_iV_j\cos\theta_{ij}\right) \\ &= -b_{ij}^{sh}\left(V_i^2 + V_j^2\right) - b_{ij}|E_i - E_j|^2 \end{aligned} \quad (3.118)$$

where,

$|E_i - E_j|$ = the magnitude of the voltage drop across the line.

$g_{ij}|E_i - E_j|^2$ = the active power losses.

$-b_{ij}|E_i - E_j|^2$ = the reactive power losses.

$-b_{ij}^{sh}\left(V_i^2 + V_j^2\right)$ = the reactive power generated by the shunt elements of the equivalent π model with $b_{ij} < 0$ and $b^{sh}_{ij} > 0$ for realistic transmission line sections.

ii. **In-phase transformer**

The complex current I_{ij} in an in-phase transformer is given as,

$$I_{ij} = a_{ij}y_{ij}\left(a_{ij}E_i - E_j\right) \quad (3.119)$$

The conjugate complex power flow $\left(S_{ij}^* = P_{ij} - jQ_{ij}\right)$ is given as,

$$S_{ij}^{*} = E_i^{*} I_{ij} = y_{ij} a_{ij} V_i e^{-j\theta i}\left(a_{ij} V_i e^{j\theta i} - V_j e^{-j\theta j}\right) \quad (3.120)$$

$$= y_{ij} a_{ij}^2 V_i^2 e^{j(\theta_i - \theta_i)} - y_{ij} a_{ij} V_i V_j e^{-j\theta ij}$$

$$= y_{ij} a_{ij}^2 V_i^2 - y_{ij} a_{ij} V_i V_j \cos\theta_{ij} + j y_{ij} a_{ij} V_i V_j \sin\theta_{ij}$$

but $y_{ij} = g_{ij} + jb_{ij}$

Therefore,

$$S_{ij}^{*} = a_{ij}^2 V_i^2\left(g_{ij} + jb_{ij}\right) - a_{ij} V_i V_j\left(g_{ij} + jb_{ij}\right)\cos\theta_{ij}$$

$$+ j\left(g_{ij} + jb_{ij}\right) a_{ij} V_i V_j \sin\theta_{ij}$$

=

$$a_{ij}^2 V_i^2 g_{ij} + j a_{ij}^2 b_{ij} V_i^2 - a_{ij} V_i V_j g_{ij} \cos\theta_{ij} - j a_{ij} b_{ij} V_i V_j \cos\theta_{ij} + a_{ij} g_{ij} V_i V_j \sin\theta_{ij} - a_{ij} b_{ij} V_i V_j \sin\theta_{ij}$$

Separating the real and reactive parts give,

$$P_{ij} = \left(a_{ij} V_i\right)^2 g_{ij} - a_{ij} V_i V_j g_{ij} \cos\theta_{ij} - a_{ij} b_{ij} V_i V_j \sin\theta_{ij} \quad (3.121)$$

$$Q_{ij} = -\left(a_{ij} V_i\right)^2 b_{ij} + a_{ij}\, b_{ij} V_i V_j \cos\theta_{ij} - a_{ij} g_{ij} V_i V_j \sin\theta_{ij} \quad (3.122)$$

iii. **Phase-shifting transformer with $a_{ij} = 1$**

The complex current I_{ij} in phase-shifting transformer with $a_{ij} = 1$ is given as,

$$I_{ij} = y_{ij}\left(E_i - e^{\ j\varphi ij} E_j\right) = y_{ij} e^{\ j\varphi ij}\left(E_i e^{j\varphi ij} - E_j\right) \quad (3.123)$$

The conjugate complex power flow $S_{ij}^{*} = P_{ij} - jQ_{ij}$ is given as,

$$S_{ij}^{*} = E_i^{*} I_{ij} = y_{ij} V_i e^{-j(\theta_i + \varphi_{ij})}\left(V_i e^{j(\theta_i + \varphi_{ij})} - V_j e^{j\theta j}\right) \quad (3.124)$$

$$= y_{ij} V_i^2 e^{j[(\theta_i + \varphi_{ij}) - (\theta_i + \varphi_{ij})]} - y_{ij} V_i V_j e^{-j(\theta_{ij} + \varphi ij)}$$

$$= y_{ij}V_i^2 - y_{ij}V_iV_j[\cos(\theta_{ij} + \varphi_{ij}) - j\sin(\theta_{ij} + \varphi_{ij})]$$

$$= y_{ij}V_i^2 - y_{ij}V_{ij}V_{ij}\cos(\theta_{ij} + \varphi_{ij}) + y_{ij}V_iV_j\sin(\theta_{ij} + \varphi_{ij})$$

but $y_{ij} = g_{ij} + jb_{ij}$

Therefore,

$$S_{ij}^* - E_i^* I_{ij} - V_i^2(g_{ij} + jb_{ij}) - V_iV_j(g_{ij} + jb_{ij})\cos(\theta_{ij} + \varphi_{ij})$$

$$+jV_iV_j(g_{ij} + jb_{ij})\sin(\theta_{ij} + \varphi_{ij})$$

$$= V_i^2 g_{ij} + jV_i^2 b_{ij} - V_iV_j g_{ij}\cos(\theta_{ij} + \varphi_{ij}) - jV_iV_j b_{ij}\cos(\theta_{ij} + \varphi_{ij})$$

$$+V_iV_j g_{ij}\sin(\theta_{ij} + \varphi_{ij}) - V_iV_j b_{ij}\sin(\theta_{ij} + \varphi_{ij})$$

Separating the real and reactive parts give,

$$P_{ij} = V_i^2 g_{ij} - V_iV_j g_{ij}\cos(\theta_{ij} + \varphi_{ij}) - V_iV_j b_{ij}\sin(\theta_{ij} - \varphi_{ij}) \qquad (3.125)$$

$$Q_{ij} = V_i^2 b_{ij} + V_iV_j b_{ij}\cos(\theta_{ij} + \varphi_{ij}) - V_iV_j g_{ij}\sin(\theta_{ij} + \varphi_{ij}) \qquad (3.126)$$

3.3.6 The Unified Power Flow Equation

The active and reactive power for unified power flow equations are given as,

$$P_{ij} - (a_{ij}V_i)^2 g_{ij} - (a_{ij}V_i)(a_{ij}V_j)g_{ij}\cos(\theta_{ij} + \varphi_{ij} - \varphi_{ji})$$
$$-(a_{ij}V_i)(a_{ji}V_j)b_{ij}\sin(\theta_{ij} + \varphi_{ij} - \varphi_{ji}) \qquad (3.127)$$

$$Q_{ij} = (a_{ij}V_i)^2(b_{ij} + b_{ij}^{sh}) + (a_{ij}V_i)(a_{ji}V_j)b_{ij}\cos(\theta_{ij} + \varphi_{ij} - \varphi_{ji})$$

$$-(a_{ij}V_i)(a_{ji}V_j)g_{ij}\sin(\theta_{ij} + \varphi_{ij} - \varphi_{ji}) \qquad (3.128)$$

The following substitutions are made for transmission lines, in-phase transformers and phase-shifting transformers respectively in equations (3.127) and (3.128):

(a) For transmission lines,

$a_{ij} = a_{ji} = 1$, and $\varphi_{ij} = \varphi_{ji} = 0$

(b) For in-phase transformers,

$y^{sh}_{ij} = y^{sh}_{ji} = 0$, $a_{ji} = 1$, and $\varphi_{ij} = \varphi_{ji} = 0$

(c) For a phase-shifting transformers,

$y^{sh}_{ij} = y^{sh}_{ji} = 0$, $a_{ij} = 1$, and $\varphi_{ji} = 0$

3.3.7 Substation Controls

These include load – break switches, circuit breakers etc.

3.3.7.1 Load – Break Switches

These switches are designed to interrupt load level current, but not the much larger fault currents. They are not designed to interrupt fault currents, but are suitable for closing on to short – circuit.

3.3.7.2 Circuit Breakers

These are switches designed to interrupt fault currents. The circuit breaker is a mechanical device for breaking and reclosing a circuit under all conditions including when the system is faulted and currents are at their greatest values. When electrical contacts are parted, the formation arc results, and the function breaker is to extinguish this arc formed in the process as quickly as possible. The classification of circuit breaker is therefore based on the medium where the arc is interrupted. These include air blast breakers, oil circuit breakers sulfur hexafluoride,$SF_{6,}$ and vacuum circuit breakers.

Breakers are usually designed to recover their dielectric strength faster than the voltage stress across their open contacts can build up (Davies, 1984).

3.4 Power System Protection

Protection scheme is the science, skill and art of applying and setting relays and fuses to provide maximum sensitivity to faults and undesirable conditions but to avoid their operations on all tolerable conditions (Davies, 1984). The two basic principles of power system protection include unit protection and Non – unit protection. Unit protection schemes operate on the principle of discrimination by comparison. This is because they protect only the unit with which they are associated and do not provide the back up protection which all discrimination by time schemes provide. In unit protection, each component of the power system is uniquely protected independent of the other parts, for instance generator protection, Transformer protection, bus-bar protection etc. For non – unit protection scheme, several relays and associated equipment are used to provide protection covering more than one zone. Example of non – unit protection include over current, earth fault, distance protection etc.

3.4.1 Generator Protection

Synchronous generators are usually protected against various forms of faults such as loss of excitation, loss of synchronism, real power flow reversal and generator over speed etc.

(a) Loss of excitation

Synchronous generators are normally over excited so as to deliver reactive power, Q to the power network.

The loss of generator excitation leads to reactive power, Q, flow reversal, drop in voltage, and impedance transition from basically resistive to

capacitive. The loss of excitation could lead to system instability. The protection can be implemented via a relay scheme sensitive to impedance, and voltage drop.

b) **Loss of synchronism**

Generators are usually protected against loss of Synchronism indirectly by over speed protection associated with the prime mover. Over frequency relays can also be used.

c) **Reverse flow of real power**

It is quite undesirable to permit real power flow in generators to reverse. The effect can be hazardous to the generator prime mover. This can be prevented through directional relay unit which detects the real power reversal.

d) **Generator over speed.**

Generator over speed protection is provided by the prime mover governor. Back up protection may be provided via an over frequency relay set to respond to about 5% over speed. The protection scheme's response to this type of generator fault is to trip the generator off line and shut the prime mover.

3.4.2 Line Protection

The transmission line is usually spread over a significant geographical area, and hence it is exposed to a variety of hazards. Causes of line faults include lightning, wind, birds, airplanes, automobiles etc.

The essential consideration for line protection is proper coordination between circuit breakers and relays. Proper coordination implies that relays will operate in a sequence such that service is minimally interrupted when clearing a fault. Typical line protection schemes include over current directional relays and impedance (distance) relays protection.

a) **Over current protection for radial lines**

This scheme is usually implemented for medium voltage systems using time delay over current technique. The application is feasible where fault currents are much greater than load currents.

b) **Directional Relays protection for complex system**

In a complex system, time delay coordination of over current relays become complicated and in some instance impossible to implement. Under such circumstances, the use of directional relays becomes imperative. In this case, the relay responds to fault in a particular direction thereby making implementation of proper coordination feasible.

c) **Impedance (Distance) Relays**

When it becomes impossible to use directional relay for line protection due to the possibility of multiple relay operations occasioned by a fault at a particular location, the impedance relays can be deployed to respond to impedance rather than voltage or current. This scheme is based on the fact that line impedance is directly proportional to the distance from the sending end; hence a fault halfway down the line could have half the line impedance. The 'reach' of a distance relay refers to how far down the line relay will respond to faults. A reach of 100% implies that the relay is set to detect faults at any point down to the far end.

3.5 National Grid Data

The National grid under review comprises of existing and proposed 330KV Network, and the grid data are made up of generators data and transmission lines data.

3.5.1 Generator Data

The Generator data for the existing and proposed 330KV national grid systems are given in tables 3.1 and 3.2 respectively.

Table 3.1 Generator data for existing 330KV National Grid (TCN, 2003)

Generator Name	Bus No	R_a (pu)	X'_d (pu)	H (sec)	D	X_d (pu)	T'_{do}
Egbin	1	0	0.437	18.54	0.0764	0.3117	7.1
Delta iv	2	0	0.417	53.46	0.105	0.3617	8.8
Kainji	3	0	0.0329	26.28	0.1273	0.0935	5.9
Shiroro	4	0	0.075	12.96	0.2546	0.2	5.57
Sapele	5	0	0.039	34.2	0.0097	0.36	8.6
Jebba	6	0	0.0433	20.34	0.0955	0.1083	5.2
Afam iv	7	0	0.0417	54.06	0.0098	0.3617	8.8
Okpai	8	0	0.0833	18	0.0044	0.843	0.99

Table 3.2 Generators data for proposed 330KV National Grid (TCN, 2003)

Generator Name	Bus No	R_a (pu)	X'_d (pu)	H (sec)	D	X_d (pu)	T'_{do}
Egbin	1	0	0.437	18.54	0.0764	0.3117	7.1
Delta iv	2	0	0.417	53.46	0.105	0.3617	8.8
Kainji	3	0	0.0329	26.28	0.1273	0.0935	5.9
Shiroro	4	0	0.075	12.96	0.2546	0.2	5.57
Sapele	5	0	0.039	34.2	0.0097	0.36	8.6
Jebba	6	0	0.0433	20.34	0.0955	0.1083	5.2
Afam iv	7	0	0.0417	36	0.0098	0.3832	8.8
Okpai	8	0	0.0833	18	0.0044	0.843	0.99
Alaoji	9	0	0.0578	5.48	0.0075	0.455	1.29
Papalanto	10	0	0.0289	32	0.0117	0.25	0.7
Omotosho	11	0	0.0289	32	0.0125	0.2975	0.574
Geregu	12	0	0.077	4.11	0	0.61	1.29
Calabar	13	0	0.0462	6.85	0.0094	0.364	1.29

Omoku	14	0	0.1155	2.74	0.0038	0.91	1.29
Egbema	15	0	0.007	4.11	0.0056	0.6067	1.29
Eyaen	16	0	0.0578	5.48	0.0075	0.455	1.29

3.5.2 Transmission Line Data

Tables 3.3 and 3.4 show the transmission lines data for existing and proposed 330KV National grid systems.

Table 3.3 Existing National grid transmission lines data (TCN, 2003)

Line Name		Bus Number		Line Type / Length (km)	R(pu)	X(pu)	B/2(pu)	Tap Ratio
From	To	From	To					
Egbin	Ikeja West	1	16	DC (62)	0.0011	0.0086	0.2574	1
Egbin	Aja	1	15	DC(16)	0.0003	0.0019	0.0581	1
Delta	Benin	2	13	SC(107)	0.0042	0.0316	0.2102	1
Delta	Aladja	2	14	SC(17)	0.0009	0.0072	0.1079	1
Kainji	Jebba T_s	3	20	SC/SC(81)	0.0015	0.0113	0.3363	1
Shiroro	Katampe	4	21	DC(144)	0.0025	0.0195	0.3221	1
Shiroro	Kaduna	4	23	SC/SC(96)	0.0017	0.0132	0.3944	1
Sapele	Benin	5	13	DC(50)	0.0009	0.007	0.2078	1
Sapele	Aladja	5	14	SC(63)	0.0025	0.0186	0.1237	1
Jebba	Jebba T_s	6	20	DC(8)	0.0001	0.0007	0.0208	1
Afam	Alaoji	7	9	DC(25)	0.0006	0.0043	0.1278	1
Okpai	Ontisha	8	10	DC(80)	0.0005	0.0042	0.1245	1
Alaoji	Ontisha	9	10	SC(138)	0.0054	0.00408	0.2711	1
Ontisha	New haven	10	11	SC(96)	0.0038	0.0284	0.1886	1
Ontisha	Benin	10	13	SC/SC(137)	0.0054	0.0405	0.2691	1
Ajaokuta	Benin	12	13	SC/SC(195)	0.0035	0.0271	0.8095	1
Benin	Ikeja West	13	16	DC(280)	0.0051	0.0039	1.1624	1
Benin	Oshgbo	13	18	SC(251)	0.0099	0.0742	0.4932	1
Ikeja West	Akangba	16	17	DC(17)	0.0004	0.0027	0.0707	1
Ikeja West	Oshogbo	16	18	SC(256)	0.0099	0.0745	0.495	1
Ikeja West	Ayede	16	19	SC/SC(137)	0.0054	0.0405	0.2691	1

Oshogbo	Ayede	18	19	SC(119)	0.0045	0.0345	0.2259	1
Oshogbo	Jebba T_s	18	20	SC/SC/SC(157)	0.002	0.0154	0.9192	1
Kaduna	Jos	23	25	SC(197)	0.0081	0.0609	0.4046	1
Kaduna	Kano	23	24	SC(230)	0.009	0.068	0.4518	1
Jos	Gombe	25	26	SC(265)	0.0118	0.0887	0.5893	1

Table 3.4 Proposed National grid transmission lines data (TCN, 2003)

Line Name		Bus Number		Line Type / Length (km)	R(pu)	X(pu)	B/2(pu)	Tap Ratio
From	To	From	To					
Egbin	Aja	1	33	DC(14)	0.0007	0.0057	0.771	1
Egbin	Erukan	1	35	SC(42)	0.004	0.00304	0.171	1
Egbin	Ikeja West	1	36	DC(62)	0.0004	0.0029	0.771	1
Delta	Benin	2	31	SC(107)	0.0008	0.0063	0.3585	1
Delta	Aladja	2	32	SC(32)	0.0008	0.0063	0.3585	1
Delta	Aja	2	33	SC(275)	0.0036	0.269	1.6089	1
Kainji	Jebba T_s	3	44	DC(81)	0.000097	0.0082	0.924	1
Kainji	Birnin Kebbi	3	48	SC(310)	0.004151	0.03041	1.8135	1
Shiroro	Katempe	4	23	DC(144)	0.0009	0.0067	1.7933	1
Shiroro	Jebba T_s	4	44	SC/SC(244)	0.0022	0.0234	1.3905	1
Shiroro	Kaduna	4	45	SC/SC(96)	0.0011	0.0097	0.546	1
Sapele	Benin	5	31	SC/DC(50)	0.0002	0.0015	0.936	1
Sapele	Aladja	5	32	SC(63)	0.0008	0.00063	0.3585	1
Jebba GS	Jebba TS	6	44	DC (8)	0.0001	0.0004	0.096	1
Afam	Alaoji	7	9	DC(25)	0.0015	0.0012	0.312	1
Afam	Ikot Ekpene	7	28	DC(90)	0.0054	0.0042	1.1208	1
Okpai	Onitsha	8	29	DC (80)	0.0015	0.0012	0.312	1
Alaoji	Onitsha	9	29	SC(138)	0.0163	0.014	0.786	1
Alaoji	Owerri	9	30	DC (60)	0.0004	0.0028	0.7472	1
Papalanto	Ikeja west	10	36	SC (30)	0.0004	0.003	0.171	1
Papalanto	Ayede	10	39	SC (60)	0.0007	0.0061	0.3421	1
Omotosho	Benin	11	31	SC(120)	0.0014	0.0122	0.6841	1
Omotosho	Ikeja west	11	36	SC(160)	0.0019	0.0162	0.91222	1

Geregu	Ajaokuta	12	40	DC (5)	0.00001	0.0005	0.057	1
Calabar	IkotEkpene	13	28	DC (72)	0.0004	0.0033	0.8967	1
Omoku	Egbema	14	15	DC(30)	0.0002	0.0014	0.3736	1
Egbema	Owerri	15	30	DC(30)	0.0002	0.0014	0.3736	1
Eyaen	Benin	16	31	DC(5)	0.0001	0.0002	0.0623	1
Damaturu	Maiduguri	17	18	SC (308)	0.004	0.0302	1.8018	1
Damturu	Gombe	17	19	SC(30)	0.0004	0.0029	0.1695	1
Gombe	Yola	19	20	SC(217)	0.003	0.022	1.2371	1
Gombe	Jos	19	22	SC(265)	0.0032	0.027	1.515	1
Yola	Jalingo	20	21	SC(132)	0.0016	0.0134	0.7525	1
Jos	Gwagwa	22	24	DC (180)	0.0013	0.0099	2.3517	1
Jos	Makurdi	22	25	DC(230)	0.0017	0.0126	3.0069	1
Katempe	Gwagwa	23	24	DC (30)	0.0018	0.0014	0.3736	
Gwagwa	Makurdi	24	25	DC (201)	0.0014	0.0107	2.8644	1
Gwagwa	Lokoja	24	42	DC (140)	0.0008	0.0065	1.7435	1
Makurdi	Aliade	25	26	DC (50)	0.0003	0.0023	0.6227	1
Aliade	New haven	26	27	DC (150)	0.0009	0.007	1.8681	1
Newhaven	Ikotekpene	27	28	DC143)	0.0005	0.0033	3.5618	1
New Haven	Onitsha	27	29	DC (96)	0.0011	0.0097	0.5475	1
Onitsha	Owerri	29	30	DC (137)	0.0008	0.0064	1.7062	1
Onitsha	Benin	29	31	DC (137)	0.0016	0.0139	1.781	1
Benin	Ajaokuta	31	40	SC(195)	0.0023	0.0198	0.748	1
Benin	Oshogbo	31	41	SC(251)	0.003	0.0254	1.431	1
Aja	Alagbon	33	34	DC(26)	0.0002	0.0012	0.3238	1
Erukan	Ikeja west	35	36	SC(32)	0.0004	0.0032	0.1824	1
Ikeja west	Akangba	36	37	SC/SC(18)	0.0007	0.0057	0.3855	1
Ikeja West	Sekete	36	38	SC (70)	0.00084	0.00709	0.3991	1
Ajaokuta	Lokoja	40	42	DC (38)	0.0002	0.0018	0.4732	1
Oshogbo	Ilorin	41	43	SC (90)	0.0012	0.0088	0.5265	1
Oshogbo	Jebba Ts	41	44	SC/SC(157)	0.0019	0.00159	0.8955	1
Ilorin	Jebba Ts	43	44	SC (84)	0.0011	0.0083	0.4914	1
Kaduna	Zaria	45	46	SC(81)	0.0011	0.0079	0.4722	1

Kaduna	Kano	45	47	SC(230)	0.0027	0.0233	1.311	1
Zaria	Kano	46	47	SC(147)	0.0019	0.0144	0.8307	1

3.6 Theory of Power Flow and Stability Computations

3.6.1 Single Machine to Infinite Bus System

A single machine to infinite bus system is used here to explain the following scenarios in the power system network:

a. A fault cleared without altering pre-fault network configuration

b. The influence of actual clearing time t_f and critical clearing time t_{cr} in system stability

c. Effect of pre-fault load condition and fault distance on critical clearing time and generator stability.

Figure 3.17 Shows machine to infinite bus schematic diagram inter-linked via double transmission lines with fault occurring in line 2.

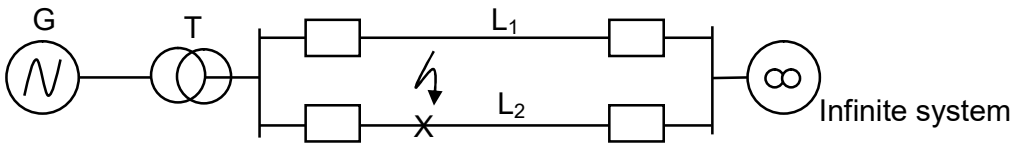

Figure 3.17 Machine to infinite bus system schematic

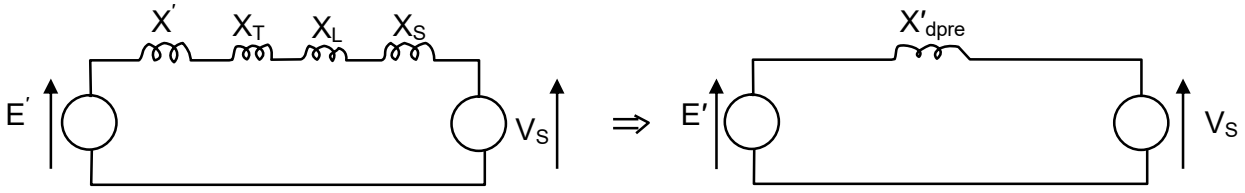

(b) Equivalent circuit for pre-and post-faults states.

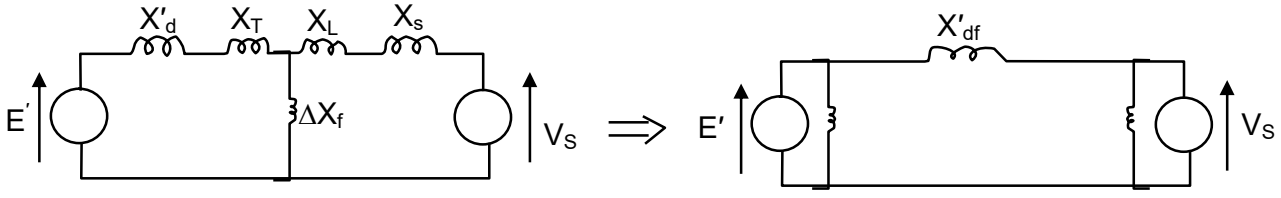

(c) Fault-on equivalent circuit

Figure 3.18 Equivalent circuits for machine to infinite bus system

The prefault equivalent reactance of the power system is given as,

$$X'_{dpre} = X'_d + X_T + X_L + X_S \quad (3.129)$$

The fault-on equivalent reactance of the system is given as

$$X'_{df} = X'_d + X_T + X_L + X_S + \frac{(x'_d + X_T)(X_L + X_S)}{\Delta X_f} \quad (3.130)$$

From equation (3.130), it can be observed that X'_{df} is largely dependent on the value of the fault shunt reactance ΔX_f.

When the fault is cleared by opening the circuit-breaker in line L_2, the equivalent circuit becomes the same again as pre-fault period, hence, X'_{dpost}= X'_{dpre}.

The effect of a three-phase fault on the power network is explained using the principle of equal area criterion as shown in figure 3.19.

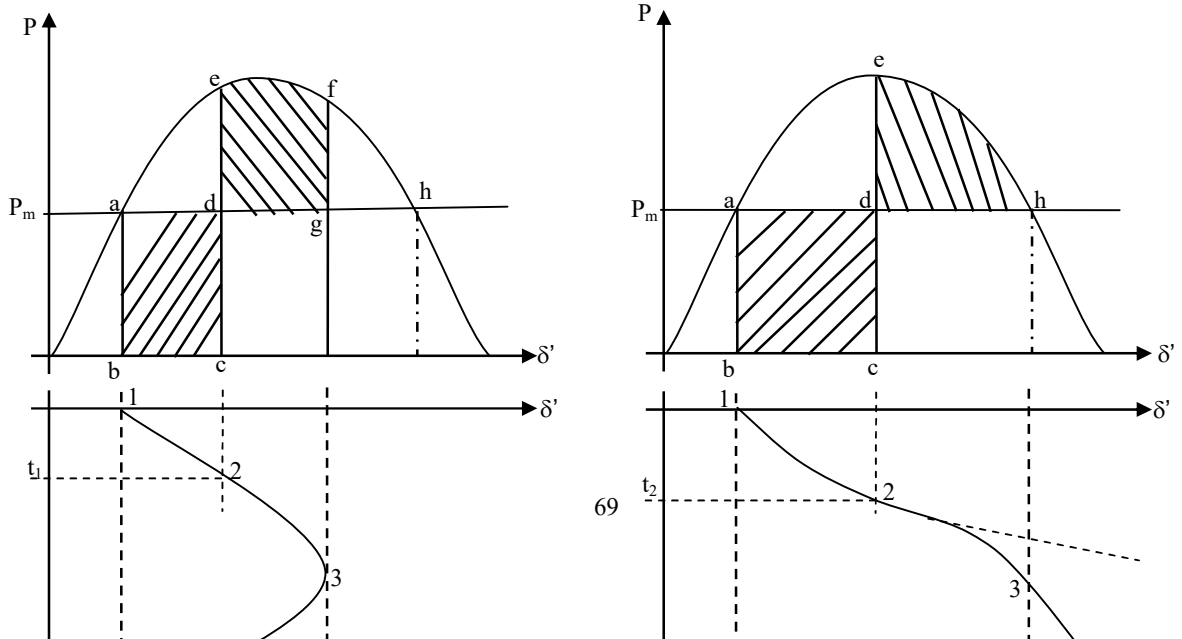

Figure 3.19: Machine energy changes after a disturbance

The following assumptions are made:

1. The effect of damper is neglected
2. The rotor speed deviation is too small for the governor's system response, hence the input power P_m from the turbine is assumed constant.

When a three-phase fault occurs in the system, ΔX_f becomes zero, and from equation (3.130), the transient reactance at fault becomes infinity. Thus, the power transfer from the generation to the system is completely blocked by the fault. At fault-on, the electrical power P_e drops from its pre-fault value to zero as indicated by line a-b in figure3.19, and remains at zero until the fault is cleared through opening of the line circuit breaker. The expression describing the rotor dynamics is given as,

$$M \frac{d^2\delta'}{dt^2} = P_m - P_e - P_D \qquad (3.131)$$

During fault period, the rotor acceleration α is obtained by substituting $P_e = 0$, $P_D = 0$ and dividing equation (3.131) by M.

$$\alpha = \frac{d^2\delta'}{dt^2} = \frac{P_m}{M} = \text{constant} \qquad (3.132)$$

Integrating equation (3.132) twice with the initial conditions $\delta'(t=0)$, and $\Delta\omega(t=0)$, gives the power angle trajectory as:

$$\delta' = \delta'_0 + \frac{\alpha t^2}{2}$$

or $$\Delta\delta' = \delta' - \delta_0 = \frac{\alpha t^2}{} \qquad (3.133)$$

2

Equation (3.133) corresponds to the curve 1-2-3- in figure 3.19(a).

Prior to the fault clearing, the rotor moves from point b to c on the power angle curve, and acquires a kinetic energy proportional to the hatched area abcd. When the fault is cleared by opening the circuit beaker, rotor again moves from point c to e on the power angle curve, following the path corresponding to the reactance given by equation (3.129). At point *e*, the rotor experiences a deceleration torque of magnitude proportional to the length of line *d-e*, and thus starts to decelerate. But because of its momentum, its angle continues to increase until the work done during deceleration area *defg*, equals the kinetic energy acquired during acceleration area abcd. The rotor again attains synchronous speed at point *f* when,

Acceleration area (*abcd)* = Deceleration area (*defg*) (3.134)

In the absence of damping, the cycle repeats and the rotor continues to undergo synchronous swings around point *a*. Under this condition, the system is stable and the generator does not lose synchronism.

Figure 3.19(b) presents similar situation but with longer fault clearing time t = t_2, where the kinetic energy acquired during rotor acceleration (proportional to the area abcd) is longer than that in figure 3.19(a). Consequently, the work done during deceleration (proportional to the area *deh*) is not sufficient to absorb the kinetic energy acquired during acceleration, hence the net rotor speed deviation does not become zero prior to the rotor reaching point *h*. Beyond point *h*, the electrical power $P_e(\delta')$ becomes less than the mechanical power P_m, and the rotor further experiences net acceleration torque resulting to increase in its angle. At point 3 in figure 3.19(b), the rotor makes an asynchronous rotation and loses synchronism with the system.

From the above illustrations, the stability margins can be established by exploring to equal area concept and fault clearing time concept (Machowski et al., 1997).

In the first case, the corresponding transient stability condition stipulates that the available deceleration area must be larger than the acceleration area forced by the fault.

Fom figure 3.19(a), the criterion demands that,

Area (deh) > Area (abcd) (3.135)

But since the generator did not use up the whole available deceleration area, the left over area (*fgh*), divided by the entire available deceleration area, gives the transient stability margin based on Area concept as,

$$K_{Area} = \frac{Area(fgh)}{Area(deh)} \quad (3.136)$$

Also, the fault clearing time being another major factor in determining the stability of the generator as can be deduced from equation (3.133), where the acceleration area (*abcd*) is observed to be proportional to the square of the fault clearing time. The critical clearing time is thus defined as the largest clearing time for which the generator will remain in synchronism. Exploring the relative difference between the critical clearing time and the actual fault clearing time to establish another measure of the transient stability margin as;

$$K_{time} = \frac{t_{cr} - t_f}{t_{cr}} \quad (3.137)$$

Effect of pre-fault load and influence of fault distance: The pre-fault load is an important factor with regards to determining the critical clearing time and generator stability. The higher the pre-fault load, the lower the critical clearing time (Machowski et al., 1997). By increasing the pre-fault load, acceleration power P_a increases by the same proportion resulting to same margin power angle $\Delta\delta'$ increase. The impedance of the faulted line Δx_L is

proportional to the fault distance; and the per-unit length reactance of the line.

Figure 3.20 illustrates the effect of fault distance on the critical clearing time.

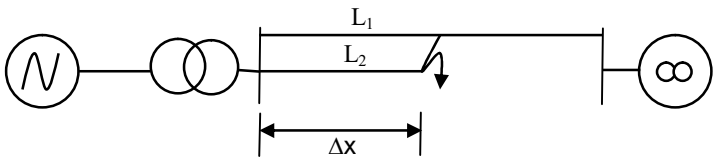

(a) Machine to infinite bus system

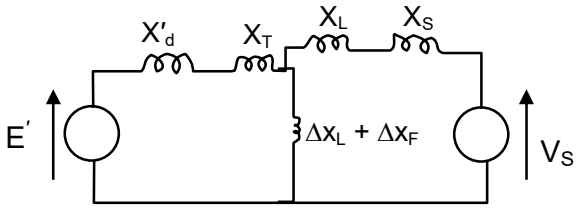

(b) Equivalent circuit diagram

Figure 3.20 Influence of the fault distance in machine to infinite bus system.

For the case of unbalanced fault, $\Delta x_f \neq 0$, the further the distance to the fault the less severe the fault and the longer the critical clear time. From equation (3.130), Δx_f is replaced by $\Delta x = \Delta x_F + \Delta x_L$.

Figure 3.21 shows the effect of various fault modes on the power angle characteristics curve. These faults in the order of decreasing severity include: (i) a three – phase fault (3ph); (ii) a phase – to – phase – to – ground faults (2ph-g); (iii) a phase – to – phase fault (2ph); (iv) a single – phase fault (1ph).

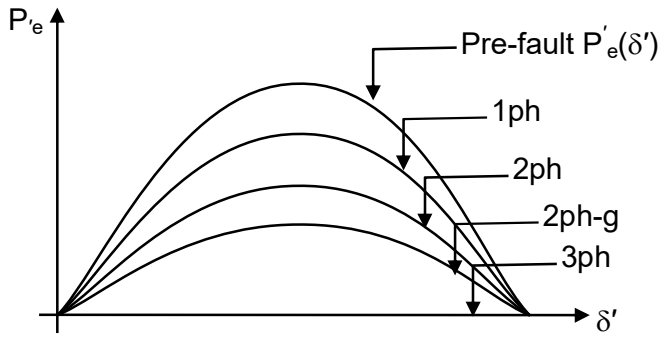

Figure 3.21 Effect of faults on power angle characteristics (curves).

3.6.2 Method of Solutions of Power Flow Problems

Power flow equations consist of a set of algebraic nonlinear equations, having larger number of unknowns than the number of equations. The solution to nonlinear problems involve linearization, that is, specifying some variables and setting some equal to zero to make the number of unknown variables equal the number of equations.

Each power system busbar is associated with four variables which include voltage magnitude |V|, voltage angle δ, net active power P, and net reactive power Q.

The power system buses are therefore classified based on the known / specified variables as follows:

(i) **PQ bus (or Load bus):** In this bus, the active power P and reactive power Q are specified, while both the voltage magnitude |V|, and angle δ are calculated.

(ii) **PV bus (or Generator bus):** In this bus, the active power P and voltage magnitude |V| are specified, while the reactive power Q and voltage angle δ are calculated.

(iii) **Reference bus (or Slack bus):** In this bus, both the voltage magnitude |V| and angle δ are specified, while the active power P and reactive power Q are calculated.

This bus serves as voltage angle reference and to balance generation, load and losses, since active power losses are unknown apriori.

3.6.3 Power Flow Eqaution

Figure 3.22 shows a generic bus with positive sign conventions for currents and power flows.

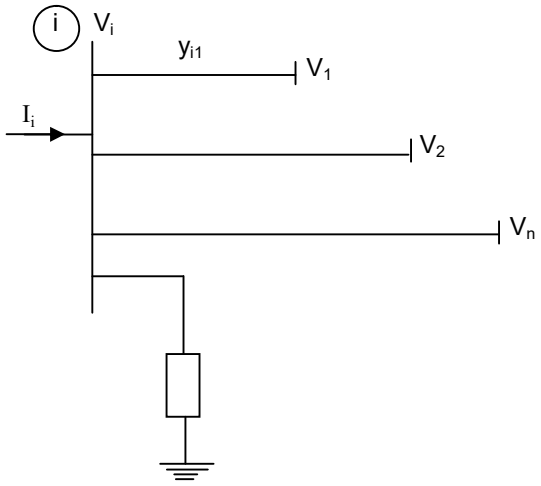

Figure 3.22 Generic power network.

By applying the Kirchhoff's current law, the current entering the i^{th} bus of an n-bus system shown in figure 3.22 is given by,

$$I_{ij} = y_{i0}V_i + y_{i1}(V_i - V_1) + y_{i2}(V_i - V_2) + \ldots + y_{in}(V_i - V_n)$$
$$= (y_{io} + y_{i1} + y_{i2} + \ldots + y_{in})V_i - y_{i1}V_1 - y_{i2}V_2 \ldots.$$
$$- y_{in}V_n \qquad (3.138)$$

$$I_i = V_i \sum_{j=1}^{n} y_{ij} - \sum_{j=1}^{n} y_{ij} V_j \quad for\ j \neq i \qquad (3.139)$$

The conjugate apparent power injection at bus *i* gives,

$$S_i^* = P_i - jQ_i = V_i^* I_i \qquad (3.140)$$

OR

$$I_i = \frac{P_i - jQ_i}{V_i^*} \qquad (3.141)$$

Substituting equation (3.141) into (3.139) gives,

$$\frac{P_i - jQ_i}{V_i^*} = V_i \sum_{j=1}^{n} y_{ij} - \sum_{j=1}^{n} y_{ij} V_{\substack{j \\ for\ j \neq i}} \quad (3.142)$$

Equation (3.141) constitutes a set of nonlinear algebraic equations which can be solved by iterative method. The iterative methods considered in this text include Gauss-Seidel method and Newton-Raphson method.

3.6.4 Gauss-Seidel Method.

Applying Gauss-Seidel iterative techniques to solve for V_i for equation (3.141) gives,

$$V_i^{(k+1)} = \frac{\frac{P_i^{sp} - jQ_i^{sp} + \sum y_{ij} V_j^{(k)}}{V_i^{*(k)}}}{\substack{\sum y_{ij} \\ for\ j \neq i}} \quad (3.143)$$

where,

y_{ij} = the actual admittance in per unit

P_i^{sp} = the specified net active power in power unit

Q_i^{sp} = the specified net reactive power in per unit.

From equation (3.143), the active and reactive power can be expressed as,

$$P_i^{(k+1)} = Real\left\{V_i^{*(k)} \left[V_i^{(k)} \sum_{j=0}^{n} y_{ij} - \sum_{\substack{j=1 \\ for\ j \neq 1}}^{n} y_{ij} V_j^{(k)}\right]\right. \quad (3.144)$$

$$Q_i^{(k+1)} = Img\left\{V_i^{*(k)} \left[V_i^{(k)} \sum_{j=0}^{n} y_{ij} - \sum_{\substack{j=1 \\ for\ j \neq 1}}^{n} y_{ij} V_j^{(k)}\right]\right. \quad (3.145)$$

Expressing the power flow equation in terms of the elements of the bus admittance matrix Y_{bus} by substituting $Y_{ij} = -y_{ij}$ and $Y_{ii} = \sum y_{ij}$ in the equations (3.143), (3.144) and (3.145), give,

$$V_i^{(k+1)} = \frac{P_i^{sp} - jQ_i^{sp}}{V_i^{*(k)}} - \sum_{j\neq 1} Y_{ij}\, V_{ij}^{(k)} \quad (3.146)$$

$$P_i^{(k+1)} = Real\left\{V_i^{*(k)} \left[V_i^{(k)} Y_{ii} + \sum^{n}_{\substack{j=1 \\ for\ j\neq 1}} Y_{ij}\, V_j^{(k)}\right]\right. \quad (3.147)$$

$$Q_i^{(k+1)} = Img\left\{V_i^{*(k)} \left[V_i^{(k)} Y_{ii} + \sum^{n}_{\substack{j=1 \\ for\ j\neq 1}} y_{ij}\, V_j^{(k)}\right]\right. \quad (3.148)$$

Where,

$Y_{ij} = -y_{ij}$ = the off-diagonal elements of the bus admittance matrix.

$Y_{ii} = \sum y_{ij}$ = the diagonal elements, including the admittance to ground of line charging susceptance and any other admittance to ground.

For an n-bus system, a total of 2(n-1) equations are required to be solved iteratively.

Solution procedures are as follows:

For PQ buses, the active and reactive powers are known (P_i^{sp}, Q_i^{sp}). Solve for real and imaginary components of voltage using equation (3.146).

For PV buses, P_i^{sp} and $|V_i|$ are specified, hence solve for $Q_i^{(k+1)}$ using equation (3.148), then substitute the result into equation (3.146) to solve for $V_i^{(k+1)}$. Since in this bus $|V_i|$ is specified, and only the imaginary part of $V_i^{(k+1)}$ is retained, and its real part is selected such that equation (3.149) is satisfied.

$$\left(e_i^{(k+1)}\right)^2 + \left(f_i^{(k+1)}\right)^2 = |V_i|^2 \quad (3.149)$$

OR

$$e_i^{(k+1)} = \sqrt{|V_i|^2 + \left(f_i^{(k+1)}\right)^2} \quad (3.150)$$

Where,

$e_i^{(k+1)}$ = the real component of the voltage, $V_i^{(k+1)}$

$f_i^{(k+1)}$ = the imaginary component of the voltage, $V_i^{(k+1)}$

In order to increase the rate of convergence, an acceleration factor α with typical values of 1.3 to 1.7 is applied to the approximate solution obtained from each iteration as expressed by equation (3.151).

$$V_i^{(k+1)} = V_i^{(k)} + \alpha \left(V_{ical}^{(k)} + V_i^{(k)} \right) \quad (3.151)$$

Where,

α = the acceleration factor.

The updated voltages immediately replace the former values in the solution of the subsequent equations. The iteration continues until changes in the real and imaginary parts of voltages between successive iterations are within a specified accuracy as defined by the equation (3.152),

$$|e_i^{(k+1)} - e_i^{(k)}| \leq \varepsilon \quad (3.152)$$
$$|f_i^{(k+1)} - f_i^{(k)}| \leq \varepsilon$$

The method for determining the completion of a solution is based on an accuracy index set up on power mismatch (Saadat, 2002). The iteration is continued until the magnitude of the largest element in the ΔP and ΔQ columns is less than the specified value. Typical power mismatch accuracy is 0.001 p.u. When a solution is converged, the net real and reactive powers at the slack bus are calculated from equations (3.147) and (3.148).

The power loss in line i-j is given by,

$$S_{Lij} = S_{ij} + S_{ji}$$

(3.153)

Where,

$$S_{ij} = V_i I_{ij}^*$$

and

$$S_{ji} = V_j I_{ji}^*$$

3.6.5 Newton-Raphson Method

For large power system, the Newton-Raphson technique is found to be more efficient and practical. The method is adjudged mathematically superior to Gauss-Seidel technique due to its quadratic convergence (Saadat, 2002). The power flow equation is formulated in polar form.

From figure 3.22, the current entering bus i is given by,

$$I_i = \sum_{j=1}^{n} Y_{ij} V_j \tag{3.154}$$

Putting equation (3.154) in polar form, gives,

$$I_i = \sum_{j=1}^{n} |Y_{ij}||V_j| < \theta_{ij} + \delta_j \tag{3.155}$$

The injected complex power at bus i is given by,

$$S_i^* = P_i - jQ_i = V_i^* I_i \tag{3.156}$$

Substituting (3.155) into (3.156) gives,

$$P_i - jQ_i = |V_i| < -\delta_i \sum_{j=1}^{n} |Y_{ij}||V_j| < \theta_{ij} + \delta_j \tag{3.157}$$

$$= V_i e^{-j\delta i} \sum_{j=1}^{n} Y_{ij} V_j e^{j(\theta ij + \delta j)}$$

$$- \sum_{j=1}^{n} |V_i \left|\left|V_j\right|\right| Y_{ij} | [\cos(0ij - \delta i + \delta j) + \sin(0ij - \delta i + \delta j)]$$

$$= \sum_{j=1}^{n} |V_i \left|\left|V_j\right|\right| Y_{ij} | \cos(\theta_{ij} - \delta i + \delta j) + \sum_{j=1}^{n} j|V_i| |V_j||Y_{ij}| \sin(\theta ij - \delta i + \delta j) \tag{3.158}$$

Separating the real and imaginary parts gives,

$$P_i = \sum_{j=1}^{n} |V_i||V_j||Y_{ij}| \cos(\theta ij - \delta i + \delta j) \quad (3.159)$$

$$Q_i = \sum_{j=1}^{n} |V_i||V_j||Y_{ij}| \sin(\theta ij - \delta i + \delta j) \quad (3.160)$$

Expanding equations (3.159) and (3.160) in Taylor's series about the initial estimate and negating all higher order terms, gives,

$$\begin{bmatrix} \Delta P_2^{(k)} \\ \vdots \\ \Delta P_n^{(k)} \\ \hline \Delta Q_2^{(k)} \\ \vdots \\ \Delta Q_n^{(k)} \end{bmatrix} = \left[\begin{array}{ccc|ccc} \frac{\partial P_2^{(k)}}{\partial \delta_2} & \cdots & \frac{\partial P_2^{(k)}}{\partial \delta_n} & \frac{\partial P_2^{(k)}}{\partial |V_2|} & \cdots & \frac{\partial P_2^{(k)}}{\partial |V_n|} \\ \vdots & \ddots & \vdots & \vdots & \ddots & \vdots \\ \frac{\partial P_n^{(k)}}{\partial \delta_2} & \cdots & \frac{\partial P_n^{(k)}}{\partial \delta_n} & \frac{\partial P_n^{(k)}}{\partial |V_2|} & \cdots & \frac{\partial P_n^{(k)}}{\partial |V_n|} \\ \hline \frac{\partial Q_2^{(k)}}{\partial \delta_2} & \cdots & \frac{\partial Q_2^{(k)}}{\partial \delta_n} & \frac{\partial Q_2^{(k)}}{\partial |V_2|} & \cdots & \frac{\partial Q_2^{(k)}}{\partial |V_n|} \\ \vdots & \ddots & \vdots & \vdots & \ddots & \vdots \\ \frac{\partial Q_n^{(k)}}{\partial \delta_2} & \cdots & \frac{\partial Q_n^{(k)}}{\partial \delta_n} & \frac{\partial Q_n^{(k)}}{\partial |V_2|} & \cdots & \frac{\partial Q_n^{(k)}}{\partial |V_n|} \end{array}\right] \begin{bmatrix} \Delta \delta_2^{(k)} \\ \vdots \\ \Delta \delta_n^{(k)} \\ \hline \Delta |\delta_2^{(k)}| \\ \vdots \\ \Delta |\delta_n^{(k)}| \end{bmatrix} \quad (3.161)$$

The middle term of equation (3.161) is known as Jacobian matrix and it gives the linearized relationship between small changes in voltage angle $\Delta\delta_i^{(k)}$ and voltage magnitude $\Delta|V_i^{(k)}|$ with the small changes in real and reactive power $\Delta P_i^{(k)}$ and $\Delta Q_i^{(k)}$ (Saadat,2002; Elgerd, 1979). In equation (3.161), bus 1 is assumed to be slack bus, and elements of the Jacobian matrix are the partial derivative of equations (3.159) and (3.160), evaluated at $\Delta\delta_i^{(k)}$ and $\Delta|V_i^{(k)}|$. Putting equation (3.161) in compact form gives,

$$\begin{bmatrix} \Delta P \\ \Delta Q \end{bmatrix} = \begin{bmatrix} J_1 & J_2 \\ J_3 & J_4 \end{bmatrix} \begin{bmatrix} \Delta \delta \\ \Delta |V| \end{bmatrix} \quad (3.162)$$

The diagonal and the off-diagonal elements of Jaobian matrix, J_1, J_2, J_3, and J_4 can be determined as follows:

For J_1,

$$\frac{\partial P_i}{\partial \delta_i} = \sum_{j\neq i}^{n} |V_i|\,|V_j||Y_{ij}|\sin(\theta ij - \delta i + \delta j) \quad (3.163)$$

$$\frac{\partial P_i}{\partial \delta_j} = -|V_i|\,|V_j|\,|Y_{ij}|\sin(\theta ij - \delta i + \delta j) \quad (3.164)$$

$$for\ j \neq i$$

For J_1,

$$\frac{\partial P_i}{\partial |V_i|} = 2|V_i||V_{ii}|\cos\theta ii + \sum_{j\neq i}|V_j||Y_{ij}|\cos(\theta ij - \delta i + \delta j) \quad (3.165)$$

$$\frac{\partial P_i}{\partial |V_j|} = |V_i||V_{ii}|\cos(\theta ij - \delta i + \delta j) \quad (3.166)$$

$$for\ j \neq i$$

For J_1,

$$\frac{\partial Q_i}{\partial \delta_i} = \sum_{j\neq i}^{n} |V_i|\,|V_j||Y_{ij}|\cos(\theta ij - \delta i + \delta j) \quad (3.167)$$

$$\frac{\partial Q_i}{\partial \delta_j} = -|V_i|\,|V_j|\,|Y_{ij}|\cos(\theta ij - \delta i + \delta j) \quad (3.168)$$

$$for\ j \neq i$$

For J_4,

$$\frac{\partial Q_i}{\partial |V_i|} = -2|V_i||V_{ii}|\sin\theta ii - \sum_{j\neq i}|V_j||Y_{ij}|\sin(\theta ij - \delta i + \delta j) \quad (3.169)$$

$$\frac{\partial Q_i}{\partial |V_j|} = -|V_i||Y_{ij}|\sin(\theta ij - \delta i + \delta j) \quad (3.170)$$

$$for\ j \neq i$$

The power residuals are given as,

$\Delta P_i^{(k)} = P_i^{sp} - P_i^{(k)}$ (3.171)

$\Delta Q_i^{(k)} = Q_i^{sp} - Q_i^{(k)}$ (3.172)

Equations (3.171) and (3.172) are the difference between the specified and calculated values of real and reactive powers.

The new estimates for bus voltages are given by,

$$\delta_i^{(k+1)} = \delta_i^{(k)} + \Delta\delta_i^{(k)} \quad (3.173)$$

$$|V_i^{(k+1)}| = |V_i^{(k)}| + \Delta|V_i^{(k)}| \quad (3.174)$$

Solution procedures for Newton-Raphson technique are as follows:

(i) For load buses, P_i^{sp} and Q_i^{sp} are specified, while voltage magnitudes and phase angles are set equal to the slack bus values, that is $|V_i^{(0)}| = 1.0$, and $\delta_i^{(0)} = 0.0$.

For generator buses, $|V_i|$ and P_i^{sp} are specified, while phase angles are set equal to the slack bus angle.

(ii) For load buses, $P_i^{(k)}$ and $Q_i^{(k)}$ are calculated from equations (3.159) and (3.160), while $\Delta P_i^{(k)}$ and $\Delta Q_i^{(k)}$ are computed from equations (3.171) and (3.172).

(iii) For generator buses, $P_i^{(k)}$ and $\Delta P_i^{(k)}$ are computed from equations (3.159) and (3.171) respectively.

(iv) The elements of Jacobian, J_1, J_2, J_3, and J_4 are computed from equations (3.163) to (3.170).

(v) The linear equation (3.162) is solved by triangular factorization and Gaussian elimination.

(vi) The new voltage magnitudes and phase angles are calculated from equations (3.173) and (3.174).

(vii) The process is continued until residuals $\Delta P_i^{(k)}$ and $\Delta Q_i^{(k)}$ are less than the specified accuracy.

i.e.

$$|\Delta P_i^{(k)}| \leq \varepsilon \quad (3.175)$$

$$|\Delta Q_i^{(k)}| \leq \varepsilon$$

Figure 3.23 shows Newton – Raphson Power Flow Algorithm

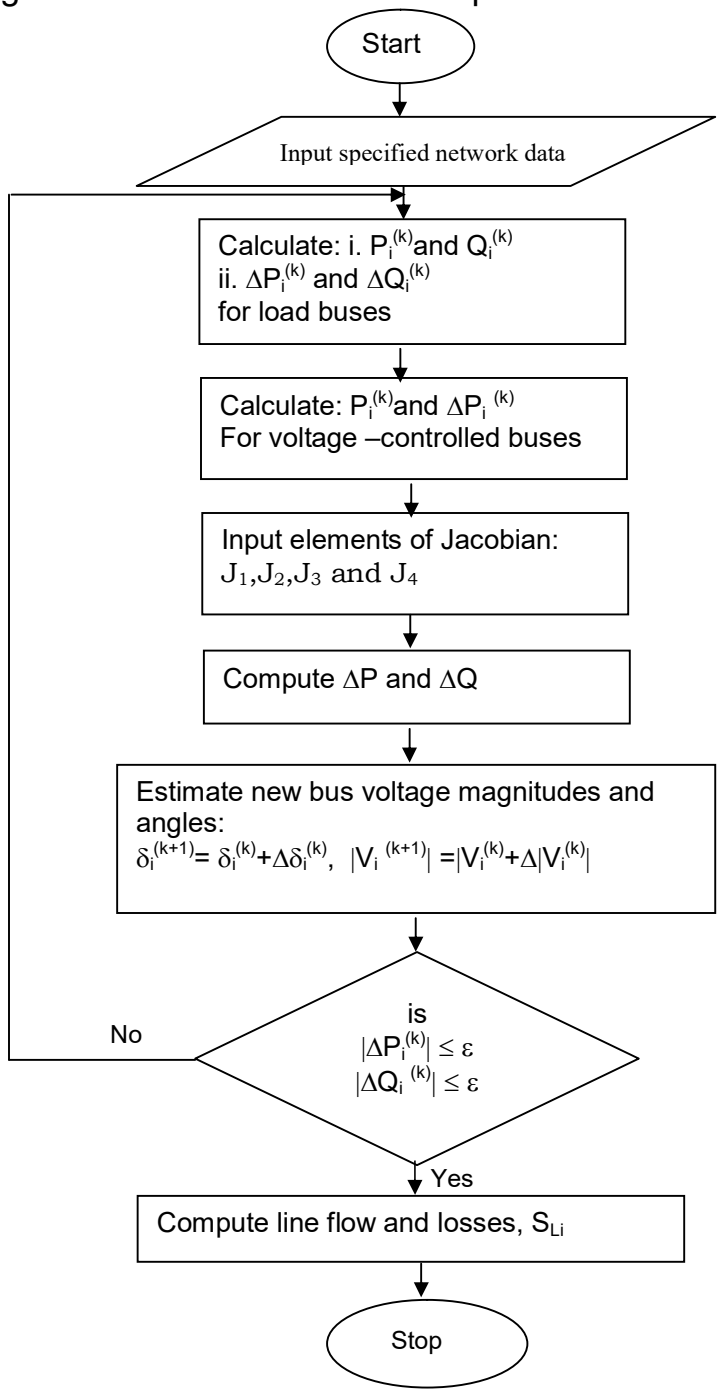

Figure 3.23 Newton –Raphson Power Flow Algorithm.

3.7 Modelling of Multimachine Power System

The figure 3.24 shown below represents a large power network consisting of n-generator buses.

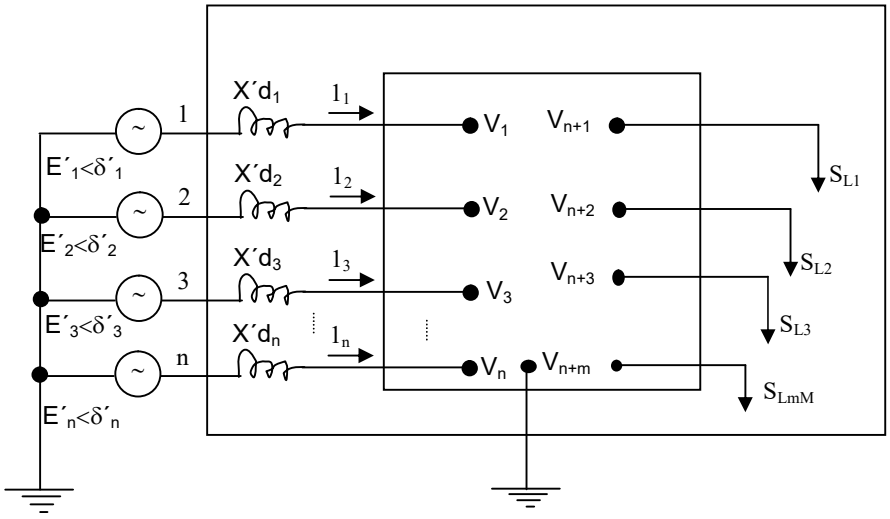

Figure 3.24 classical model of a large power network.

The node current equation for the network shown in figure 3.24 can be written in matrix form as,

$$\begin{bmatrix} I_1 \\ I_2 \\ \vdots \\ I_n \\ \hline I_{n+1} \\ \vdots \\ I_{n+m} \end{bmatrix} = \left[\begin{array}{ccc|ccc} Y_{11} & \cdots & Y_{1n} & Y_{1(n+1)} & \cdots & Y_{1(n+m)} \\ Y_{21} & \cdots & Y_{2n} & Y_{2(n+1)} & \cdots & Y_{2(n+m)} \\ \vdots & \ddots & \vdots & \vdots & \ddots & \\ Y_{n1} & & Y_{nn} & Y_{2(n+1)} & \cdots & Y_{n(n+m)} \\ \hline Y_{(n+1)} & \cdots & Y_{(n+1)n} & Y_{(n+1)(n+1)} & & Y_{(n+1)(n+m)} \\ \vdots & \ddots & & \vdots & \ddots & \vdots \\ Y_{(n+m)1} & \cdots & Y_{(n+m)n} & Y_{(n+m)(n+1)} & \cdots & Y_{(n+m)(n+m)} \end{array}\right] \begin{bmatrix} V_1 \\ V_2 \\ \vdots \\ V_n \\ \hline E'_{n+1} \\ \vdots \\ E'_{n+m} \end{bmatrix} \quad (3.176)$$

The model considers the following assumptions (Kimbark, 1948; Anderson, 2002):

1. The mechanical power input to each synchronous machine is constant.
2. Damping or asynchronous power is negligible.
3. The synchronous machines are represented electrically by constant voltage behind transient reactance models.

4. The motion of each synchronous machine rotor (relative to a synchronously rotating reference frame) is at a fixed angle relative to the angle of the voltage behind the transient reactance.
5. Loads are represented by constant impedances.

The constant voltage source $|E'|<\delta$ is determined from the initial conditions (that is, predisturbance power flow conditions). During the transient, the magnitude is held constant, while the variation of angle δ is governed by the swing equation (Bergen and Vittal, 2000). The representation of the loads as constant impedances enable the elimination of algebraic network equations and hence reduce the system of equations for the multimachine system consisting of only differential equations.

The complex electric power injected into the network shown in figure 3.22 by each machine is given as follows:

$$P_1 + jQ_1 = E_1^* I_1 \tag{3.177}$$

$$P_2 + jQ_2 = E_2^* I_2 \tag{3.178}$$

$$\vdots$$

$$P_n + jQ_n = E_n^* I_n \tag{3.179}$$

The injected current by each machine,

$$I_1 = Y_{11}E_1^* + Y_{12}E_2^* + \cdots + Y_{1n}E_n^* = \sum_{k=1}^{n} Y_{1k}E_k^* \tag{3.180}$$

$$I_2 = Y_{21}E_1^* + Y_{22}E_2^* + \cdots + Y_{2n}E_n^* = \sum_{k=1}^{n} Y_{2k}E_k^* \tag{3.181}$$

$$I_n = Y_{n1}E_1^* + Y_{n2}E_2^* + \cdots + Y_{nn}E_n^* = \sum_{k=1}^{n} Y_{nk}E_k^* \tag{3.182}$$

Where, Y's are the terminal self-and mutual admittances of the network, (which are also known as the driving point and transfer admittances). Each terminal self-admittance is the sum of the element admittances of all elements connected to that terminal; while each terminal mutual admittance

(between two given terminals) is the negative of the element admittance of the elements connected between the terminals.

Substituting equations (3.180) to (3.182) into equations (3.177) to (3.179) give,

$$P_1 + jQ_1 = E_1^* Y_{11} E_1 + E_1^* Y_{12} E_2 + \cdots + E_1^* Y_{1n} E_n = E_1^* \sum_{k=1}^{n} Y_{1k} E_k \quad (3.183)$$

$$P_2 + jQ_2 = E_2^* Y_{21} E_1 + E_2^* Y_{22} E_2 + \cdots + E_2^* Y_{2n} E_n - E_2^* \sum_{k=1}^{n} Y_{2k} E_k \quad (3.184)$$

$$\vdots$$

$$P_n + jQ_n = E_n^* Y_{n1} E_1 + E_n^* Y_{n2} E_2 + \cdots + E_n^* Y_{nn} E_n = E_n^* \sum_{k=1}^{n} Y_{nk} E_k \quad (3.185)$$

Taking into account the machines angular displacement, δ and the admittance angle θ, equations (3.183) to (3.185), become,

$$P_1 + jQ_1 = E_1^2 Y_{11} < \theta_{11} + E_1 E_2 Y_{12} < \theta_{12} - \delta_1 + \delta_2 + \cdots + E_1 E_n Y_{1n} < \theta_{1n} - \delta_1 + \delta_n = \sum_{k=1}^{n} E_1 E_k Y_{1k} < \theta_{1k} - \delta_1 + \delta_k \quad (3.186)$$

$$P_2 + jQ_2 = E_2 E_1 Y_{21} < \theta_{21} - \delta_2 + \delta_1 + E_2^2 Y_{22} < \theta_{22} + \cdots + E_2 E_n Y_{2n} < \theta_{2n} - \delta_2 + \delta_n = \sum_{k=1}^{n} E_1 E_k Y_{1k} < \theta_{1k} - \delta_1 + \delta_k \quad (3.187)$$

$$\vdots$$

$$P_n + jQ_n = E_n E_1 Y_{n1} < \theta_{n1} - \delta_n + \delta_1 + + E_n E_2 Y_{n2} < \theta_{2n} - \delta_2 + \delta_n + \cdots + E_n^2 Y_{nn} < \theta_{nn} \quad (3.188)$$

Applying the relation, $< \theta = \cos\theta + j\sin\theta$ and separating the real parts from the equations (3.186) to (3.188), give,

$$P_1 = E_1^2 Y_{11}\cos\theta_{11} + E_1E_2Y_{12}\cos(\theta_{12} - \delta_1 + \delta_2) + \cdots + E_1E_2Y_{1n}\cos(\theta_{1n} - \delta_1 + \delta_n)$$

$$= \sum_{k=1}^{n} E_1E_kY_{1k}\cos(\theta_{1n} - \delta_1 + \delta_k) \quad (3.189)$$

$$P_2 = E_2^2 Y_{22}\cos\theta_{22} + E_2E_1Y_{12}\cos(\theta_{21} - \delta_2 + \delta_1) + \cdots + E_2E_nY_{2n}\cos(\theta_{2n} - \delta_2 + \delta_n)$$

$$= \sum_{k=1}^{n} E_2E_kY_{2k}\cos(\theta_{2k} - \delta_2 + \delta_k) \quad (3.190)$$

$$\vdots$$

$$P_n = E_n^2 Y_{nn}\cos\theta_{nn} + E_nE_1Y_{n1}\cos(\theta_{n1} - \delta_n + \delta_1) + \cdots + E_nE_{n-1}Y_{2n-1}\cos(\theta_{nn-1} - \delta_n + \delta_{n-1})$$

$$= \sum_{k-1}^{n} E_nE_kY_{nk}\cos(\theta_{nk} - \delta_n + \delta_k) \quad (3.191)$$

Equations (3.189) to (3.191) are known as power-angle equations since they give the electric power output of each machine (power input to the network) as functions of the angular positions of the machines.

3.8 Multimachine Transient Stability Equations

3.8.1 The Rotor swing equation

The following assumptions are made when deriving the rotor swing equation for transient stability analysis (Arrillaga and Arnold, 1990):

1. Machine rotor speed does not vary greatly from synchronous speed (1.0pu).
2. Machine rotational power losses due to windage and friction are neglected.
3. Mechanical shaft power is smooth that is the shaft power is constant except for the results of speed governor action.

The assumption (1) permits the per unit power to be equated with per unit torque. From assumption (2), the accelerating power of the machine is expressed as the difference between the shaft power (P_m) as supplied by the prime mover or absorbed by the load and the electrical power (P_e).

When a power system is subjected to disturbance and unbalanced torque is created which acts on the rotor resulting in the acceleration or deceleration of the rotor in accordance to newton's second law,

$$J\frac{d\omega_m}{dt} + D_d\omega_m = T_t - T_e \qquad (3.192)$$

Where,

J = the total moment of inertia of the turbine and generator rotor in (kgm^2)

ω_m = the rotor shaft velocity in (mechanical radians per second)

T_t = the torque produced by the turbine (Nm)

T_e = the counter – acting electromagnetic torque

D_d = the damping – torque coefficient (Nm), and it accounts for the mechanical rotational loss due to windage and friction.

The turbine torque T_t changes relatively slowly, due to the long thermal time constants associated with the boiler and turbine, when compared with the electromagnetic torque T_e, which may change its value almost instantaneously. In the steady-state, the rotor angular speed is the synchronous speed ω_{sm}, while the turbine torque T_t is equal to the sum of the electromagnetic torque T_e and the damping (or rotational loss) torque $D_d\omega_{sm}$. That is,

$$T_t = T_e + D_d\omega_{sm} \quad \text{or} \quad T_m = T_t - D_d\omega_{sm} = T_e \qquad (3.193)$$

Where,

T_m = the net mechanical shaft torque

i.e. the turbine torque minus the rotational loses at $\omega_m = \omega_{sm}$.

This torque (T_m) is the torque that is converted into electromagnetic torque (T_e). If as a result of some system disturbance, T_m becomes greater than T_e, ($T_m > T_e$), the rotor accelerates, but if T_m becomes less than Te,($T_m < T_e$), then it decelerates.

The rotor velocity can thus be expressed as,

$$\omega_m = \omega_{sm} + \Delta\omega_{sm} = \omega_{sm} + \frac{d\delta_m}{dt} \qquad (3.194)$$

Where,

δ_m = the rotor angle expressed in mechanical radians.

$\Delta\omega_m = \frac{d\delta_m}{dt}$ = the speed deviation in mechanical radians per second.

From equation (3.194),

$\frac{d\omega_m}{dt} = \frac{d^2\delta_m}{dt^2}$ = angular acceleration

By making appropriate substitutions, equation (3.193) becomes,

$$J\frac{d^2\delta_m}{dt^2} + D_d\frac{d\delta_m}{dt} = T_m - T_e \qquad (3.195)$$

Multiplying both sides of equation (3.195) by the rotor synchronous speed ω_{sm} gives,

$$J\omega_{sm}\frac{d^2\delta_m}{dt^2} + \omega_{sm}D_d\frac{d\delta_m}{dt} = \omega_{sm}T_m - \omega_{sm}T_e \qquad (3.196)$$

Since power is the product of angular velocity and torque, the terms on the right hand side of equation (3.196) can be expressed as power to give,

$$J\omega_{sm}\frac{d^2\delta_m}{dt^2} + \omega_{sm}Dd\frac{d\delta_m}{dt} = \frac{\omega_{sm}}{\omega_m}P_m - \frac{\omega_{sm}}{\omega_m}P_e \qquad (3.197)$$

Where,

P_m = the net power input to the generator

P_e = the electrical air-gap power

During a disturbance the speed of a synchronous machine is usually very close to synchronous speed, such that $\omega_m \approx \omega_{sm}$, thus equation (3.197) becomes,

$$J\omega_{sm}\frac{d^2\delta_m}{dt^2} + \omega_{sm}Dd\frac{d\delta_m}{dt} = P_m - P_e \quad (3.198)$$

From equation (3.198), the coefficient $J\omega_{sm} = M_m$ = the angular momentum of the rotor at synchronous speed; therefore, the expression becomes;

$$M_m\frac{d^2\delta_m}{dt^2} = P_m - P_e - D_m\frac{d\delta_m}{dt} \quad (3.199)$$

Where,

$D_m = \omega_{sm}D_d$ = the damping coefficient.

Equation (3.199) is known as the swing equation which is the fundamental equation governing the rotor dynamics. This equation states that the product of rotor moment of inertia and its angular acceleration is equal to the net torque applied to the rotor (mechanical shaft torque and electromagnetic torque) (Fitzgerald and Kingsley, 1961).

It is conventional to express the angular momentum of the rotor in terms of a normalized inertia constant when all generators of a particular type will have similar “inertia” values irrespective of their rating (Machowski et al., 1997). The inertia constant (H) is therefore defined as the ratio of the stored kinetic energy in mega joules at synchronous speed to the machine’s apparent power rating S_n in MVA (Kimbark, 1948; Machowski et al., 1997).

The expressions for inertia constant and moment of inertia are given as,

$$H = \frac{0.5J\omega_{sm}^2}{S_n} \quad (3.200)$$

$$M_m = \frac{2HS_n}{\omega_{sm}}$$

The inertia constant, H measured in seconds quantifies the kinetic energy of the rotor at synchronous speed in terms of the number of seconds (time duration) it would take the generator to provide an equivalent amount of electrical energy, when operating at a power output equal to its MVA rating (Machowski et al., 1997).

When T_m is used for mechanical time constant, equation (3.200) becomes,

$$T_m = \frac{J\omega^2_{sm}}{S_n} \tag{3.201}$$

$$M_m = \frac{T_m S_n}{\omega_{sm}}$$

Equation (3.201) implies that if the generator is at rest, and a mechanical torque equal to $\frac{S_n}{\omega_{sm}}$ is suddenly applied to the turbine shaft, the rotor will accelerate, with its velocity increasing linearly and the machine will reach its synchronous speed ω_{sm} at T_m seconds.

Expressing the power angle in electrical radians and angular speed in electrical radians per second rather than their mechanical equivalents give,

$$\delta = \frac{\delta_m}{P/2}$$

$$\omega_s = \frac{\omega_{sm}}{P/2} \tag{3.202}$$

Where P = the number of poles.

Introducing the inertia constant and substituting equation (3.202) into (3.199) transforms the swing equation to,

$$\frac{2HS_n}{\omega_s}\frac{d^2\delta}{dt^2} + \frac{Dd\delta}{dt} = P_m - P_e$$

Or (3.203)

$$\frac{T_m S_n}{\omega_s}\frac{d^2\delta}{dt^2} + \frac{Dd\delta}{dt}\ P_m - P_e$$

Where,

$D = 2D_m/P$ = the damping coefficient

On rationalization by defining the inertia coefficient M and damping power P_D as follows:

$$M = \frac{2HSn}{\omega s} = \frac{TmSn}{\omega s} \text{ and}$$

$$P_D = D\frac{d\delta}{dt},$$

The swing equation takes a general form,

$$M\frac{d^2\delta}{dt^2} = P_m - P_e - P_D = P_a \quad (3.204)$$

Where P_a = accelerating power of the machine.

The expression relating the mechanical angular velocity to the electrical angular velocity is given by

$$\omega_{sm} = (\frac{2}{P})\omega_s \quad (3.205)$$

Equation (3.204) can expressed in per unit by normalizing to a common MVA base. If the base is the MVA rating of the generator, then dividing both sides of equation (3.203) by S_n and neglecting the effect of damping gives,

$$\frac{2Hd^2\delta}{\omega_s dt^2} = P_m(pu) - P_e(pu) \quad (3.206)$$

Expressing (3.206) in terms of system frequency f_0 gives the swing equation as:

$$\frac{H}{180f_0}\frac{d^2\delta}{dt^2} = P_m - P_e \quad (3.207)$$

It is usually more convenient to replace the second-order differential equation (3.204) by two first-order equations as,

$$\frac{Md\Delta\omega}{dt} = P_m - P_e - P_D = P_a$$

$$\frac{d\delta}{dt} = \Delta\omega \quad (3.208)$$

The time derivative of the rotor angle $\frac{d\delta}{dt} = \Delta\omega = \omega - \omega_s$ = the rotor speed deviation in electrical radians per second.

The solution of equation (3.204) gives δ as a function of t, while the graph of the solution is known as a swing curve. In multimachine systems, the output and the accelerating power of each machine depend upon the angular positions and the angular speeds of all the machines of thesystem. Thus, for an n – machines system, there are n – simultaneous differential equations written in the form of equation (3.204) as follows:

$$M_1\ddot{\delta}_1 = P_{m1} - P_{e1}\left(\delta_1, \delta_2, \ldots, \delta_{n-1}, \delta_n, \dot{\delta}_1, \dot{\delta}_2, \cdots, \dot{\delta}_{n-1}, \dot{\delta}_n\right)$$

$$M_2\ddot{\delta}_2 = P_{m2} - P_{e2}\left(\delta_1, \delta_2, \ldots, \delta_{n\ 1}, \delta_n, \dot{\delta}_1, \dot{\delta}_2, \cdots, \dot{\delta}_{n\ 1}, \dot{\delta}_n\right) \qquad (3.209)$$

$$M_n\ddot{\delta}_n = P_{mn} - P_{en}\left(\delta_1, \delta_2, \ldots, \delta_{n-1}, \delta_n, \dot{\delta}_1, \dot{\delta}_2, \cdots, \dot{\delta}_{n-1}, \dot{\delta}_n\right)$$

Where, $\ddot{\delta} = \frac{d^2\delta}{dt^2}, and\ \dot{\delta} = \frac{d\delta}{dt}$

3.9 Step-by-step Solution of Swing Equation

Step-by-step method is thereby applied to the solution of swing equations. In the application, the following considerations are made:

1. The acceleration as calculated at the beginning of a particular time interval is assumed to remain constant from the middle of the proceeding interval to the middle of the interval being considered.
2. The values of δ and ω are computed at the beginning and at the end of the interval for each machine.
3. The difference between the input and output power of each machine is computed.

4. P_m is assumed constant due to slowness of governor action.
5. P_e is a function of the relative angular positions of all the machines of the system and can be determined by solving the network to which the machines are connected.
6. If damping power is taken into account, the output, including damping will depend also on the relative angular speeds of all the machines.

From equation (3.204),

$$M\frac{d^2\delta}{dt^2} = P_a \qquad (3.210)$$

Dividing equation (3.210) by M and integrating twice with respect to time, t gives,

$$\frac{d^2\delta}{dt^2} = \frac{P_a}{M}$$

$$\frac{d\delta}{dt} = \omega = \omega_0 + \frac{P_a t}{M} \qquad (3.211)$$

And,

$$\delta = \delta_0 + \omega_0 t + \frac{P_a t^2}{2M} \qquad (3.212)$$

Where,

δ_0 = the value of δ at the beginning of the interval

ω_0 = the value of ω at the beginning of the interval.

These equations hold for any instant of time t during the interval in which P_a is constant. But since the interest here is particularly centered in the values of δ and ω at the end of the interval, by letting subscript n represent quantities at the end of the n^{th} interval, and n-1 represents quantities at the end of the $(n-1)^{th}$ interval, which coincides with the beginning of the n^{th} interval, and Δt as the length of the interval.

Substituting Δt for t in equations (3.211) and (3.212), and inserting appropriate subscripts, the speed and angle at the end of the n^{th} interval is obtained as,

$$\omega_n = \omega_{n-1} + \frac{\Delta t}{M} P_{a(n-l)} \tag{3.213}$$

$$\delta_n = \delta_{n-1} + \Delta t\omega_{n-1} + \frac{(\Delta t)^2}{2M} P_{a(n-1)} \tag{3.214}$$

From equations (3.213) and (3.214), the speed and angle increments during the n^{th} interval can be written as,

$$\Delta\omega_n = \omega_n - \omega_{n-1} = \frac{\Delta t}{M} P_{a(n-1)} \tag{3.215}$$

$$\Delta\delta_n = \delta_n - \delta_{n-1} = \Delta t\omega_{n-1} + \frac{(\Delta t)^2}{2M} P_{a(n-1)} \tag{3.216}$$

These sets of equations (3.213), (3.214) and (3.215), (3.216) are suitable for step-by-step calculation of the machines speed and angular variations.

For improved accuracy, the calculations for the n^{th} interval begins at $t = (n-1)\Delta t$, while $\Delta\delta_{n-1}$ is the angular position at this instant. The acceleration, α_{n-1} calculated at this instant is assumed to be constant from, $t = (n - 3/2)\ \Delta t$ to $t = (n - ½)\Delta t$. Over this period, a change in speed occurs and is determined as,

$$\Delta\omega_{n-½} = \Delta t\alpha_{n-1} = \frac{\Delta t}{M} P_{a(n-1)} \tag{3.217}$$

And the speed at the end of this time is given by,

$$\omega_{n-½} = \omega_{n-3/2} + \Delta\omega_{n-½} \tag{3.218}$$

Figure 3.25 show the actual and assumed curves of acceleration speed and angular position plotted against time for step-by-step solution.

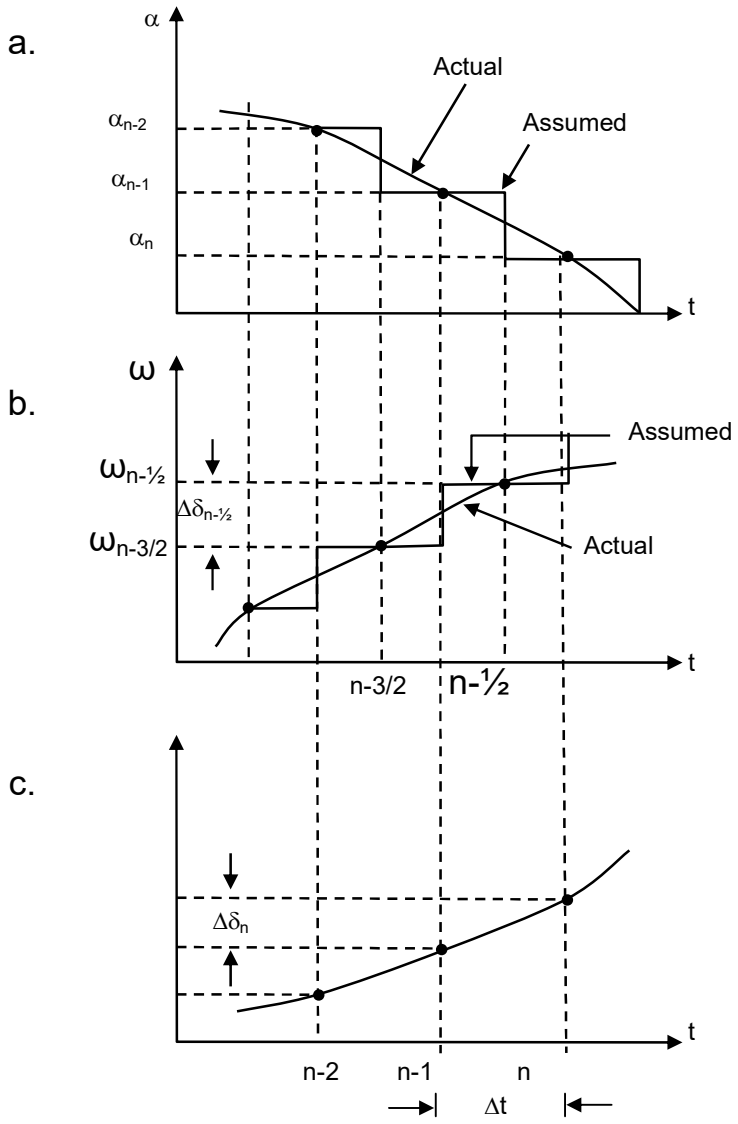

Figure 3.25 step-by-step method for solution of swing equation.

If it is assumed that the change in speed occurred as a step at the middle of the period (that is, t = (n-1) Δt), which is the same instant for which the acceleration was calculated. Then, between steps, the speed is assumed constant as shown in figure 3.25(b). From the interval

t = (n-1)Δt to t = nΔt or all through the n^{th} interval, the speed will be constant at the value $\omega_{n-½}$. The change in angular position during the n^{th} interval as shown in figure 3.25(c) is given by,

$$\Delta\delta_n = \Delta t\omega_{n-½} \qquad (3.219)$$

And the position at the end of the interval is given by,

$$\delta_n = \delta_{n-1} + \Delta\delta_n \tag{3.220}$$

Equations (3.217) – (3.220) can be used for the computation. But if the interest is only to determine the angular position, δ, then the speed term ω can be eliminated by putting equation (3.217) into (3.218) and then substituting the results into equation (3.219) as follows:

$$\Delta\delta_n = \Delta t\omega_{n-½} + \frac{(\Delta t)^2}{M} P_{a(n-1)} \tag{3.221}$$

Similar to equation (3.219),

$$\Delta\delta_{n-1} = \Delta t\omega_{n-3/2} \tag{3.222}$$

Substituting equation (3.222) into (3.221) gives

$$\Delta\delta_n = \Delta\delta_{n-1} + \frac{(\Delta t)^2}{M} P_{a(n-1)} \tag{3.223}$$

When the speed is desired, the expression is given by,

$$\omega_{n-½} = \frac{\Delta\delta_n}{\Delta_t} \tag{3.224}$$

Equation (3.223) gives the increment in angle at any time interval in terms of the increment for the previous interval. The effects of discontinuities in the accelerating power P_a before the fault occurred and after it is cleared are taken care of as follows:

Prior to the fault, the system is assumed to be in the steady state; therefore the accelerating power, P_{a0}^-, and the preceding increment in angle, $\Delta\delta_o$ are both equal to zero. Assuming that the fault is cleared at the beginning of the k^{th} interval, the value for $P_{a(k-1)}$ to be used for calculation should be,

$$½(P_{a(k-1)}^- + P_{a(k-1)}^+) \tag{3.225}$$

Where,

$P_{a(k-1)}^-$ = the accelerating power just prior to fault clearing

$P_{a(k-1)}^+$ = the accelerating power just after fault is cleared.

3.10 Data preparation for Transient Stability

The following steps are adopted in data preparation (Bergen and Vittal, 2000):

1. The conversion of the system data to a common base; a system base of 100MVA is conventionally chosen.
2. Load data from the pre-fault power flow are converted to equivalent impedances or admittances. For instance, if a certain load bus has a voltage solution V_{Li} and complex power demand, $S_{Li} = P_{Li} + jQ_{Li}$, then, using $S_{Li} = V_{Li}I_{Li}^*$ which implies, $I_{Li} = \frac{S_{Li}^*}{V_{Li}^*}$, hence,

$$Y_{Li} = \frac{I_{Li}}{V_{Li}} = \frac{S_{Li}^*}{|V_{Li}|^2} = \frac{P_{Li} - jQ_{Li}}{|V_{Li}|^2} \quad (3.226)$$

Where,

$Y_{Li} = g_{Li} + jb_{Li}$ = the equivalent shunt load admittance.

3. The internal voltage of the generators $|E_i| < \delta_i^0$ are calculated from the power flow data using the predisturbance terminal voltage $|V_i| < \beta_i$ as follows:

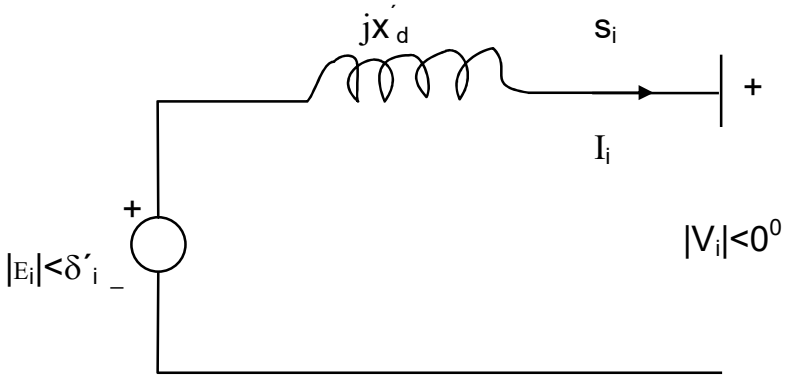

Figure 3.26 Generator model

From figure 3.26, the generator internal voltage is given by,

$$|E_i| < \delta_i' = |V_i| + jX_{di}'I_i \quad (3.227)$$

$$= |V_i| + \frac{jX_{di}'}{|V_i|}(P_i - jQ_i)$$

$$= |V_i| + Q_i \frac{X'_{di}}{|V_i|} + j\left(P_i \frac{X'_{di}}{V_i}\right)$$

However, the angle difference between internal and terminal voltage of the generator shown in figure 3.26 is δ'_i. Since the actual terminal voltage angle is β_i, and the initial generator angle δ'_i, by adding the predisturbance voltage angle β_i to δ'_i gives the initial generator angle. That is,

$$\delta_i^o = \delta'_i + \beta_i \qquad (3.228)$$

4. Calculation of Y_{bus} matrices for the prefault, fault-on and post fault network conditions are determined as follows:

i. The equivalent load admittances earlier computed are connected between the load buses and the reference node. Additional nodes are provided for the internal generator nodes (nodes 1, 2,…, n) and the appropriate values of admittances corresponding to x'_d are connected between these nodes and the generator terminal nodes.

ii. In order to obtain the Y_{bus} corresponding to the faulted system, (usually three-phase-to-ground fault is assumed); the row and column corresponding to the faulted node are set to zero to get the fault-on Y_{bus}.

iii. The post fault Y_{bus} is obtained by removing the faulted line that would have been isolated via protective relay operation.

4. In the final step, all the nodes except the internal generator nodes are eliminated using kron reduction; the reduced Y_{bus} matrix is obtained. The reduced Y_{bus} matrix is denoted by $\hat{Y}$.

The reduced matrix $\hat{Y}$ can also be derived as follows:

The system Y_{bus} for each network condition provides the following relationship between the voltages and currents;

$$I = Y_{bus}\, V \qquad (3.229)$$

Where,

I = the current vector given by the injected currents at each bus. In the classical model, the injected current is considered to exist only at the n-internal generator buses. All other currents are zero. Therefore, the injected current vector has the form,

$$I = \begin{bmatrix} I_n \\ \dots \\ 0 \end{bmatrix}$$

Partitioning the Y_{bus} and V matrices appropriately gives,

$$I = \begin{bmatrix} I_n \\ \dots \\ 0 \end{bmatrix} = \begin{bmatrix} Y_{nn} & \vdots & Y_{ns} \\ \dots & \vdots & \dots \\ Y_{sn} & \vdots & Y_{ss} \end{bmatrix} \begin{bmatrix} E_n \\ \dots \\ V_s \end{bmatrix} \quad (3.230)$$

Where,

the subscript n denotes the internal generator nodes, and the subscript s denotes all the remaining nodes.

The voltage at the internal generator nodes are given by the internal emfs.

From equation (3.230),

$$I_n = Y_{nn}E_n + Y_{ns}V_s \quad (3.231)$$

$$0 = Y_{sn}E_n + Y_{ss}V_s \quad (3.232)$$

$$V_s = \frac{-Y_{sn}E_n}{Y_{ss}} = -Y_{ss}^{-1}Y_{sn}E_n \quad (3.233)$$

Putting equation (3.233) into (3.231) gives,

$$I_n = Y_{nn}E_n + (-Y_{ss}^{-1}Y_{sn}E_n)$$

$$= [Y_{nn} - Y_{ns}Y_{ss}^{-1}Y_{sn}]E_n = \hat{Y}E_n \quad (3.234)$$

Where,

$\hat{Y} = Y_{nn} - Y_{ns}Y_{ss}^{-1}Y_{sn}$ = reduced system admittance matrix with the dimension of (nxn).

n = the number of the generators.

The reduced admittance matrix as expressed in equation (3.234) provides the complete description of all the injected currents in terms of the internal generator voltages.

From equation (3.125),

The active power injected into the network at node i, which is the electrical power output of machine i is given by,

$$P_{ei} = real E_i I_i^*$$

$$= |E_i|^2 \hat{G}_{ii} \sum_{\substack{j=1 \\ j \neq i}}^{n} E_i E_j \hat{B}_{ij} \sin(\delta_i - \delta_j) + \hat{G}_{ij} \cos(\delta_i - \delta_j) \quad (3.235)$$

$$for\ i = 1,2,\cdots,n$$

Substituting equation (3.235) into the differential equations in (3.204) with the damping coefficient neglected, gives,

$$M_i \ddot{\delta}_i = P_{mi}^0 - |E_i|^2 \hat{G}_{ii} - \sum_{\substack{j=1 \\ j \neq i}}^{n} E_i E_j \{\hat{B}_{ij} \sin(\delta_i - \delta_j) + \hat{G}_{ij} \cos(\delta_i - \delta_j)\} \quad (3.236)$$

$$for\ i = 1,2,\cdots,n$$

Equation (3.236) are second-order differential equations and can be solved by numerical integration but must first be converted to a set of coupled first-order differential equation expressed as,

$$M_i \dot{\omega}_i = P_{mi}^0 - |E_i|^2 \hat{G}_{ii} - \sum_{\substack{j=1 \\ j \neq i}}^{n} E_i E_j \{\hat{B}_{ij} \sin(\delta_i - \delta_j) + \hat{G}_{ij} \cos(\delta_i - \delta_j)\} \quad (3.237)$$

$$for\ i = 1,2,\cdots,n$$

where,

$$\dot{\delta}_i = \omega_i$$

The value of the mechanical power for each machine in equation (3.236) is determined from the prefault conditions. The mechanical power is set equal to the active electrical power output of each generator at the prefault conditions. This provides the equilibrium condition and the initial angles for each generator as given by δ_i^0 in equation (3.228).

Figure 3.27 shows the transient stability analysis algorithm.

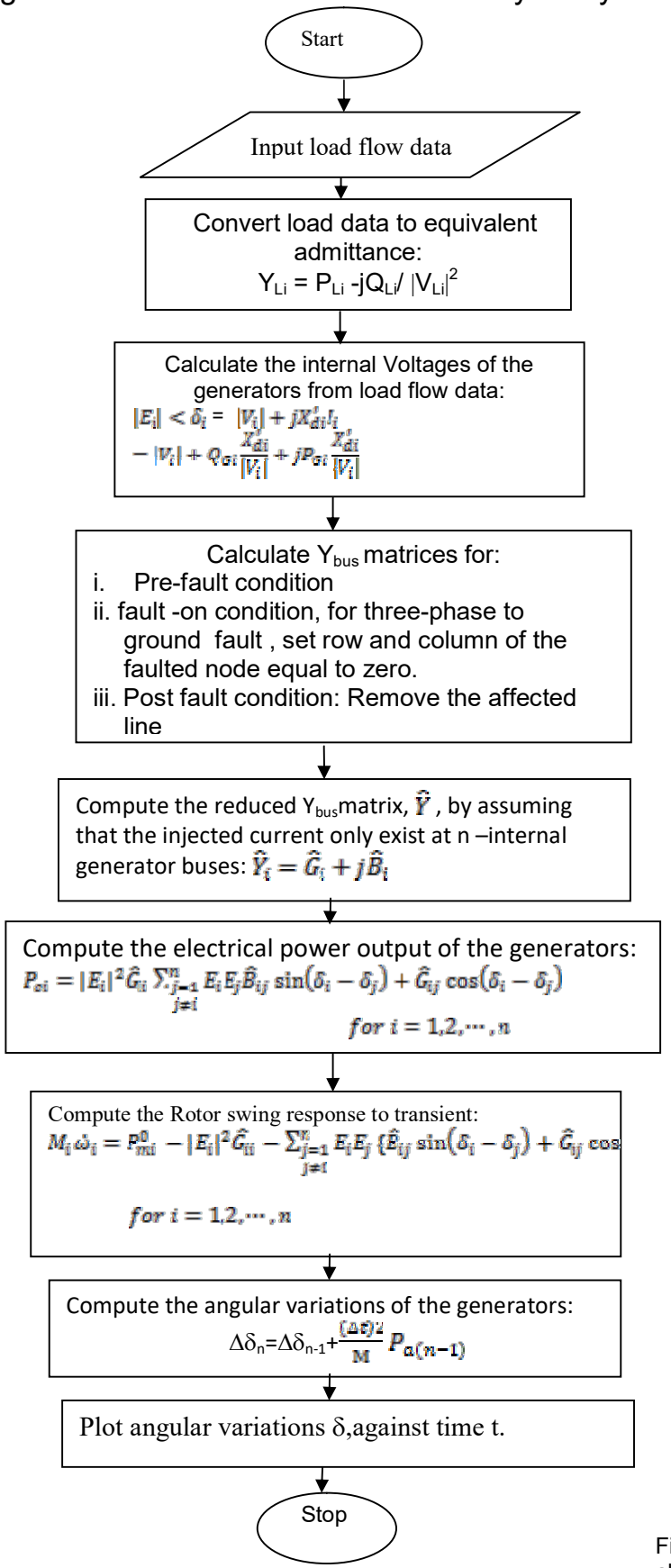

Figure 3.27 Transient stability Analysis algorithm

3.11 Coherent Genrator Identification

Due to large interconnections that make up the present day power networks, its complexity has equally increased thereby demanding for a simplified but accurate method of transient stability analysis with minimal computer time and memory space. The method of transient stability analysis of a large power system via simplified dynamic equivalents is attracting increased attention by researchers across the globe (Rau and Hussian, 1998). The Coherent generator technique is an elegant and powerful technique for system simplification leading to the construction of simplified reduced order dynamic models which can represent the entire system without loss of any significant characteristic behaviour. The method of Coherent generators identification deployed in this text is based on equal acceleration and velocity concept; with the effects of damping and transfer conductance taken into account in power system model.

The principle of the swing generators coherency is anchored on the concept that when any disturbance occurs in the power system, the differences in the Coherent machines rotor angles remain constant in time.

3.11.1 Mathematical Formulation

From equation (3.204), the rotor dynamic equation for the i^{th} machine of an n-generator bus system is given by,

$$M_i\ddot{\delta}_i = P_{mi} - P_{ei} - D_i\dot{\delta}_i \tag{3.238}$$

For i^{th} and j^{th} generators to be coherent,

$$\delta_{i(t)} - \delta_{j(t)} - \delta_{ij} - constant - \delta_{ij}^0 \tag{3.239}$$

where,

$\delta_{ij}^0 = \delta_i^0 - \delta_j^0 =$ prefault value of the difference between the i^{th} and j^{th} rotor angles.

Linearizing equation (3.238) on the assumption that the power variation is small and that the generator coherency is independent of the magnitude of the disturbance (Podmore, 1978), gives,

$$M_i \Delta\ddot{\delta}_i = \Delta P_{mi} - \Delta P_{ei} - D_i \Delta\omega_i \qquad (3.240)$$

Where,

$\Delta\ddot{\delta}_i$ = the change in acceleration of the ith machine

$\Delta\omega_i$= change in the velocity of the ith machine

The mechanical power input to the machine is assumed constant for a short duration of the fault, hence the term ΔP_{mi} in equation (3.240) becomes zero.

While the resultant electrical power output of the ith machine with respect to variation in its rotor angle δ_i is given by,

$$P_{ei}(\delta) = P_{ei}(\delta^0 + \Delta\delta)$$

$$= P_{ei}(\delta^0) + \sum_{j=1}^{n} \frac{\partial P_{ei}}{\partial \delta_j} |\Delta\delta_j{}_{\delta^0}$$

where,

$$\Delta P_{ei}(\delta) = \sum_{j=1}^{n} \frac{\partial P_{ei}}{\partial \delta_j} |\Delta\delta_j{}_{\delta^0} \qquad (3.241)$$

and,

$$P_{ei} = \sum_{j=1}^{n} E_i E_j Y_{ij} \cos(\theta_{ij} - \delta_{ij}) \qquad (3.142)$$

Equation (3.241) is the change in electrical power of the ith generator due to a small change in the angle of the jth generator evaluated at the time of initiating the fault (Lee and Schweppe, 1973).

From equation (3.242), the $\frac{\partial P_{ei}}{\partial \delta_j}$ is given by,

$$\frac{\partial P_{ei}}{\partial \delta_j} = E_i \sum_{\substack{j=1 \\ j\neq 1}}^{n} Y_{ij} E_j \sin\left(\theta_{ij} - \delta_i + \delta_j\right) \Delta\delta_i - E_i \sum_{j=1}^{n} Y_{ij} E_j \sin\left(\theta_{ij} - \delta_i + \delta_j\right) \Delta\delta_j$$

(3.243)

The following assumptions are made:

1. Internal voltages of the machines are equal to 1.0 pu
2. The angular difference $\left(\delta_i - \delta_j\right)$ is within 30^0.
3. The network is highly reactive, while the conductances are not neglected.

Consequently, the equation (3.243) simplifies to,

$$\Delta P_{ei} = \sum_{\substack{j=1 \\ j\neq i}}^{n} Y_{ij}\left(\Delta\delta_i - \delta_j\right) \quad (3.244)$$

Substituting equation (3.244) into equation (3.240) gives,

$$M_i \Delta\ddot{\delta}_i = \sum_{\substack{j=1 \\ j\neq i}}^{n} Y_{ij}\left(\Delta\delta_j - \Delta\delta_i\right) - D_i \Delta\omega_i \quad (3.245)$$

Introducing a dummy variable $Y'_{ij,}$ relating the actual system admittance matrix element Y_{ij} as follows:

$$Y'_{ij} = Y_{ij}$$

and (3.246)

$$Y'_{ii} = -\sum_{\substack{j-1 \\ j\neq i}}^{n} Y_{ij}$$

Substituting equation (3.246) into (3.245) and dividing by M_i gives,

$$\Delta\ddot{\delta}_i = M_i^{-1} \sum_{\substack{j=1 \\ j\neq i}}^{n} Y'_{ij} \Delta\delta_j - M_i^{-1} D_i \Delta\omega_i \quad (3.247)$$

For a given set of machines to be considered candidates for coherency check, it is required that such machines must form a sensible geographical area, which is a measure of their mutual admittances.

Electrical proximity for any two machines depends upon their mutual admittance (Sankaranarayanan et al., 1983). As the mutual admittance between two machines becomes larger, that pair of machines are considered more close to each other (Rau and Hussian, 1998). Therefore, the mutual admittance between a pair of machines is a measure of coupling between then (Monticelli, 1999; Rau and Hussian, 1998).

It can thus be deduced from equation (3.246) that if all the machines have equal mutual admittance to the $_i^{th}$ machine, then,

$$Y'_{ii} = (n-1)|Y'_{ij}| \tag{3.248}$$

From equation (3.248), an electric proximity index α_{ij} can be defined by the expression,

$$\alpha_{ij} = (n-1)\frac{Y'_{ij}}{|Y'_{ii}|} \geq 1.0 \tag{3.249}$$

$$for\ j = 1,2,\cdots,n$$

$$j \neq 1$$

The generators that satisfy equation (3.249) are deemed eligible for coherency grouping test with the i^{th} machine.

The linearized acceleration equation (3.245) for i^{th} and j^{th} machines can be re-written as,

$$\Delta\ddot{\delta}_i = M_i^{-1}Y_{ij}\left(\Delta\delta_j - \Delta\delta_i\right) + M_i^{-1}\sum_{\substack{k=1 \\ k\neq i,j}}^{n} Y_{ik}(\Delta\delta_k - \Delta\delta_i) - M_i^{-1}D_i\Delta\omega_i \tag{3.250}$$

$$\Delta\ddot{\delta}_j = M_j^{-1}Y_{ji}\left(\Delta\delta_i - \Delta\delta_j\right) + M_j^{-1}\sum_{\substack{k=1 \\ k\neq i,j}}^{n} Y_{jk}\left(\Delta\delta_k - \Delta\delta_j\right) - M_j^{-1}D_j\Delta\omega_j \tag{3.251}$$

Comparing the terms of both equations (3.250) and (3.251), and resolving as follows:

1. The first terms, $M_i^{-1}Y_{ij}(\Delta\delta_j - \Delta\delta_i)$ and $M_j^{-1}Y_{ji}(\Delta\delta_i - \Delta\delta_j)$ are opposite in sign to one another, while $Y_{ij} = Y_{ji}$.

   The differences in magnitude between the two terms are due to the difference in M_i and M_j values. The i^{th} and j^{th} machines are considered as coherent if $\Delta\delta_i - \Delta\delta_j$, which implies that $|(\Delta\delta_j - \Delta\delta_i)|$ or $|(\Delta\delta_i - \Delta\delta_j)|$ will be equal to zero or very negligible. Consequently, the first terms of equations (3.250) and (3.251) will only contribute an insignificant amount to the change in the respective accelerations.

2. In the second terms of equations (3.250) and (3.251), it can be observed that $(\Delta\delta_k - \Delta\delta_i)$ and $(\Delta\delta_k - \Delta\delta_j)$ may have significant values if the i^{th} and j^{th} machines are considered coherent, therefore $\Delta\delta_i = \Delta\delta_j$ and $\Delta\omega_i = \Delta\omega_j$. Hence, the second terms of both equations (3.250) and (3.251) have significant values and thus, contribute more reasonably than the first terms to the change in accelerations.

For equal acceleration of the i^{th} and j^{th} machines, the coefficients of the second and third terms of equations (3.250) and (3.251) must be equal to each other (for perfect coherency). That is,

$$M_i^{-1}\sum_{\substack{k=1\\k\neq i,j}}^{n} Y_{ik} = M_j^{-1}\sum_{\substack{k=1\\k\neq i,j}}^{n} Y_{jk}$$

Or

$$M_i^{-1}a_i = M_i^{-1}a_i \qquad (3.252)$$

Where,

$$a_i = \sum Y_{ik}, \quad a_j = \sum Y_{jk}$$

And

$$M_i^{-1} D_i = M_j^{-1} D_j \quad (3.253)$$

From the equations (3.252) and (3.253), the two normalized indices β and γ are defined for coherency check as follows:

$$\beta_{ij} = \frac{|M_i^{-1} a_i - M_j^{-1} a_i|}{Max(M_i^{-1} a_i, M_j^{-1} a_j)} \leq 0.2 \quad (3.254)$$

and,

$$\gamma_{ij} = \frac{|M_i^{-1} D_i - M_j^{-1} D_i|}{Max(M_i^{-1} D_i, M_j^{-1} D_j)} \leq 0.5 \quad (3.255)$$

where,

β_{ij} = Inertia index for i^{th} and j^{th} machines

γ_{ij} = Damping index for i^{th} and j^{th} machines

If machines i and j are perfectly coherent, then both β and γ must be identically equal to zero. But when one of the inertias tends to infinity, then both β and γ tend to 1.0, which indicates the machines deviation from each other. The tolerance values of 0.2 for β and 0.5 for γ are found to give acceptable results (Guruprasada and Hussian, 1998). In a situation whereby the damping coefficient is zero or the ratio D/M becomes uniform, the coherency grouping is conducted based on β criterion alone.

3.11.2 Coherent Generators Dynamic Equivalent Construction Technique

The generators whose transient behaviour is similar to each other are aggregated into one equivalent generator. The coherency based dynamic equivalent construction has the advantage of transforming the large power network into a reduced model with the basic physical structure of the original

system being preserved. The concept of dynamic equivalent construction technique deployed in this text is based on the power invariance at the terminal buses and at the internal buses of the coherent machines (Kimbark, 1948; Hussian and Rau, 1993; Sankaranarayan et al., 1983). According to (Kimbark, 1948), the synchronous machines are represented by the classical models with the voltage sources behind the transient reactances. For the machines considered to be coherent, the fictitious points between the voltage sources and the transient reactances of the coherent machines are assumed to be connected together. Hence, the voltage sources of the coherent machines become parallel to each other. All the transient reactances are then connected together to this fictitious point. The other ends of the reactances connect different point of the network. The parallel voltage sources are therefore replaced by a single equivalent voltage source such that it can deliver the active and reactive power equal to the sum of the active and reactive powers delivered by the machines of the coherent group being replaced.

3.11.2.1 Mathematical Formulation

Considering a coherent machine group containing p number of terminal buses and are connected by p_t tie buses. Figure 3.28 shows a large power network model with coherent generator groups.

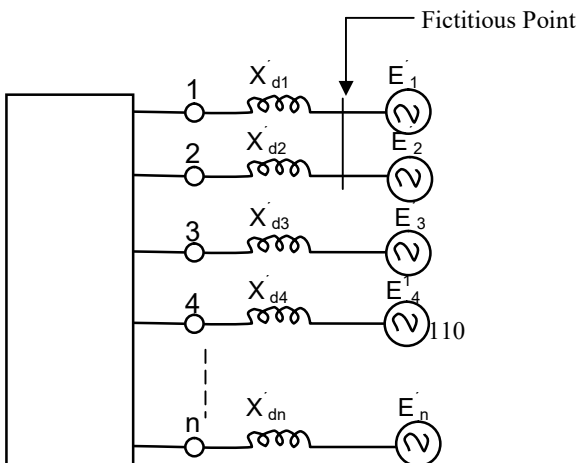

Figure 3.28 large power network with coherent generator groups.

The real and reactive power received by the i^{th} terminal bus from the corresponding coherent machine and the internal voltages of i^{th} machine given by,

$$S_i = V_i^* I_i \tag{3.256}$$

and

$$E_i = V_i + X'_{di} I_i \tag{3.257}$$

Where,

V_i = terminal voltage of i^{th} machine

I_i = current flowing to the terminal bus of i^{th} machine.

The sum of the powers received by *p* buses of the coherent group is given by,

$$S_T = \sum_{i=1}^{p} S_i = \sum_{i=1}^{p} V_i^* I_i \tag{3.258}$$

The equivalent terminal bus of the coherent group must be such that it can receive the total power S_T and current I_T from the equivalent machine replacing the coherent group of machines.

That is,

$$S_T = V_e^* I_T$$

$$V_e^* I_T = \sum_{i=1}^{p} V_i^* I_i$$

Hence,

$$V_e = \left[\sum_{i-1}^{p} \frac{V_i^* I_i}{I_T}\right]^* \quad (3.259)$$

Where,

I_T = the vector sum of the currents and is given by,

$$I_T = \sum_{i-1}^{p} I_i \quad (3.260)$$

The equivalent machine internal voltage, E_e is given by,

$$E_e = \left(\sum_{i=1}^{p} \frac{E_i^* I_i}{I_e}\right)^* \quad (3.261)$$

Where,

$I_e = \sum_{i=1}^{p} I_{i=}$ vector of currents of the coherent group being replaced.

p = the number of the machine in the coherent group.

The equivalent machine transient reactance X'_{de} is given by,

$$X'_{de} = \frac{(E_e - V_e)}{\sum_{i=1}^{p} I_i} \quad (3.262)$$

The equivalent inertia constant, H_e of the coherent group is the sum of the inertia constants of the individual machines, and is given by,

$$H_e = \sum_{i=1}^{p} H_i \quad (3.263)$$

The equivalent damping coefficient, D_e of the coherent group is the sum of the damping coefficients of the individual machines, and is given by,

$$D_e - \sum_{i=1}^{p} D_i \quad (3.264)$$

The equivalent mechanical power, P_{me} is the sum of mechanical powers required to accelerate the individual machines, and is given by,

$$P_{me} = \sum_{i-1}^{p} P_{mi} \quad (3.265)$$

The following conditions are considered in forming the equivalent group (Kimbark, 1948):

1. When the machines to be combined to form an equivalent machine are connected in parallel at their terminals. By applying the Thevenin's theorem, their effect upon the network is the same as if they were replaced by a single source of emf, equal to the open circuit voltage of the group of machines, in series with single impedance, equal to the impedance seen from the terminals when the machines emfs are equal to zero. Hence, the impedance of the equivalent machine is a reactance equal to the parallel combination of the reactances of the individual machines referred to a common Megavolts-Ampere base, if expressed in per unit.

   The equivalent emf is sort of average of the emfs' of the individual machines. If the machines swing together, the equivalent emf is constant in magnitude and has the same frequency as the emfs of the machines. The emf of the equivalent machine is such that the equivalent machine initially supplies to the network the same active and reactive power as the group of machines that it replaces.
2. When the machines to be combined are not in parallel at their terminals, their reactances cannot be combined. The fictitious points between the reactance and the source of internal voltage of each machine are connected together. However, by paralleling the several voltage sources and connecting together at one end all the reactances, the other ends of which go to different points of the network. The

parallel voltage sources are replaced by a single source which is adjusted to deliver to the network the same active and reactive power as the sources which it replaces. For instance, two or more stations which are connected together by low-impedance ties may likewise be combined to form an equivalent machine.

3.11.2.2 The Algorithm for the Coherent Machines Identification and Dynamic Equivalents Construction

Figure 3.29 shows the algorithm for the coherent machines identification and construction of dynamic equivalents.

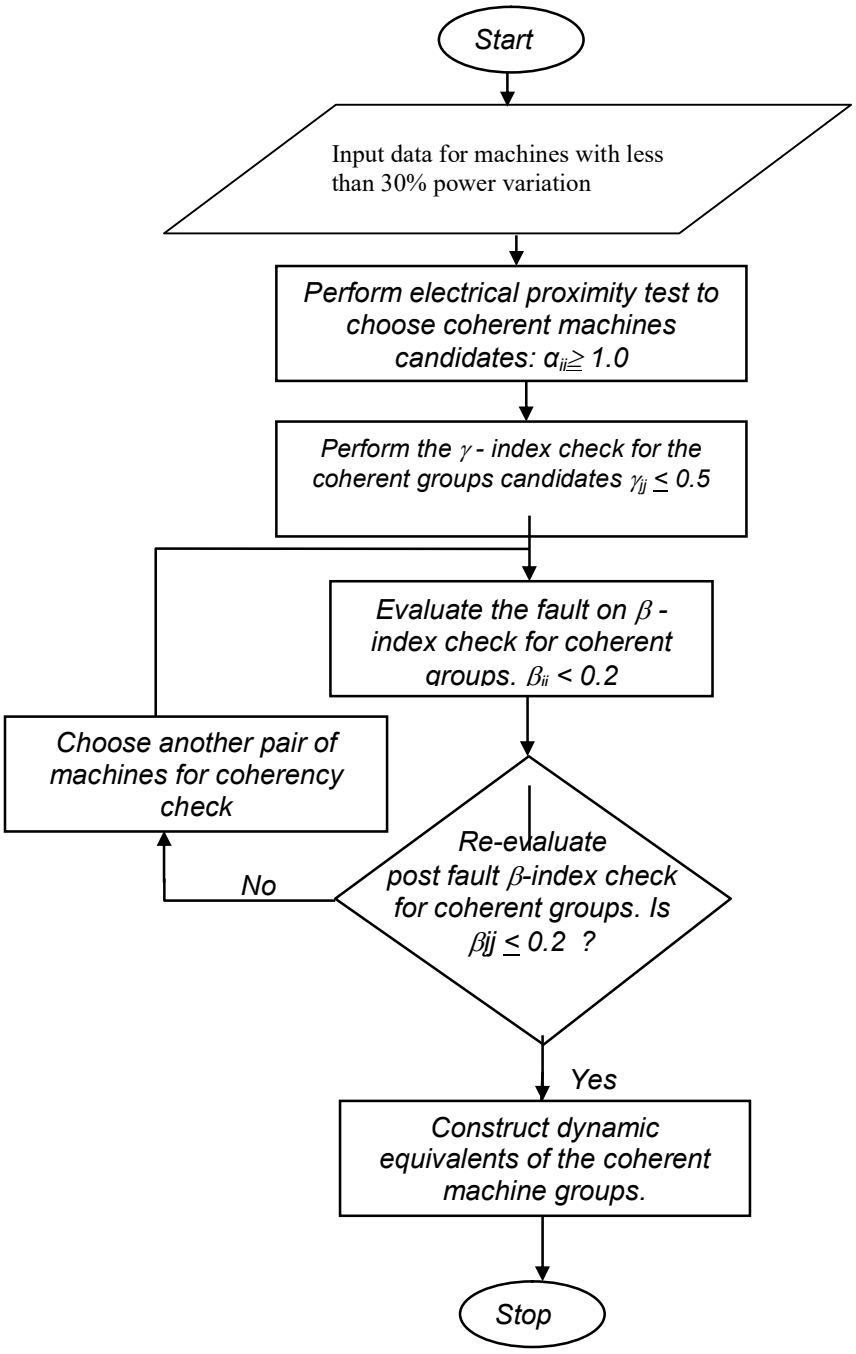

Figure 3.29 Algorithm for coherent machines identification and dynamic equivalents construction.

Chapter Four

4.0 Power Flow and Stability evaluation of the Existing and Proposed National Grids

4.1 Derivation of existing national grid injected current equations.

Figure 4.1 shows the existing 330KV Nigeria power network.

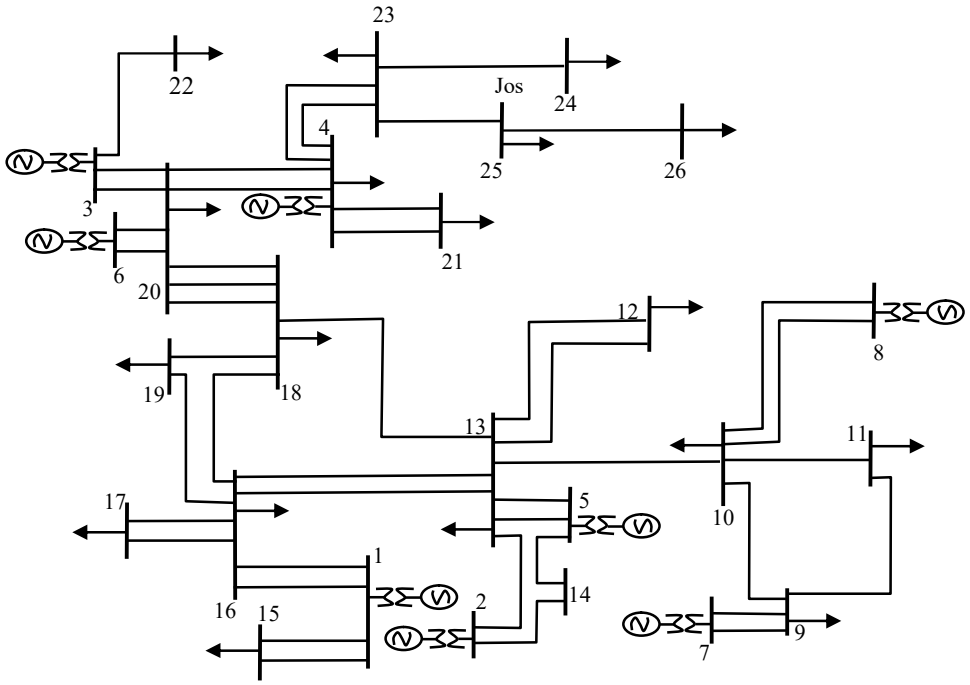

Figure 4.1 Existing 330KV Nigeria power network.

From figure 4.1, the net injected current into the network are given as follows:

$$i_1 = V_1y_{10} + (V_1 - V_{15})\, y_{1(15)} + (V_1 - V_{16})\, y_{1(16)} \quad (4.1)$$

$$i_2 = V_2y_{20} + (V_2 - V_{13})\, y_{2(13)} + (V_2 - V_{14})\, y_{2(14)} \quad (4.2)$$

$$i_3 = V_3y_{30} + (V_3 - V_{20})\, y_{3(20)} + (V_3 - V_{22})\, y_{3(22)} \quad (4.3)$$

$$i_4 = V_4y_{40} + (V_4 - V_{20})\, y_{4(20)} + (V_4 - V_{21})\, y_{4(21)} + (V_4 - V_{23})y_{4(23)} \quad (4.4)$$

$$i_5 = V_5y_{50} + (V_5 - V_{12})\, y_{5(12)} + (V_5 - V_{14})\, y_{5(14)} \quad (4.5)$$

$$i_6 = V_6y_{60} + (V_6 - V_{20})\, y_{6(20)} \quad (4.6)$$

$$i_7 = V_7y_{70} + (V_7 - V_9)\, y_{7(9)} \quad (4.7)$$

$$i_8 = V_8 y_{80} + (V_8 - V_{10})\, y_{8(10)} \quad (4.8)$$

$$0 = V_9 y_{90} + (V_9 - V_7)\, y_{9(7)} + (V_9 - V_{10})\, y_{9(10)} \quad (4.9)$$

$$0 = V_{10} y_{100} + (V_{10} - V_8)\, y_{10(8)} + (V_{10} - V_9)\, y_{10(9)} + (V_{10} - V_{11}) y_{10(11)} + (V_{10} - V_{13}) y_{10(13)} \quad (4.10)$$

$$0 = V_{11} y_{110} + (V_{11} - V_{10})\, y_{11(10)} \quad (4.11)$$

$$0 = V_{12} y_{120} + (V_{12} - V_{13})\, y_{12(13)} \quad (4.12)$$

$$0 = V_{13} y_{130} + (V_{13} - V_2)\, y_{13(2)} + (V_{13} - V_5)\, y_{13(5)} + (V_{13} - V_{10}) y_{13(10)} + (V_{13} - V_{12}) y_{13(12)} \quad (4.13)$$

$$0 = V_{14} y_{140} + (V_{14} - V_2)\, y_{14(2)} + (V_{14} - V_5)\, y_{14(5)} \quad (4.14)$$

$$0 = V_{15} y_{150} + (V_{15} - V_1)\, y_{15(1)} \quad (4.15)$$

$$0 = V_{16} y_{160} + (V_{16} - V_1)\, y_{16(1)} + (V_{16} - V_{13})\, y_{16(13)} + (V_{16} - V_{17}) y_{16(17)} + (V_{16} - V_{18})\, y_{16(18)} + (V_{16} - V_{19}) y_{16(19)} \quad (4.16)$$

$$0 = V_{17} y_{170} + (V_{17} - V_{16})\, y_{17(16)} \quad (4.17)$$

$$0 = V_{18} y_{180} + (V_{18} - V_{13})\, y_{18(13)} + (V_{18} - V_{19})\, y_{18(19)} + (V_{18} - V_{20}) y_{18(20)} \quad (4.18)$$

$$0 = V_{19} y_{190} + (V_{19} - V_{16})\, y_{19(16)} + (V_{19} - V_{18})\, y_{19(18)} \quad (4.19)$$

$$0 = V_{20} y_{200} + (V_{20} - V_3)\, y_{20(3)} + (V_{20} - V_4)\, y_{20(4)} + (V_{20} - V_6) y_{20(6)} + (V_{20} - V_{18}) y_{20(18)} \quad (4.20)$$

$$0 = V_{21} y_{210} + (V_{21} - V_4)\, y_{21(4)} \quad (4.21)$$

$$0 = V_{22} y_{220} + (V_{22} - V_3)\, y_{22(3)} \quad (4.22)$$

$$0 = V_{23} y_{230} + (V_{23} - V_4)\, y_{23(4)} + (V_{23} - V_{24})\, y_{23(24)} + (V_{23} - V_{25})\, y_{23(25)} \quad (4.23)$$

$$0 = V_{24} y_{240} + (V_{24} - V_{23})\, y_{24(23)} \quad (4.24)$$

$$0 = V_{25} y_{250} + (V_{25} - V_{23})\, y_{25(23)} + (V_{25} - V_{26})\, y_{25(26)} \quad (4.25)$$

$$0 = V_{26} y_{260} + (V_{26} - V_{25})\, y_{26(25)} + (V_{19} - V_{18})\, y_{19(18)} \quad (4.26)$$

Putting these equations in matrix form gives,

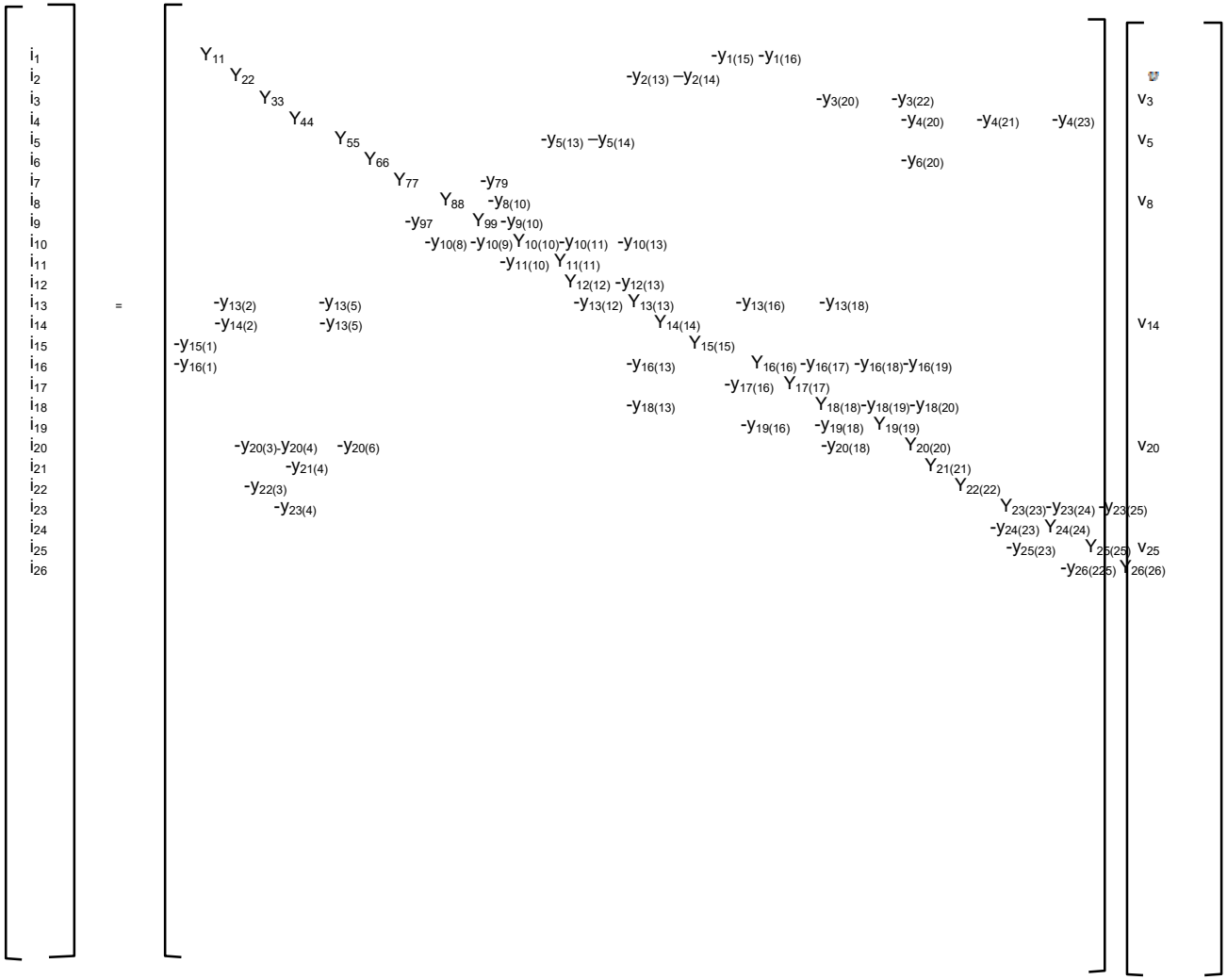

Designating the network admittance in terms of self-admittance of each node gives:

$Y_{11} = Y_{10} + Y_{1(15)} + Y_{1(16)}$
$Y_{22} = Y_{20} + Y_{2(13)} + Y_{2(14)}$
$Y_{33} = Y_{30} + Y_{3(20)} + Y_{3(22)}$
$Y_{44} = Y_{40} + Y_{4(20)} + Y_{4(21)} + Y_{4(23)}$
$Y_{55} = Y_{50} + Y_{5(12)} + Y_{5(14)}$
$Y_{66} = Y_{60} + Y_{6(20)}$
$Y_{77} = Y_{70} + Y_{7(9)}$
$Y_{88} = Y_{80} + Y_{8(10)}$
$Y_{99} = Y_{90} + Y_{9(7)} + Y_{9(10)}$
$Y_{10(10} = Y_{100} + Y_{10(8)} + Y_{10(9)} + Y_{10(11)} + Y_{10(13)}$
$Y_{11(11)} = Y_{100} + Y_{11(10)}$
$Y_{12(12)} = Y_{120} + Y_{12(13)}$
$Y_{13(13)} = Y_{130} + Y_{13(2)} + Y_{13(5)} + Y_{13(10)} + Y_{13(12)}$
$Y_{14(14)} = Y_{140} + Y_{14(2)} + Y_{14(5)}$
$Y_{15(15)} = Y_{150} + Y_{15(1)}$
$Y_{16(16)} = Y_{160} + Y_{16(1)} + Y_{16(13)} + Y_{16(17)} + Y_{16(18)} + Y_{16(19)}$
$Y_{17(17)} = Y_{170} + Y_{17(16)}$
$Y_{18(18)} = Y_{180} + Y_{18(13)} + Y_{18(19)} + Y_{18(20)}$
$Y_{19(19)} = Y_{190} + Y_{19(16)} + Y_{19(18)}$
$Y_{20(20)} = Y_{200} + Y_{20(3)} + Y_{20(4)} + Y_{20(6)} + Y_{20(18)}$
$Y_{21(21)} = Y_{210} + Y_{21(4)}$
$Y_{22(22)} = Y_{220} + Y_{22(3)}$
$Y_{23(23)} = Y_{230} + Y_{23(4)}\ Y_{23(24)} + Y_{23(25)}$
$Y_{24(24)} = Y_{240} + Y_{24(23)}$
$Y_{25(25)} = Y_{250} + Y_{25(23)} + Y_{25(26)}$
$Y_{26(26)} = Y_{260} + Y_{26(25)} + Y_{19(18)}$

$Y_{12} = Y_{21} + Y_{12}$
$Y_{13} = Y_{31} + Y_{13}$
etc.

4.2 Derivation of Proposed National Grid Injected Current Equations

Figure 4.2 shows the Proposed 330KV Nigeria power network.

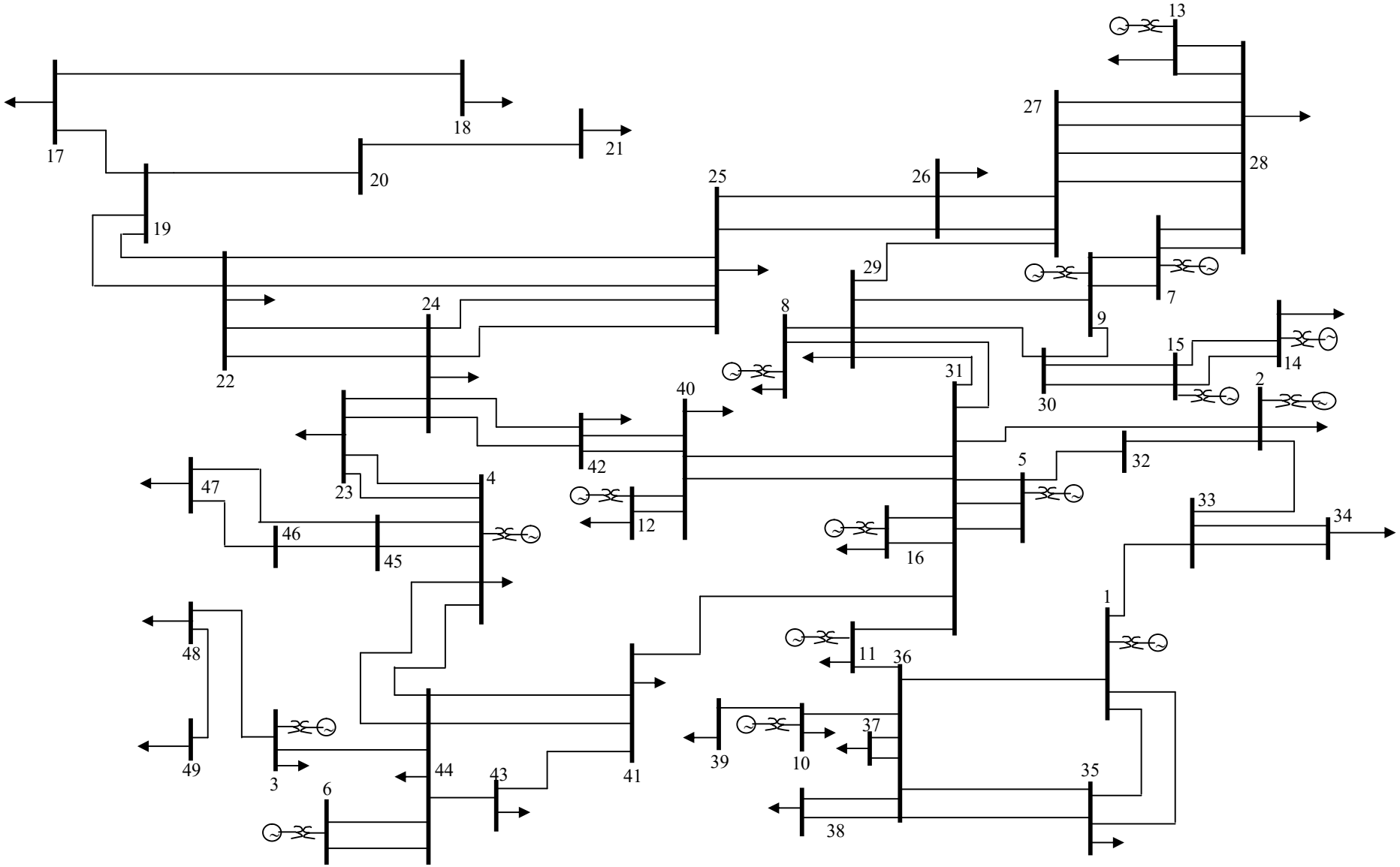

Figure 4.2 Proposed 330KV Nigeria Power Network (16machines-49 Bus System)

From figure 4.2, the net injected current into the Network are given as follows:

$$i_1 = V_1y_{10} + (V_1 - V_{33})\, y_{1(33)} + (V_1 - V_{35})\, y_{1(35)} + (V_1 - V_{36})y_{1(36)} \quad (4.27)$$

$$i_2 = V_2y_{20} + (V_2 - V_{31})\, y_{2(31)} + (V_2 - V_{32})\, y_{2(32)} + (V_2 - V_{33})y_{2(33)} \quad (4.28)$$

$$i_3 = V_3y_{30} + (V_3 - V_{44})\, y_{3(44)} + (V_3 - V_{48})\, y_{3(48)} \quad (4.29)$$

$$i_4 = V_4y_{40} + (V_4 - V_{23})\, y_{4(23)} + (V_4 - V_{44})\, y_{4(44)} + (V_4 - V_{45})y_{4(45)} \quad (4.30)$$

$$i_5 = V_5y_{50} + (V_5 - V_{31})\, y_{5(31)} + (V_5 - V_{32})\, y_{5(32)} \quad (4.31)$$

$$i_6 = V_6y_{60} + (V_6 - V_{44})\, y_{6(44)} \quad (4.32)$$

$$i_7 = V_7y_{70} + (V_7 - V_9)\, y_{79} + (V_7 - V_{28})\, y_{7(28)} \quad (4.33)$$

$$i_8 = V_8y_{80} + (V_8 - V_{29})\, y_{8(29)} \quad (4.34)$$

$$i_9 = V_9y_{90} + (V_9 - V_7)\, y_{97} + (V_9 - V_{29})\, y_{9(29)} + (V_9 - V_{30})y_{9(30)} \quad (4.35)$$

$$i_{10} = V_{10}y_{100} + (V_{10} - V_{36})\, y_{10(36)} + (V_{10} - V_{39})\, y_{10(39)} \quad (4.36)$$

$$i_{11} = V_{11}y_{110} + (V_{11} - V_{31})\, y_{11(31)} + (V_{11} - V_{36})\, y_{11(36)} \quad (4.37)$$

$$i_{12} = V_{12}y_{120} + (V_{12} - V_{40})\, y_{12(40)} \quad (4.38)$$

$$i_{13} = V_{13}y_{130} + (V_{13} - V_{28})\, y_{13(28)} \quad (4.39)$$

$$i_{14} = V_{14}y_{140} + (V_{14} - V_{15})\, y_{14(15)} \quad (4.40)$$

$$i_{15} = V_{15}y_{150} + (V_{15} - V_{14})\, y_{15(14)} + (V_{15} - V_{30})\, y_{15(30)} \quad (4.41)$$

$$i_{16} = V_{16}y_{160} + (V_{16} - V_{31})\, y_{16(31)} \quad (4.42)$$

$$0 = V_{17}y_{170} + (V_{17} - V_{18})\, y_{17(18)} + (V_{17} - V_{19})\, y_{17(19)} \quad (4.43)$$

$$0 = V_{18}y_{180} + (V_{18} - V_{17})\, y_{18(17)} \quad (4.44)$$

$$0 = V_{19}y_{190} + (V_{19} - V_{17})\, y_{19(17)} + (V_{19} - V_{20})\, y_{19(20)} + (V_{19} - V_{22})y_{19(22)} \quad (4.45)$$

$$0 = V_{20}y_{200} + (V_{20} - V_{19})\, y_{20(19)} + (V_{20} - V_{21})\, y_{20(21)} \quad (4.46)$$

$$0 = V_{21}y_{210} + (V_{21} - V_{20})\, y_{21(20)} \quad (4.47)$$

$$0 = V_{22}y_{220} + (V_{22} - V_{19})\, y_{22(19)} + (V_{22} - V_{24})\, y_{22(24)} + (V_{22} - V_{25})y_{22(25)} \quad (4.48)$$

$$0 = V_{23}y_{230} + (V_{23} - V_4)\, y_{23(4)} + (V_{23} - V_{24})\, y_{23(24)} \quad (4.49)$$

$$0 = V_{24}y_{240} + (V_{24} - V_{22})\, y_{24(22)} + (V_{24} - V_{23})\, y_{24(23)} + (V_{24} - V_{25})y_{24(25)}$$

$$+ (V_{24} - V_{42})y_{24(42)} \quad (4.50)$$

$$0 = V_{25}y_{250} + (V_{25} - V_{22})\, y_{25(22)} + (V_{25} - V_{24})\, y_{25(24)} + (V_{25} - V_{26})y_{25(26)} \quad (4.51)$$

$$0 = V_{26}y_{260} + (V_{26} - V_{25})\, y_{26(25)} + (V_{26} - V_{27})\, y_{26(27)} \quad (4.52)$$

$$0 = V_{27}y_{270} + (V_{27} - V_{26})\, y_{27(26)} + (V_{27} - V_{28})\, y_{27(28)} + (V_{27} - V_{29})y_{27(29)} \quad (4.53)$$

$$0 = V_{28}y_{280} + (V_{28} - V_{7})\, y_{28(7)} + (V_{28} - V_{13})\, y_{28(13)} + (V_{28} - V_{27})y_{28(27)} \quad (4.54)$$

$$0 = V_{29}y_{290} + (V_{29} - V_{8})\, y_{29(8)} + (V_{29} - V_{9})\, y_{29(9)} + (V_{29} - V_{27})y_{29(27)}$$
$$+ (V_{29} - V_{30})\, y_{29(30)} + (V_{29} - V_{31})y_{29(31)} \quad (4.55)$$

$$0 = V_{30}y_{300} + (V_{30} - V_{9})\, y_{30(9)} + (V_{30} - V_{15})\, y_{30(15)} + (V_{30} - V_{29})y_{30(29)} \quad (4.56)$$

$$0 = V_{31}y_{310} + (V_{31} - V_{2})\, y_{31(2)} + (V_{31} - V_{5})\, y_{31(5)} + (V_{31} - V_{11})y_{31(11)}$$
$$+ (V_{31} - V_{29})\, y_{31\,(29)} + (V_{31} - V_{40})y_{31(40)} + (V_{31} - V_{41})y_{31(41)} \quad (4.57)$$

$$0 = V_{32}y_{320} + (V_{32} - V_{2})\, y_{32(2)} + (V_{32} - V_{5})\, y_{32(5)} \quad (4.58)$$

$$0 = V_{33}y_{330} + (V_{33} - V_{1})\, y_{33(1)} + (V_{33} - V_{2})\, y_{33(2)} + (V_{33} - V_{34})y_{33(34)} \quad (4.59)$$

$$0 = V_{34}y_{340} + (V_{34} - V_{33})\, y_{34(33)} \quad (4.60)$$

$$0 = V_{35}y_{350} + (V_{35} - V_{1})\, y_{35(1)} + (V_{35} - V_{36})\, y_{35(36)} \quad (4.61)$$

$$0 = V_{36}y_{360} + (V_{36} - V_{1})\, y_{36(1)} + (V_{36} - V_{10})\, y_{36(10)} + (V_{36} - V_{11})y_{36(11)}$$
$$+ (V_{36} - V_{35})\, y_{36(35)} + (V_{36} - V_{37})\, y_{36(37)} + (V_{36} - V_{38})y_{36(38)} \quad (4.62)$$

$$0 = V_{37}y_{370} + (V_{37} - V_{36})\, y_{37(36)} \quad (4.63)$$

$$0 = V_{38}y_{380} + (V_{38} - V_{36})\, y_{38(36)} \quad (4.64)$$

$$0 = V_{39}y_{390} + (V_{39} - V_{10})\, y_{39(10)} \quad (4.65)$$

$$0 = V_{40}y_{400} + (V_{40} - V_{12})\, y_{40(12)} + (V_{40} - V_{31})\, y_{40(31)} + (V_{40} - V_{42})y_{40(42)} \quad (4.66)$$

$$0 = V_{41}y_{410} + (V_{41} - V_{31})\, y_{41(31)} + (V_{41} - V_{43})\, y_{41(43)} + (V_{41} - V_{44})y_{41(44)} \quad (4.67)$$

$$0 = V_{42}y_{420} + (V_{42} - V_{24})\, y_{42(24)} + (V_{42} - V_{40})\, y_{42(40)} \quad (4.68)$$

$$0 = V_{43}y_{430} + (V_{43} - V_{41})\, y_{43(41)} + (V_{43} - V_{44})\, y_{43(44)} \quad (4.69)$$

$$0 = V_{44}y_{440} + (V_{44} - V_{3})\, y_{44(3)} + (V_{44} - V_{4})\, y_{44(4)} + (V_{44} - V_{6})y_{44(6)}$$
$$+ (V_{44} - V_{41})\, y_{44(41)} + (V_{44} - V_{43})\, y_{44(43)} \quad (4.70)$$

$$0 = V_{45}y_{450} + (V_{45} - V_{4})\, y_{45(4)} + (V_{45} - V_{46})\, y_{45(46)} + (V_{45} - V_{47})y_{45(47)} \quad (4.71)$$

$$0 = V_{46}y_{460} + (V_{46} - V_{45})\, y_{46(45)} + (V_{46} - V_{47})\, y_{46(47)} \quad (4.72)$$

$$0 = V_{47}y_{470} + (V_{47} - V_{45})\, y_{47(45)} + (V_{47} - V_{46})\, y_{47(46)} \quad (4.73)$$

$$0 = V_{48}y_{480} + (V_{48} - V_{3})\, y_{48(3)} + (V_{48} - V_{49})\, y_{48(49)} \quad (4.74)$$

$$0 = V_{49}y_{490} + (V_{49} - V_{48})\, y_{49(48)} \quad (4.75)$$

Putting these equations in matrix form gives,

Designating network admittance in terms of self-admittance of each node gives:

$$Y_{11} = Y_{10} + Y_{1(33)} + Y_{1(35)} + Y_{1(36)}$$

$$Y_{22} = Y_{20} + Y_{2(31)} + Y_{2(32)} + Y_{2(36)}$$

$$Y_{33} = Y_{30} + Y_{3(44)} + Y_{4(48)}$$

$$Y_{44} = Y_{40} + Y_{4(23)} + Y_{4(44)} + Y_{4(45)}$$

$$Y_{55} = Y_{50} + Y_{5(31)} + Y_{5(32)}$$

$$Y_{66} = Y_{60} + Y_{6(44)}$$

$$Y_{77} = Y_{70} + Y_{79} + Y_{7(28)}$$

$$Y_{88} = Y_{80} + Y_{8(29)}$$

$$Y_{99} = Y_{90} + Y_{97} + Y_{9(29)} + Y_{9(30)}$$

$$Y_{10(10)} = Y_{100} + Y_{10(36)} + Y_{10(39)}$$

$$Y_{11(11)} = Y_{110} + Y_{11(31)} + Y_{11(36)}$$

$$Y_{12(12)} = Y_{120} + Y_{12(40)}$$

$$Y_{13(13)} = Y_{130} + Y_{13(28)}$$

$$Y_{14(14)} = Y_{140} + Y_{14(15)}$$

$$Y_{15(15)} = Y_{150} + Y_{15(14)} + Y_{15(30)}$$

$$Y_{16(16)} = Y_{160} + Y_{16(31)}$$

$$Y_{17(17)} = Y_{170} + Y_{17(18)} + Y_{17(19)}$$

$$Y_{18(18)} = Y_{180} + Y_{18(17)}$$

$$Y_{19(19)} = Y_{190} + Y_{19(17)} + Y_{19(20)} + Y_{19(22)}$$

$$Y_{20(200} = Y_{200} + Y_{20(19)} + Y_{20(21)}$$

$$Y_{21(21)} = Y_{210} + Y_{21(20)}$$

$$Y_{22(22)} = Y_{220} + Y_{22(19)} + Y_{22(22)} + Y_{22(25)}$$

$$Y_{23(23)} = Y_{230} + Y_{23(4)} + Y_{23(34)}$$

$$Y_{24(24)} = Y_{240} + Y_{24(22)} + Y_{24(23)} + Y_{24(45)} + Y_{24(42)}$$

$$Y_{25(25)} = Y_{250} + Y_{25(22)} + Y_{25(24)} + Y_{25(26)}$$

$$Y_{26(26)} = Y_{260} + Y_{26(25)} + Y_{26(27)}$$

$$Y_{27(27)} = Y_{270} + Y_{27(26)} + Y_{27(28)} + Y_{27(29)}$$

$Y_{28(28)} = Y_{280} + Y_{28(7)} + Y_{28(13)} + Y_{28(27)}$

$Y_{29(29)} = Y_{290} + Y_{29(8)} + Y_{29(9)} + Y_{29(27)} + Y_{29(30)} + Y_{29(31)}$

$Y_{30(30} = Y_{300} + Y_{30(9)} + Y_{30(15)} + Y_{31(11)} + Y_{31(29)}$

$Y_{31(31)} = Y_{310} + Y_{31(2)} + Y_{31(5)} + Y_{31(11)} + Y_{31(29)} + Y_{31(40)} + Y_{31(41)}$

$Y_{32(32)} = Y_{320} + Y_{32(2)} + Y_{32(5)}$

$Y_{33(33)} = Y_{330} + Y_{33(1)} + Y_{33(2)} + Y_{33(34)}$

$Y_{34(34)} = Y_{340} + Y_{34(33)}$

$Y_{35(35)} = Y_{350} + Y_{35(1)} + Y_{35(36)}$

$Y_{36(36)} = Y_{360} + Y_{36(1)} + Y_{36(10)} + Y_{36(11)} + Y_{36(35)} + Y_{36(37)} + Y_{36(38)}$

$Y_{37(37)} = Y_{370} + Y_{37(36)}$

$Y_{38(38)} = Y_{380} + Y_{38(36)}$

$Y_{39(39)} = Y_{390} + Y_{39(10)}$

$Y_{40(40)} = Y_{400} + Y_{40(12)} + Y_{40(31)} + Y_{40(42)}$

$Y_{41(41)} = Y_{410} + Y_{41(31)} + Y_{41(43)} + Y_{41(44)}$

$Y_{42(42)} = Y_{420} + Y_{42(24)} + Y_{42(40)}$

$Y_{43(43)} = Y_{430} + Y_{43(41)} + Y_{43(44)}$

$Y_{44(44)} = Y_{440} + Y_{44(3)} + Y_{44(4)} + Y_{44(6)} + Y_{44(41)} + Y_{44(43)}$

$Y_{45(45)} = Y_{450} + Y_{45(4)} + Y_{45(46)}\ Y_{45(47)}$

$Y_{46(46)} = Y_{460} + Y_{46(45)} + Y_{46(47)}$

$Y_{47(47)} = Y_{470} + Y_{47(45)} + Y_{47(46)}$

$Y_{48(48)} = Y_{480} + Y_{48(3)} + Y_{48(49)}$

$Y_{49(49)} = Y_{490} + Y_{49(48)}$

The complex electric power injected into the pre-reform network is given as follows:

$$P_1 + jQ_1 = E_1^* + I_1 \quad (4.76)$$

$$P_2 + jQ_2 = E_2^* + I_2 \quad (4.77)$$

$$P_3 + jQ_3 = E_3^* + I_3 \quad (4.78)$$

$$P_4 + jQ_4 = E_4^* + I_4 \quad (4.79)$$

$$P_5 + jQ_5 = E_5^* + I_5 \quad (4.80)$$

$$P_6 + jQ_6 = E_6^* + I_6 \quad (4.81)$$

$$P_7 + jQ_7 = E_7^* + I_7 \quad (4.82)$$

$$P_8 + jQ_8 = E_8^* + I_8 \quad (4.83)$$

The complex electric power injected into the post-reform network is given as follows:

$$P_1 + jQ_1 = E_1^* + I_1 \quad (4.84)$$

$$P_2 + jQ_2 = E_2^* + I_2 \quad (4.85)$$

$$P_3 + jQ_3 = E_3^* + I_3 \quad (4.86)$$

$$P_4 + jQ_4 = E_4^* + I_4 \quad (4.87)$$

$$P_5 + jQ_5 = E_5^* + I_5 \quad (4.88)$$

$$P_6 + jQ_6 = E_6^* + I_6 \quad (4.89)$$

$$P_7 + jQ_7 = E_7^* + I_7 \quad (4.90)$$

$$P_8 + jQ_8 = E_8^* + I_8 \quad (4.91)$$

$$P_9 + jQ_9 = E_9^* + I_9 \quad (4.92)$$

$$P_{10} + jQ_{10} = E_{10}^* + I_{10} \quad (4.93)$$

$$P_{11} + jQ_{11} = E_{11}^* + I_{11} \quad (4.94)$$

$$P_{12} + jQ_{12} = E_{12}^* + I_{12} \quad (4.95)$$

$$P_{13} + jQ_{13} = E_{13}^* + I_{13} \quad (4.96)$$

$$P_{14} + jQ_{14} = E_{14}^* + I_{14} \quad (4.98)$$

$$P_{15} + jQ_{15} = E_{15}^* + I_{15} \quad (4.99)$$

$$P_{16} + jQ_{16} = E_{16}^* + I_{16} \quad (4.100)$$

The electric power output of each existing grid machine as functions of the angular positions of other machines in the network is given as follows:

$$P_1 = E_1^2 Y_{11}\cos\theta_{11} + E_1E_2Y_{12}\cos(\theta_{12} - \delta_1 + \delta_2) + E_1E_3Y_{13}\cos(\theta_{13} - \delta_1 + \delta_3) + E_1E_4Y_{14}\cos(\theta_{14} - \delta_1 + \delta_4) + E_1E_5Y_{15}\cos(\theta_{15} - \delta_1 + \delta_5) + E_1E_6Y_{16}\cos(\theta_{16} - \delta_1 + \delta_6) + E_1E_7Y_{17}\cos(\theta_{17} - \delta_1 + \delta_7) + E_1E_8Y_{18}\cos(\theta_{18} - \delta_1 + \delta_8)$$

(4.101)

$$P_2 = E_2^2 Y_{22}\cos\theta_{22} + E_2E_1Y_{21}\cos(\theta_{21} - \delta_2 \div \delta_1) + E_2E_3Y_{23}\cos(\theta_{23} - \delta_2 + \delta_3) + E_2E_4Y_{24}\cos(\theta_{24} - \delta_2 + \delta_4) + E_2E_5Y_{25}\cos(\theta_{25} - \delta_2 + \delta_5) + E_2E_6Y_{26}\cos(\theta_{26} - \delta_2 + \delta_6) + E_2E_7Y_{27}\cos(\theta_{27} - \delta_2 + \delta_7) + E_2E_8Y_{28}\cos(\theta_{28} - \delta_2 + \delta_8) \quad (4.101)$$

$$P_3 = E_3^2 Y_{33}\cos\theta_{33} + E_3E_1Y_{31}\cos(\theta_{31} - \delta_3 \div \delta_1) + E_3E_2Y_{32}\cos(\theta_{32} - \delta_3 + \delta_2) + E_3E_4Y_{34}\cos(\theta_{34} - \delta_3 + \delta_4) + E_3E_5Y_{35}\cos(\theta_{35} - \delta_3 + \delta_5) + E_3E_6Y_{36}\cos(\theta_{36} - \delta_3 + \delta_6) + E_3E_7Y_{37}\cos(\theta_{37} - \delta_3 + \delta_7) + E_3E_8Y_{38}\cos(\theta_{38} - \delta_3 + \delta_8) \quad (4.102)$$

$$P_4 = E_4^2 Y_{44}\cos\theta_{44} + E_4E_1Y_{41}\cos(\theta_{41} - \delta_4 + \delta_1) + E_4E_2Y_{42}\cos(\theta_{42} - \delta_4 + \delta_2) + E_4E_3Y_{43}\cos(\theta_{43} - \delta_4 + \delta_3) + E_4E_5Y_{45}\cos(\theta_{45} - \delta_4 + \delta_5) + E_4E_6Y_{46}\cos(\theta_{46} - \delta_4 + \delta_6) + E_4E_7Y_{47}\cos(\theta_{47} - \delta_4 + \delta_7) + E_4E_8Y_{48}\cos(\theta_{48} - \delta_4 + \delta_8) \quad (4.103)$$

$$P_5 = E_5^2 Y_{55}\cos\theta_{55} + E_5E_1Y_{51}\cos(\theta_{51} - \delta_5 \div \delta_1) + E_5E_2Y_{52}\cos(\theta_{52} - \delta_5 + \delta_2) + E_5E_3Y_{53}\cos(\theta_{53} - \delta_5 + \delta_3) + E_5E_4Y_{54}\cos(\theta_{54} - \delta_5 + \delta_4) + E_5E_6Y_{56}\cos(\theta_{56} - \delta_5 + \delta_6) + E_5E_7Y_{57}\cos(\theta_{57} - \delta_5 + \delta_7) + E_5E_8Y_{58}\cos(\theta_{58} - \delta_5 + \delta_8) \quad (4.104)$$

$$P_6 = E_6^2 Y_{66}\cos\theta_{66} + E_6E_1Y_{61}\cos(\theta_{61} - \delta_6 \div \delta_1) + E_6E_2Y_{62}\cos(\theta_{62} - \delta_6 + \delta_2) + E_6E_3Y_{63}\cos(\theta_{63} - \delta_6 + \delta_3) + E_6E_4Y_{64}\cos(\theta_{64} - \delta_6 + \delta_4) + E_6E_5Y_{65}\cos(\theta_{65} - \delta_6 + \delta_5) + E_6E_7Y_{67}\cos(\theta_{67} - \delta_6 + \delta_7) + E_6E_8Y_{68}\cos(\theta_{68} - \delta_6 + \delta_8) \quad (4.105)$$

$$P_7 = E_7^2 Y_{77}\cos\theta_{77} + E_7E_1Y_{71}\cos(\theta_{71} - \delta_7 \div \delta_1) + E_7E_2Y_{72}\cos(\theta_{72} - \delta_7 + \delta_2) + E_7E_3Y_{73}\cos(\theta_{73} - \delta_7 + \delta_3) + E_7E_4Y_{74}\cos(\theta_{74} - \delta_7 + \delta_4) + E_7E_5Y_{75}\cos(\theta_{75} - \delta_7 + \delta_5) + E_7E_6Y_{76}\cos(\theta_{76} - \delta_7 + \delta_6) + E_7E_8Y_{78}\cos(\theta_{78} - \delta_7 + \delta_8) \quad (4.106)$$

$$P_8 = E_8^2 Y_{88}\cos\theta_{88} + E_8E_1Y_{81}\cos(\theta_{81} - \delta_8 \div \delta_1) + E_8E_2Y_{82}\cos(\theta_{82} - \delta_8 + \delta_2) + E_8E_3Y_{83}\cos(\theta_{83} - \delta_8 + \delta_3) + E_8E_4Y_{84}\cos(\theta_{84} - \delta_8 + \delta_4)$$

$$+E_8E_5Y_{85}\cos(\theta_{85}-\delta_8+\delta_5)+E_8E_6Y_{86}\cos(\theta_{86}-\delta_8+\delta_6)$$
$$+E_8E_7Y_{87}\cos(\theta_{87}-\delta_8+\delta_7) \quad (4.107)$$

The electric power output of each proposed grid machine as functions of the angular positions of other machines in the network is given as follows:

$$P_1=E_1^2Y_{11}\cos\theta_{11}+E_1E_2Y_{12}\cos(\theta_{12}-\delta_1+\delta_2)+E_1E_3Y_{13}\cos(\theta_{13}-\delta_1+\delta_3)$$
$$+E_1E_4Y_{14}\cos(\theta_{14}-\delta_1+\delta_4)+E_1E_5Y_{15}\cos(\theta_{15}-\delta_1+\delta_5)$$
$$+E_1E_6Y_{16}\cos(\theta_{16}-\delta_1+\delta_6)+E_1E_7Y_{17}\cos(\theta_{17}-\delta_1+\delta_7)$$
$$+E_1E_8Y_{18}\cos(\theta_{18}-\delta_1+\delta_8)+E_1E_9Y_{19}\cos(\theta_{19}-\delta_1+\delta_9)$$
$$+E_1E_{10}Y_{1(10)}\cos(\theta_{1(10)}-\delta_1+\delta_{10})+E_1E_{11}Y_{1(11)}\cos(\theta_{1(11)}-\delta_1+\delta_{11})$$
$$+E_1E_{12}Y_{1(12)}\cos(\theta_{1(12)}-\delta_1+\delta_{12})+E_1E_{13}Y_{1(13)}\cos(\theta_{1(13)}-\delta_1+\delta_{13})$$
$$+E_1E_{14}Y_{1(14)}\cos(\theta_{1(14)}-\delta_1+\delta_{14})+E_1E_{15}Y_{1(15)}\cos(\theta_{1(15)}-\delta_1+\delta_{15})+$$
$$E_1E_{16}Y_{1(16)}\cos(\theta_{1(16)}-\delta_1+\delta_{16})$$

(4.108)

$$P_2=E_2^2Y_{22}\cos\theta_{22}+E_2E_1Y_{21}\cos(\theta_{21}-\delta_2+\delta_1)+E_2E_3Y_{23}\cos(\theta_{23}-\delta_2+\delta_3)$$
$$+E_2E_4Y_{24}\cos(\theta_{24}-\delta_2+\delta_4)+E_2E_5Y_{25}\cos(\theta_{25}-\delta_2+\delta_5)$$
$$+E_2E_6Y_{26}\cos(\theta_{26}-\delta_2+\delta_6)+E_2E_7Y_{27}\cos(\theta_{27}-\delta_2+\delta_7)$$
$$+E_2E_8Y_{28}\cos(\theta_{28}-\delta_2+\delta_8)+E_2E_9Y_{29}\cos(\theta_{29}-\delta_2+\delta_9)$$
$$+E_2E_{10}Y_{2(10)}\cos(\theta_{2(10)}-\delta_2+\delta_{10})+E_2E_{11}Y_{2(11)}\cos(\theta_{2(11)}-\delta_2+\delta_{11})$$
$$+E_2E_{12}Y_{2(12)}\cos(\theta_{2(12)}-\delta_2+\delta_{12})+E_2E_{13}Y_{2(13)}\cos(\theta_{2(13)}-\delta_2+\delta_{13})$$
$$+E_2E_{14}Y_{2(14)}\cos(\theta_{2(14)}-\delta_2+\delta_{14})+E_2E_{15}Y_{2(15)}\cos(\theta_{2(15)}-\delta_2+\delta_{15})+$$
$$E_2E_{16}Y_{2(16)}\cos(\theta_{2(16)}-\delta_2+\delta_{16})$$

(4.109)

$$P_3=E_3^2Y_{33}\cos\theta_{33}+E_3E_1Y_{31}\cos(\theta_{31}-\delta_3+\delta_1)+E_3E_2Y_{32}\cos(\theta_{32}-\delta_3+\delta_2)$$
$$+E_3E_4Y_{34}\cos(\theta_{34}-\delta_3+\delta_4)+E_3E_5Y_{35}\cos(\theta_{35}-\delta_3+\delta_5)$$
$$+E_3E_6Y_{36}\cos(\theta_{36}-\delta_3+\delta_6)+E_3E_7Y_{37}\cos(\theta_{37}-\delta_3+\delta_7)$$
$$+E_3E_8Y_{38}\cos(\theta_{38}-\delta_3+\delta_8)+E_3E_9Y_{39}\cos(\theta_{39}-\delta_3+\delta_9)$$
$$+E_3E_{10}Y_{3(10)}\cos(\theta_{3(10)}-\delta_3+\delta_{10})+E_3E_{11}Y_{3(11)}\cos(\theta_{3(11)}-\delta_3+\delta_{11})$$

$$+E_3E_{12}Y_{3(12)}\cos(\theta_{3(12)}-\delta_3+\delta_{12})+E_3E_{13}Y_{3(13)}\cos(\theta_{3(13)}-\delta_3+\delta_{13})$$
$$+E_3E_{14}Y_{3(14)}\cos(\theta_{3(14)}-\delta_3+\delta_{14})+E_3E_{15}Y_{3(15)}\cos(\theta_{3(15)}-\delta_3+\delta_{15})+$$
$$E_3E_{16}Y_{3(16)}\cos(\theta_{3(16)}-\delta_3+\delta_{16}) \quad (4.110)$$

$$P_4=E_4^2Y_{44}\cos\theta_{44}+E_4E_1Y_{41}\cos(\theta_{41}-\delta_4+\delta_1)+E_4E_2Y_{42}\cos(\theta_{42}-\delta_4+\delta_2)$$
$$+E_4E_3Y_{43}\cos(\theta_{43}-\delta_4+\delta_3)+E_4E_5Y_{45}\cos(\theta_{45}-\delta_4+\delta_5)$$
$$+E_4E_6Y_{46}\cos(\theta_{46}-\delta_4+\delta_6)+E_4E_7Y_{47}\cos(\theta_{47}-\delta_4+\delta_7)$$
$$+E_4E_8Y_{48}\cos(\theta_{48}-\delta_4+\delta_8)+E_4E_9Y_{49}\cos(\theta_{49}-\delta_4+\delta_9)$$
$$+E_4E_{10}Y_{4(10)}\cos(\theta_{4(10)}-\delta_4+\delta_{10})+E_4E_{11}Y_{4(11)}\cos(\theta_{4(11)}-\delta_4+\delta_{11})$$
$$+E_4E_{12}Y_{4(12)}\cos(\theta_{4(12)}-\delta_4+\delta_{12})+E_4E_{13}Y_{4(13)}\cos(\theta_{4(13)}-\delta_4+\delta_{13})$$
$$+E_4E_{14}Y_{4(14)}\cos(\theta_{4(14)}-\delta_4+\delta_{14})+E_4E_{15}Y_{4(15)}\cos(\theta_{4(15)}-\delta_4+\delta_{15})+$$
$$E_4E_{16}Y_{4(16)}\cos(\theta_{4(16)}-\delta_4+\delta_{16})$$
(4.111)

$$P_5=E_5^2Y_{55}\cos\theta_{55}+E_5E_1Y_{51}\cos(\theta_{51}-\delta_5+\delta_1)+E_5E_2Y_{52}\cos(\theta_{52}-\delta_5+\delta_2)$$
$$+E_5E_3Y_{53}\cos(\theta_{53}-\delta_5+\delta_3)+E_5E_4Y_{54}\cos(\theta_{54}-\delta_5+\delta_4)$$
$$+E_5E_6Y_{56}\cos(\theta_{56}-\delta_5+\delta_6)+E_5E_7Y_{57}\cos(\theta_{57}-\delta_5+\delta_7)$$
$$+E_5E_8Y_{58}\cos(\theta_{58}-\delta_5+\delta_8)+E_5E_9Y_{59}\cos(\theta_{59}-\delta_5+\delta_9)$$
$$+E_5E_{10}Y_{5(10)}\cos(\theta_{5(10)}-\delta_5+\delta_{10})+E_5E_{11}Y_{5(11)}\cos(\theta_{5(11)}-\delta_5+\delta_{11})$$
$$+E_5E_{12}Y_{5(12)}\cos(\theta_{5(12)}-\delta_5+\delta_{12})+E_5E_{13}Y_{5(13)}\cos(\theta_{5(13)}-\delta_5+\delta_{13})$$
$$+E_5E_{14}Y_{5(14)}\cos(\theta_{5(14)}-\delta_5+\delta_{14})+E_5E_{15}Y_{5(15)}\cos(\theta_{5(15)}-\delta_5+\delta_{15})$$
$$+E_5E_{16}Y_{5(16)}\cos(\theta_{5(16)}-\delta_5+\delta_{16}) \quad (4.112)$$

$$P_6=E_6^2Y_{66}\cos\theta_{66}+E_6E_1Y_{61}\cos(\theta_{61}-\delta_6+\delta_1)+E_6E_2Y_{62}\cos(\theta_{62}-\delta_6+\delta_2)$$
$$+E_6E_3Y_{63}\cos(\theta_{63}-\delta_6+\delta_3)+E_6E_4Y_{64}\cos(\theta_{64}-\delta_6+\delta_4)$$
$$+E_6E_5Y_{65}\cos(\theta_{65}-\delta_6+\delta_5)+E_6E_7Y_{67}\cos(\theta_{67}-\delta_6+\delta_7)$$
$$+E_6E_8Y_{68}\cos(\theta_{68}-\delta_6+\delta_8)+E_6E_9Y_{69}\cos(\theta_{69}-\delta_6+\delta_9)$$
$$+E_6E_{10}Y_{6(10)}\cos(\theta_{6(10)}-\delta_6+\delta_{10})+E_6E_{11}Y_{6(11)}\cos(\theta_{6(11)}-\delta_6+\delta_{11})$$
$$+E_6E_{12}Y_{6(12)}\cos(\theta_{6(12)}-\delta_6+\delta_{12})+E_6E_{13}Y_{6(13)}\cos(\theta_{6(13)}-\delta_6+\delta_{13})$$
$$+E_6E_{14}Y_{6(14)}\cos(\theta_{6(14)}-\delta_6+\delta_{14})+E_6E_{15}Y_{6(15)}\cos(\theta_{6(15)}-\delta_6+\delta_{15})$$

$$+E_6E_{16}Y_{6(16)}\cos(\theta_{6(16)}-\delta_6+\delta_{16}) \quad (4.113)$$

$$P_7 = E_7^2Y_{77}\cos\theta_{77}+E_7E_1Y_{71}\cos(\theta_{71}-\delta_7+\delta_1)+E_7E_2Y_{72}\cos(\theta_{72}-\delta_7+\delta_2)$$
$$+E_7E_3Y_{73}\cos(\theta_{73}-\delta_7+\delta_3)+E_7E_4Y_{74}\cos(\theta_{74}-\delta_7+\delta_4)$$
$$+E_7E_5Y_{75}\cos(\theta_{75}-\delta_7+\delta_5)+E_7E_6Y_{76}\cos(\theta_{76}-\delta_7+\delta_6)$$
$$+E_7E_8Y_{78}\cos(\theta_{78}-\delta_7+\delta_8)+E_7E_9Y_{79}\cos(\theta_{79}-\delta_7+\delta_9)$$
$$+E_7E_{10}Y_{7(10)}\cos(\theta_{7(10)}-\delta_7+\delta_{10})+E_7E_{11}Y_{7(11)}\cos(\theta_{7(11)}-\delta_7+\delta_{11})$$
$$+E_7E_{12}Y_{7(12)}\cos(\theta_{7(12)}-\delta_7+\delta_{12})+E_7E_{13}Y_{7(13)}\cos(\theta_{7(13)}-\delta_7+\delta_{13})$$
$$+E_7E_{14}Y_{7(14)}\cos(\theta_{7(14)}-\delta_7+\delta_{14})+E_7E_{15}Y_{7(15)}\cos(\theta_{7(15)}-\delta_7+\delta_{15})$$
$$+E_7E_{16}Y_{7(16)}\cos(\theta_{7(16)}-\delta_7+\delta_{16}) \quad (4.114)$$

$$P_8 = E_8^2Y_{88}\cos\theta_{88}+E_8E_1Y_{81}\cos(\theta_{81}-\delta_8+\delta_1)+E_8E_2Y_{82}\cos(\theta_{82}-\delta_8+\delta_2)$$
$$+E_8E_3Y_{83}\cos(\theta_{83}-\delta_8+\delta_3)+E_8E_4Y_{84}\cos(\theta_{84}-\delta_8+\delta_4)$$
$$+E_8E_5Y_{85}\cos(\theta_{85}-\delta_8+\delta_5)+E_8E_6Y_{86}\cos(\theta_{86}-\delta_8+\delta_6)$$
$$+E_8E_7Y_{87}\cos(\theta_{87}-\delta_8+\delta_7)+E_8E_9Y_{89}\cos(\theta_{89}-\delta_8+\delta_9)$$
$$+E_8E_{10}Y_{8(10)}\cos(\theta_{8(10)}-\delta_8+\delta_{10})+E_8E_{11}Y_{8(11)}\cos(\theta_{8(11)}-\delta_8+\delta_{11})$$
$$+E_8E_{12}Y_{8(12)}\cos(\theta_{8(12)}-\delta_8+\delta_{12})+E_8E_{13}Y_{8(13)}\cos(\theta_{8(13)}-\delta_8+\delta_{13})$$
$$+E_8E_{14}Y_{8(14)}\cos(\theta_{8(14)}-\delta_8+\delta_{14})+E_8E_{15}Y_{8(15)}\cos(\theta_{8(15)}-\delta_8+\delta_{15})$$
$$+E_8E_{16}Y_{8(16)}\cos(\theta_{8(16)}-\delta_8+\delta_{16}) \quad (4.115)$$

$$P_9 = E_9^2Y_{99}\cos\theta_{99}+E_9E_1Y_{91}\cos(\theta_{91}-\delta_9+\delta_1)+E_9E_2Y_{92}\cos(\theta_{92}-\delta_9+\delta_2)$$
$$+E_9E_3Y_{93}\cos(\theta_{93}-\delta_9+\delta_3)+E_9E_4Y_{94}\cos(\theta_{94}-\delta_9+\delta_4)$$
$$+E_9E_5Y_{95}\cos(\theta_{95}-\delta_9+\delta_5)+E_9E_6Y_{96}\cos(\theta_{96}-\delta_9+\delta_6)$$
$$+E_9E_7Y_{97}\cos(\theta_{97}-\delta_9+\delta_7)+E_9E_0Y_{90}\cos(\theta_{90}-\delta_9+\delta_0)$$
$$+E_9E_{10}Y_{9(10)}\cos(\theta_{9(10)}-\delta_9+\delta_{10})+E_9E_{11}Y_{9(11)}\cos(\theta_{9(11)}-\delta_9+\delta_{11})$$
$$+E_9E_{12}Y_{9(12)}\cos(\theta_{9(12)}-\delta_9+\delta_{12})+E_9E_{13}Y_{9(13)}\cos(\theta_{9(13)}-\delta_9+\delta_{13})$$

$$+E_9E_{14}Y_{9(14)}\cos(\theta_{9(14)}-\delta_9+\delta_{14})+E_9E_{15}Y_{9(15)}\cos(\theta_{9(15)}-\delta_9+\delta_{15})+ E_9E_{16}Y_{9(16)}\cos(\theta_{9(16)}-\delta_9+\delta_{16})$$

(4.115)

$$P_{10}=E_{10}^2Y_{(10)(10)}\cos\theta_{(10)(10)}+E_{10}E_1Y_{(10)1}\cos(\theta_{(10)1}-\delta_{10}+\delta_1)+E_{10}E_2Y_{(10)2}\cos(\theta_{(10)2}-\delta_{10}+\delta_2)$$
$$+E_{10}E_3Y_{(10)3}\cos(\theta_{(10)3}-\delta_{10}+\delta_3)+E_{10}E_4Y_{(10)4}\cos(\theta_{(10)4}-\delta_{10}+\delta_4)$$
$$+E_{10}E_5Y_{(10)5}\cos(\theta_{(10)5}-\delta_{10}+\delta_5)+E_{10}E_6Y_{(10)6}\cos(\theta_{(10)6}-\delta_{10}+\delta_6)$$
$$+E_{10}E_7Y_{(10)7}\cos(\theta_{(10)7}-\delta_{10}+\delta_7)+E_{10}E_8Y_{(10)8}\cos(\theta_{(10)8}-\delta_{10}+\delta_8)$$
$$+E_{10}E_9Y_{(10)9}\cos(\theta_{(10)9}-\delta_{10}+\delta_9)+E_{10}E_{11}Y_{10(11)}\cos(\theta_{10(11)}-\delta_{10}+\delta_{11})$$
$$+E_{10}E_{12}Y_{10(12)}\cos(\theta_{10(12)}-\delta_{10}+\delta_{12})+E_{10}E_{13}Y_{10(13)}\cos(\theta_{10(13)}-\delta_{10}+\delta_{13})$$
$$+E_{10}E_{14}Y_{10(14)}\cos(\theta_{10(14)}-\delta_{10}+\delta_{14})+E_{10}E_{15}Y_{10(15)}\cos(\theta_{10(15)}-\delta_{10}+\delta_{15})$$
$$+E_{10}E_{16}Y_{10(16)}\cos(\theta_{10(16)}-\delta_{10}+\delta_{16})$$

(4.116)

$$P_{11}=E_{11}^2Y_{(11)(11)}\cos\theta_{(11)(11)}+E_{11}E_1Y_{(11)1}\cos(\theta_{(11)1}-\delta_{11}+\delta_1)+E_{11}E_2Y_{(11)2}\cos(\theta_{(11)2}-\delta_{11}+\delta_2)$$
$$+E_{11}E_3Y_{(11)3}\cos(\theta_{(11)3}-\delta_{11}+\delta_3)+E_{11}E_4Y_{(11)4}\cos(\theta_{(11)4}-\delta_{11}+\delta_4)$$
$$+E_{11}E_5Y_{(11)5}\cos(\theta_{(11)5}-\delta_{11}+\delta_5)+E_{11}E_6Y_{(11)6}\cos(\theta_{(11)6}-\delta_{11}+\delta_6)$$
$$+E_{11}E_7Y_{(11)7}\cos(\theta_{(11)7}-\delta_{11}+\delta_7)+E_{11}E_0Y_{(10)0}\cos(\theta_{(10)0}-\delta_{10}+\delta_0)$$
$$+E_{10}E_9Y_{(10)9}\cos(\theta_{(10)9}-\delta_{10}+\delta_9)+E_{10}E_{11}Y_{10(11)}\cos(\theta_{10(11)}-\delta_{10}+\delta_{11})$$
$$+E_{10}E_{12}Y_{10(12)}\cos(\theta_{10(12)}-\delta_{10}+\delta_{12})+E_{10}E_{13}Y_{10(13)}\cos(\theta_{10(13)}-\delta_{10}+\delta_{13})$$
$$+E_{10}E_{14}Y_{10(14)}\cos(\theta_{10(14)}-\delta_{10}+\delta_{14})+E_{10}E_{15}Y_{10(15)}\cos(\theta_{10(15)}-\delta_{10}+\delta_{15})$$
$$+E_{10}E_{16}Y_{10(16)}\cos(\theta_{10(16)}-\delta_{10}+\delta_{16})$$

(4.117)

$$P_{12}=E_{12}^2Y_{(12)(12)}\cos\theta_{(12)(12)}+E_{12}E_1Y_{(12)1}\cos(\theta_{(12)1}-\delta_{12}+\delta_1)+E_{12}E_2Y_{(12)2}\cos(\theta_{(12)2}-\delta_{12}+\delta_2)$$
$$+E_{12}E_3Y_{(12)3}\cos(\theta_{(12)3}-\delta_{12}+\delta_3)+E_{12}E_4Y_{(12)4}\cos(\theta_{(12)4}-\delta_{12}+\delta_4)$$
$$+E_{12}E_5Y_{(12)5}\cos(\theta_{(12)5}-\delta_{12}+\delta_5)+E_{12}E_6Y_{(12)6}\cos(\theta_{(12)6}-\delta_{12}+\delta_6)$$
$$+E_{12}E_7Y_{(12)7}\cos(\theta_{(12)7}-\delta_{12}+\delta_7)+E_{12}E_8Y_{(12)8}\cos(\theta_{(12)8}-\delta_{12}+\delta_8)$$
$$+E_{12}E_9Y_{(12)9}\cos(\theta_{(12)9}-\delta_{12}+\delta_9)+E_{12}E_{10}Y_{12(10)}\cos(\theta_{12(10)}-\delta_{12}+\delta_{10})$$
$$+E_{12}E_{11}Y_{12(11)}\cos(\theta_{12(11)}-\delta_{12}+\delta_{11})+E_{12}E_{13}Y_{12(13)}\cos(\theta_{12(13)}-\delta_{12}+\delta_{13})$$
$$+E_{12}E_{14}Y_{12(14)}\cos(\theta_{12(14)}-\delta_{12}+\delta_{14})+E_{12}E_{15}Y_{12(15)}\cos(\theta_{12(15)}-\delta_{12}+\delta_{15})$$

$$+E_{12}E_{16}Y_{12(16)}\cos(\theta_{12(16)}-\delta_{12}+\delta_{16}) \quad (4.118)$$

$$P_{13}=E_{13}^2Y_{(13)(13)}\cos\theta_{(13)(13)}+E_{13}E_1Y_{(13)1}\cos(\theta_{(13)1}-\delta_{13}+\delta_1)+E_{13}E_2Y_{(13)2}\cos(\theta_{(13)2}-\delta_{13}+\delta_2)$$
$$+E_{13}E_3Y_{(13)3}\cos(\theta_{(13)3}-\delta_{13}+\delta_3)+E_{13}E_4Y_{(13)4}\cos(\theta_{(13)4}-\delta_{13}+\delta_4)$$
$$+E_{13}E_5Y_{(13)5}\cos(\theta_{(13)5}-\delta_{13}+\delta_5)+E_{13}E_6Y_{(13)6}\cos(\theta_{(13)6}-\delta_{13}+\delta_6)$$
$$+E_{13}E_7Y_{(13)7}\cos(\theta_{(13)7}-\delta_{13}+\delta_7)+E_{13}E_8Y_{(13)8}\cos(\theta_{(13)8}-\delta_{13}+\delta_8)$$
$$+E_{13}E_9Y_{(13)9}\cos(\theta_{(13)9}-\delta_{13}+\delta_9)+E_{13}E_{11}Y_{13(11)}\cos(\theta_{13(11)}-\delta_{13}+\delta_{11})$$
$$+E_{13}E_{12}Y_{13(12)}\cos(\theta_{13(12)}-\delta_{13}+\delta_{12})+E_{13}E_{14}Y_{13(14)}\cos(\theta_{13(14)}-\delta_{13}+\delta_{14})$$
$$+E_{13}E_{15}Y_{13(15)}\cos(\theta_{13(15)}-\delta_{13}+\delta_{15})+E_{13}E_{16}Y_{13(16)}\cos(\theta_{13(16)}-\delta_{13}+\delta_{16}) \quad (4.119)$$

$$P_{14}=E_{14}^2Y_{(14)(14)}\cos\theta_{(14)(14)}+E_{14}E_1Y_{(14)1}\cos(\theta_{(14)1}-\delta_{14}+\delta_1)+E_{14}E_2Y_{(14)2}\cos(\theta_{(14)2}-\delta_{14}+\delta_2)$$
$$+E_{14}E_3Y_{(14)3}\cos(\theta_{(14)3}-\delta_{14}+\delta_3)+E_{14}E_4Y_{(14)4}\cos(\theta_{(14)4}-\delta_{14}+\delta_4)$$
$$+E_{14}E_5Y_{(14)5}\cos(\theta_{(14)5}-\delta_{14}+\delta_5)+E_{14}E_6Y_{(14)6}\cos(\theta_{(14)6}-\delta_{14}+\delta_6)$$
$$+E_{14}E_7Y_{(14)7}\cos(\theta_{(14)7}-\delta_{14}+\delta_7)+E_{14}E_8Y_{(14)8}\cos(\theta_{(14)8}-\delta_{14}+\delta_8)$$
$$+E_{14}E_9Y_{(14)9}\cos(\theta_{(14)9}-\delta_{14}+\delta_9)+E_{14}E_{10}Y_{14(10)}\cos(\theta_{14(10)}-\delta_{14}+\delta_{10})$$
$$+E_{14}E_{11}Y_{14(11)}\cos(\theta_{14(11)}-\delta_{14}+\delta_{11})+E_{14}E_{12}Y_{14(12)}\cos(\theta_{14(12)}-\delta_{14}+\delta_{12})$$
$$+E_{14}E_{13}Y_{14(13)}\cos(\theta_{14(13)}-\delta_{14}+\delta_{13})+E_{14}E_{15}Y_{14(15)}\cos(\theta_{14(15)}-\delta_{14}+\delta_{15})$$
$$+E_{14}E_{16}Y_{14(16)}\cos(\theta_{14(16)}-\delta_{14}+\delta_{16}) \quad (4.120)$$

$$P_{15}=E_{15}^2Y_{(15)(15)}\cos\theta_{(15)(15)}+E_{15}E_1Y_{(15)1}\cos(\theta_{(15)1}-\delta_{15}+\delta_1)+E_{15}E_2Y_{(15)2}\cos(\theta_{(15)2}-\delta_{15}+\delta_2)$$
$$+E_{15}E_3Y_{(15)3}\cos(\theta_{(15)3}-\delta_{15}+\delta_3)+E_{15}E_4Y_{(15)4}\cos(\theta_{(15)4}-\delta_{15}+\delta_4)$$
$$+E_{15}E_5Y_{(15)5}\cos(\theta_{(15)5}-\delta_{15}+\delta_5)+E_{15}E_6Y_{(15)6}\cos(\theta_{(15)6}-\delta_{15}+\delta_6)$$
$$+E_{15}E_7Y_{(15)7}\cos(\theta_{(15)7}-\delta_{15}+\delta_7)+E_{15}E_8Y_{(15)8}\cos(\theta_{(15)8}-\delta_{15}+\delta_8)$$
$$+E_{15}E_9Y_{(15)9}\cos(\theta_{(15)9}-\delta_{15}+\delta_9)+E_{15}E_{10}Y_{15(10)}\cos(\theta_{15(10)}-\delta_{15}+\delta_{10})$$
$$+E_{15}E_{11}Y_{15(11)}\cos(\theta_{15(11)}-\delta_{15}+\delta_{11})+E_{15}E_{12}Y_{15(12)}\cos(\theta_{15(12)}-\delta_{15}+\delta_{12})$$
$$+E_{15}E_{13}Y_{15(13)}\cos(\theta_{15(13)}-\delta_{15}+\delta_{13})+E_{15}E_{14}Y_{15(14)}\cos(\theta_{15(14)}-\delta_{15}+\delta_{14})$$
$$+E_{15}E_{16}Y_{15(16)}\cos(\theta_{15(16)}-\delta_{15}+\delta_{16}) \quad (4.121)$$

$$P_{16}=E_{16}^2Y_{(16)(16)}\cos\theta_{(16)(16)}+E_{16}E_1Y_{(16)1}\cos(\theta_{(16)1}-\delta_{16}+\delta_1)+E_{16}E_2Y_{(16)2}\cos(\theta_{(16)2}-\delta_{16}+\delta_2)$$

$$+E_{16}E_3Y_{(16)3}\cos(\theta_{(16)3}-\delta_{16}+\delta_3)+E_{16}E_4Y_{(16)4}\cos(\theta_{(16)4}-\delta_{16}+\delta_4)$$
$$+E_{16}E_5Y_{(16)5}\cos(\theta_{(16)5}-\delta_{16}+\delta_5)+E_{16}E_6Y_{(16)6}\cos(\theta_{(16)6}-\delta_{16}+\delta_6)$$
$$+E_{16}E_7Y_{(16)7}\cos(\theta_{(16)7}-\delta_{16}+\delta_7)+E_{16}E_8Y_{(16)8}\cos(\theta_{(16)8}-\delta_{16}+\delta_8)$$
$$+E_{16}E_9Y_{(16)9}\cos(\theta_{(16)9}-\delta_{16}+\delta_9)+E_{16}E_{10}Y_{16(10)}\cos(\theta_{16(10)}-\delta_{16}+\delta_{10})$$
$$+E_{16}E_{11}Y_{16(11)}\cos(\theta_{16(11)}-\delta_{16}+\delta_{11})+E_{16}E_{12}Y_{16(12)}\cos(\theta_{16(12)}-\delta_{15}+\delta_{12})$$
$$+E_{16}E_{13}Y_{16(13)}\cos(\theta_{16(13)}-\delta_{16}+\delta_{13})+E_{16}E_{14}Y_{16(14)}\cos(\theta_{16(14)}-\delta_{16}+\delta_{14})$$
$$+E_{16}E_{15}Y_{16(15)}\cos(\theta_{16(15)}-\delta_{16}+\delta_{15}) \quad (4.122)$$

The rotor swing equations for the existing Network generators are given as follows:

$$M_1\ddot{\delta}_1 = P_{m1}-P_{e1}\left(\delta_1,\delta_2,\delta_3,\delta_4,\delta_5,\delta_6,\delta_7,\delta_8,\dot{\delta}_1,\dot{\delta}_2,\dot{\delta}_3,\dot{\delta}_4,\dot{\delta}_5,\dot{\delta}_6,\dot{\delta}_7,\dot{\delta}_8\right) \quad (4.123)$$
$$M_2\ddot{\delta}_2 = P_{m2}-P_{e2}\left(\delta_1,\delta_2,\delta_3,\delta_4,\delta_5,\delta_6,\delta_7,\delta_8,\dot{\delta}_1,\dot{\delta}_2,\dot{\delta}_3,\dot{\delta}_4,\dot{\delta}_5,\dot{\delta}_6,\dot{\delta}_7,\dot{\delta}_8\right) \quad (4.124)$$
$$M_3\ddot{\delta}_3 = P_{m3}-P_{e3}\left(\delta_1,\delta_2,\delta_3,\delta_4,\delta_5,\delta_6,\delta_7,\delta_8,\dot{\delta}_1,\dot{\delta}_2,\dot{\delta}_3,\dot{\delta}_4,\dot{\delta}_5,\dot{\delta}_6,\dot{\delta}_7,\dot{\delta}_8\right) \quad (4.125)$$
$$M_4\ddot{\delta}_4 = P_{m4}-P_{e4}\left(\delta_1,\delta_2,\delta_3,\delta_4,\delta_5,\delta_6,\delta_7,\delta_8,\dot{\delta}_1,\dot{\delta}_2,\dot{\delta}_3,\dot{\delta}_4,\dot{\delta}_5,\dot{\delta}_6,\dot{\delta}_7,\dot{\delta}_8\right) \quad (4.126)$$
$$M_5\ddot{\delta}_5 = P_{m5}-P_{e5}\left(\delta_1,\delta_2,\delta_3,\delta_4,\delta_5,\delta_6,\delta_7,\delta_8,\dot{\delta}_1,\dot{\delta}_2,\dot{\delta}_3,\dot{\delta}_4,\dot{\delta}_5,\dot{\delta}_6,\dot{\delta}_7,\dot{\delta}_8\right) \quad (4.127)$$
$$M_6\ddot{\delta}_6 = P_{m6}-P_{e6}\left(\delta_1,\delta_2,\delta_3,\delta_4,\delta_5,\delta_6,\delta_7,\delta_8,\dot{\delta}_1,\dot{\delta}_2,\dot{\delta}_3,\dot{\delta}_4,\dot{\delta}_5,\dot{\delta}_6,\dot{\delta}_7,\dot{\delta}_8\right) \quad (4.128)$$
$$M_7\ddot{\delta}_7 = P_{m7}-P_{e7}\left(\delta_1,\delta_2,\delta_3,\delta_4,\delta_5,\delta_6,\delta_7,\delta_8,\dot{\delta}_1,\dot{\delta}_2,\dot{\delta}_3,\dot{\delta}_4,\dot{\delta}_5,\dot{\delta}_6,\dot{\delta}_7,\dot{\delta}_8\right) \quad (4.129)$$
$$M_8\ddot{\delta}_8 = P_{m8}-P_{e8}\left(\delta_1,\delta_2,\delta_3,\delta_4,\delta_5,\delta_6,\delta_7,\delta_8,\dot{\delta}_1,\dot{\delta}_2,\dot{\delta}_3,\dot{\delta}_4,\dot{\delta}_5,\dot{\delta}_6,\dot{\delta}_7,\dot{\delta}_8\right) \quad (4.130)$$

The rotor swing equations for the proposed network generators are given as follows:

$$M_1\ddot{\delta}_1 = P_{m1} \quad P_{e1}\left(\delta_1,\delta_2,\delta_3,\delta_4,\delta_5,\delta_6,\delta_7,\delta_8,\delta_9,\delta_{10},\delta_{11},\delta_{12},\delta_{13},\delta_{14},\delta_{15},\delta_{16},\dot{\delta}_1,\right.$$
$$\left.\dot{\delta}_2,\dot{\delta}_3,\dot{\delta}_4,\dot{\delta}_5,\dot{\delta}_6,\dot{\delta}_7,\dot{\delta}_0,\dot{\delta}_9,\dot{\delta}_{10},\dot{\delta}_{11},\dot{\delta}_{12},\dot{\delta}_{13},\dot{\delta}_{14},\dot{\delta}_{15},\dot{\delta}_{16}\right) \quad (4.131)$$
$$M_2\ddot{\delta}_2 - P_{m2} - P_{e2}\left(\delta_1,\delta_2,\delta_3,\delta_4,\delta_5,\delta_6,\delta_7,\delta_8,\delta_9,\delta_{10},\delta_{11},\delta_{12},\delta_{13},\delta_{14},\delta_{15},\delta_{16},\dot{\delta}_1,\right.$$
$$\left.\dot{\delta}_2,\dot{\delta}_3,\dot{\delta}_4,\dot{\delta}_5,\dot{\delta}_6,\dot{\delta}_7,\dot{\delta}_8,\dot{\delta}_9,\dot{\delta}_{10},\dot{\delta}_{11},\dot{\delta}_{12},\dot{\delta}_{13},\dot{\delta}_{14},\dot{\delta}_{15},\dot{\delta}_{16}\right) \quad (4.132)$$
$$M_3\ddot{\delta}_3 = P_{m3} - P_{e3}\left(\delta_1,\delta_2,\delta_3,\delta_4,\delta_5,\delta_6,\delta_7,\delta_8,\delta_9,\delta_{10},\delta_{11},\delta_{12},\delta_{13},\delta_{14},\delta_{15},\delta_{16},\dot{\delta}_1,\right.$$
$$\left.\dot{\delta}_2,\dot{\delta}_3,\dot{\delta}_4,\dot{\delta}_5,\dot{\delta}_6,\dot{\delta}_7,\dot{\delta}_8,\dot{\delta}_9,\dot{\delta}_{10},\dot{\delta}_{11},\dot{\delta}_{12},\dot{\delta}_{13},\dot{\delta}_{14},\dot{\delta}_{15},\dot{\delta}_{16}\right) \quad (4.133)$$

$$M_4\ddot{\delta}_4 = P_{m4} - P_{e4}\left(\delta_1,\delta_2,\delta_3,\delta_4,\delta_5,\delta_6,\delta_7,\delta_8,\delta_9,\delta_{10},\delta_{11},\delta_{12},\delta_{13},\delta_{14},\delta_{15},\delta_{16},\dot{\delta}_1,\right.$$
$$\left.\dot{\delta}_2,\dot{\delta}_3,\dot{\delta}_4,\dot{\delta}_5,\dot{\delta}_6,\dot{\delta}_7,\dot{\delta}_8,\dot{\delta}_9,\dot{\delta}_{10},\dot{\delta}_{11},\dot{\delta}_{12},\dot{\delta}_{13},\dot{\delta}_{14},\dot{\delta}_{15},\dot{\delta}_{16}\right) \quad (4.134)$$

$$M_5\ddot{\delta}_5 = P_{m5} - P_{e5}\left(\delta_1,\delta_2,\delta_3,\delta_4,\delta_5,\delta_6,\delta_7,\delta_8,\delta_9,\delta_{10},\delta_{11},\delta_{12},\delta_{13},\delta_{14},\delta_{15},\delta_{16},\dot{\delta}_1,\right.$$
$$\left.\dot{\delta}_2,\dot{\delta}_3,\dot{\delta}_4,\dot{\delta}_5,\dot{\delta}_6,\dot{\delta}_7,\dot{\delta}_8,\dot{\delta}_9,\dot{\delta}_{10},\dot{\delta}_{11},\dot{\delta}_{12},\dot{\delta}_{13},\dot{\delta}_{14},\dot{\delta}_{15},\dot{\delta}_{16}\right) \quad (4.135)$$

$$M_6\ddot{\delta}_6 = P_{m6} - P_{e6}\left(\delta_1,\delta_2,\delta_3,\delta_4,\delta_5,\delta_6,\delta_7,\delta_8,\delta_9,\delta_{10},\delta_{11},\delta_{12},\delta_{13},\delta_{14},\delta_{15},\delta_{16},\dot{\delta}_1,\right.$$
$$\left.\dot{\delta}_2,\dot{\delta}_3,\dot{\delta}_4,\dot{\delta}_5,\dot{\delta}_6,\dot{\delta}_7,\dot{\delta}_8,\dot{\delta}_9,\dot{\delta}_{10},\dot{\delta}_{11},\dot{\delta}_{12},\dot{\delta}_{13},\dot{\delta}_{14},\dot{\delta}_{15},\dot{\delta}_{16}\right) \quad (4.136)$$

$$M_7\ddot{\delta}_7 = P_{m7} - P_{e7}\left(\delta_1,\delta_2,\delta_3,\delta_4,\delta_5,\delta_6,\delta_7,\delta_8,\delta_9,\delta_{10},\delta_{11},\delta_{12},\delta_{13},\delta_{14},\delta_{15},\delta_{16},\dot{\delta}_1,\right.$$
$$\left.\dot{\delta}_2,\dot{\delta}_3,\dot{\delta}_4,\dot{\delta}_5,\dot{\delta}_6,\dot{\delta}_7,\dot{\delta}_8,\dot{\delta}_9,\dot{\delta}_{10},\dot{\delta}_{11},\dot{\delta}_{12},\dot{\delta}_{13},\dot{\delta}_{14},\dot{\delta}_{15},\dot{\delta}_{16}\right) \quad (4.137)$$

$$M_8\ddot{\delta}_8 = P_{m8} - P_{e8}\left(\delta_1,\delta_2,\delta_3,\delta_4,\delta_5,\delta_6,\delta_7,\delta_8,\delta_9,\delta_{10},\delta_{11},\delta_{12},\delta_{13},\delta_{14},\delta_{15},\delta_{16},\dot{\delta}_1,\right.$$
$$\left.\dot{\delta}_2,\dot{\delta}_3,\dot{\delta}_4,\dot{\delta}_5,\dot{\delta}_6,\dot{\delta}_7,\dot{\delta}_8,\dot{\delta}_9,\dot{\delta}_{10},\dot{\delta}_{11},\dot{\delta}_{12},\dot{\delta}_{13},\dot{\delta}_{14},\dot{\delta}_{15},\dot{\delta}_{16}\right) \quad (4.138)$$

$$M_9\ddot{\delta}_9 = P_{m9} - P_{e9}\left(\delta_1,\delta_2,\delta_3,\delta_4,\delta_5,\delta_6,\delta_7,\delta_8,\delta_9,\delta_{10},\delta_{11},\delta_{12},\delta_{13},\delta_{14},\delta_{15},\delta_{16},\dot{\delta}_1,\right.$$
$$\left.\dot{\delta}_2,\dot{\delta}_3,\dot{\delta}_4,\dot{\delta}_5,\dot{\delta}_6,\dot{\delta}_7,\dot{\delta}_8,\dot{\delta}_9,\dot{\delta}_{10},\dot{\delta}_{11},\dot{\delta}_{12},\dot{\delta}_{13},\dot{\delta}_{14},\dot{\delta}_{15},\dot{\delta}_{16}\right) \quad (4.139)$$

$$M_{10}\ddot{\delta}_{10} = P_{m10} - P_{e10}\left(\delta_1,\delta_2,\delta_3,\delta_4,\delta_5,\delta_6,\delta_7,\delta_8,\delta_9,\delta_{10},\delta_{11},\delta_{12},\delta_{13},\delta_{14},\delta_{15},\delta_{16},\dot{\delta}_1,\right.$$
$$\left.\dot{\delta}_2,\dot{\delta}_3,\dot{\delta}_4,\dot{\delta}_5,\dot{\delta}_6,\dot{\delta}_7,\dot{\delta}_8,\dot{\delta}_9,\dot{\delta}_{10},\dot{\delta}_{11},\dot{\delta}_{12},\dot{\delta}_{13},\dot{\delta}_{14},\dot{\delta}_{15},\dot{\delta}_{16}\right) \quad (4.140)$$

$$M_{11}\ddot{\delta}_{11} = P_{m11} - P_{e11}\left(\delta_1,\delta_2,\delta_3,\delta_4,\delta_5,\delta_6,\delta_7,\delta_8,\delta_9,\delta_{10},\delta_{11},\delta_{12},\delta_{13},\delta_{14},\delta_{15},\delta_{16},\dot{\delta}_1,\right.$$
$$\left.\dot{\delta}_2,\dot{\delta}_3,\dot{\delta}_4,\dot{\delta}_5,\dot{\delta}_6,\dot{\delta}_7,\dot{\delta}_8,\dot{\delta}_9,\dot{\delta}_{10},\dot{\delta}_{11},\dot{\delta}_{12},\dot{\delta}_{13},\dot{\delta}_{14},\dot{\delta}_{15},\dot{\delta}_{16}\right) \quad (4.141)$$

$$M_{12}\ddot{\delta}_{12} = P_{m12} - P_{e12}\left(\delta_1,\delta_2,\delta_3,\delta_4,\delta_5,\delta_6,\delta_7,\delta_8,\delta_9,\delta_{10},\delta_{11},\delta_{12},\delta_{13},\delta_{14},\delta_{15},\delta_{16},\dot{\delta}_1,\right.$$
$$\left.\dot{\delta}_2,\dot{\delta}_3,\dot{\delta}_4,\dot{\delta}_5,\dot{\delta}_6,\dot{\delta}_7,\dot{\delta}_8,\dot{\delta}_9,\dot{\delta}_{10},\dot{\delta}_{11},\dot{\delta}_{12},\dot{\delta}_{13},\dot{\delta}_{14},\dot{\delta}_{15},\dot{\delta}_{16}\right) \quad (4.142)$$

$$M_{13}\ddot{\delta}_{13} = P_{m13} - P_{e13}\left(\delta_1,\delta_2,\delta_3,\delta_4,\delta_5,\delta_6,\delta_7,\delta_8,\delta_9,\delta_{10},\delta_{11},\delta_{12},\delta_{13},\delta_{14},\delta_{15},\delta_{16},\dot{\delta}_1,\right.$$
$$\left.\dot{\delta}_2,\dot{\delta}_3,\dot{\delta}_4,\dot{\delta}_5,\dot{\delta}_6,\dot{\delta}_7,\dot{\delta}_8,\dot{\delta}_9,\dot{\delta}_{10},\dot{\delta}_{11},\dot{\delta}_{12},\dot{\delta}_{13},\dot{\delta}_{14},\dot{\delta}_{15},\dot{\delta}_{16}\right) \quad (4.143)$$

$$M_{14}\ddot{\delta}_{14} = P_{m14} - P_{e14}\left(\delta_1,\delta_2,\delta_3,\delta_4,\delta_5,\delta_6,\delta_7,\delta_8,\delta_9,\delta_{10},\delta_{11},\delta_{12},\delta_{13},\delta_{14},\delta_{15},\delta_{16},\dot{\delta}_1,\right.$$
$$\left.\dot{\delta}_2,\dot{\delta}_3,\dot{\delta}_4,\dot{\delta}_5,\dot{\delta}_6,\dot{\delta}_7,\dot{\delta}_8,\dot{\delta}_9,\dot{\delta}_{10},\dot{\delta}_{11},\dot{\delta}_{12},\dot{\delta}_{13},\dot{\delta}_{14},\dot{\delta}_{15},\dot{\delta}_{16}\right) \quad (4.144)$$

$$M_{15}\ddot{\delta}_{15} = P_{m15} - P_{e15}\left(\delta_1,\delta_2,\delta_3,\delta_4,\delta_5,\delta_6,\delta_7,\delta_8,\delta_9,\delta_{10},\delta_{11},\delta_{12},\delta_{13},\delta_{14},\delta_{15},\delta_{16},\dot{\delta}_1,\right.$$
$$\left.\dot{\delta}_2,\dot{\delta}_3,\dot{\delta}_4,\dot{\delta}_5,\dot{\delta}_6,\dot{\delta}_7,\dot{\delta}_8,\dot{\delta}_9,\dot{\delta}_{10},\dot{\delta}_{11},\dot{\delta}_{12},\dot{\delta}_{13},\dot{\delta}_{14},\dot{\delta}_{15},\dot{\delta}_{16}\right) \quad (4.145)$$

$$M_{16}\ddot{\delta}_{16} = P_{m16} - P_{e16}\left(\delta_1,\delta_2,\delta_3,\delta_4,\delta_5,\delta_6,\delta_7,\delta_8,\delta_9,\delta_{10},\delta_{11},\delta_{12},\delta_{13},\delta_{14},\delta_{15},\delta_{16},\dot{\delta}_1,\right.$$

$$\dot{\delta}_2, \dot{\delta}_3, \dot{\delta}_4, \dot{\delta}_5, \dot{\delta}_6, \dot{\delta}_7, \dot{\delta}_8, \dot{\delta}_9, \dot{\delta}_{10}, \dot{\delta}_{11}, \dot{\delta}_{12}, \dot{\delta}_{13}, \dot{\delta}_{14}, \dot{\delta}_{15}, \dot{\delta}_{16}) \quad (4.146)$$

CHAPTER FIVE

5.0 Results and Discussion

The transient stability analysis of the existing 330KV (8 machines-26 bus) and proposed 330KV (16 machines-49 bus) Nigeria power systems were carried out through direct method. Prior to the analysis, the power flow studies conducted on the system exposed the inadequacies of the existing network in terms of transmission capacity, unbalanced network arrangement with respect to the geographical spread of the generation stations.

The power flow study conducted on the proposed network showed remarkable improvement in the geographical spread of the generation stations, reinforcement of the transmission capacities, and a better looped network with more alternative transmission links.

5.1 Existing Network power flow results

The power flow result for existing 330KV Nigeria power system shown in Appendix A2, indicates flat voltage profile within acceptable limits in all the 26 buses. The voltage angles variations between buses are all below 25^{o}, with the highest voltage angle of 26.612^{o} occurring between Egbin and Afam, followed by 21.789^{o} and 20.132^{o} voltage angles deviations between Egbin and Alaoji, and Egbin and Gombe respectively. With reference to the steady-state stability limit of 90^{o}, the system can be considered safe with no threat of disintegration in terms of static stability limit violation under the prevailing loading conditions. Appendix A3 shows that the computed line losses stood at 119.662MW under the generators schedule and loading conditions as shown in Appendix A1. The losses in the lines 10-9, 10-8, 9-7 and 13-16 were quite significant (above 10MW) under this loading condition. Table 5.1 shows the lines with losses above 10MW in existing Network.

Table 5.1 Lines with losses above 10MW in existing.

Bus No		Bus Name		Losses (MW)
From	To	From	To	
10	9	Ontisha	Alaoji	25.520
10	8	Ontisha	Okpai	20.970
9	7	Alaoji	Afam	17.109
13	16	Benin	Ikeja West	10.875

5.2 Proposed Network load flow result

The proposed 330KV Nigeria power system power flow result shown in Appendix B2, indicates that 11 out of 49 buses were found to have voltage magnitudes in excess of +10%, while the rest fall within acceptable limit. The vulnerable buses and their percentage voltage magnitudes violations include: bus 17 (Damaturu, 71.6%), bus 18 (Maiduguri, 80%), bus 19 (Gombe, 69.9%), bus 20 (Yola, 79.4%), bus 21 (Jalingo, 80.9%), bus 22 (Jos, 31.3%), bus 23 (Katempe, 14.4%),bus 24 (Gwagwa, 16.8%), bus 25 (Makurdi, 21.8%), bus 26 (Aliade, 19.6%), and bus 27 (New haven, 11%). This is shown in table 5.2.

Table 5.2 Buses with intolerable voltage profile violation in proposed Network.

Bus		Voltage profile (p.u)	% Violation
No	**Name**		
17	Damaturu	1.716	71.6%
18	Maiduguri	1.800	80%
19	Gombe	1.699	69.9%
20	Yola	1.794	79.4%
21	Jalingo	1.809	80.9%
22	Jos	1.313	31.3%
23	Katempe	1.144	14.4%
24	Gwagwa	1.168	16.8%
25	Makurdi	1.218	21.8%
26	Aliade	1.196	19.6%
27	New Haven	1.110	11.0%

These buses have higher voltage magnitudes beyond acceptable limits due to reactive power build-up in between the transmission lines inter-connecting them, since the lines are comparatively long lines. Placement of properly sized synchronous reactors in these buses will help to absorb the excess reactive power and hence bring down the voltage profile within tolerable limits.

The computed line flow and losses shown in Appendix B3 indicated that the line losses of 421.953MW occurred in the network under the generation schedule and loading conditions given in Appendix B1. The losses in the following lines were quite significant: 19-22 (73.211MW), 11-36 (40.872MW), 7-28 (40.734MW), 24-23 (32.899MW), 22-24 (29.229MW), 11-

31 (22.269MW), 26-27 (20.965MW), 4-23 (17.480MW), 24-42 (17.445MW), 1-35 (14.096MW), and 25-22 (12.875MW). This is shown in table 5.3.

Table 5.3 Lines with losses above 10MW in proposed Network.

Bus No		Bus Name		Losses (MW)
From	To	From	To	
19	22	Gombe	Jos	73.211
11	36	Omotosho	Ikeja West	40.872
7	28	Afam	Ikot ekpene	40.734
24	23	Gwagwa	Katempe	32.899
22	24	Jos	Gwagwa	29.229
11	31	Omotosho	Benin	22.269
26	27	Aliade	New Haven	20.965
4	23	Shiroro	Katempe	17.480
24	42	Gwagwa	Lokoja	17.445
1	35	Egbin	Erukan	14.096
15	22	Makurdi	Jos	12.875

The losses could be minimized by introducing more lines to increase their power transmission capacities.

5.3 Results of transient stability analysis of existing Network under three-phase fault at some selected buses and lines

When a three-phase fault was impressed on line 4-20 with bus 4 as the faulted bus, the generators rotor swing curves shown in figure 5.1 indicates that Shiroro generating plant connected to bus 4 became unstable even at a clearing time of 0.16s. Figure 5.2 also shows that the same generator (Shiroro) still experienced instability when bus 20 became the faulted bus, while line 4-20 remained the faulted line.

Figure 5.3 shows the rotor swing curves of the systems' generators response to a three-phase fault on line 13-16, with bus 13 as faulted bus. The system was quite stable under this fault condition at a clearing time of 0.16s.

When the faulted bus was switched to bus 16, the rotor angles swings of Afam and Okpai generators oscillate between 90^0 and above 100^o, even at the clearing time of 0.16s. At a clearing time of 0.20s, the oscillating angles of the system generators increased beyond 120^o as shown in figure 5.5. The system thus experienced instability at a clearing time of 0.22s as shown in figure 5.6.

The critical clearing time for this fault condition is 0.21s, and the rotors swing curves at this time is shown in figure 5.7.

Figure 5.8 shows the swing curves in response to a three-phase fault at bus 10, line 10-13 with a clearing time of 0.16s. Under this fault condition, Okpai and Afam generators became unstable due to their rotors acceleration in response to the fault, while other generators in the network remained stable.

When the faulted bus was switched to bus 13, the same generators (Okpai and Afam) remained unstable, while others were stable at the clearing time of 0.16s as shown in figure 5.9.

Figures 5.10 and 5.11 show the swing curves in response to a three-phase fault on line 13-18 with the faulted buses of 18 and 13 respectively at a clearing time of 0.3s. In both cases, the system was stable. Table 5.4 shows the summary of the transient stability analysis of existing Nigeria power system under three-phase faults at selected buses and lines.

Table 5.4 The Summary of transient stability analysis of existig Nigeria power system.

Faulted bus	Faulted line	Type of fault	Clearing time (s)	Critical clearing time (s)	Stability margin	System Response
4	4-20	Three-phase	0.16	-	-	Gen. at bus 4:unstable
20	4-20	Three-phase	0.16	-	-	Gen. at bus 4:unstable
13	13-16	Three-phase	0`.16	-	-	System stable
16	13-16	Three-phase	0.16	0.21	0.238	System stable
16	13-16	Three-phase	0.22	-	-	System unstable
10	10-13	Three-phase	0.16	-	-	Generators (Okpai and Afam) unstable
13	10-13	Three-phase	0.16	-	-	Generators (Okpai and Afam) unstable
18	13-18	Three-phase	0.3	-	-	System stable
13	13-18	Three-phase	0.3	-	-	System stable

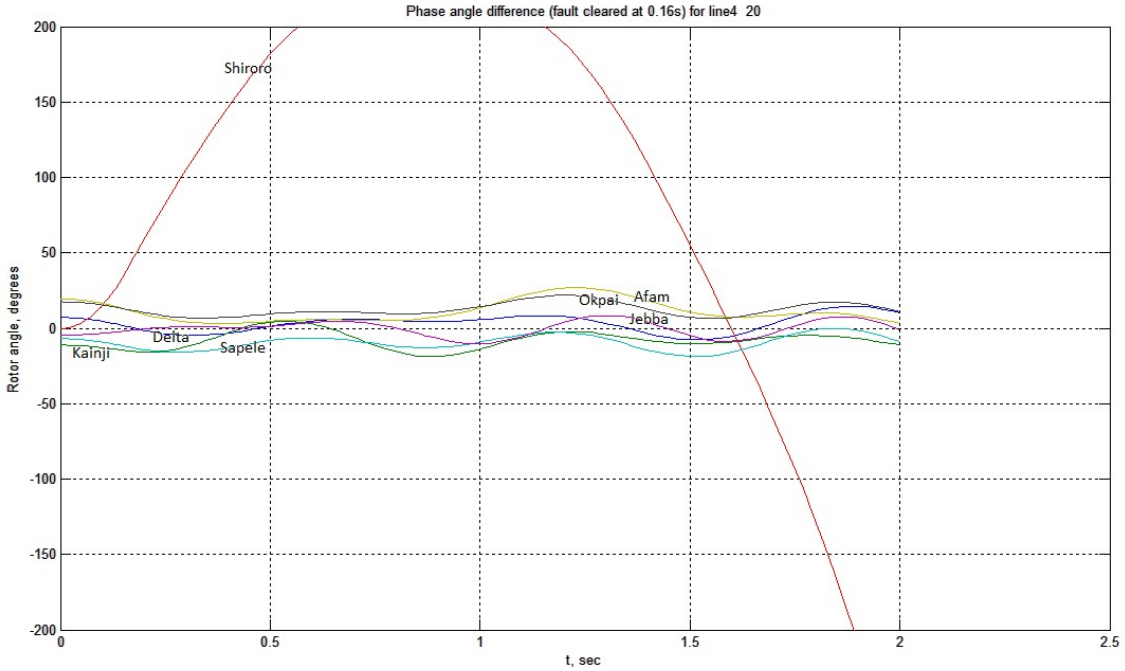

Figure 5.1 Swing curves for fault at bus 4, line 4 – 20 (Clearing Time:0.16s)

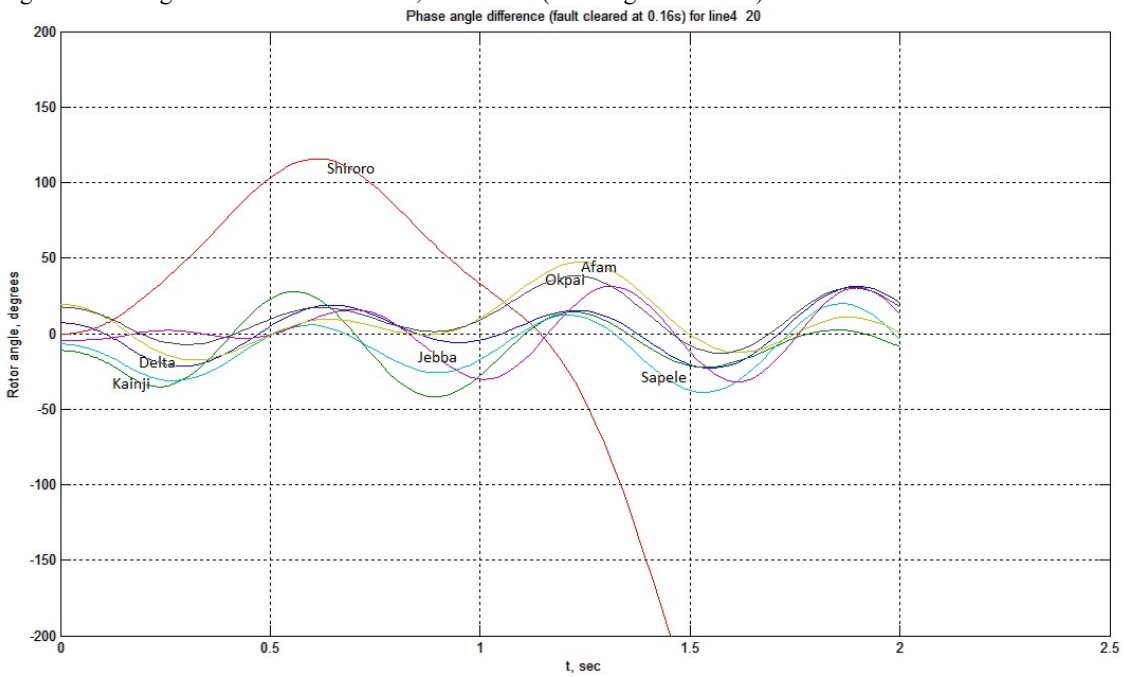

Figure 5.2 Swing curves for fault at bus 20, line 4 – 20 (Clearing Time:0.16s)

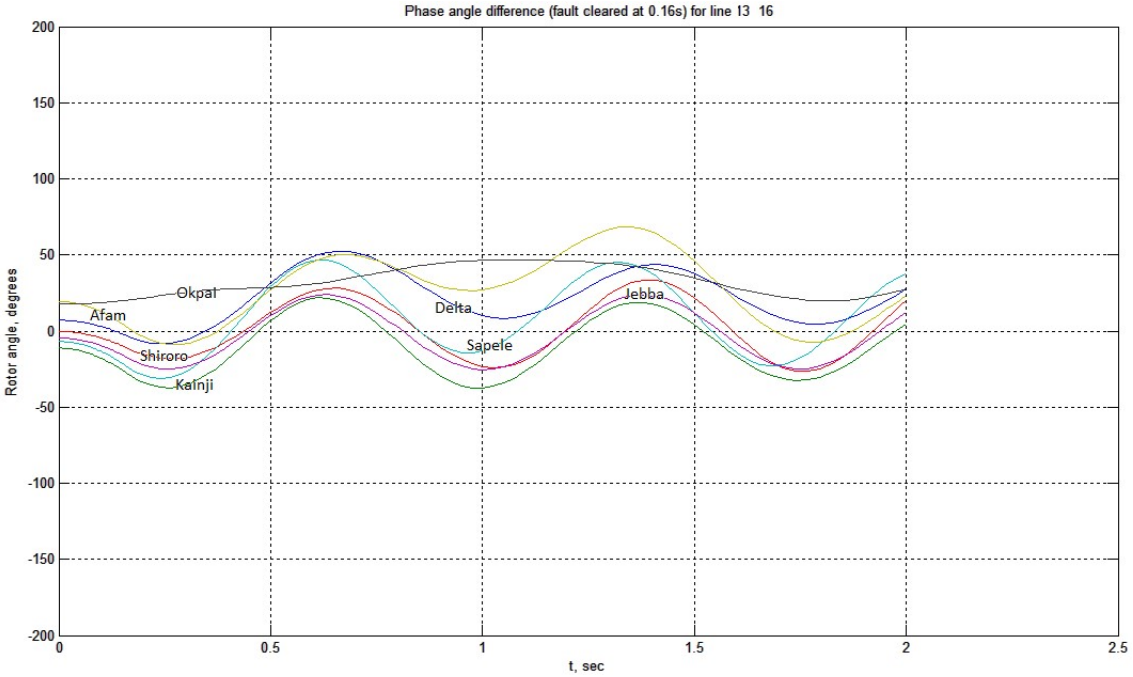

Figure 5.3 Swing curves for fault at bus 13, line 13 – 16 (Clearing Time:0.16s)

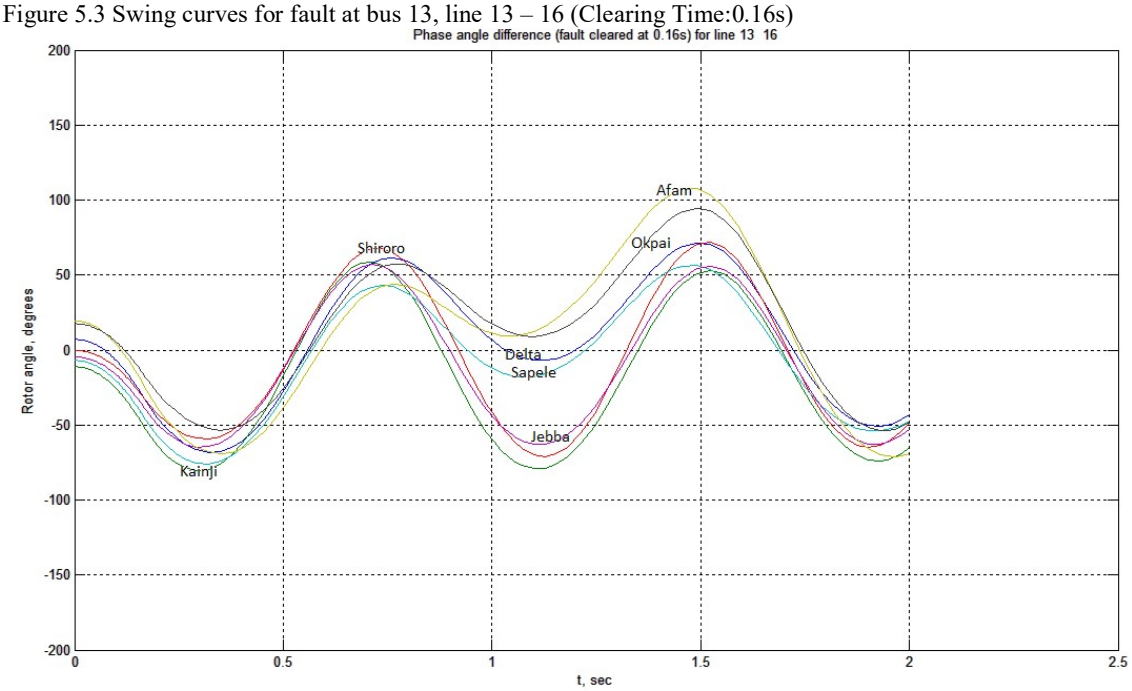

Figure 5.4 Swing curves for fault at bus 16, line 13 – 16 (Clearing Time:0.16s)

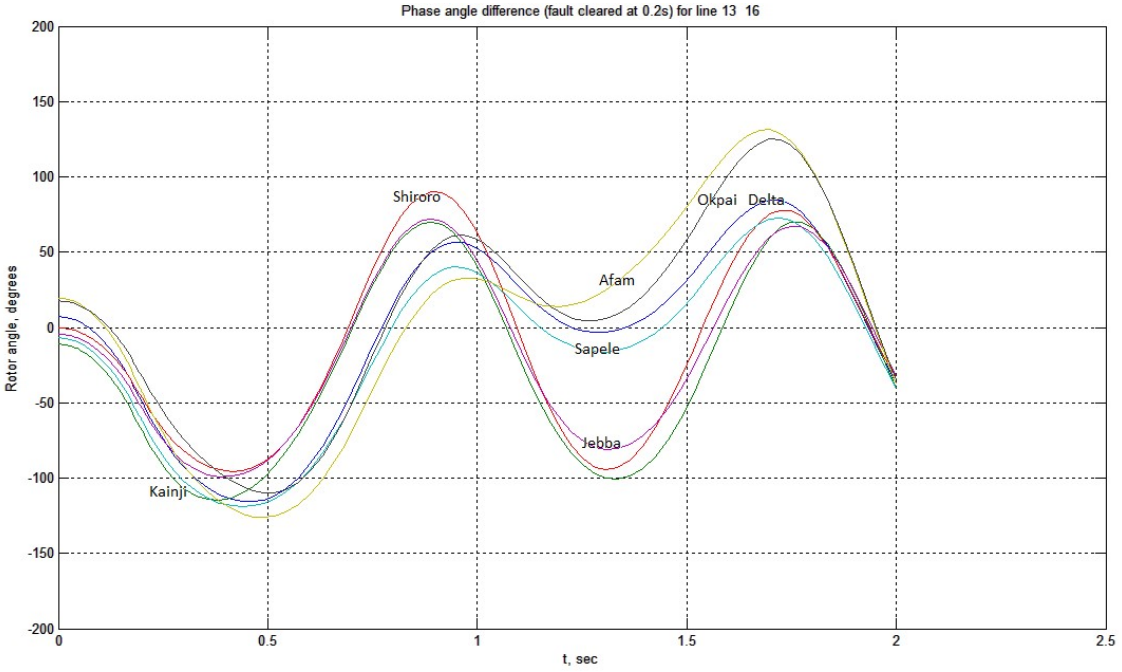

Figure 5.5 Swing curves for fault at bus 16, line 13 – 16 (Clearing Time:0.20s)

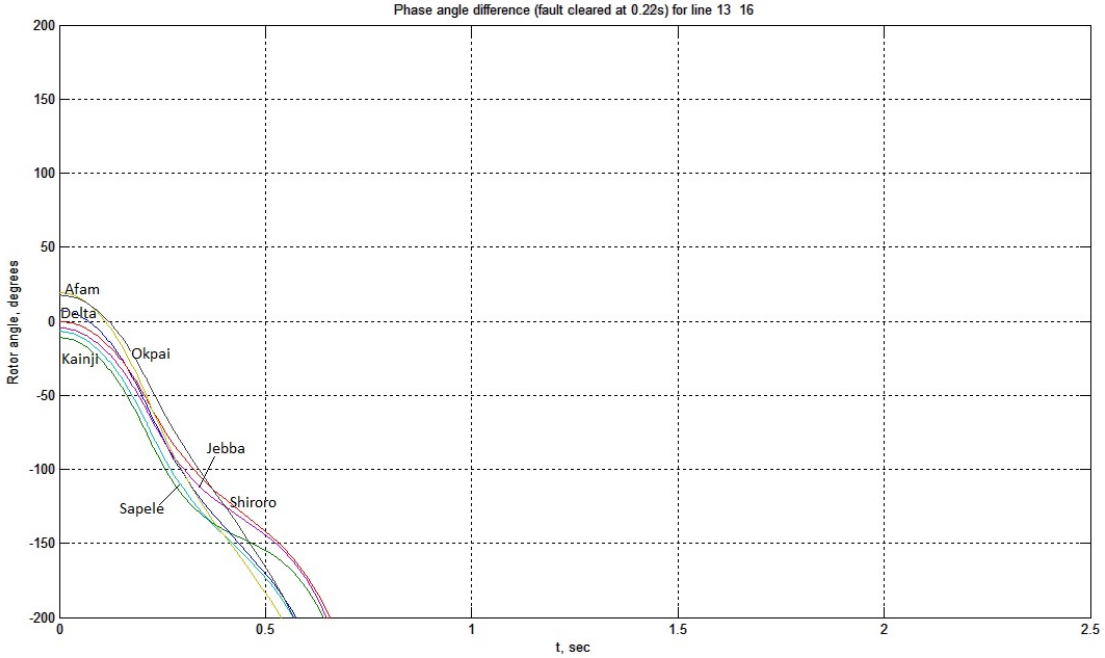

Figure 5.6 Swing curves for fault at bus 16, line 13 – 16 (Clearing Time:0.22s)

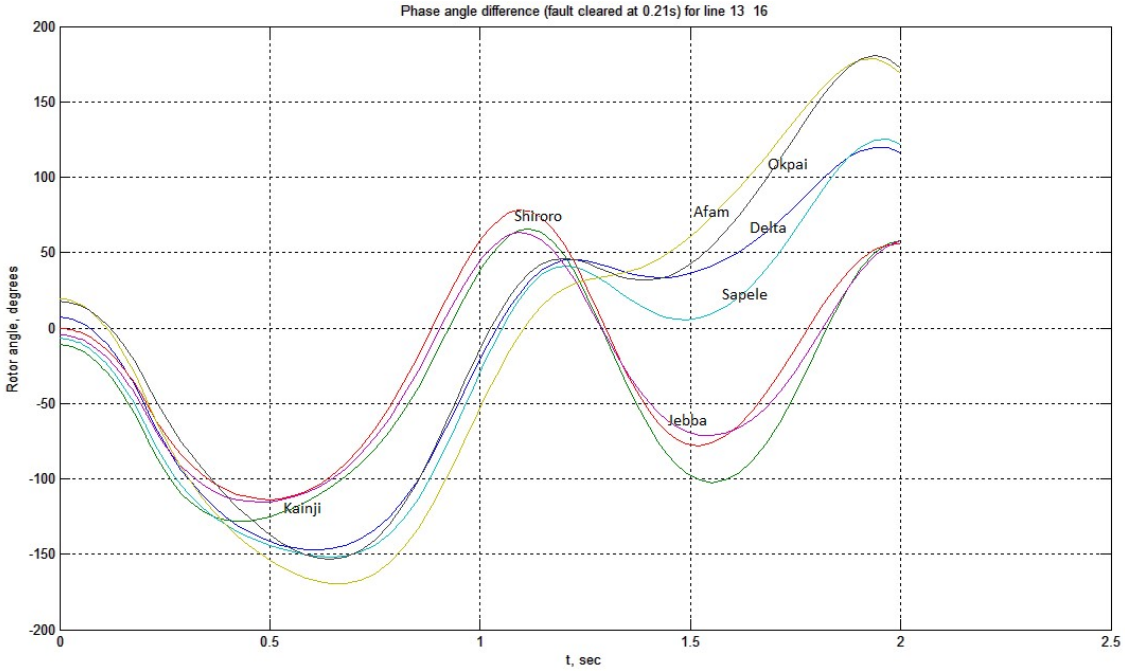

Figure 5.7 Swing curves for fault at bus 16, line 13 – 16 (Critical clearing Time:0.21s)

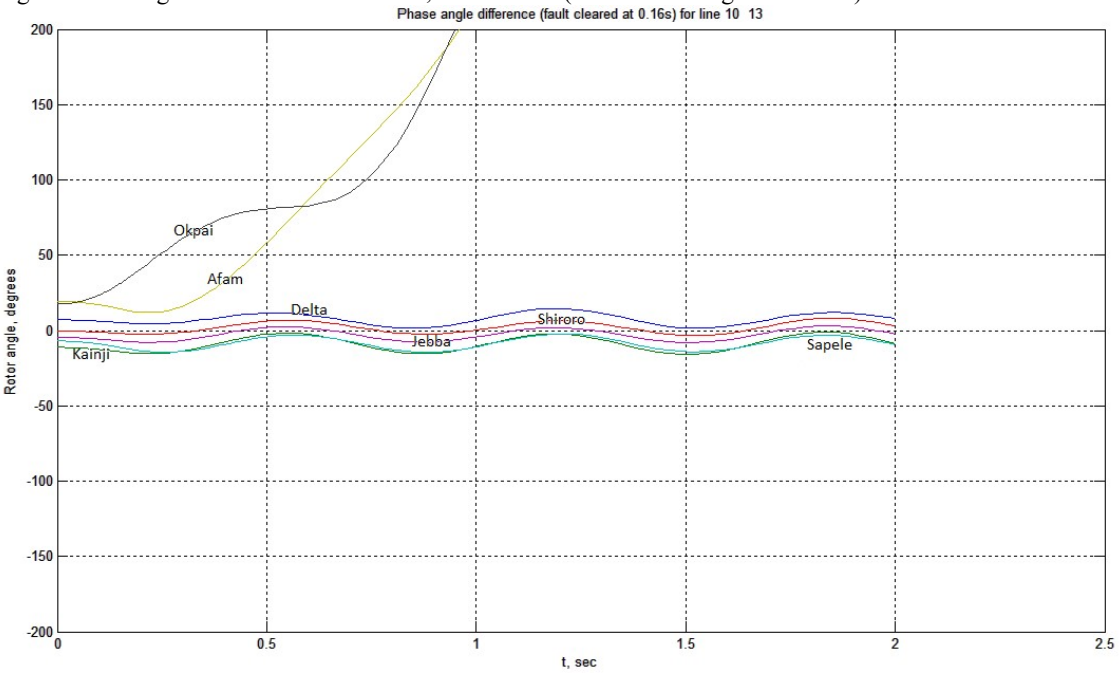

Figure 5.8 Swing curves for fault at bus 10, line 10 – 13 (Clearing Time:0.16s)

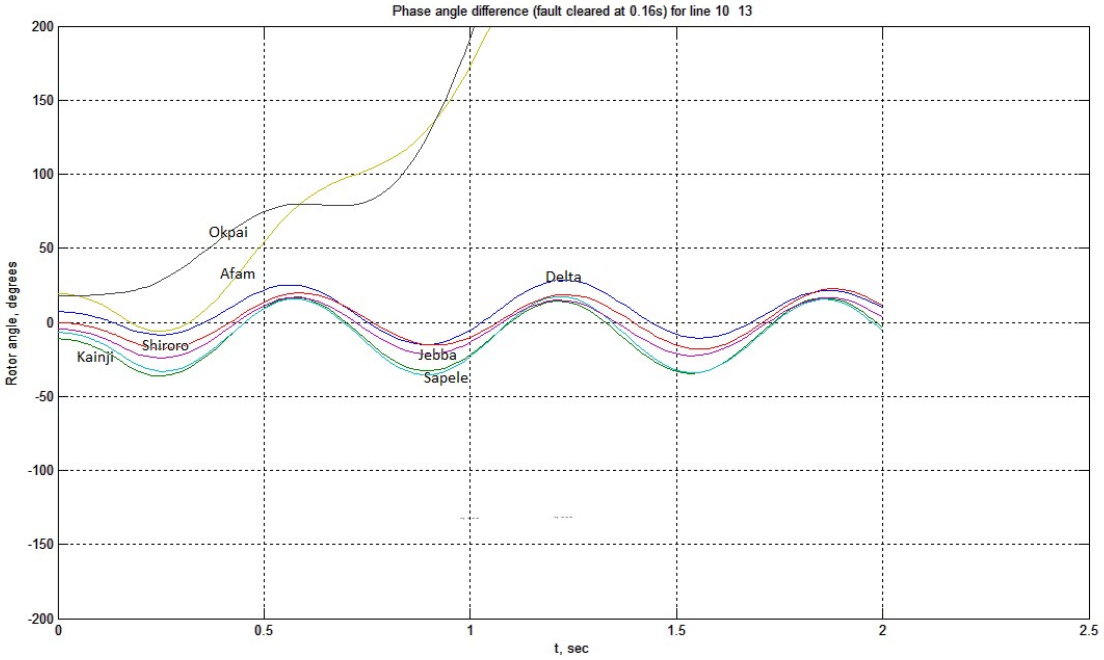

Figure 5.9 Swing curves for fault at bus 13, line 10 – 13 (Clearing Time:0.16s)

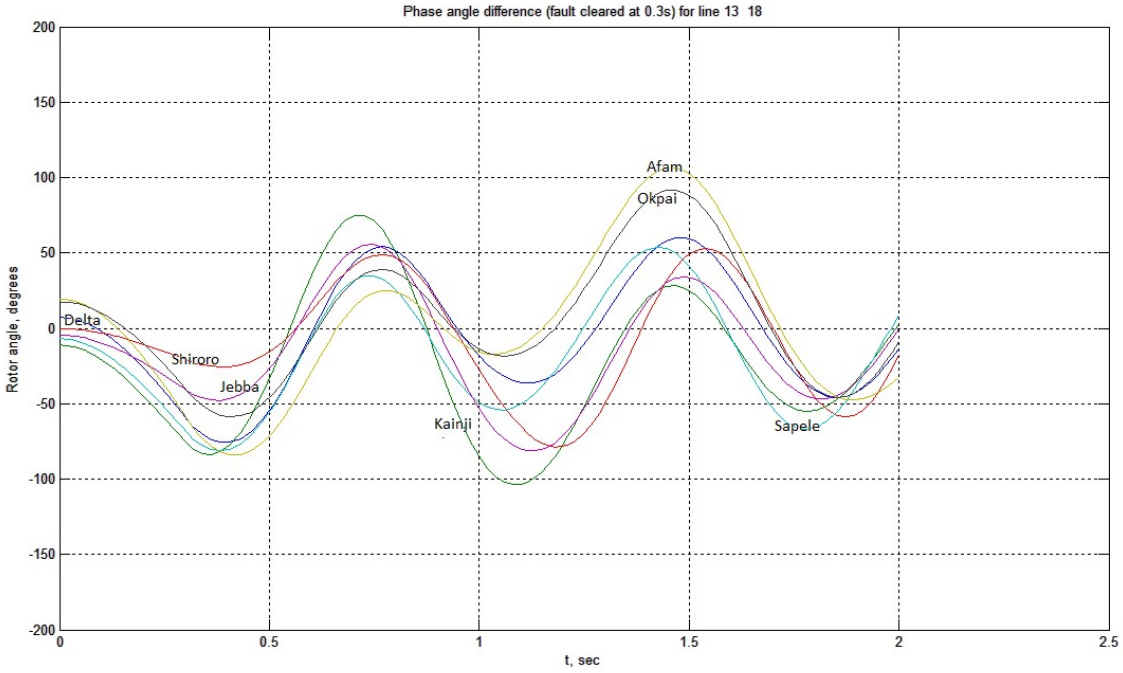

Figure 5.10 Swing curves for fault at bus 18, line 13 – 18 (Clearing Time:0.3s)

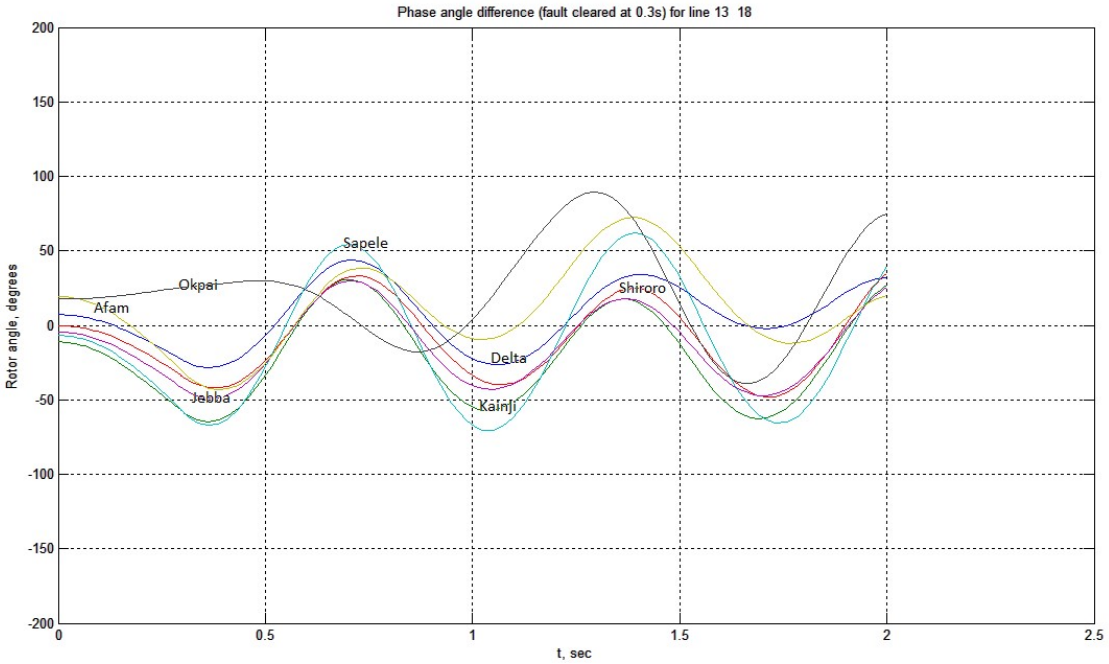

Figure 5.11 Swing curves for fault at bus 13, line 13 – 18 (Clearing Time:0.3s)

5.4 Results of transient stability analysis of proposed Network under three-phase fault at selected buses and lines.

When a three-phase fault was impressed at bus 40, line 31-40, of figure 4.2, under the generators schedule and network loading condition shown in Appendix B1, the system's response to the disturbance is shown in figure 5.12. At clearing times of 0.16s and 0.3s respectively as indicated in figures 5.12 and 5.13, the generators (Shiroro, Geregu, and Omoku) experienced instability, while the rest of system generators remained stable.

At faulted bus 31, line 31-40, and clearing times of 0.16s and 0.3s respectively, figure 5.14 and 5.15 indicate that in both cases, four generators (Shiroro, Geregu, Omoku and Eyean) experienced instability, while the rest of the generators were stable.

At faulted bus 2, line 2-31, figures 5.16, 5.17 and 5.18 show that the critical clearing time for this fault condition is 0.17s, beyond which generators (Shiroro and Omoku) became unstable in addition to generators (Geregu and Eyean) which had earlier been lost due to instability occasioned by rotor acceleration of these generators at the instant of the initiated fault.

At faulted bus 31, line 2-31, figures 5.19, 5.20 and 5.21 show that the critical clearing time for the fault condition is 0.29s, beyond which the generator (Okpai) becomes unstable in addition to loss of four generators (Shiroro, Geregu, Omoku and Eyean) which had become unstable at the instant of the fault initiation.

When the three-phase fault is impressed on line 22-25 and bus 22 as faulted bus, figures 5.22, 5.23 and 5.24, respectively indicate that three generators (Shiroro, Geregu and Omoku) remained unstable, while the rest of the system generators were stable.

By switching the faulted bus to bus 25, while faulted line remained line 22-25, figure 5.25, 5.26, and 5.27 show that the unstable generators

remained those of Shiroro, Geregu and Omoku, while the rest of the system generators remained stable.

At faulted bus 3, line 3-44, figure 5.28 indicates the loss of three generators (Shiroro, Geregu, and Kainji) as a result of rotor acceleration in response to the initiated three-phase fault. The rest of the system's generators remained stable.

By switching the faulted bus to bus 44, and faulted line retained as line 3-44, figures 5.29, 5.30 and 5.31 show that the critical clearing time for this fault condition is 0.21s, beyond this time, Omoku generator will become unstable in addition to Shiroro, Geregu and Kainji generators which became unstable at the instant of the initiated fault.

Table 5.5 shows the summary of the transient stability analysis of proposed Nigeria power system under three-phase fault at selected buses and lines.

Table 5.5 The Summary of transient stability analysis of proposed Nigeria power system.

Faulted bus	Faulted line	Type of fault	Clearing time (sec)	Critical clearing time (s)	Stability margin	System Response
40	31-40	Three-phase	0.16	-	-	Shiroro, Geregu and Omoku: Unstable
40	31-40	Three-phase	0.3	-	-	″
31	31-40	Three-phase	0.16	-	-	Shiroro, Geregu, Omoku and Eyean: unstable
31	31-40	Three-phase	0.3	-	-	″
2	2-31	Three-phase	0.16	0.17	0.058	Geregu unstable
2	2-31	Three-phase	0.17	0.17	0	Geregu and Eyean: Unstable
2	2-31	Three-phase	0.18	0.17	-0.888	Shiroro, Geregu, Omoku and Eyean: Unstable
31	2-31	Three-phase	0.16	0.29	0.448	Shiroro, Geregu, Omoku and Eyean: Unstable
31	2-31	Three-phase	0.29	0.29	0	Shiroro, Geregu, Omoku and Eyean: Unstable
31	2-31	Three-phase	0.3	0.29	-0.034	Shiroro, Geregu, Omoku Eyean and Okpai: Unstable
22	22-25	Three-phase	0.16	-	-	Shiroro, Geregu and Omoku: Unstable
22	22-25	Three-phase	0.2	-	-	
22	22-25	Three-phase	0.3	-	-	
25	22-25	Three-phase	0.16	-	-	Shiroro, Geregu and Omoku: Unstable
25	22-25	Three-phase	0.2	-	-	
25	22-25	Three-phase	0.3	-	-	

3	3-44	Three-phase	0.16	0.21	0.238	Shiroro, Geregu and Kainji: Unstable
3	3-44	Three-phase	0.21	0.21	0	Shiroro, Geregu and Kainji: Unstable
3	3-44	Three-phase	0.22	0.21	-0.047	Shiroro, Geregu, Kainji and Omoku: Unstable

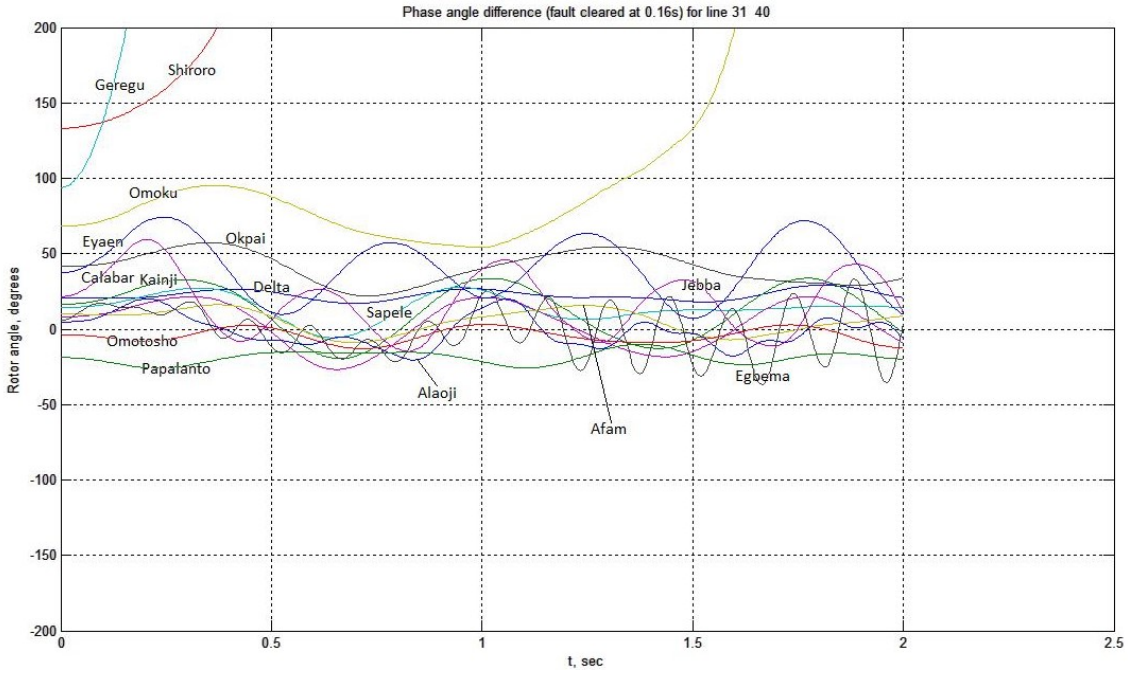

Figure 5.12 Swing curves for fault at bus 40, line 31 – 40 (Clearing Time: 0.16s)

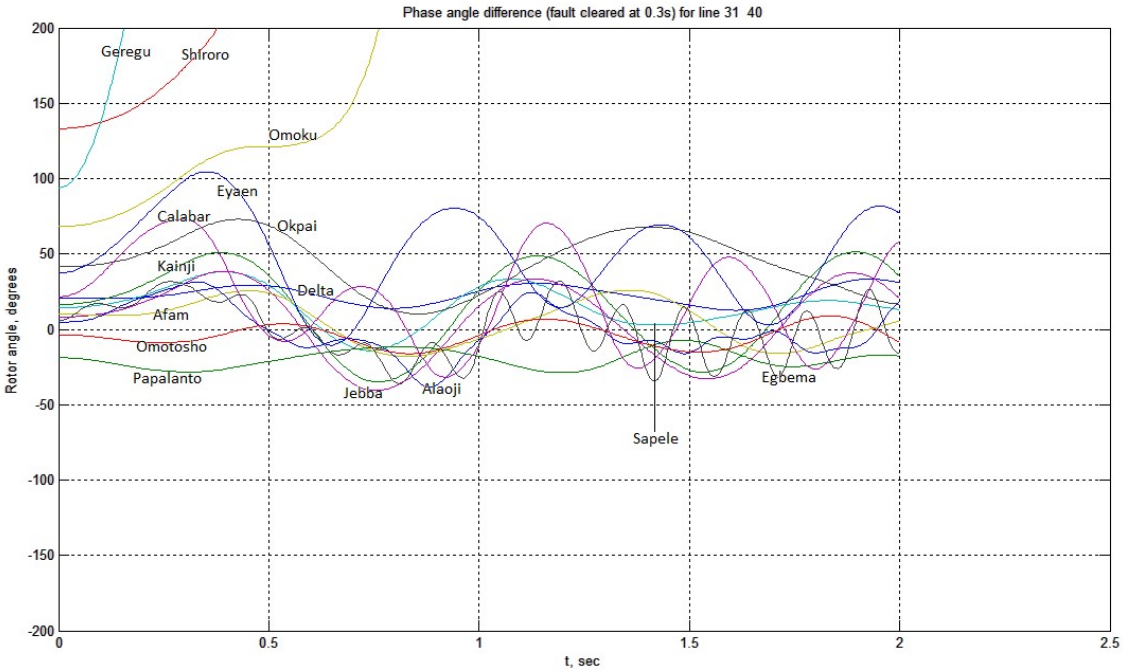

Figure 5.13 Swing curves for fault at bus 40, line 31 – 40 (Clearing Time: 0.3s)

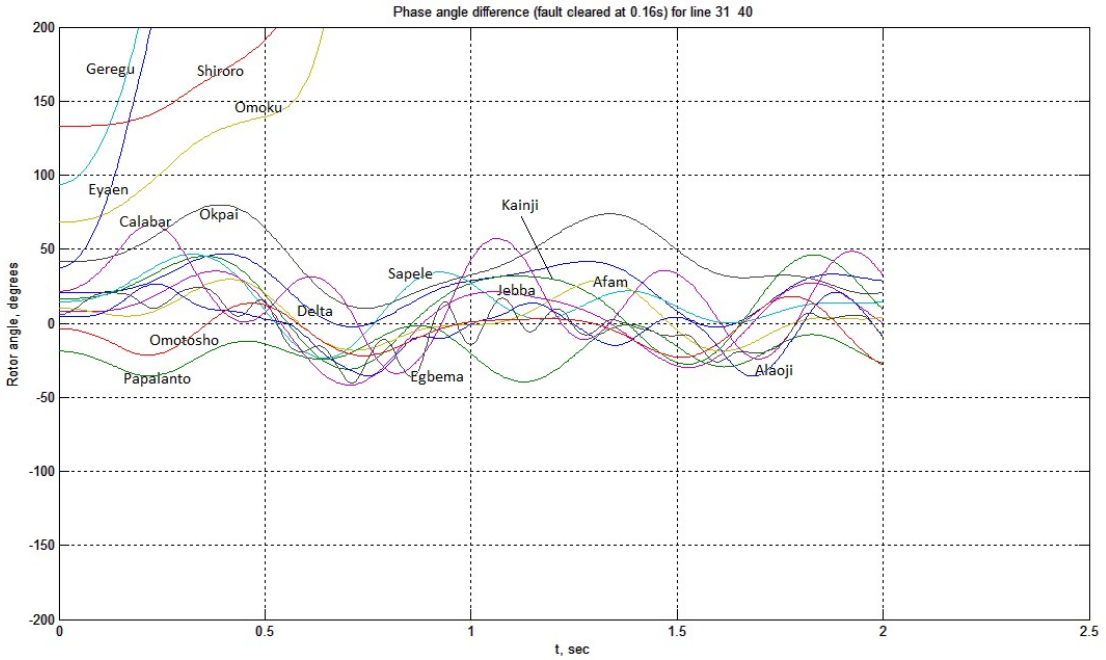

Figure 5.14 Swing curves for fault at bus 31, line 31 – 40 (Clearing Time: 0.16s)

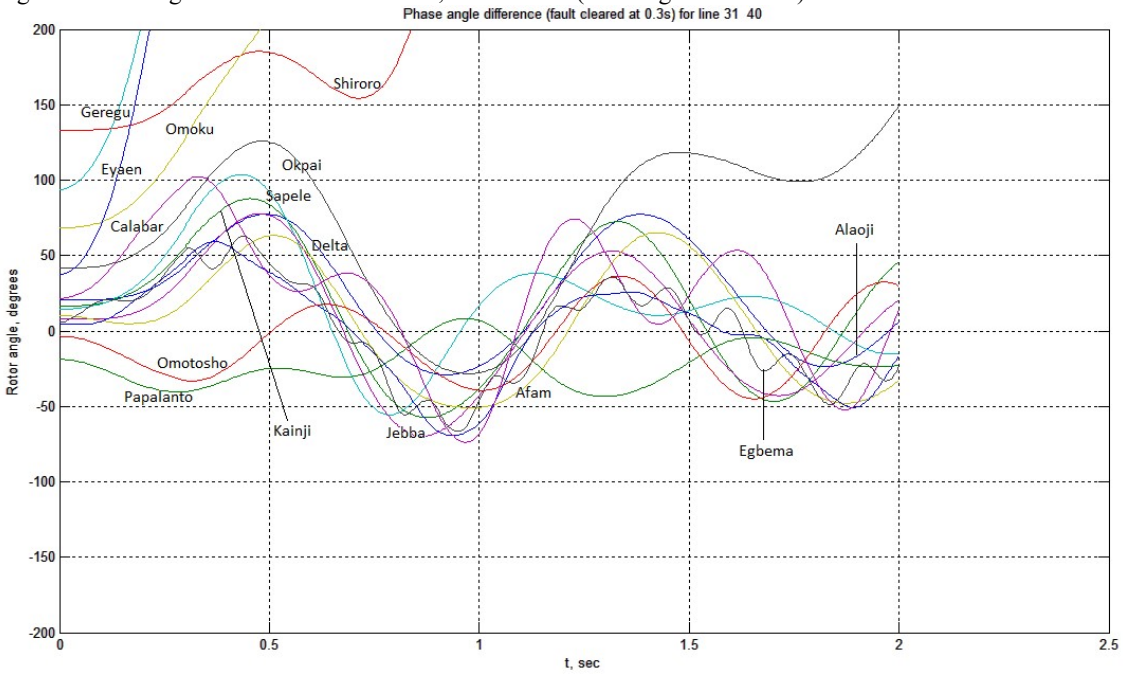

Figure 5.15 Swing curves for fault at bus 31, line 31 – 40 (Clearing Time: 0.3s)

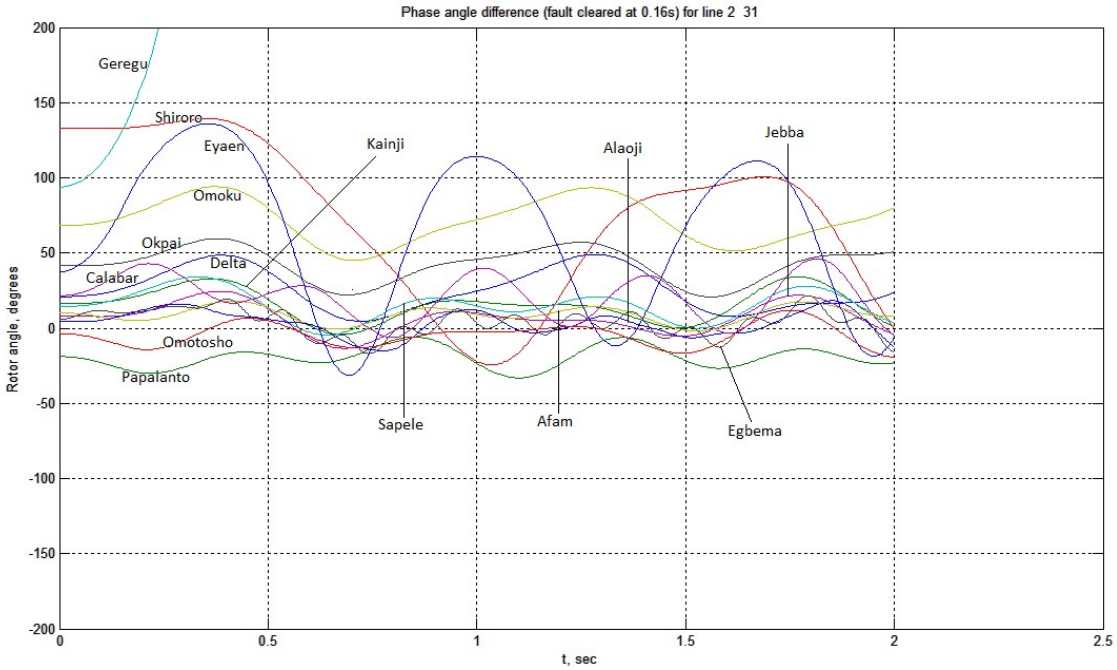

Figure 5.16 Swing curves for fault at bus 2, line 2 – 31 (Clearing Time: 0.16s)

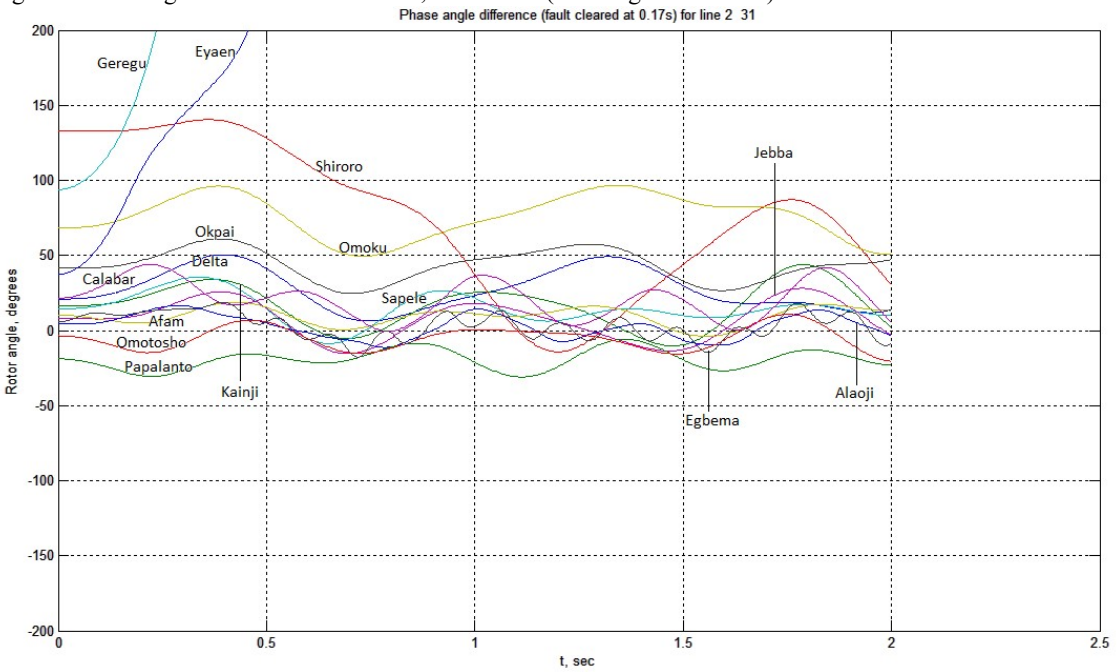

Figure 5.17 Swing curves for fault at bus 2, line 2 – 31 (Critical clearing Time: 0.17s)

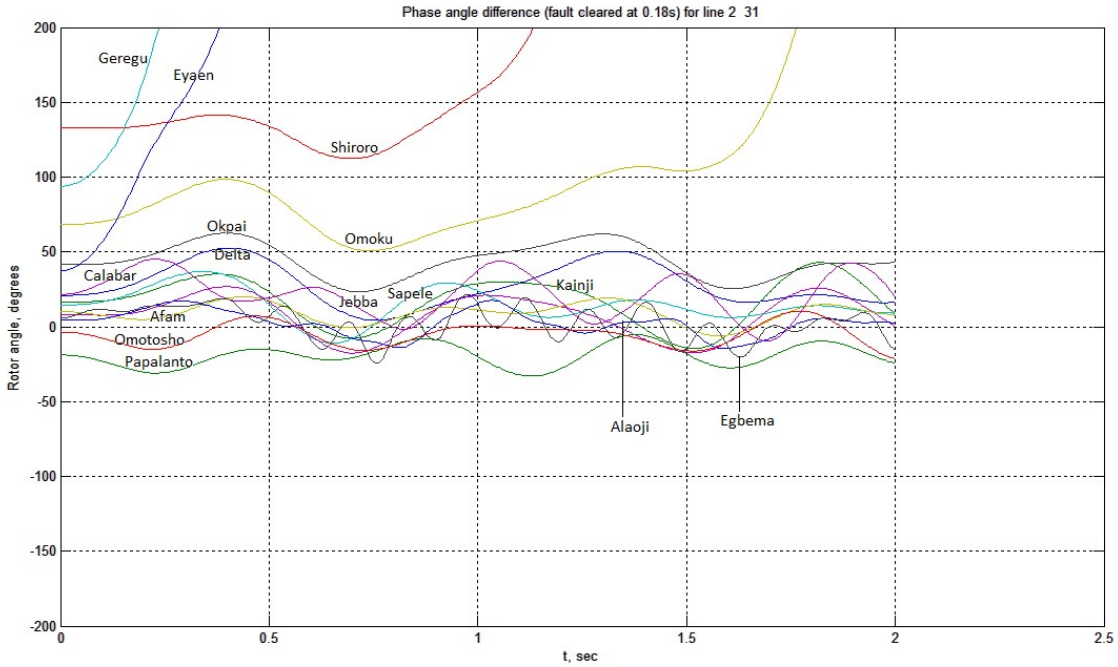

Figure 5.18 Swing curves for fault at bus 2, line 2 – 31 (Clearing Time: 0.18s)

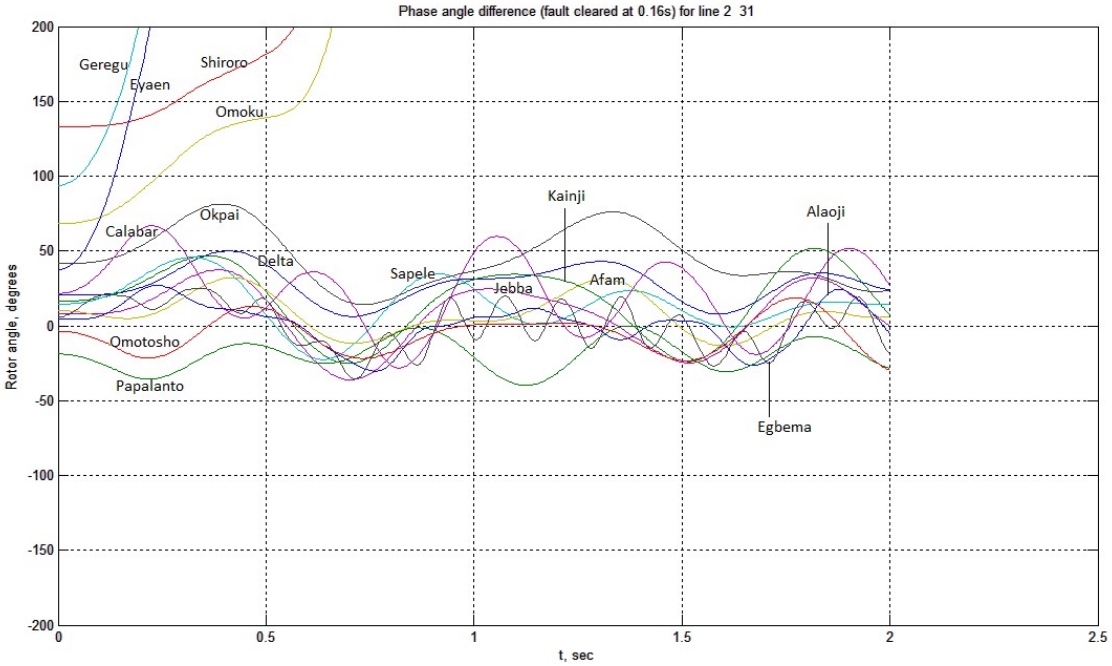

Figure 5.19 Swing curves for fault at bus 31, line 2 – 31 (Clearing Time: 0.16s)

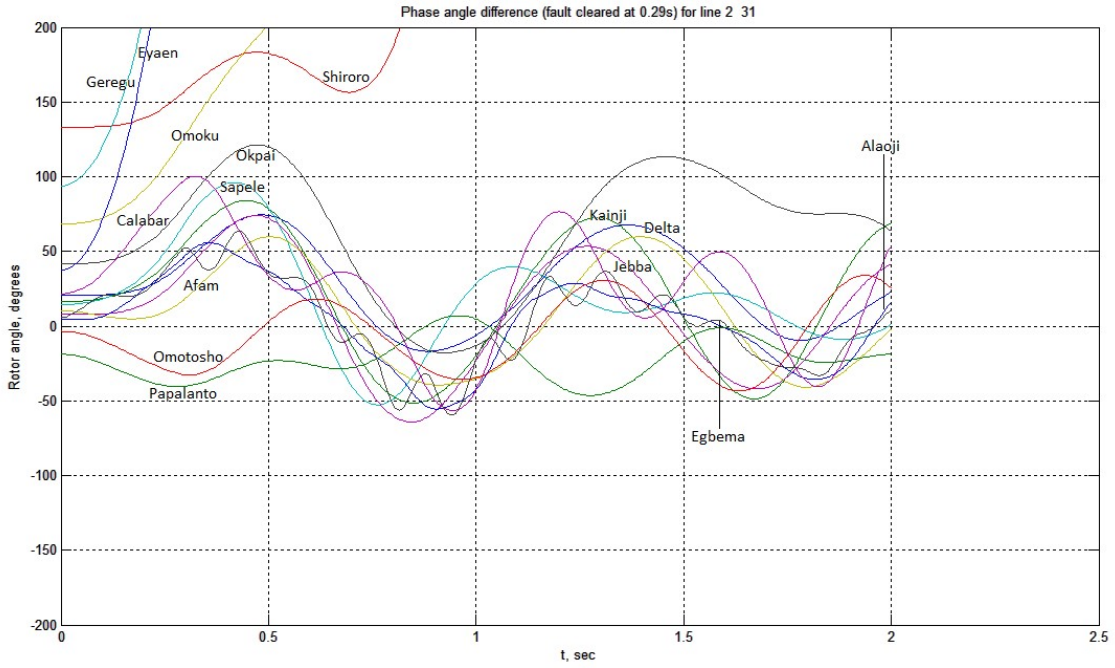

Figure 5.20 Swing curves for fault at bus 31, line 2 – 31 (Critical clearing Time: 0.29s)

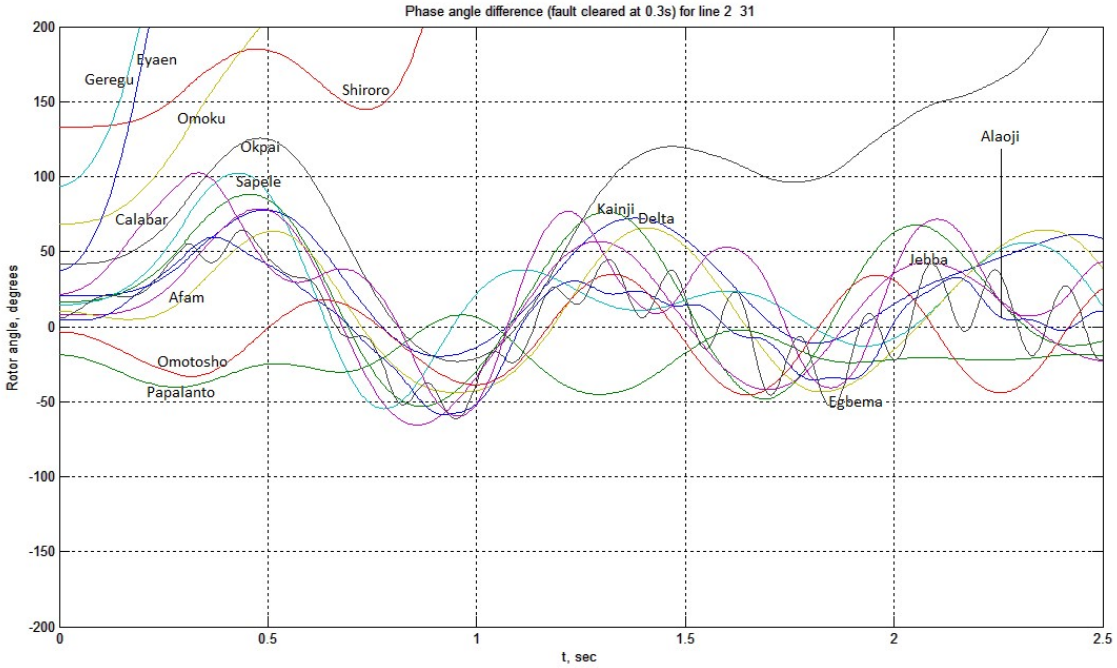

Figure 5.21 Swing curves for fault at bus 31, line 2 – 31 (Clearing Time: 0.3s)

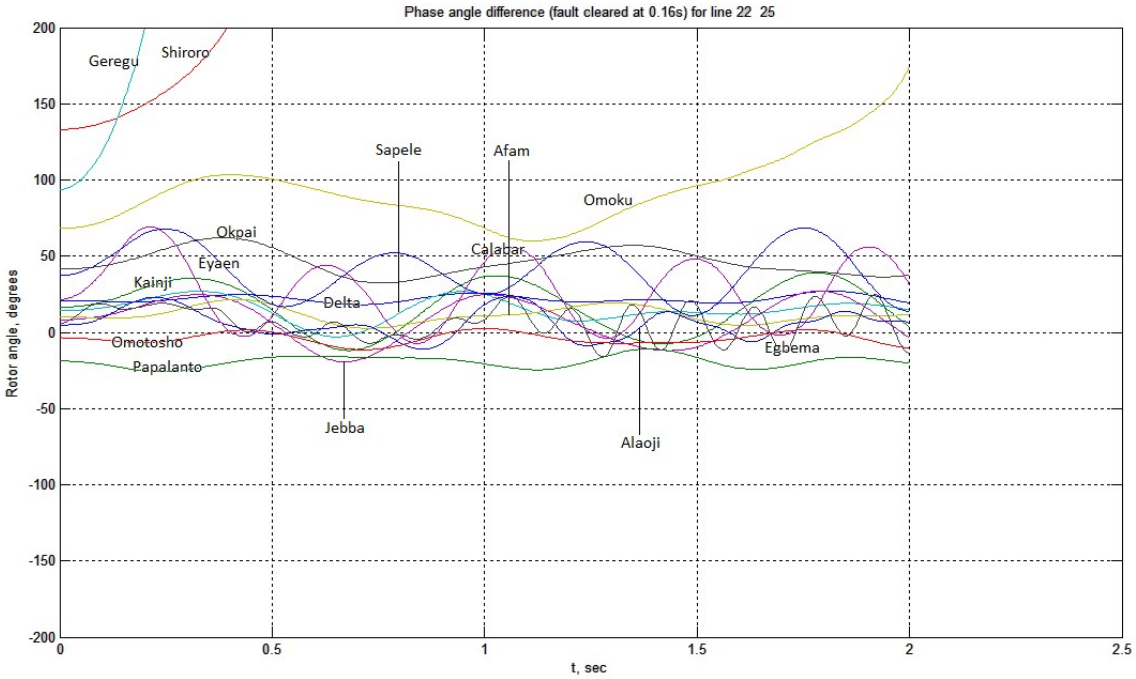

Figure 5.22 Swing curves for fault at bus 22, line 22 – 25 (Clearing Time: 0.16s)

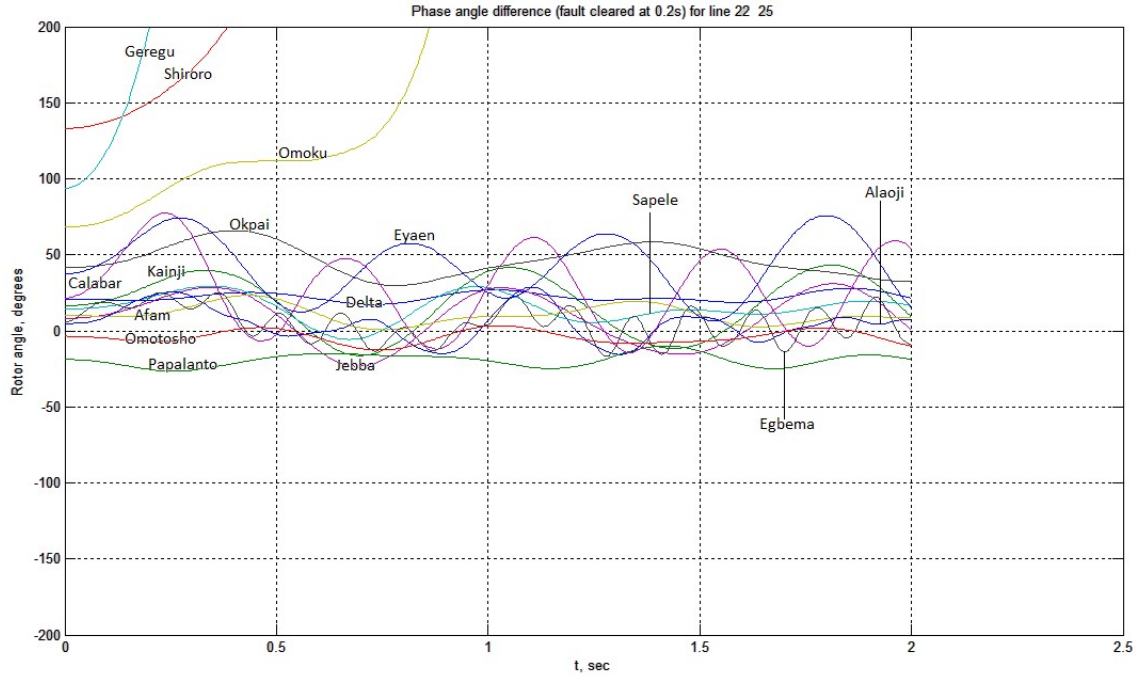

Figure 5.23 Swing curves for fault at bus 22, line 22 – 25 (Clearing Time: 0.2s)

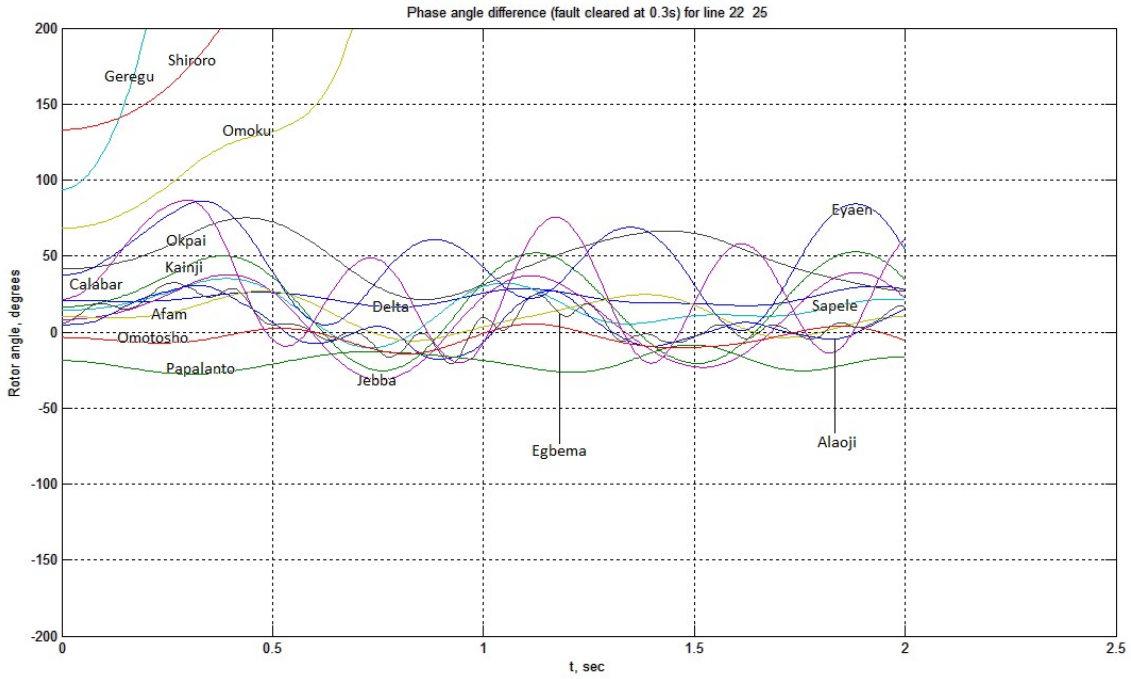

Figure 5.24 Swing curves for fault at bus 22, line 22 – 25 (Clearing Time: 0.3s)

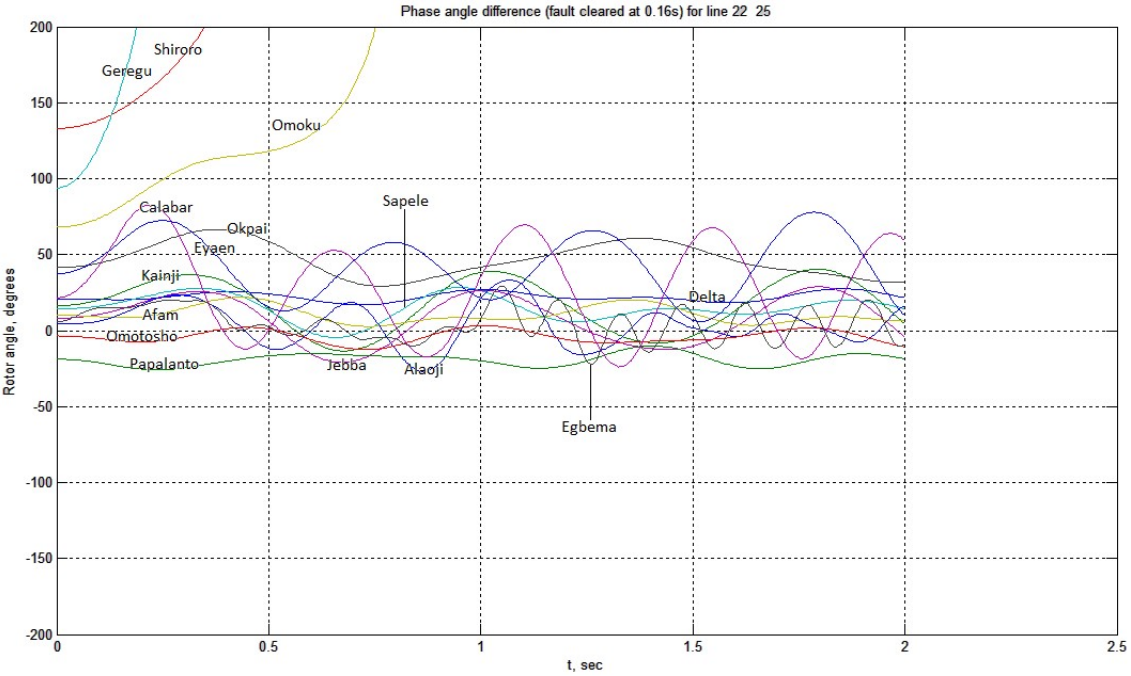

Figure 5.25 Swing curves for fault at bus 25, line 22 – 25 (Clearing Time: 0.16s)

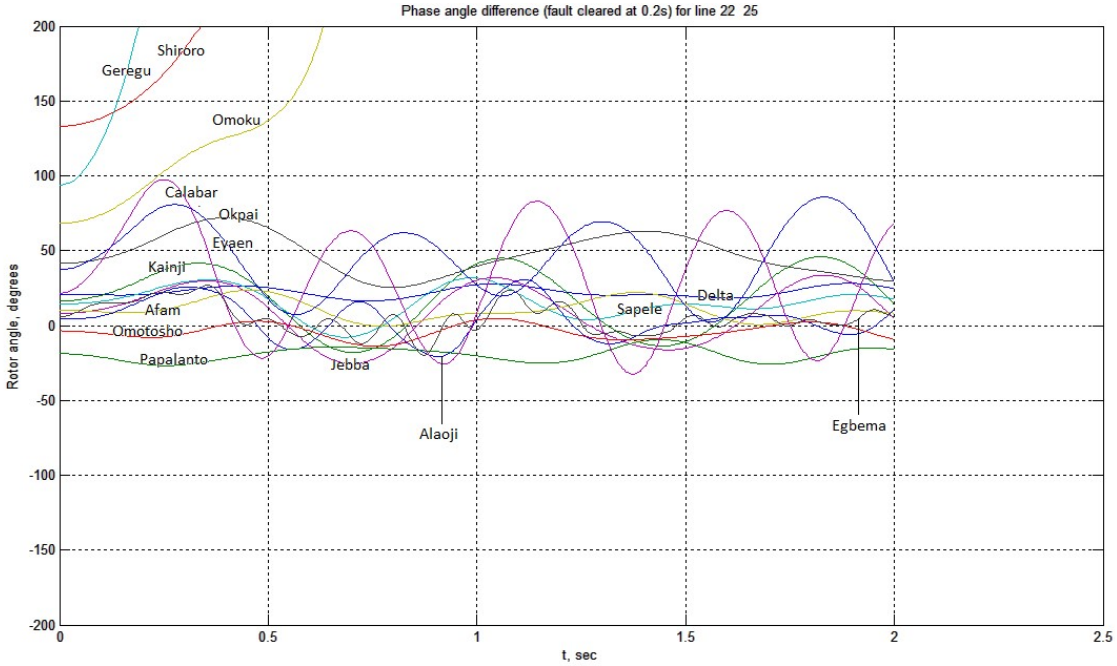

Figure 5.26 Swing curves for fault at bus 25, line 22 – 25 (Clearing Time: 0.2s)

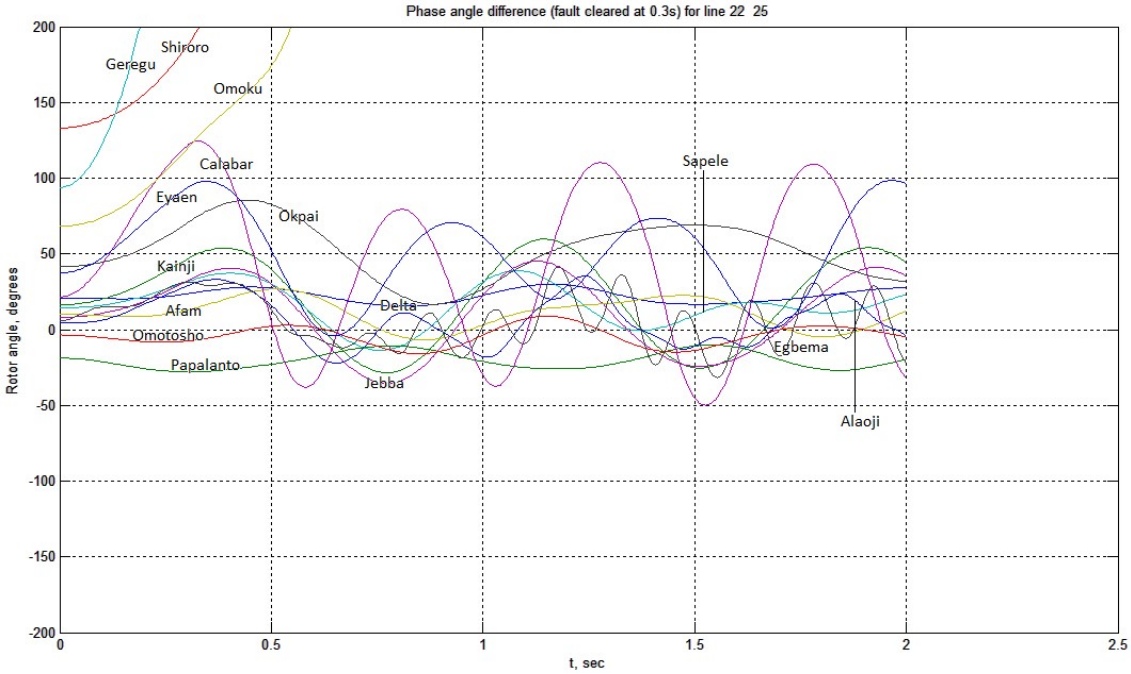

Figure 5.27 Swing curves for fault at bus 25, line 22 – 25 (Clearing Time: 0.3s)

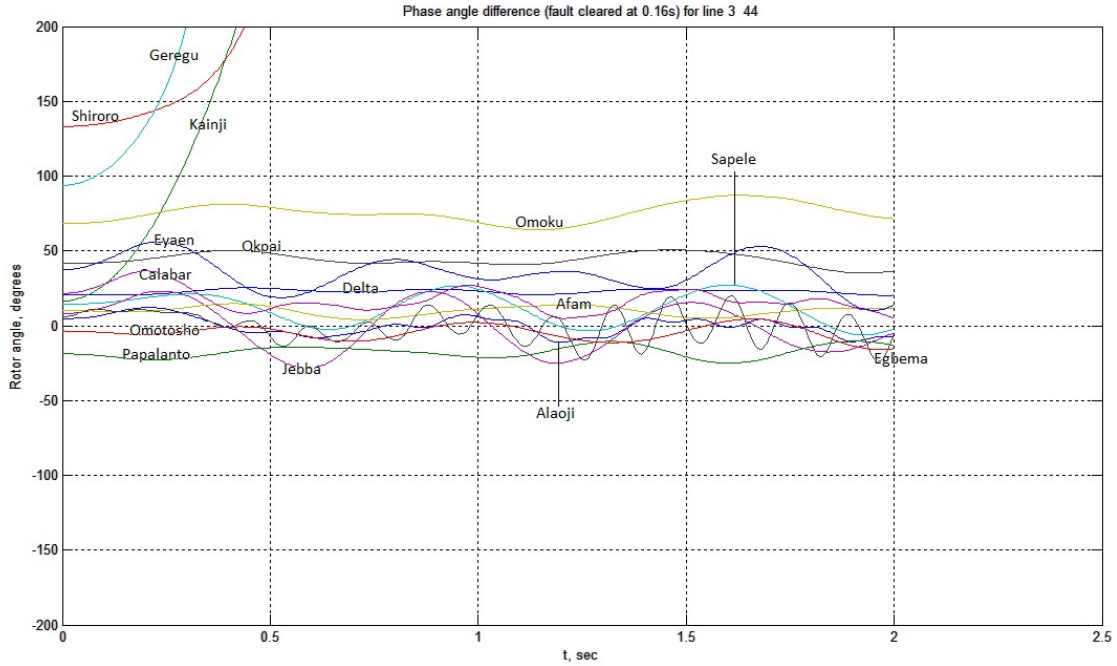

Figure 5.28 Swing curves for fault at bus 3, line 3 – 44 (Clearing Time: 0.16s)

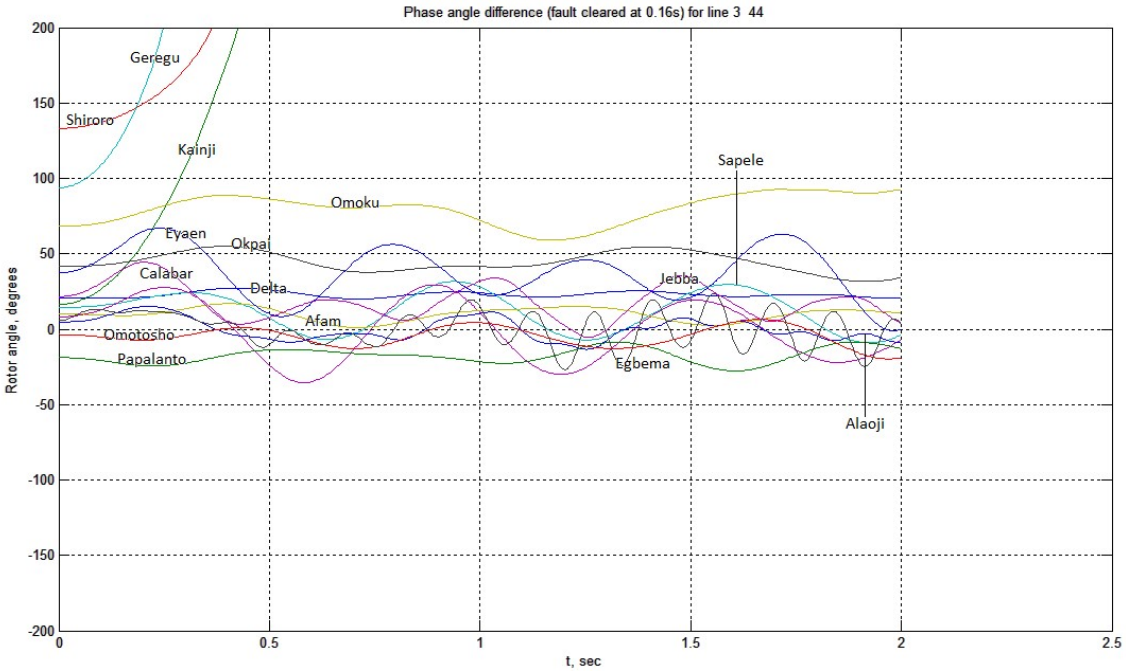

Figure 5.29 Swing curves for fault at bus 44, line 3 – 44 (Clearing Time: 0.16s)

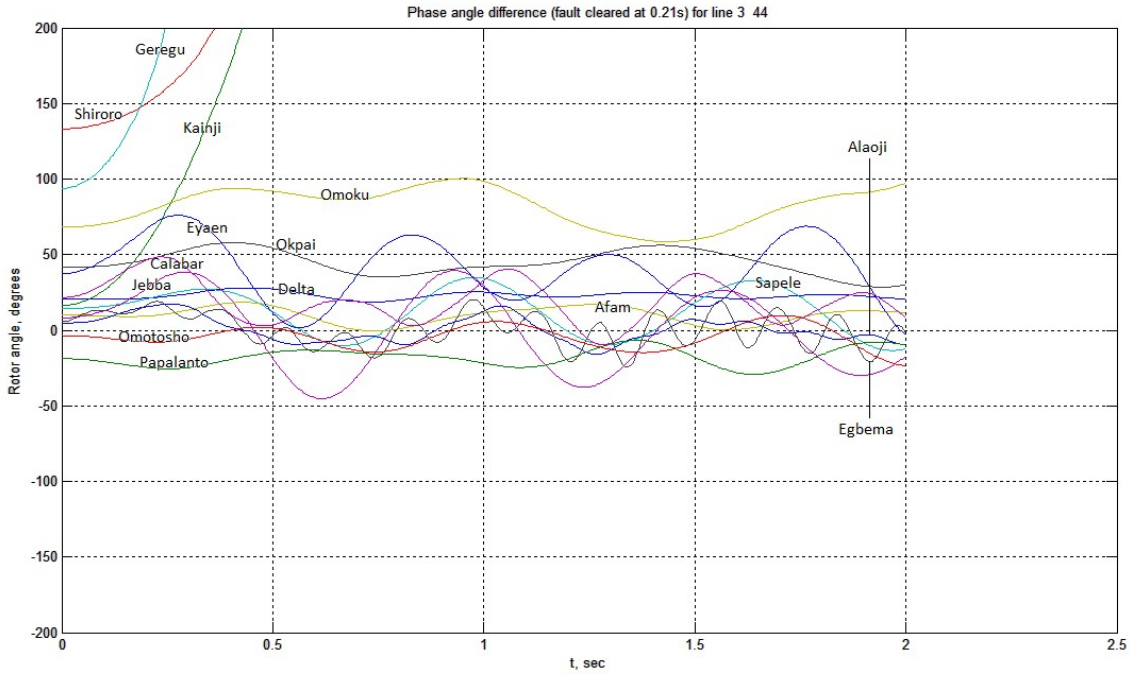

Figure 5.30 Swing curves for fault at bus 44, line 3 – 44 (Critical clearing Time: 0.21s)

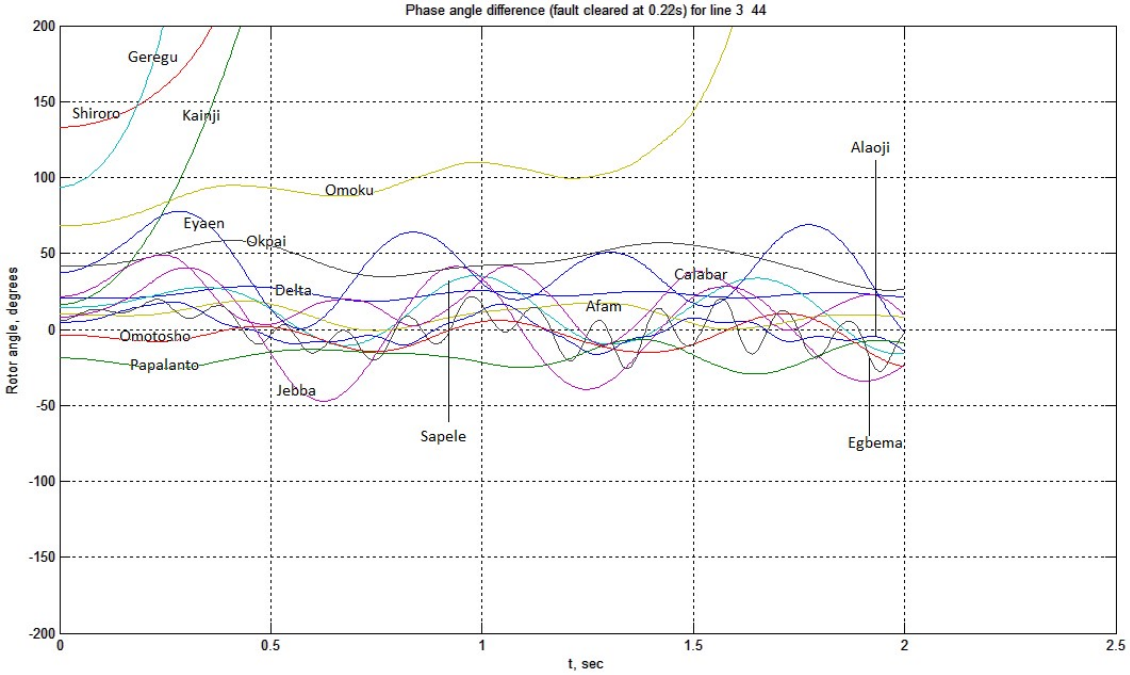

Figure 5.31 Swing curves for fault at bus 44, line 3 – 44 (Clearing Time: 0.22s)

5.4.1 Results of generators-coherency check and aggregation for a three-phase fault at bus 3 line 3-44.

The fault on power variations was carried out using the reduced bus admittance matrix, $\hat{Y}$, and the generators with real power variations of less than 30% were classified as external area generators, while those with higher power variations became study area generators. Electrical proximity index check was thereafter conducted on external area machines to determine the degree of coupling among the generators which is a function of mutual admittances. The machines that satisfied the index condition qualify for coherent groups check. The γ- and β- indices checks were subsequently performed on the machines with the following generators found to reasonably form coherent groups:

Group I: Delta (2) and Eyaen (16)

Group II: Afam (7) and Okpai (8)

Group III: Papalanto (10) and Omotosho (11)

Figure 5.32 shows the swing curves for group I coherent generators, while figure 5.33 shows their equivalent swing curve after aggregation.

Figure 5.34 on the other hand shows the swing curves for group II coherent generators, while figure 5.35 shows their equivalent swing curve after aggregation.

Also figure 5.36 shows the swing curves for group III coherent generators, while figure 5.37 shows their equivalent swing curve after aggregation.

Figure 5.38 shows the swing curves of the new network after integrating the aggregated generators to the rest of the power system, thereby reducing the 16 machines system to 13 machines. Hence, through coherent generators aggregation, the complexity of the original network is simplified, and the computational time for the system simulation reduced.

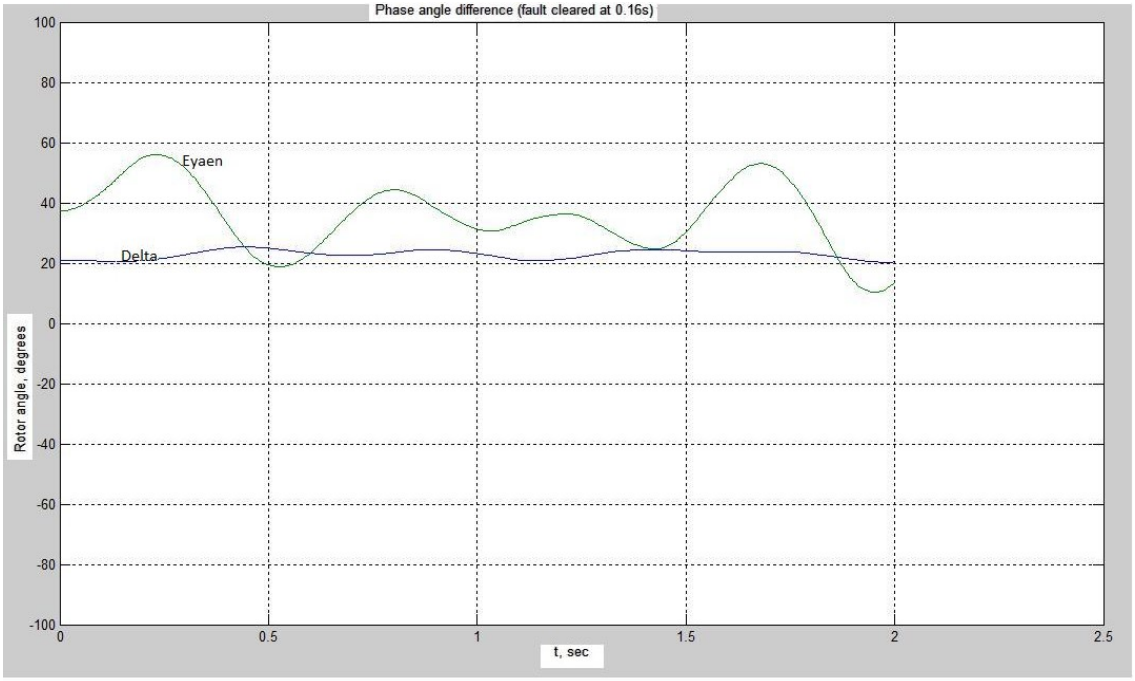

Figure 5.32 Swing curves for machines 2 and 6 for fault at bus 3, line 3 – 44

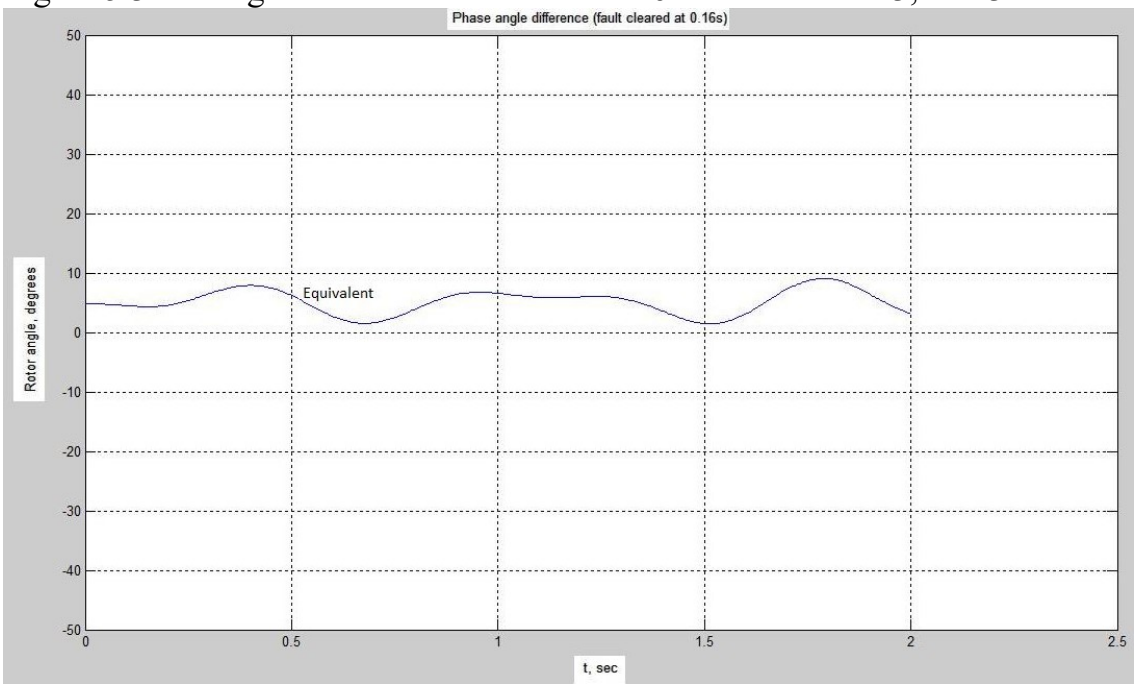

Figure 5.33 Equivalent swing curve for machines 2 and 6

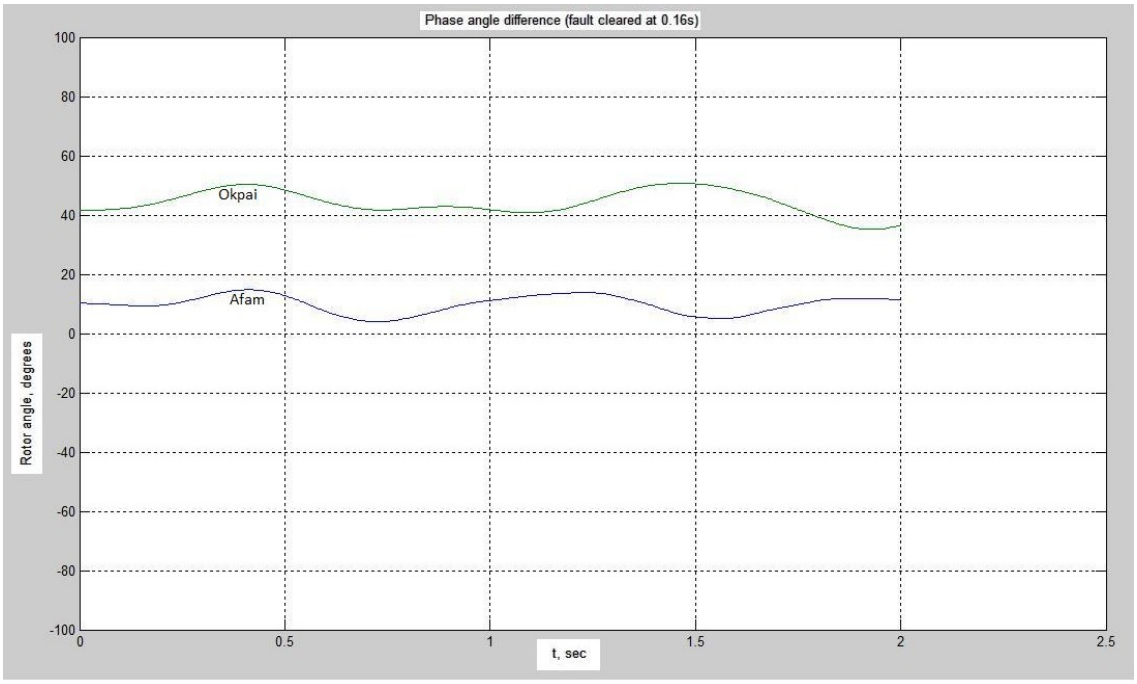

Figure 5.34 Swing curves for machines 7 and 8 for fault at bus 3, line 3 – 44

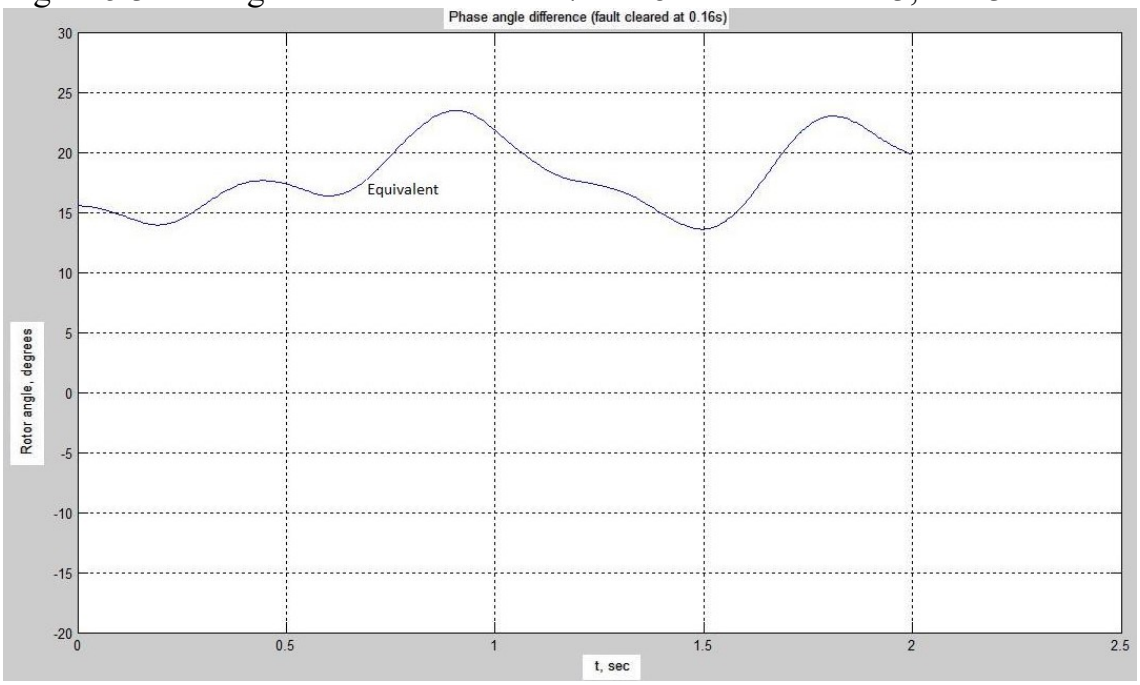

Figure 5.35 Equivalent swing curve for machines 7 and 8

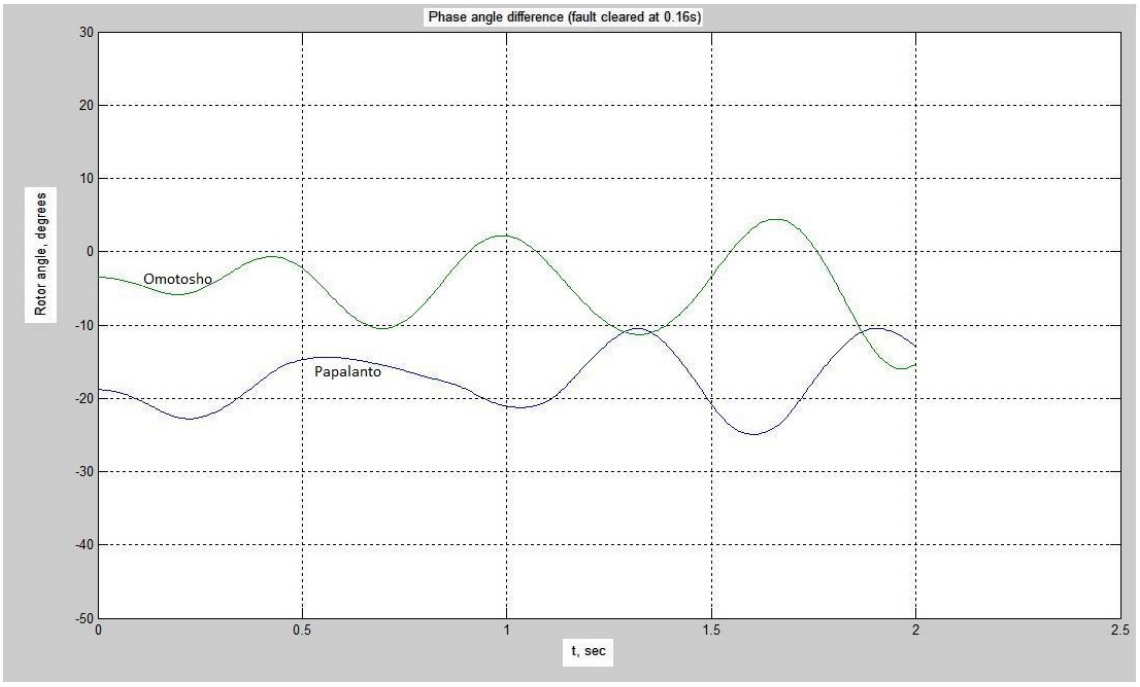

Figure 5.36 Swing curves for machines 10 and 11 for fault at bus 3, line 3 – 44

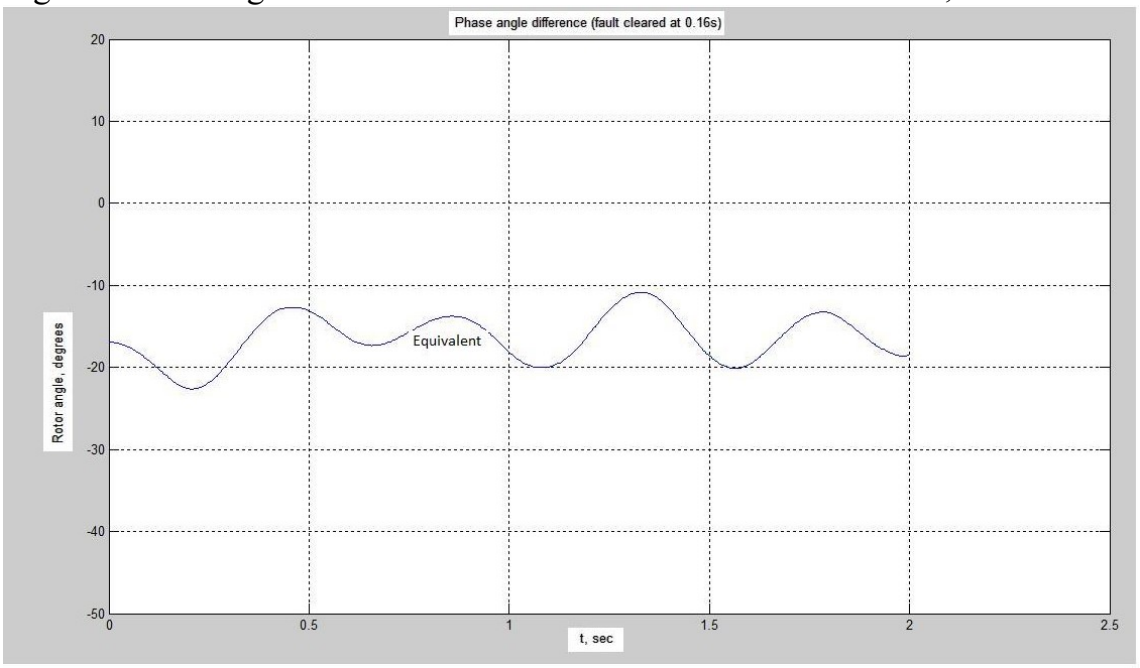

Figure 5.37 Equivalent swing curve for machines 10 and 11

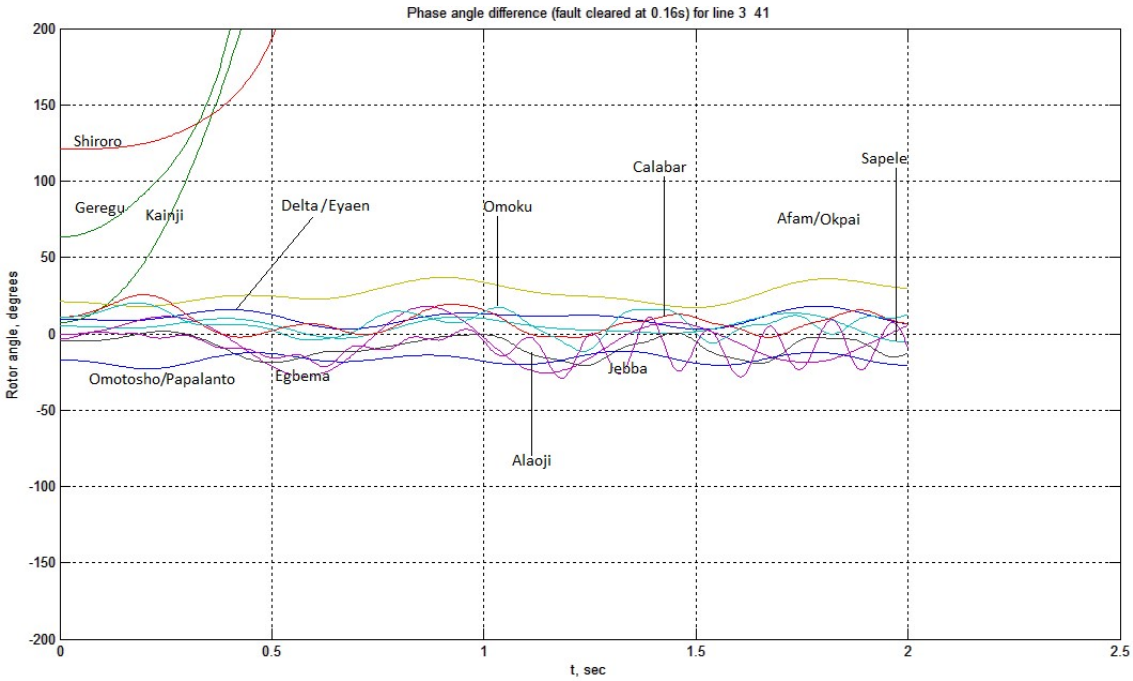

Figure 5.38 Swing curves of New Network after aggregation for fault at bus 3, line 3 – 44/41

CHAPTER SIX

6.0 Conclusion and Recommendations

The result of this research has thrown up many challenges facing the Nigeria power system in the areas of transmission capacity inadequacies of the Network for efficient power evacuation. The power flow results of the proposed 330KV Nigeria power system show that the following load buses have high voltage magnitudes above recommended + 10% tolerance: Damaturu, Maiduguri, Gombe, Yola, Jalingo, Jos, Katempe, Gwagwa, Makurdi, Aliade and New Haven.

6.1 Conclusion

The transient stability Analysis over the years has been the tool used to test the effectiveness of any given power system as well as its operational conditions. It helps the power system operators to make informed decisions when updating the network facilities in terms of transmission capacities, relay scheme and system controllers settings; and efficient power flow management.

In the course of this research, the concept of reducing the Nigeria power system to single machine - infinite bus system, and thereafter apply the principle of equal area criterion to analyze its transient stability was discarded because the network structure would have been altered, thereby producing highly compromised results. The direct method of transient stability assessment was deployed, by aggregating the generators of each generating station linking the 330KV grid system as one equivalent generator through dynamic generators aggregation technique. The power flow studies of the present operated network (existing, 8 machines – 26 bus) and expanded network (proposed, 16 machines–49 bus) systems were carried out using MATLAB-programmed Newton-Raphson technique. The results of the two systems show drastic improvement in the proposed system in terms of power

flow capacities which stood at 8476.6MW as against proposed Network power flow capacity of 3491.2MW. The multi machine transient stability study was conducted on the two networks under the most adverse fault conditions (three-phase fault at selected buses and lines). The processes include the conversion of system load data to equivalent admittances and calculation of the following system parameters:

(1) The internal voltages of the generators.
(2) Y_{bus} matrices for pre-fault, fault on and post fault conditions.
(3) Reduced Y_{bus} matrix, $\hat{Y}$.
(4) Electrical power output of the generators
(5) Rotor swings response to transient conditions
(6) Rotor angle variations of the system generators at the instant of fault initiation.

Then plotting of rotor angles variations against time t for various fault situations and clearing times.

The research also deployed the dynamic generators aggregation technique based on rotor swing coherency of the candidate generators, dependent on electrical proximity index which defines the degree of coupling between two machines. The damping and inertia indices, γ and β respectively were equally used to check generators group coherency for possible aggregation. The technique proved useful since it helped to reduce the network complexity without altering the structure. It equally ensured power invariance at the aggregated generators terminals before and after aggregation.

The simulation software is Ode45 MATLAB function based on the Fehlberg fourth-and fifth-order pair for higher accuracy. This enables very low fault clearing time to be entered unlike Ode23 function.

The results of this research show accurate prediction of critical clearing times for certain fault conditions, establishment of stability margins for

some system generators under certain fault conditions. This offers useful information to proper setting of system relaying schemes.

The effect of system controllers was not evaluated since the research only considers first swing stability which will be too short for system controllers such as governor system to respond.

6.2 Recommendations

Placement of appropriately sized synchronous reactors at these buses may be helpful in absorbing the excess reactive power build-up along the transmission lines linking them.

The amount of power losses observed in some transmission lines can be minimized by reinforcing those lines through introduction of more lines or converting single circuit lines to double circuit status where applicable thereby increasing their power evacuating capabilities.

In the area of transient stability analysis which concerns maintenance of system security when subjected to a large disturbance without tripping of generator unit(s) due to loss of synchronism, and preventing the possibility of system blackout as a result of cascaded outage. The swing curves of the simulated transient stability analysis of the Pre-Reform Nigeria power system show that at almost all the fault locations, the network experienced multiple generators losses which is unacceptable. Each of these generators contributes more than 100MW to the Network, therefore loosing two or more of such units will further stress the power system. Considering that the dominant system parameters that influence transient stability include:

(a) Generators reactances and inertia.

(b) Transmission system reactances under normal and post fault conditions.

Therefore the following steps could be taken to improve the transient stability of the power system:

(1) Increasing the inertia, H and reducing the reactance's of the vulnerable machines.

(2) Reinforcing the transmission lines in order to improve on the system reactances.

(3) Introduction of quick opening circuit breakers of high interrupting capacities will improve the transient stability limit of a given fault situation. For instance, a typical maximum fault clearing time for a three-phase fault is 8 cycles (including relay operating and circuit breakers opening times). While modern circuit breakers open within 3 cycles with relay operating time inclusive.

(4) Installation of discrete supplementary controllers such as dynamic braking system such as shunt braking resistors and series braking resistors.

- The shunt braking resistors are usually switched in following a fault clearing, to correct the temporary imbalance b\etween the mechanical power input and electrical power output of generators.
- Series braking resistors are effective in controlling the relative angle between the sending and generators with small inertia and receiving end generator with higher inertia.

The preference for this scheme over primary controllers like speed governor and excitation systems is that its action is not continuous, but only initiated following a disturbance and is temporary in nature.

Contribution to knowledge

This research has provided a suite of specifications and standards veritable for system planning, operation and management of the expanded 330KV National grid system.

It has provided insight on the anticipated expanded national grid performance in terms of power flow and system stability; and established critical clearing times for some system fault locations as well as stability margins for some grid generators under three-phase short circuits on transmission lines.

The research also provided an algorithm for coherent generator based transient stability analysis through generators aggregation and dynamic equivalents construction.

REFERENCES

Fouad A. A. and Vijay Vittal, V. (1992), ' Power System Transient Stability Analysis using the Transient Energy Function Method,' Prentice Hall Inc.,.

Fouad A. A. and Vittal V. (1988), 'The Transient Energy Function Method', Int. J. of Electrical Power and Energy System, vol. 10, No. 4, pp 233 – 246.

Fouad A. A. and Stanton S. E. (1981), 'Transient Stability of Multimachine Power Systems, Part 1: Investigation of System Trajectories', IEEE Trans., vol. PAS – 100, pp 3408 – 3414.

Fitzgerald A. E. and Kingsley C. (1961), ' Electric Machinery,' Second Edition, McGraw Hill.

Edris A. (1991), 'Enhancement of First-swing Stability using a High-speed Phase Shifter', IEEE Trans. on Power Systems, vol. PWRS – 6, No. 3, pp 1113 – 1118.

Behera A. K. (1988), 'Transient Stability Analysis of Multimachine Power Systems using Detailed Models', Ph.D Thesis, University of Illinois at Urbana-Champaign.

El-Abiad A. H. and Nagappan K. (1966), 'Transient Stability Regions of Multimachine Power Systems', IEEE Trans., vol. PAS – 85, No. 2, pp 169 – 178.

Germond A. J. and Podmore R. (1978), 'Dynamic Aggregation of Generating Unit Models', IEEE Trans., vol. PAS – 97, No. 4, pp 1060 – 1069.

Monticelli A. (1999), 'State Estimation in Electric Power Systems, A Generalized Approach', Kluwer Academic Publishers.

Omoigui M. O. and Ojo O. J. (2007), 'Investigation of steady-state and Transient Stabilities of the Restructured Nigerian 330KV Electric Power

Network' Proc. Of Inter. Conf. and Exhibition on Power systems, University of Lagos, Nigeria, July, pp 75 – 83.

Onohaebi O. S. and Apeh S. T. (2007), 'Voltage Instability in Electrical Network: A case study of the Nigerian 330KV Transmission Grids', Research Journal of Applied Sciences, Medwell, vol. 8, pp 865 – 874.

Onohaebi O. S. and Igbinovoa S. O. (2007), 'Voltage dips reduction in the Nigerian 330KV Transmission Grids, Journal of Engineering and Applied Sciences, Medwell vol.6, pp 496 – 503.

Okafor E. N. C. (2009), 'Evaluation of the Impact of power sector Reforms on the Nigerian Economy', Global Journal of Engineering and Technology, vol. 8, pp 411 – 421.

Balogun A. O. (2007), 'Impact of Power Sector Reform on Nigeria Electricity Industry', International Conference on Power Systems, Lagos, Nigeria, July, Pp 123 – 128.

Transmission Company of Nigeria (2003), 'Grid Network for Evacuation of proposed 10,000MW power generation'.

Stein R. and Hunt W. T. (1979), 'Electric Power System Components Transformers and Rotating machines', Van Nostrand Reinhold Company, New York.

Ekwue A. O. and Macqueen J. F. (1991), 'Comparison of Load Flow Solution Methods', Electric Power Systems Research, 22, pp 213 – 222.

Okoro C. C. (2010), 'Energy Conversion Principles & Systems For Power Engineering', University of Lagos press, Lagos.

Izuegbunam F.I. (2002), 'Improvement of Power Supply Services in Owerri Metropolis and Environs', M.sc thesis, Federal University of Technology, Owerri.

Davies T. (1984), 'Protection of Industrial Power Systems', Pergamon Press, England.

Gupta B. R. (1998), 'Power System Analysis and Design', S.Chand & Company Ltd.

Bergen A. R. and Hill D. J. (1981), 'A Structure-Preserving Model for Power System Stability Analysis', IEEE Trans., vol. PAS – 100, No. 1, pp 25 – 35.

Bergen A. R., Hill D.J. and De Marcot C. L. (1986), 'Lyapunov Functions for Multimachine Power Systems with Generator Flux Decay and Voltage Dependent Loads', Int. J. of Electrical Power and Energy System, vol. 8, No. 1, pp 2 – 10.

Bergen A. R. and Vittal V. (2000), 'Power Systems Analysis', 2nd Edition, Prentice Hall Inc.

Al-Fuhaid A. S. (1987), 'Coherency Identification for Power System', Int. J. Electr. Power and Energy Syst. Vol. 9, No. 3, July, PP. 149-56.

Adkins B. and Harley R. G. (1979), 'The General Theory of Alternating Current Machines: Application to Practical Problems', Chapman and Hall Ltd.

Spalding B. D., Yee H. and Goudie D. B. (1977), 'Coherency Recognition for Transient stability studies using singular points', IEEE Trans., Vol. PAS-96, PP. 1368-75.

Toumi B., Dhifaorei R., Cutsem T. V. and Ribbens – Pavella M. (1986), 'Fast Transient Stability Assessment Revisited', IEEE Trans. of Power Systems, vol. PWRS – 1, No. 2, pp 211 – 220.

Okoro C. C. (1986), 'Theoretical Foundations for Dynamic Transient Stability Evaluation of a Machine Infinite-bus System', NJET vol. 9, no. 1, August , 105 – 124.

Okoro C. C. and Awosope C. O. A. (1987), 'Transient Stability of a Machine Infinite-Bus System with Particular Reference to the Nigerian National Grid', Project Sponsored by the Central Research-Committee, University of Lagos, Nigeria.

Njemanze C. (2001), ' NEPA and the economy' Business Times, Vol. 26, No. 33, August 13 – 19, pp. 20 – 21.

Taylor C.W. (1994), ' Power System Voltage Stability', McGraw Hill Inc.

Taylor C. W., Nassief F. R. and Cresap R. L. (1981), 'Northwest Power Pool Transient Stability Enhancement by 120-degree Phase Rotation', IEEE Trans., vol. PAS – 100, July, pp 3486 – 3495.

Okoro C. C. and Achugbu K. C. (2007), ' Contingency Assessment of the Nigeria 330KV Power Grid', Proc. of inter. Conf. And exhibition on Pow. Systems University of Lagos, Nigeria, 23rd -25th July, pp. 84-93.

Vorley D. H. (1974), 'Numerical Techniques for Analyzing the Stability of Large Power Systems', Ph.D Thesis, University of Manchester (England).

Larson E. V. and Swan D.A. (1981), 'Applying Power System Stabilizers, Parts I, II, III' IEEE Trans., PAS – 100, pp 3017 – 3046.

Kimbark E. W. (1948), 'Power System Stability, Vol. 1: Synchronous Machine', John Wiley & Sons.

Rahimi F A., Lamby M. G., Wrubel J. N. and Lee, K. L. (1993), 'Evaluation of the Transient Energy Function Method for on-line Dynamic Security Analysis', IEEE Trans. on Power Systems, vol. 8, No. 2, pp 497 – 507.

Lüders G. A. (1971), 'Transient Stability of Multimachine Power System via the Direct Method of Lyaponuv', IEEE Trans., PAS – 90, No. 1.

Maria G. A., Tang C. and Kim J. (1990), 'HYBRID Transient Stability Analysis', IEEE Trans. on Power Systems, vol. 5, No. 2, pp 384 – 391.

Anderson G. (2003), 'Modeling and Analysis of Electric Power Systems', EEH – Power Systems Laboratory, ETH Zurich.

Gless G. E. (1966), 'Direct Method of Lyapunov Applied to Transient Power System Stability', IEEE Trans., vol. PAS – 85, No. 2, pp 159 – 168.

Gross G., Imperato C. F. and Look P. M. (1982), 'A Tool for the Comprehensive Analysis of Power System Dynamic Stability', IEEE Trans., vol. PAS – 101, No. 4, pp 226 – 234.

Benson G. H. and Dunn R. W. (2000), 'A High-speed Transient Simulator for On-line and Off-line Analysis', Proc. of the Universities' Power Engineering Conference, Belfast.

Chiang H. D. (1989), 'Study of the Existence of Energy Functions for Power Systems with Losses', IEEE Trans. on Circuits and Systems, vol. CAS – 36, Nov., pp 1423 – 1429.

Chiang H. G., Wu F. F. and Varaiya P. P. (1987), 'Foundations of Direct Methods for Power System Transient Stability Analysis', IEEE Trans. on Circuits and Systems, vol. CAS – 34, No. 2, pp 160 -173.

Rudnick H., Patino R. I., and Brameller A. (1981), 'Power System Dynamic Equivalents: Coherency Recognition via the rate of change of Kinetic Energy', Proceedings of the IEE, Vol. 128, Pt C, No. 6, Nov., PP. 325-33.

Saadat H. (2002), 'Power System Analysis', Tata McGraw Hill.

Dommel H. W. and Sato N. (1972), 'Fast Transient Stability Solutions', IEEE Trans., Power Apparatus and Systems, PAS – 91, pp 1643 – 1650.

Achibong I. (2007), 'Vision 2010 – The place of IEEE Nigeria in the Present Electric Power Reforms', A technical paper presented at the IEEE National Meeting/Technical Session, Port Harcourt.

IEEE Task Force, Subcommittee of System Dynamic Performance, Power Systems Engineering Committee PES. (1982), 'Proposed Terms and Definitions for Power System Stability', IEEE Transactions PAS – 101, pp 1894 – 1898.

IEEE Task Force on Load Representation for Dynamic Performance,(1995) , 'Standard Load Models for Power Flow and Dynamic Performance Simulation' IEE Trans., PWRS – 10, No. 3, pp 1302 – 1312.

IEEE Committee Report (1992), 'Transient Stability Test Systems for Direct Stability Methods', IEEE Trans. on Power Systems, vol. 7, Feb., pp 37 – 43.

IEEE Committee Report (1985), 'Application of Direct Methods to Transient Stability Analysis of Power Systems', IEEE Trans., vol. PAS – 104, May, pp 1629 – 1636.

IEEE Committee Report (1987), 'Bibliography on the Application of Siscrete Supplimentary Controls to Improve Power System Stability', IEEE Trans. on Power Systems, vol. PWRS – 2, May, pp 474 – 485.

Arrillaga J. and Arnold C. P. (1990), 'Computer Analysis of Power Systems', John Wiley & Sons.

Robert J. D. and Hiskens I. A. (1997), 'Lyapunov Functions for Multimachine Power Systems with Dynamic Loads, IEEE Transactions on Circuits and Systems – I: Fundamental Theory and Applications, vol. 44, no. 9, Sept., 796 – 811.

Machowski J. and Nelles D. (1994), 'Power System Transient Stability Enhancement by Optimal Control of Static VAR Compensators' Int. J. on Electrical Power and Energy Systems, 16, No. 5.

Machowski J., Bialek J. W. and Bumby J. R. (1997), 'Power System Dynamics and Stability', John Wiley & Sons.

Undrill J. M. and Turner A. E. (1971), 'Construction of Power System Electro-Mechanical Equivalents by Modal Analysis', IEEE Trans., Vol. PAS-90 Sept./Oct., PP 2049-59.

Tong J., Chiang H. D. and Conneen T. P. (1993), 'A Sensitivity-based BCU Method for Fast Derivation of Stability Limits in Electric Power Systems', IEEE Trans. on Power Systems, vol. 8, No. 4, pp 1418 – 1428.

Padiyar K. R. (1996), 'Power System Dynamics, Stability and Control', John Wiley & Sons Pte Ltd.

Padiyar K. R. (1993), 'Improvement of System Stability with SVC Control in Recent Advances in Control and Management of Energy Systems', Interline Publishing, Bangalore, pp 136 – 156.

Padiyar K. R. and Sastry H. S. Y. (1987), 'Topological Energy Function Stability Analysis of Power Systems', Int. J. of Electrical Power and Energy System, vol. 9, No. 1, pp 9 – 16.

Padiyar K. R. and Ghosh K. K. (1989), 'Direct Stability Evaluation of Power Systems with Detailed Generator Models using Structure-Preserving Energy Functions', Int. J. of Electrical Power and Energy System, vol. 11, No. 1, pp 47 – 56.

Padiyar K. R. and Ghosh K. K. (1989), 'Dynamic Security Assessment of Power Systems using Structure-Preserving Energy Functions', Int. J. of Electrical Power and Energy Systems, vol. 11, No. 1.

Padiyar K. R. and Ghosh K. K. (1987), 'A Novel Structure-Preserving Energy Function for Direct Stability Evaluation of Power Systems with known Modes of Instability', Electric Machines and Power Systems, vol. 13, pp 135 – 148.

Padiyar K. R. and Sastry H. S. Y. (1986), 'Fast Evaluation of Transient Stability of Power Systems using a Structure-Preserving Energy Function', Electric Machines and Power Systems, vol. 11, pp 421 – 441.

Padiyar K. R. and Immanuel V. (1995), 'Direct Evaluation of Transient Stability Improvement with Static VAR Compensators using a Structure-Preserving Energy Function', Electric Machines and Power Systems, vol. 23, No. 3.

El-Kady M. A., Tang C. K., Carvalho V. F., Fouad A. A. and Vittal V. (1986), 'Dynamic Security Assessment Utilizing the Transient Energy Function Method', IEEE Trans. on Power Systems, vol. PWRS – 1, pp 284 – 291.

Klien M., Rogers G. J. and Kundur P. (1991), 'A Fundamental Study of Inter-area Oscillations in Power Systems', IEEE Trans. on Power Systems, vol. 6, No. 3, pp 914 – 921.

Al-Rawi M. N., Anwar A. and Abdul-Majeed A. M. (2007), 'Computer-aided Transient Stability Analysis, Journal of Computer Science 3(3): 149 – 153.

Ribbens – Pavella M. and Evans F. J. (1985), 'Direct Methods for Studying Dynamics of Large-scale Electric Power Systems – A Survey', Automatica, vol. 32, Januay, pp 1 -21.

Hussian M. Y. and Rau V. G. (1993), 'Coherency Identification and Construction of Dynamic Equivalent for large power system', Proceedings of 2nd Inter. Confr. On Avances in powr. Syst. Control, operation and management, Hongkong.

Tsolas N. A., Arapostathis A. and Varaiya P. P. (1985), 'A Structure-Preserving Energy Function for Power System Transient Stability Analysis', IEEE Trans. on Circuits and Systems, vol. CAS – 32, No. 10, pp 1041 – 1049.

Narasimhamurthi N. and Musavi M. R. (1984), 'A General Energy Function for Transient Stability Analysis of Power Systems', IEEE Trans. on Circuits and Systems, vol. CAS – 31, No. 7, pp 637 – 645.

Elgerd O. I. (1979), 'Electric Energy Systems Theory: An Introduction', McGraw Hill Inc.

Kundur P. (1994), 'Power System Stability and Control', McGraw Hill Inc.

Anderson P. M. and Fouad A. A. (1977), 'Power System Control and Stability', Iowa State University Press, Ames, Iowa.

Anderson P. M. and Fouad A. A. (2002), 'Power System Control and Stability, Second Edition, Wiley – IEEE Press.

Oirsouw P. M. V. (1990), 'A Dynamic Equivalent Using Modal Coherency and Frequency Response', IEEE Trans., Vol. PS-5, No.1, Feb., PP. 289-95.

Varaiya P. P., Wu F. F. and Chen R. L. (1985), 'Direct Methods for Transient Stability Analysis of Power Systems: Recent Results', Proc. of IEEE, vol. 73, pp 1703 – 1715.

Sauer P. W. and Pai M. A. (1998), 'Power System Dynamics and Stability', Prentice Hall.

Cresap R. L; Taylor C. W. and Kreipe M. J.(1981), 'Transient Stability Enhancement by 120-degree Phase Rotation', IEEE Trans., vol. PAS – 100, Feb., pp 745 – 753.

Podmore R. (1978), 'Identification of Coherent Generators for Dynamic Equivalents', IEEE Trans., vol. PAS – 97, No. 4, pp 1060 – 1069.

Stanton S. E. (1982), 'Assessment of the Stability of a Multimachine Power System by the Transient Energy Margin', Ph.D Thesis, Iowa State University, Ames, IA, United States.

Geeves S. (1988), 'A Modal-Coherency Technique for Derving Dynamic Equivalents', IEEE Trans., Vol. PS-3, No. 1, Feb., PP. 44-51.

Nishida S. and Takeda S. (1992), 'A Method to Construct a Control Strategy in Emergency Control of Power Systems on the Basis of Energy Function', Electrical Engineering in Japan, vol. 102, No. 5, pp 77 – 84.

Lee S. T. Y. and Schweppe F. C. (1973), 'Distance measures and Coherency Recognition for Transient Stability Equivalents' IEEE Trans., vol. PAS – 82, Sept./Oct., pp 1550 – 1557.

Krishnaparandhama T., Elvangovan S., and Kuppurajulu A., 'Method for Identifying Coherent Generators', Int. J. Electr. Power and Energy Syst. Vol. 3, No. 2, April, PP. 85-90.

Rau V. G. and Hussian M. Y. (1998), 'Coherent Generators', Allied Publishers Limited, New Delhi.

Immanuel V. (1993), 'Application of Structure-Preserving Energy Functions for Stability Evaluation of Power Systems with Static VAR Compensators', Ph.D Thesis Submitted to Indian Institute of Science, Bangalore.

Sankaranarayanan V., Venugopal M., Elangovan S., and R.N. Dharma R. N. (1983), 'Coherency Identification and Equivbalents for Transiet Stability Studies', Electr. Pwr. Syst., Res. Vol. 6, PP. 51-60.

Prince W. W., Gulachenki E. K., Kundur P., Lange F. J., Loehr G. C., Roth B. A., and Silva R. F. (1978), 'Testing of the Modal Dynamic Equivalents Technique', IEEE Trans., Vol. PAS-97, July / Aug., PP. 1366-72.

Sue Y., Wehenkel L., Belhomme R., Rousseaux P., Pavella M., Eusibie E., Heilbronn B. and Lasigne J. F. (1992), 'Extended Equal Area Criterion Revisited', IEEE Trans. on Power Systems, vol. 7, No. 3, pp 1012 – 1022.

Sue Y., Pavella M. (1993), 'Critical-Cluster Identification in Transient Stability Studies', IEE Proc. (London) Parc C, vol. 140, No. 6, pp 481 – 489.

Sue Y., Cutsem T. V. and Ribbens-Pavella M. (1989), 'Extended Equal Area Criterion: Justifications, Generalizations, Applications', IEEE Trans. on Power Systems, vol. 4, No. 1, pp 44 – 52.

Cutsem T. V. and Vournas C. (1998), 'Voltage Stability of Electric Power Systems, Kluwer Academic Publishers.

A1: Existing 330KV National Grid Bus Data

Bus No.	Bus code	Voltage (pu)	Angle (Deg.)	P_{load} MW	Q_{load} MW	P_{gen} MW	Q_{gen} Mvar	Q_{min} Mvar	Q_{max} Mvar	Injected Mvar
1.	1	1.0	0.0	260	161.13	0	0	-550	800	0
2.	2	1.0	0.0	44	277.3	500	0	-100	120	0
3.	2	1.0	0.0	0	0	164	0	-250	300	0
4.	2	1.0	0.0	0	0	530	0	-300	270	0
5.	2	1.0	0.0	0	0	77	0	-280	430	0
6.	2	1.0	0.0	0	0	415	0	-200	270	0
7.	2	1.0	0.0	64	39.7	500	0	-150	280	0
8.	2	1.0	0.0	0	0	450	0	-260	330	0
9.	0	1.0	0.0	250	154.9	0	0	0	0	0
10.	0	1.0	0.0	152	94.2	0	0	0	0	0
11.	0	1.0	0.0	135.6	84.02	0	0	0	0	0
12.	0	1.0	0.0	15	9.3	0	0	0	0	0
13.	0	1.0	0.0	120	74.38	0	0	0	0	0
14.	0	1.0	0.0	43	26.65	0	0	0	0	0
15.	0	1.0	0.0	200	123.9	0	0	0	0	0
16.	0	1.0	0.0	550	340.9	0	0	0	0	0
17.	0	1.0	0.0	400	247.9	0	0	0	0	0
18.	0	1.0	0.0	180	111.55	0	0	0	0	0
19.	0	1.0	0.0	240	148.7	0	0	0	0	0
20.	0	1.0	0.0	12	7.43	0	0	0	0	0
21.	0	1.0	0.0	185	114.7	0	0	0	0	0
22.	0	1.0	0.0	85	52.68	0	0	0	0	0
23.	0	1.0	0.0	260	161.1	0	0	0	0	0
24.	0	1.0	0.0	135.6	84	0	0	0	0	0
25.	0	1.0	0.0	80	49.6	0	0	0	0	0

26.	0	1.0	0.0	80	49.6	0	0	0	0	0

A2: Existing 330KV National Grid Power Flow Results

Bus No.	Voltage mag.	Angle degree	Load		Generation		Injected Mvar
			MW	Mvar	MW	MVar	
1.	1.000	0.000	260.000	161.130	974.862	622.862	0.000
2.	0.970	9.059	44.000	277.300	500.000	58.175	0.000
3.	1.000	0.220	0.000	0.000	164.000	-79.358	0.000
4.	1.000	-5.449	0.000	0.000	530.000	146.842	0.000
5.	1.000	6.041	0.000	0.000	77.00	215.882	0.000
6.	1.000	-0.366	0.000	0.000	415.000	-32.960	0.000
7.	1.000	23.612	64.00	39.700	500.000	33.670	0.000
8.	1.000	13.940	0.000	0.000	450.000	169.443	0.000
9.	0.961	21.789	250.000	154.900	0.000	0.000	0.000
10.	0.947	12.986	152.000	94.200	0.000	0.000	0.000
11.	0.920	10.518	135.600	84.020	0.000	0.000	0.000
12.	1.006	5.029	15.000	9.300	0.000	0.000	0.000
13.	0.988	5.405	120.000	74.380	0.000	0.000	0.000
14.	0.984	7.287	43.000	26.650	0.000	0.000	0.000
15.	0.976	-1.890	200.000	123.900	0.000	0.000	0.000
16.	0.930	-4.997	550.000	340.900	0.000	0.000	0.000
17.	0.903	-7.190	400.000	247.900	0.000	0.000	0.000
18.	0.969	-3.108	180.000	111.550	0.000	0.000	0.000
19.	0.922	-6.774	240.000	148.700	0.000	0.000	0.000
20.	0.999	-0.895	12.000	7.430	0.000	0.000	0.000
21.	0.948	-9.646	185.000	114.700	0.000	0.000	0.000
22.	0.992	-4.443	85.000	52.680	0.000	0.000	0.000
23.	0.972	-10.182	260.000	161.100	0.000	0.000	0.000
24.	0.919	-16.030	135.600	84.000	0.000	0.000	0.000
25.	0.970	-16.146	80.000	49.600	0.000	0.000	0.000
26.	0.956	-20.132	80.000	49.600	0.000	0.000	0.000
Total			**3491.200**	**2413.640**	**3610.862**	**1134.511**	**0.000**

A3: Existing 330KV National Grid Line Flow and Losses

From	To	Power flow			Line Losses	
		MW	Mvar	MVA	MW	Mvar
1		714.862	461.688	850.990		
	16	513.764	355.188	624.589	8.001	43.175
	15	201.098	106.500	227.558	1.098	-17.400
2		456.000	-219.125	505.917		
	13	309.518	-124.037	333.447	2.307	-0.987
	14	146.482	-95.088	174.639	0.606	-17.059
3		164.000	-79.358	182.191		
	20	78.190	-22.078	81.247	0.185	-29.269
	22	85.810	-57.280	103.172	0.810	-109.960
4		530.000	146.842	549.966		
	20	-222.853	-60.023	230.794	1.776	-167.498
	21	187.469	85.882	206.205	2.469	-28.818
	23	565.383	120.983	578.183	5.166	-20.493
5		77.000	215.882	229.203		
	13	179.479	130.941	222.167	0.552	-37.253
	14	-102.479	84.941	133.104	0.398	-19.739
6		415.000	-32.960	416.307		
	20	415.000	-32.960	416.307	0.520	0.492
7		436.000	-6.030	436.042		
	9	436.000	-6.030	436.042	17.109	3.301
8		450.000	169.443	480.844		
	10	450.000	169.443	480.844	20.970	6.443
9		-250.000	-154.900	294.099		
	7	-418.891	9.331	418.995	17.109	3.301
	10	168.891	-164.231	235.576	25.520	-25.906
10		-152.000	-94.200	178.823		
	8	-429.030	-163.000	458.951	20.970	6.443
	10	-143.371	138.326	199.221	25.520	-25.906
	11	136.418	60.139	149.086	0.818	-23.881
	13	283.983	-129.665	312.185	5.122	-6.184
11		-135.600	-84.020	159.520		
	10	-135.600	-84.020	159.520	0.818	-23.881
12		-15.000	-9.300	17.649		
	13	-15.000	-9.300	17.649	0.159	-146.743
13		-120.000	-74.380	141.182		
	2	-307.211	123.050	330.938	2.307	-0.987
	5	-178.926	-168.195	245.569	0.552	37.253
	10	-278.862	123.481	304.978	5.122	-6.184
	12	15.159	-137.443	138.276	0.159	-146.743
	16	442.256	15.489	442.527	10.875	-129.105
	18	187.584	-30.762	190.090	3.269	-63.621

14		-43.000	-26.650	50.589		
	2	-145.876	78.029	165.434	0.606	-17,059
	5	102.876	-104.679	146.770	0.398	-19.739
15		-200.000	-123.900	235.268		
	1	-200.000	-123.900	235.268	1.098	-17.400
16		-550.000	-340.900	647.080		
	1	-505.762	-312.014	594.263	8.001	43.175
	13	-431.381	-144.593	454.969	10.875	-129.105
	17	402.593	227.025	462.192	2.593	-20.875
	18	-80.641	-99.535	128.103	0.719	-41.004
	19	65.191	-11.782	66.248	0.252	-42.562
17		-400.000	-247.900	470.589		
	16	-400.000	-247.900	470.589	2.593	-20.875
18		-180.000	-111.550	211.763		
	13	-184.315	-32.859	187.221	3.269	-63.621
	16	81.360	58.531	100.227	0.719	-41.004
	19	176.968	95.463	201.074	1.907	-22.457
	20	-254.013	-232.686	344.479	1.844	-158.902
19		-240.000	-148.700	282.333		
	16	-64.939	-30.780	71.864	0.252	-42.562
	18	-175.061	-117.920	211.072	1.907	-22.457
20		-12.000	-7.430	14.114		
	3	-78.005	-7.191	78.336	0.185	-29.269
	4	224.628	-107.475	249.016	1.776	-167.498
	6	-414.480	33.452	415.828	0.520	0.492
	18	255.857	73.784	266.284	1.844	-158.902
21		-185.000	-114.700	217.672		
	4	-185.000	-114.700	217.672	2.469	-28.818
22		-85.000	-52.680	100.001		
	3	-85.000	-52.680	100.001	0.810	-109.960
23		-260.000	-161.100	305.865		
	4	-560.217	-141.476	577.805	5.166	-20.493
	25	162.666	-42.471	168.119	1.965	-53.686
	24	137.551	22.847	139.435	1.951	-61.153
24		-135.600	-84.000	159.510		
	23	-135.600	-84.000	159.510	1.951	-61.153
25		-80.000	-49.600	94.128		
	23	-160.701	-11.215	161.092	1.965	-53.686
	26	80.701	-38.385	89.365	0.701	-87.985
26		-80.000	-49.600	94.128		
	25	-80.000	-49.600	94.128	0.701	-87.985
				Total loss	**119.662**	**-1279.129**

B1: Proposed national grid bus data

Bus no	Bus code	V (pu)	Angle (Deg.)	P_load MW	Q _load Mvar	P_gen MW	Q _gen Mvar	Qmin Mvar	Qmax Mvar	Injected Mvar
1	1	1	0	0	0	1254	777	-550	800	0
2	2	1	0	0	0	682	423	-100	120	0
3	2	1	0	0	0	699	433	-250	300	0
4	2	1	0	200	123.9	600	372	-300	370	0
5	2	1	0	0	0	683	348	-280	340	0
6	2	1	0	19	11.8	303.5	376	-200	270	0
7	2	1	0	117	72.5	302	187	-150	200	0
8	2	1	0	0	0	536	332	-260	330	0
9	2	1	0	454	281.4	480	298	-250	290	0
10	2	1	0	0	0	326	202	-160	200	0
11	2	1	0	0	0	323	200	-160	200	0
12	2	1	0	0	0	444	275	-220	270	0
13	2	1	0	90	55.76	600	372	-280	370	0
14	2	1	0	0	0	240	149	-100	140	0
15	2	1	0	0	0	360	223	-180	220	0
16	2	1	0	0	0	480	298	-250	290	0
17	0	1	0	62	38	0	0	0	0	0
18	0	1	0	115	71	0	0	0	0	0
19	0	1	0	141	87	0	0	0	0	0
20	0	1	0	82	51	0	0	0	0	0
21	0	1	0	61	38	0	0	0	0	0
22	0	1	0	141	87	0	0	0	0	0
23	0	1	0	307	190	0	0	0	0	0
24	0	1	0	173	107	0	0	0	0	0
25	0	1	0	90	56	0	0	0	0	0
26	0	1	0	61	38	0	0	0	0	0
27	0	1	0	247	153	0	0	0	0	0
28	0	1	0	82	51	0	0	0	0	0
29	0	1	0	276	171	0	0	0	0	0
30	0	1	0	90	56	0	0	0	0	0
31	0	1	0	218	135	0	0	0	0	0
32	0	1	0	78	48	0	0	0	0	0
33	0	1	0	380	236	0	0	0	0	0
34	0	1	0	302	187	0	0	0	0	0
35	0	1	0	340	211	0	0	0	0	0
36	0	1	0	925	573	0	0	0	0	0
37	0	1	0	650	403	0	0	0	0	0
38	0	1	0	110	68	0	0	0	0	0
39	0	1	0	420	260	0	0	0	0	0
40	0	1	0	26	16	0	0	0	0	0
41	0	1	0	430	266	0	0	0	0	0
42	0	1	0	70	43	0	0	0	0	0
43	0	1	0	78	48	0	0	0	0	0
44	0	1	0	19	12	0	0	0	0	0
45	0	1	0	433	268	0	0	0	0	0
46	0	1	0	131	81	0	0	0	0	0
47	0	1	0	135.6	84	0	0	0	0	0
48	0	1	0	141	87	0	0	0	0	0
49	0	1	0	112	69	0	0	0	0	0

B2: Proposed national grid power flow result

Power flow solution by Newton –Raphson Method

Maximum power mismatch =5.72795e-008

No. of iterations =11

Bus No.	Voltage Mag.(pu)	Angle (Degree)	Load MW	Load Mvar	Generated MW	Generated Mvar	Injected Mvar
1	1.000	0.000	400.000	247.900	1840.053	1694.541	0.000
2	1.010	23.771	0.000	0.000	682.000	-370.504	0.000
3	1.050	24.063	0.000	0.000	699.000	-425.568	0.000
4	1.050	17.216	200.000	123.900	600.000	-1775.149	0.000
5	1.020	22.966	0.000	0.000	683.000	415.426	0.000
6	1.050	21.769	19.000	11.800	303.500	-355.418	0.000
7	1.050	24.897	117.000	72.500	302.000	-919.643	0.000
8	1.050	24.500	0.000	0.000	536.000	-641.801	0.000
9	1.050	24.960	454.000	281.400	480.000	-105.417	0.000
10	0.960	-0.856	150.000	92.960	326.000	144.198	0.000
11	0.970	13.761	120.000	74.000	323.000	-140.745	0.000
12	1.050	19.137	0.000	0.000	444.000	-1476.315	0.000
13	1.050	23.023	90.000	55.760	600.000	-900.514	0.000
14	1.040	25.796	0.000	0.000	240.000	-816.762	0.000
15	1.050	25.538	0.000	0.000	360.000	492.467	0.000
16	1.010	22.511	0.000	0.000	480.000	-1101.969	0.000
17	1.716	8.442	62.000	38.000	0.000	0.000	0.000
18	1.800	7.418	115.000	71.000	480.000	0.000	0.000
19	1.699	8.626	141.000	87.000	0.000	0.000	0.000
20	1.794	7.585	82.000	51.000	0.000	0.000	0.000
21	1.809	7.382	61.000	38.000	0.000	0.000	0.000
22	1.313	13.986	141.000	87.000	0.000	0.000	0.000
23	1.144	16.767	307.000	190.000	0.000	0.000	0.000
24	1.168	15.838	173.000	107.000	0.000	0.000	0.000
25	1.218	16.624	90.000	56.000	0.000	0.000	0.000
26	1.196	17.502	61.000	38.000	0.000	0.000	0.000
27	1.110	20.740	247.000	153.000	0.000	0.000	0.000
28	1.075	21.994	82.000	51.000	0.000	0.000	0.000
29	1.049	23.692	276.000	171.000	0.000	0.000	0.000
30	1.052	25.082	90.000	56.000	0.000	0.000	0.000
31	1.012	22.396	218.000	135.000	0.000	0.000	0.000
32	1.015	23.224	78.000	48.000	0.000	0.000	0.000
33	0.987	-1.668	380.000	236.000	0.000	0.000	0.000
34	0.984	-1 864	302.000	187.000	0.000	0.000	0 .000
35	0.970	-0.171	340.000	211.000	0.000	0.000	0.000
36	0.966	-0.436	925.000	573.000	0.000	0.000	0.000

37	0.938	-2.618	650.000	403.000	0.000	0.000	0.000
38	0.962	-0.901	110.000	68.000	0.000	0.000	0.000
39	0.942	-2.378	420.000	260.000	0.000	0.000	0.000
40	1.057	19.015	26.000	16.000	0.000	0.000	0.000
41	1.044	21.405	430.000	266.000	0.000	0.000	0.000
42	1.084	18.218	70.000	43.000	0.000	0.000	0.000
43	1.050	21.360	78.000	48.000	0.000	0.000	0.000
44	1.051	21.692	19.000	12.000	0.000	0.000	0.000
45	1.051	13.043	433.000	268.000	0.000	0.000	0.000
46	1.054	12.000	131.000	81.000	0.000	0.000	0.000
47	1.061	11.330	135.600	84.000	0.000	0.000	0.000
48	1.079	21.633	141.000	87.000	0.000	0.000	0.000
49	1.055	11.147	112.000	69.000	0.000	0.000	0.000
	TOTAL		**8476.600**	**5249.220**	**8898.553**	**-6283.173**	**0.000**

B3 Proposed 330KV National Grid Line flow and losses

From	To	Power Flow			Line losses	
		Mw	Mvar	MVA	MW	Mvar
1		1440.053	1446.641	2041.206		
	33	525.656	99.780	535.043	2.153	-134.623
	35	505.198	294.637	584.839	14.096	-22.487
	36	409.198	1052.223	1128.989	5.771	-107.151
2		682.000	-370.504	776.143		
	31	380.232	-107.378	395.103	1.173	-64.026
	32	142.069	-141.548	200.548	0.245	-71.611
	33	159.699	-121.578	200.711	0.964	-248.722
3		699.000	-425.568	818.357		
	44	556.742	-110.872	567.675	0.273	-180.893
	48	142.258	-314.696	345.356	1.258	-401.696
4		400.000	-1899.049	1940.718		
	23	-55.827	-1659.959	1660.897	17.480	-302.205
	44	363.945	-109.587	380.086	2.681	-278.405
	45	819.772	-129.503	829.938	6.753	-60.913
5		683.000	415.426	799.417		
	31	746.742	371.106	833.872	1. 494	-181.980
	32	-63 .742	44.321	77.636	0.082	-73.617
6		284.500	-367.218	464.531		
	44	284.500	-367.218	464.531	0.189	-20.435
7		185.00	-992.143	1009.244		
	9	-39.680	15.259	42.513	0.055	-68.752
	28	224.680	-1007.402	1032.153	40.734	-221.452
8		536.000	-641.801	836.185		
	29	536.000	-641.801	836.185	8.928	-61.613
9		26.000	-386.817	387.690		
	7	39.735	-84.011	92.934	0.055	-68.752
	29	77.169	-169.993	186.688	1.907	-171.574
	30	-90.904	-132.814	160.944	0.039	-164.749

10		176.00	51.238	183.307		
	36	-245.809	-162.663	294.756	0.356	-29.035
	39	421.809	213.901	472.944	1.809	-46.099
11		203.000	-214.745	295.507		
	31	-1219.237	-164.794	1230.323	22.269	59.670
	36	1422.237	-49.951	1423.114	40.872	177.599
12		444.000	-1476.315	1541.636		
	40	444.000	1476.315	1541.636	0.214	-1.958
13		510.000	-956.274	1083.771		
	28	510.000	-956.274	1083.771	3.611	-172.730
14		240.000	-816.762	851.293		
	15	240.000	-816.762	851.293	1.221	-73.051
15		360.000	492.467	610.020		
	14	-238.779	743.711	781.103	1.221	-73.051
	30	598.779	-251.244	649.353	0.730	-77.399
16		480.000	-1101.969	1201.971		
	31	480.000	-1101.969	1201.971	1.403	-9.927
17		-62.000	-38.000	72.719		
	18	118.407	-1017.525	1024.392	3.407	-1088.525
	19	-180.407	979.525	996.000	1.483	-88.128
18		-115.000	-71.000	135.152		
	17	-115.000	-71.000	135.152	3.407	-1088.525
19		-141.000	-87.000	165.680		
	17	181.891	-1067.657	1083.037	1.483	-88.128
	20	149.324	-1108.491	1118.503	6.094	-710.853
	22	-472.215	2089.145	2141.848	73.211	-80.812
20		-82.000	-51.000	96.566		
	19	-143.230	397.638	422.648	6.094	-710.853
	21	61.230	-448.638	452.797	0.230	-486.638
21		-61.000	-38.000	71.868		
	20	-61.000	-38.000	71.868	0.230	-486.638

22		-141.000	-87.000	165.680		
	19	545.426	-2169.956	2237.454	73.211	-80.812
	24	-244.309	1547.751	1566.914	29.229	-503.565
	25	-442.117	535.205	694.199	12.875	-869.048
23		-307.000	-190.000	361.039		
	4	73.307	-1357.754	1359.731	17.480	-302.205
	24	-380.307	-1547.754	1593.793	32.899	-74.285
24		-173.000	-107.000	203.416		
	22	273.537	-2051.316	2069.473	29.229	-503.565
	23	413.206	1473.469	1530.311	32.899	-74.285
	25	-249.630	-904.943	938.742	3.249	-790.654
	42	-610.113	1375.789	1505.003	17.445	-300.964
25		-90.000	-56.000	106.000		
	22	454.992	-1404.253	1476.125	12.875	-869.048
	24	252.979	114.289	277.597	3.349	-790.654
	26	-797.971	1233.965	1469.499	4.842	-144.337
26		-61.000	-38.000	71.868		
	25	802.813	-1378.302	1595.063	4.842	-144.337
	27	-863.813	1340.302	1594.548	20.965	-334.000
27		-247.000	-153.000	290.548		
	26	884.778	-1674.302	1893.705	20.965	-334.000
	28	-600.416	822.397	1018.251	7.920	- 798.097
	29	-531.363	698.905	877.961	7.768	-59.217
28		-82.000	-51.000	96.566		
	7	-183.947	785.950	807.189	40.734	-221.452
	13	-506.389	783.544	932.937	3.611	-172.730
	27	608.336	-1620.494	1730.916	7.920	-798.097
29		-276.000	-171.000	324.680		
	8	-527.072	580.188	783.851	8.928	-61.613
	9	-75.261	-1.582	75.278	1.907	-171.574
	27	539.130	-758.624	930.275	7.768	-59.217
	30	-415.846	-168.624	448.734	1.259	-366.534

	31	203.049	177.140	269.458	1.605	-151.998
30		-90.000	-56.000	106.000		
	9	90.943	-31.935	96.387	0.039	-164.749
	15	-598.049	173.845	622.804	0.730	-77.399
	29	417.105	-197.910	461.677	1.259	-366.534
31		-218.000	-135.000	256.416		
	2	-379.059	43.353	381.530	1.173	-64.026
	5	-745.248	-553.086	928.062	1.494	-181.980
	11	1241.506	224.464	1261.634	22.269	59.670
	16	-478.597	1092.042	1192.313	1.403	-9.927
	29	-201.444	-329.138	385.891	1.605	-151.998
	40	288.802	-331.989	440.026	3.340	-131368
	41	56.041	-280.646	286.187	0.620	-297.153
32		-78.000	-48.000	91.586		
	2	-141.824	69.937	158.131	0.245	-71.611
	5	63.824	-117.937	134.100	0.082	-73.617
33		-380.000	-236.000	447.321		
	1	-523.503	-234.403	573.586	2.153	-134.623
	2	-158.735	-127.144	203.378	0.964	-248.722
	34	302.238	125.548	327.277	0.238	-61.452
34		-302.000	-187.000	355.208		
	33	-302.000	-187.000	355.208	0.238	-61.452
35		-340.000	-211.000	400.151		
	1	-491.102	-317.124	584.593	14.096	-22.487
	36	151.102	106.124	184.646	0.162	-32.889
36		-925.000	-573.000	1088.097		
	1	-403.427	-1159.374	1227.559	5.771	-107.151
	10	246.165	133.628	280.096	0.356	-29.035
	11	-1381.365	227.551	1399.981	40.872	177.599
	35	-150.941	-139.013	205.201	0.162	-32.889
	37	654.449	369.385	751.498	4.449	-33.615
	38	110.118	-5.177	110.240	0.118	-73.177
37		-650.000	-403.000	764.793		
	36	-650.000	-403.000	764.793	4.449	-33.615

38		-110.000	-68.000	129.321		
	36	-110.000	-68.000	129.321	0.118	-73.177
39		-420.000	-260.000	493.964		
	10	-420.000	-260.000	493.964	1.809	-46.099
40		-26.000	-16.000	30.529		
	12	-443.786	1474.357	1539.700	0.214	-1.958
	31	-285.462	200.621	348.909	3.340	-131.368
	42	703.248	-1690.979	1831.384	5.689	-57.226
41		-430.000	-266.000	505.624		
	31	-55.421	-16.507	57.827	0.620	-297.153
	43	0.251	-127.294	127.294	0.054	-114.998
	44	-374.830	-122.199	394.246	2.460	-194.456
42		-70.000	-43.000	-82.152		
	24	627.558	-1676.753	1790.343	17.445	-300.964
	40	-697.558	1633.753	1776.439	5.689	-57.226
43		-78.000	-48.000	91.586		
	41	-0.197	12.296	12.298	0.054	-114.998
	44	-77.803	-60.296	98.433	0.061	-107.984
44		-19.00	-12.000	22.472		
	3	-556.469	-70.021	560.858	0.273	-180.893
	4	366.627	-168.817	403.626	2.681	-278.405
	6	-284.311	346.783	448.432	0.189	-20.435
	41	377.290	-72.257	384.147	2.460	-194.456
	43	77.864	-47.688	91.307	0.061	-107.984
45		-433.000	-268.000	509.228		
	4	-813.019	68.590	815.908	6.753	-60.913
	46	243.881	-133.052	277.815	0.658	-99.882
	47	136.138	-203.537	244.869	0.538	-287.537
46		-131.000	-81.000	154.019		
	45	-243.223	33.171	245.475	0.658	-99.882
	49	112.223	-114.171	160.091	0.223	-183.171
47		-135.600	-84.000	159.510		

	45	-135.600	-84.000	159.510	0.538	-287.537
48		-141.000	-87.000	165.680		
	3	-141.000	-87.000	165.680	1.258	-401.696
49		-112.000	-69.000	131.548		
	46	-112.000	-69.000	131.548	0.223	-183.171
				Total	**421.953**	**-11532.393**

C1: Y_{bus} matrix for proposed 330KV Nigeria power system at faulted

1	2	3	4	5	6	7	8	9	10	11	12	13	14	15
1.0000	0.6904	0	0.2506	0.7285	0.4291	0.2270	0.1615	0.1589	4.7953	2.3276	0.2813	0.2360	0.0601	1.0031
0.4856	1.0000	0	0.6485	2.0109	1.1104	0.5875	0.4181	0.4112	0.6729	1.4694	0.7279	0.6107	0.1555	2.5959
0	0	0	0	0	0	0	0	0	0	0	0	0	0	0
0.1456	0.5356	0	1.0000	0.6131	1.2015	0.4695	0.2596	0.3099	0.2052	0.4763	0.7312	0.5697	0.1089	1.8179
0.4624	1.8144	0	0.6697	1.0000	1.1468	0.6067	0.4317	0.4247	0.6505	1.5009	0.7517	0.6306	0.1606	2.6808
0.1781	0.6550	0	0.8581	0.7497	1.0000	0.3833	0.2330	0.2587	0.2509	0.5825	0.5553	0.4413	0.0934	1.5586
0.1455	0.5352	0	0.5178	0.6126	0.5919	1.0000	0.5744	1.1695	0.2050	0.4759	0.4977	1.3250	0.3526	5.8861
0.1908	0.7019	0	0.5277	0.8033	0.6630	1.0585	1.0000	0.7662	0.2689	0.6241	0.5242	0.9850	0.3025	5.0487
0.0651	0.2397	0	0.2187	0.2743	0.2555	0.7482	0.2660	1.0000	0.0918	0.2131	0.2118	0.5290	0.1723	2.8760
3.8818	0.7744	0	0.2859	0.8296	0.4895	0.2590	0.1843	0.1813	1.0000	2.7083	0.3209	0.2692	0.0686	1.1444
1.4096	1.2650	0	0.4964	1.4320	0.8501	0.4498	0.3201	0.3148	2.0262	1.0000	0.5572	0.4675	0.1191	1.9873
0.3096	1.1388	0	1.3850	1.3034	1.4729	0.8547	0.4885	0.5686	0.4363	1.0127	1.0000	1.0187	0.2017	3.3666
0.1745	0.6420	0	0.7251	0.7348	0.7864	1.5291	0.6168	0.9543	0.2460	0.5709	0.6846	1.0000	0.3081	5.1423
0.0965	0.3550	0	0.3010	0.4063	0.3613	0.8836	0.4113	0.6749	0.1360	0.3157	0.2943	0.6689	1.0000	7.1696
0.2488	0.9154	0	0.7760	1.0477	0.9316	2.2783	1.0604	1.7401	0.3507	0.8140	0.7588	1.7247	1.1075	1.0000

bus 3.

0.4408	1.6216	0	0.6442	1.8560	1.1031	0.5836	0.4153	0.4085	0.6212	1.4421	0.7231	0.6067	0.1545	2.5789

C2: Proposed grid generators fault-induced power variation

Gen No.	Pre-fault power	Fault –on power	Power Variation (ΔP_e)	% Power variation ($\%\Delta P_e$)
1.	1526.6713	1463.4118	63.2594	4.1436
2.	698.8045	546.0441	152.7604	21.8602
3	722.1478	0.0000	722.1478	100.0000
4	365.5102	254.9256	110.5846	30.2549
5	720.1548	538.0106	182.1442	25.2924
6	315.4216	58.5326	256.8890	81.4431
7	232.9139	184.2951	48.6188	20.8742
8	537.9326	463.2554	74.6772	13.8823
9.	75.6594	51.2205	24.4389	32.3012
10.	305.2420	302.0117	3.2303	1.0583
11.	281.8090	259.4960	22.3130	7.9178
12.	425.4265	325.2076	100.2188	23.5573
13.	537.2041	421.7675	115.4365	21.4884
14	237.3737	221.8550	15.5187	6.5377
15	698.3300	495.3371	202.9928	29.0683
16.	478.7144	380.4466	98.2678	20.5274

C3: Study and external systems Generators classified based on fault – on percentage power variation.

	Machines		Percentage Power Variation $\%\Delta P_e$(MW)
	No	**Name**	
Study System Machines ($\% \Delta P_e > 30\%$)	3	Kainji	100.000
	4	Shiroro	20.2549
	6	Jebba	81.4431
	9	Alaoji	32.3012
External System Machines($\%\Delta P_e < 30\%$)	1	Egbin	4.1436
	2	Delta	21.8602
	5	Sapele	25.2924
	7	Afam	20.8742
	8	Okpai	13.8823
	10	Papalanto	1.0583
	11	Omotosho	7.9178
	12	Geregu	23.5573
	13	Calabar	21.4884
	14	Omoku	6.5377
	15	Egbema	29.0683
	16	Eyaen	20.5274

C4: γ – Index data for proposed generators coherency check

	2	3	4	5	6	7	8	9	10	11	12	13	14
5234	0	0	0	0	0	0	0	0	0	0	0	0	0
1493	0.5945	0	0	0	0	0	0	0	0	0	0	0	0
7902	0.9000	0.7534	0	0	0	0	0	0	0	0	0	0	0
9312	0.8556	0.9414	0.9856	0	0	0	0	0	0	0	0	0	0
1223	0.5817	0.0307	0.7610	0.9396	0	0	0	0	0	0	0	0	0
9339	0.8614	0.9438	0.9861	0.0402	0.9420	0	0	0	0	0	0	0	0
9407	0.8755	0.9495	0.9876	0.1381	0.9479	0.1020	0	0	0	0	0	0	0
6679	0.3032	0.7175	0.9303	0.7928	0.7085	0.8011	0.8214	0	0	0	0	0	0
9113	0.8138	0.9245	0.9814	0.2243	0.9221	0.2555	0.3314	0.7328	0	0	0	0	0
9052	0.8011	0.9194	0.9801	0.2739	0.9168	0.3031	0.3742	0.7146	0.0640	0	0	0	0
0000	1.0000	1.0000	1.0000	1.0000	1.0000	1.0000	1.0000	1.0000	1.0000	1.0000	NaN	0	0
6670	0.3013	0.7167	0.9301	0.7933	0.7077	0.8016	0.8219	0.0027	0.7336	0.7153	1.0000	0	0
6635	0.2939	0.7137	0.9294	0.7955	0.7046	0.8037	0.8237	0.0132	0.7364	0.7183	1.0000	0.0105	0
6694	0.3063	0.7187	0.9306	0.7918	0.7098	0.8002	0.8206	0.0044	0.7317	0.7133	1.0000	0.0071	0.017
6679	0.3032	0.7175	0.9303	0.7928	0.7085	0.8011	0.8214	0.7328	0.7146	1.0000	0.0027	0.0132	0.004

C5: β - Index data for proposed generators coherency check

	3	4	5	6	7	8	9	10	11	12	13	14	15
.6532	0	0	0	0	0	0	0	0	0	0	0	0	0
.2945	0.5084	0	0	0	0	0	0	0	0	0	0	0	0
.3010	0.7576	0.5068	0	0	0	0	0	0	0	0	0	0	0
.4579	0.3603	0.2316	0.6211	0	0	0	0	0	0	0	0	0	0
.0885	0.6195	0.2260	0.3628	0.4053	0	0	0	0	0	0	0	0	0
.4850	0.3266	0.2700	0.6400	0.0500	0.4350	0	0	0	0	0	0	0	0
.0291	0.6633	0.3151	0.2800	0.4737	0.1150	0.5000	0	0	0	0	0	0	0
.7044	0.8975	0.7915	0.5772	0.8398	0.7306	0.8478	0.6956	0	0	0	0	0	0
.4206	0.4014	0.1787	0.5950	0.0643	0.3644	0.1111	0.4375	0.8287	0	0	0	0	0
.4206	0.4014	0.1787	0.5950	0.0643	0.3644	0.1111	0.4375	0.8287	0	0	0	0	0
.7783	0.9231	0.8436	0.6829	0.8798	0.7979	0.8858	0.7717	0.2500	0.8716	0.8716	0	0	0
.6305	0.8719	0.7393	0.4715	0.7997	0.6632	0.8097	0.6194	0.2000	0.7859	0.7859	0.4000	0	0
.8522	0.9487	0.8957	0.7886	0.9199	0.8653	0.9239	0.8478	0.5000	0.9144	0.9144	0.3333	0.6000	0
.7783	0.9231	0.8436	0.6829	0.8798	0.7979	0.8858	0.7717	0.2500	0.8716	0.8716	0.4000	0.3333	0
.7044	0.8975	0.7915	0.5772	0.8398	0.7306	0.8478	0.6956	0.8287	0.8287	0.2500	0.2000	0.500	0.2

C6: Aggregated Grid Generators groups data

Group	Candidate Machine		Equivalent Machines Parameters					
	No.	Name	Internal Voltage and angle ($E_e<\delta_e$)	Terminal voltage and angle ($V_e<\theta_e$)	Modified reactance (X^1_{de})	Initia Constant (H_e)	Damping Coefficient (D_e)	Mech Power (P_{me})
I	2/16	Delta / Eyaen	0.668 <55.7742	1.006 <23.0009	0.031	58.9	0.1125	1162.00
II	7/8	Afam / Okpai	0.605 <46.5231	1.051 <24.7112	0.033	54.0	0.142	838.00
III	10/11	Papalanto/ Omotosho	1.019 <9.8432	1.034 <5.3225	0.014	64.0	0.0242	649.00

C7: New Grid Generators data after aggregation

Gen	Ra	X'_d(pu)	H(sec)	D	X_d (pu)	T'_{do}	
1	0	0.0437	18.54	0.0764	0.3117	7.1	
2	0	0.0242	58.9	0.1125	0.3617	8.8	%2,16
3	0	0.0329	26.28	0.1273	0.0935	5.9	
4	0.	0.075	12.96	0.2546	0.2	5.57	
5	0	0.039	34.2	0.0097	0.36	8.6	
6	0	0.0433	20.34	0.0955	0.1083	5.2	
7	0	0.0278	54	0.0142	0.3832	8.8	%7,8
8	0	0.0578	5.48	0.0075	0.455	1.29	
9	0	0.0144	64	.0242	0.25	0.7	%10,11
10	0	0.077	4.11	0.0	0.61	1.29	
11	0	0.0462	6.85	0.0094	0.364	1.29	
12	0	0.1155	2.74	0.0038	0.91	1.29	
13	0	0.007	4.11	0.0056	0.6067	1.29	

C8: New Grid system bus data after aggregation

Bus No.	Bus Code	V (pu)	Angle (Deg.)	Pload MW	Qload Mvar	Pgen MW	Qgen Mvar	Qmin Mvar	Qmax Mvar	Injected Mvar	Aggre. Gen
1	1	1	0	400	247.9	1254	0	-550	800	0	
2	2	1.006	0	0	0	1162	0	-500	780	0	%2,16
3	2	1	0	0	0	699	0	-250	300	0	
4	2	1	0	200	123.9	600	0	-300	370	0	
5	2	1	0	0	0	683	0	-280	340	0	
6	2	1	0	19	11.8	303.5	0	-200	270	0	
7	2	1.051	0	117	72.5	838	0	-360	470	0	%7,8
8	2	1	0	454	281.4	480	0	-250	290	0	
9	2	1.019	0	270	166.96	649	0	-280	350	0	% 10,11
10	2	1	0	0	0	444	0	-220	270	0	
11	2	1	0	90	55.76	600	0	-280	370	0	
12	2	1	0	0	0	240	0	-100	140	0	
13	2	1	0	0	0	360	0	-180	220	0	
14	0	1	0	62	38	0	0	0	0	0	
15	0	1	0	115	71	0	0	0	0	0	
16	0	1	0	141	87	0	0	0	0	0	
17	0	1	0	82	51	0	0	0	0	0	
18	0	1	0	61	38	0	0	0	0	0	
19	0	1	0	141	87	0	0	0	0	0	
20	0	1	0	307	190	0	0	0	0	0	
21	0	1	0	173	107	0	0	0	0	0	
22	0	1	0	90	56	0	0	0	0	0	
23	0	1	0	61	38	0	0	0	0	0	
24	0	1	0	247	153	0	0	0	0	0	
25	0	1	0	82	51	0	0	0	0	0	
26	0	1	0	276	171	0	0	0	0	0	

27	0	1	0	90	56	0	0	0	0	0	
28	0	1	0	218	135	0	0	0	0	0	
29	0	1	0	78	48	0	0	0	0	0	
30	0	1	0	380	236	0	0	0	0	0	
31	0	1	0	302	187	0	0	0	0	0	
32	0	1	0	340	211	0	0	0	0	0	
33	0	1	0	925	573	0	0	0	0	0	
34	0	1	0	650	403	0	0	0	0	0	
35	0	1	0	110	68	0	0	0	0	0	
36	0	1	0	420	260	0	0	0	0	0	
37	0	1	0	26	16	0	0	0	0	0	
38	0	1	0	430	266	0	0	0	0	0	
39	0	1	0	70	43	0	0	0	0	0	
40	0	1	0	78	48	0	0	0	0	0	
41	0	1	0	19	12	0	0	0	0	0	
42	0	1	0	433	268	0	0	0	0	0	
43	0	1	0	131	81	0	0	0	0	0	
44	0	1	0	135.6	84	0	0	0	0	0	
45	0	1	0	141	87	0	0	0	0	0	
46	0	1	0	112	69	0	0	0	0	0	

C9: Line data for new Grid System after aggregation

From Bus	To Bus	R(pu)	X(pu)	B/2(pu)	Tap Ratio
1	30	0.0007	0.0057	0.771	1
1	32	0.004	0.00304	0.171	1
1	33	0.0004	0.0029	0.771	1
2	28	0.0008	0.0063	0.3585	1
2	39	0.0008	0.0063	0.3585	1
2	30	0.0036	0.269	1.6089	1
3	41	0.000097	0.0082	0.924	1
3	45	0.004151	0.03041	1.8135	1
4	20	0.0009	0.0067	1.7933	1
4	41	0.0022	0.0234	1.3905	1
4	42	0.0011	0.0097	0.546	1
5	28	0.0002	0.0015	0.936	1
5	29	0.0008	0.0063	0.3585	1
6	41	0.0001	0.0004	0.096	1
7	8	0.0015	0.0012	0.312	1
7	25	0.0054	0.0042	1.1208	1
7	26	0.0015	0.0012	0.312	1
8	26	0.0163	0.014	0.786	1
8	27	0.0004	0.0028	0.7472	1
9	33	0.0004	0.003	0.171	1
9	36	0.0007	0.0061	0.3421	1
9	28	0.0014	0.0122	0.6841	1
9	33	0.0019	0.0162	0.91222	1
10	37	0.00001	0.0005	0.057	1
11	25	0.0004	0.0033	0.8967	1

12	13	0.0002	0.0014	0.3736	1
13	27	0.0002	0.0014	0.3736	1
14	15	0.004	0.0302	1.8018	1
14	16	0.0004	0.0029	0.1695	1
16	17	0.003	0.022	1.2371	1
16	19	0.0032	0.027	1.515	1
17	18	0.0016	0.0134	0.7525	1
19	21	0.0013	0.0099	2.3517	1
19	22	0.0017	0.0126	3.0069	1
20	21	0.0018	0.0014	0.3736	1
21	22	0.0014	0.0107	2.8644	1
21	39	0.0008	0.0065	1.7435	1
22	23	0.0003	0.0023	0.6221	1
23	24	0.0009	0.007	1.8681	1
24	25	0.0005	0.0033	3.5618	1
24	26	0.0011	0.0097	0.5475	1
26	27	0.0008	0.0064	1.7062	1
26	38	0.0016	0.0139	0.781	1
28	37	0.0023	0.0198	0.748	1
28	38	0.003	0.0254	1.431	1
30	31	0.0002	0.0012	0.3238	1
32	33	0.0004	0.0032	0.1824	1
33	34	0.0007	0.0057	0.3855	1
33	35	0.00084	0.00709	0.3991	1
37	39	0.0002	0.0018	0.4732	1
38	40	0.0012	0.0088	0.5265	1
38	41	0.0019	0.00159	0.8955	1
40	41	0.0011	0.0083	0.4914	1

42	43	0.0011	0.0079	0.4722	1
42	44	0.0027	0.0233	1.311	1
43	46	0.0019	0.0144	0.8307	1

APPENDIX D: MATLAB program

POWER FLOW MATLAB PROGRAM

```
%   Power flow solution by Newton-Raphson method
%   Copyright (c) 2010 Fabian I. Izuegbunam
ns=0; ng=0; Vm=0; delta=0; yload=0; deltad=0;
nbus = length(busdata(:,1));
kb=[];Vm=[]; delta=[]; Pd=[]; Qd=[]; Pg=[]; Qg=[]; Qmin=[]; Qmax=[];  % Added
(6-8-00)
Pk=[]; P=[]; Qk=[]; Q=[]; S=[]; V=[]; % Added (6-8-00)
for k=1:nbus
n=busdata(k,1);
kb(n)=busdata(k,2); Vm(n)=busdata(k,3); delta(n)=busdata(k, 4);
Pd(n)=busdata(k,5); Qd(n)=busdata(k,6); Pg(n)=busdata(k,7); Qg(n) =
busdata(k,8);
Qmin(n)=busdata(k, 9); Qmax(n)=busdata(k, 10);
Qsh(n)=busdata(k, 11);
    if Vm(n) <= 0  Vm(n) = 1.0; V(n) = 1 + j*0;
    else delta(n) = pi/180*delta(n);
         V(n) = Vm(n)*(cos(delta(n)) + j*sin(delta(n)));
         P(n)=(Pg(n)-Pd(n))/basemva;
         Q(n)=(Qg(n)-Qd(n)+ Qsh(n))/basemva;
         S(n) = P(n) + j*Q(n);
    end
end
for k=1:nbus
if kb(k) == 1, ns = ns+1; else, end
if kb(k) == 2 ng = ng+1; else, end
ngs(k) = ng;
nss(k) = ns;
end
Ym=abs(Ybus); t = angle(Ybus);
m=2*nbus-ng-2*ns;
maxerror = 1; converge=1;
iter = 0;
%%%% added for parallel lines (Aug. 99)
mline=ones(nbr,1);
for k=1:nbr
      for m=k+1:nbr
         if((nl(k)==nl(m)) & (nr(k)==nr(m)));
            mline(m)=2;
         elseif ((nl(k)==nr(m)) & (nr(k)==nl(m)));
         mline(m)=2;
         else, end
      end
   end
%%%   end of statements for parallel lines (Aug. 99)

% Start of iterations
clear A  DC   J  DX
while maxerror >= accuracy & iter <= maxiter % Test for max. power mismatch
for ii=1:m
for k=1:m
   A(ii,k)=0;      %Initializing Jacobian matrix
end, end
iter = iter+1;
for n=1:nbus
nn=n-nss(n);
lm=nbus+n-ngs(n)-nss(n)-ns;
J11=0; J22=0; J33=0; J44=0;
```

```
   for ii=1:nbr
    if mline(ii)==1   % Added to include parallel lines (Aug. 99)
        if nl(ii) == n | nr(ii) == n
            if nl(ii) == n ,  l = nr(ii); end
            if nr(ii) == n , l = nl(ii); end
         J11=J11+ Vm(n)*Vm(l)*Ym(n,l)*sin(t(n,l)- delta(n) + delta(l));
         J33=J33+ Vm(n)*Vm(l)*Ym(n,l)*cos(t(n,l)- delta(n) + delta(l));
                if kb(n)~=1
                J22=J22+ Vm(l)*Ym(n,l)*cos(t(n,l)- delta(n) + delta(l));
                J44=J44+ Vm(l)*Ym(n,l)*sin(t(n,l)- delta(n) + delta(l));
                else, end
                if kb(n) ~= 1  & kb(l) ~=1
                    lk = nbus+l-ngs(l)-nss(l)-ns;
                    ll = l -nss(l);
                % off diagonalelements of J1
                    A(nn, ll) =-Vm(n)*Vm(l)*Ym(n,l)*sin(t(n,l)- delta(n) +
delta(l));
                    if kb(l) == 0  % off diagonal elements of J2
                    A(nn, lk) =Vm(n)*Ym(n,l)*cos(t(n,l)- delta(n) +
delta(l));end
                    if kb(n) == 0  % off diagonal elements of J3
                    A(lm, ll) =-Vm(n)*Vm(l)*Ym(n,l)*cos(t(n,l)-
delta(n)+delta(l)); end
                    if kb(n) == 0 & kb(l) == 0  % off diagonal elements of  J4
                    A(lm, lk) =-Vm(n)*Ym(n,l)*sin(t(n,l)- delta(n) +
delta(l));end
              else end
           else , end
      else, end
   end
   Pk = Vm(n)^2*Ym(n,n)*cos(t(n,n))+J33;
   Qk = -Vm(n)^2*Ym(n,n)*sin(t(n,n))-J11;
   if kb(n) == 1 P(n)=Pk; Q(n) = Qk; end   % Swing bus P
     if kb(n) == 2  Q(n)=Qk;
         if Qmax(n) ~= 0
           Qgc = Q(n)*basemva + Qd(n) - Qsh(n);
           if iter <= 7                  % Between the 2th & 6th iterations
              if iter > 2                % the Mvar of generator buses are
                if Qgc  < Qmin(n),       % tested. If not within limits Vm(n)
                Vm(n) = Vm(n) + 0.01;    % is changed in steps of 0.01 pu to
                elseif Qgc  > Qmax(n),   % bring the generator Mvar within
                Vm(n) = Vm(n) - 0.01;end % the specified limits.
             else, end
           else,end
         else,end
     end
   if kb(n) ~= 1
     A(nn,nn) = J11;  %diagonal elements of J1
     DC(nn) = P(n)-Pk;
   end
   if kb(n) == 0
     A(nn,lm) = 2*Vm(n)*Ym(n,n)*cos(t(n,n))+J22;  %diagonal elements of J2
     A(lm,nn)= J33;        %diagonal elements of J3
     A(lm,lm) =-2*Vm(n)*Ym(n,n)*sin(t(n,n))-J44;  %diagonal of elements of J4
     DC(lm) = Q(n)-Qk;
   end
end
DX=A\DC';
for n=1:nbus
  nn=n-nss(n);
  lm=nbus+n-ngs(n)-nss(n)-ns;
```

```
    if kb(n) ~= 1
    delta(n) = delta(n)+DX(nn); end
    if kb(n) == 0
    Vm(n)=Vm(n)+DX(lm); end
 end
  maxerror=max(abs(DC));
     if iter == maxiter & maxerror > accuracy
   fprintf('\nWARNING: Iterative solution did not converged after ')
   fprintf('%g', iter), fprintf(' iterations.\n\n')
   fprintf('Press Enter to terminate the iterations and print the results \n')
   converge = 0; pause, else, end

end

if converge ~= 1
   tech= ('                         ITERATIVE SOLUTION DID NOT CONVERGE'); else,
   tech=('                    Power Flow Solution by Newton-Raphson Method');
end
V = Vm.*cos(delta)+j*Vm.*sin(delta);
deltad=180/pi*delta;
i=sqrt(-1);
k=0;
for n = 1:nbus
     if kb(n) == 1
     k=k+1;
     S(n)= P(n)+j*Q(n);
     Pg(n) = P(n)*basemva + Pd(n);
     Qg(n) = Q(n)*basemva + Qd(n) - Qsh(n);
     Pgg(k)=Pg(n);
     Qgg(k)=Qg(n);
     elseif  kb(n) ==2
     k=k+1;
     S(n)=P(n)+j*Q(n);
     Qg(n) = Q(n)*basemva + Qd(n) - Qsh(n);
     Pgg(k)=Pg(n);
     Qgg(k)=Qg(n);
  end
yload(n) = (Pd(n)- j*Qd(n)+j*Qsh(n))/(basemva*Vm(n)^2);
end
busdata(:,3)=Vm'; busdata(:,4)=deltad';
Pgt = sum(Pg);  Qgt = sum(Qg); Pdt = sum(Pd); Qdt = sum(Qd); Qsht = sum(Qsh);
```

MATLAB PROGRAM FOR MULTIMACHINE TRANSIENT STABILITY ANALYSIS

```
% TRANSIENT STABILITY ANALYSIS OF MULTIMACHINE POWER SYSTEM NETWORK
% Copyright (c) 2010 Fabian I. Izuegbunam
%
%tic
global Pm f H E  Y th ngg
f=50;
ngr=gendata(:,1);
ngg=length(gendata(:,1));
for k=1:ngg
zdd(ngr(k))=gendata(k, 2)+j*gendata(k,3);
H(k)=gendata(k,4);    % new
end
for k=1:ngg
```

```
I(k) =conj(S(ngr(k)))/conj(V(ngr(k)));
Ep(k) = V(ngr(k))+zdd(ngr(k))*I(k);  % new
Pm(k)=real(S(ngr(k)));              % new
end
E=abs(Ep); d0=angle(Ep);
Er=real(Ep); Ei=imag(Ep); %mine
Ip=real(I); dp=imag(I);     %mine
Iab = abs(I); dab=angle(I);   %mine
for k=1:ngg
nl(nbr+k) = nbus+k;
nr(nbr+k) = gendata(k, 1);
R(nbr+k)  = real(zdd(ngr(k)));
X(nbr+k)  = imag(zdd(ngr(k)));
Bc(nbr+k)  = 0;
a(nbr+k) = 1.0;
yload(nbus+k)=0;
end
nbr1=nbr; nbus1=nbus;
nbrt=nbr+ngg;
nbust=nbus+ngg;
linedata=[nl, nr, R, X, -j*Bc, a];
[Ybus, Ybf]=ybusbf(linedata, yload, nbus1,nbust);
fprintf('\nPrefault reduced bus admittance matrix \n')
Ybf
Y=abs(Ybf); th=angle(Ybf);
Pm=zeros(1, ngg);
disp(['      G(i)    E''(i)     d0(i)      Pm(i)'])
for ii = 1:ngg
for jj = 1:ngg
Pm(ii) = Pm(ii) + E(ii)*E(jj)*Y(ii, jj)*cos(th(ii, jj)-d0(ii)+d0(jj));

end,
fprintf('       %g', ngr(ii)), fprintf('   %8.4f',E(ii)), fprintf('   %8.4f',
180/pi*d0(ii))
fprintf('  %8.4f \n',Pm(ii))
end
% this display of I(i) and dp is mine
disp(['       I(i)        I(imaj)     I(absolute)      I(angle)'])
for ii = 1:ngg
    fprintf('     %8.4f',Ip(ii)), fprintf('    %8.4f', dp(ii)), fprintf('
%8.4f',Iab(ii))
    fprintf('      %8.4f \n', 180/pi*dab(ii))
end
%displaying the Ep(k)
disp(['        E(real)          E(imag)'])
for ii = 1:ngg
    fprintf('       %8.4f', Er(ii)), fprintf('        %8.4f\n', Ei(ii))
end
%toc
nf = fdata;       % I changed the input type of the Faulted bus

fprintf('\nFaulted reduced bus admittance matrix\n')
Ydf=ybusdf(Ybus, nbus1, nbust, nf)
%toc
%Fault cleared
%tic
[Yaf]=ybusaf(linedata, yload, nbus1,nbust, nbrt, lrmv);  % I declared the
variable 'lrmv' in Yaf and changed the input type
fprintf('\nPostfault reduced bus admittance matrix\n')
Yaf
%toc
```

```
tc = tcl;    % this is mine
tf = tfl;   % this is mine
%resp='y';
%while resp =='y' | resp=='Y'
%tc=input('Enter clearing time of fault in sec. tc = ');
%tf=input('Enter final simulation time in sec.  tf = ');
%tic
clear t  x  del
t0 = 0;
w0=zeros(1, length(d0));
x0 = [d0,  w0];
tol=0.0001;
Y=abs(Ydf); th=angle(Ydf);
%[t1, xf] =ode23('dfpek', t0, tc, x0, tol);  % Solution during fault (use with
MATLAB 4)
tspan=[t0, tc];                                          %use with MATAB 5
[t1, xf] =ode45('dfpek', tspan, x0);  % Solution during fault (use with MATLAB
5)
x0c =xf(length(xf), :);
Y=abs(Yaf); th=angle(Yaf);
%[t2,xc] =ode23('afpek', tc, tf, x0c, tol); % Postfault solution (use with
MATLAB 4)
tspan = [tc, tf];                              % use with MATLAB 5
[t2,xc] =ode45('afpek', tspan, x0c);        % Postfault solution (use with
MATLAB 5)
t =[t1; t2]; x = [xf; xc];
fprintf('\nFault is cleared at %4.3f Sec. \n', tc)
for k=1:nbus
    if kb(k)==1
    ms=k; else, end
end
fprintf('\nPhase angle difference of each machine \n')
fprintf('with respect to the slack in degree.\n')
fprintf('   t - sec')
kk=0;
for k=1:ngg
    if k~=ms
    kk=kk+1;
      del(:,kk)=180/pi*(x(:,k)-x(:,ms));
    fprintf('    d(%g,',ngr(k)), fprintf('%g)', ngr(ms))

    else, end

end
%-------------------------------------------------------------
% code for ranking
%for k=1:ngg
 %   if k~=ms
  %  kk=kk+1;
   % del(:,kk)=180/pi*(x(:,k)-x(:,ms));
 %if del(:,kk)>=0
  %      fprintf('\n')
   % fprintf('\n Generator %g',k)
    %    fprintf(' is Transiently Unstable')
 %else, end
  %  end
%end
%-----------------------------------------------------------------
fprintf(' \n')
disp([t, del])
%t = t2(0.01:0.001,1:10);
```

```
h=figure; figure(h)
plot(t, del)
axis([0 2.5 -200 200])
%legend('d(1,2)', 'd(3,2)', 'd(4,2)', 'd(5,2)', 'd(6,2)', 'd(7,2)', 'd(8,2)',
'd(9,2)')
title(['Phase angle difference (fault cleared at ', num2str(tc),'s) ', 'for line
', num2str(lrmv)])
xlabel('t, sec'), ylabel('Rotor angle, degrees'), grid
```

MATLAB PROGRAM FOR ADMITTANCE MATRIX FORMATION

```
%  This program obtains th Bus Admittance Matrix for power flow solution
%  Copyright (c) 2010 Fabian I. Izuegbunam

j=sqrt(-1); i = sqrt(-1);
nl = linedata(:,1); nr = linedata(:,2); R = linedata(:,3);
X = linedata(:,4); Bc = j*linedata(:,5); a = linedata(:, 6);
nbr=length(linedata(:,1)); nbus = max(max(nl), max(nr));
Z = R + j*X; y= ones(nbr,1)./Z;        %branch admittance
for n = 1:nbr
if a(n) <= 0  a(n) = 1; else end
Ybus=zeros(nbus,nbus);     % initialize Ybus to zero
               % formation of the off diagonal elements
for k=1:nbr;
       Ybus(nl(k),nr(k))=Ybus(nl(k),nr(k))-y(k)/a(k);
       Ybus(nr(k),nl(k))=Ybus(nl(k),nr(k));         % showing symmetry as this
is the same in above
    end
end
              % formation of the diagonal elements
for  n=1:nbus
     for k=1:nbr
         if nl(k)==n
         Ybus(n,n) = Ybus(n,n)+y(k)/(a(k)^2) + Bc(k);
         elseif nr(k)==n
         Ybus(n,n) = Ybus(n,n)+y(k) +Bc(k);
         else, end
     end
end
clear Pgg
```

MATLAB PROGRAM FOR LINE FLOWS

```
%  This program is used in conjunction with lfgauss or lf Newton
%  for the computation of line flow and line losses.
%
%  Copyright (c) 2010 Fabian I. Izuegbunam
SLT = 0;
fprintf('\n')
fprintf('                            Line Flow and Losses \n\n')
fprintf('     --Line--  Power at bus & line flow    --Line loss--
Transformer\n')
fprintf('     from  to    MW      Mvar     MVA       MW      Mvar      tap\n')

for n = 1:nbus
busprt = 0;
   for L = 1:nbr;
       if busprt == 0
       fprintf('   \n'), fprintf('%6g', n), fprintf('      %9.3f', P(n)*basemva)
       fprintf('%9.3f', Q(n)*basemva), fprintf('%9.3f\n', abs(S(n)*basemva))

       busprt = 1;
```

```
        else, end
        if nl(L)==n      k = nr(L);
        In = (V(n) - a(L)*V(k))*y(L)/a(L)^2 + Bc(L)/a(L)^2*V(n);
        Ik = (V(k) - V(n)/a(L))*y(L) + Bc(L)*V(k);
        Snk = V(n)*conj(In)*basemva;
        Skn = V(k)*conj(Ik)*basemva;
        SL  = Snk + Skn;
        SLT = SLT + SL;
        elseif nr(L)==n  k = nl(L);
        In = (V(n) - V(k)/a(L))*y(L) + Bc(L)*V(n);
        Ik = (V(k) - a(L)*V(n))*y(L)/a(L)^2 + Bc(L)/a(L)^2*V(k);
        Snk = V(n)*conj(In)*basemva;
        Skn = V(k)*conj(Ik)*basemva;
        SL  = Snk + Skn;
        SLT = SLT + SL;
        else, end
          if nl(L)==n | nr(L)==n
          fprintf('%12g', k),
          fprintf('%9.3f', real(Snk)), fprintf('%9.3f', imag(Snk))
          fprintf('%9.3f', abs(Snk)),
          fprintf('%9.3f', real(SL)),
              if nl(L) ==n & a(L) ~= 1
              fprintf('%9.3f', imag(SL)), fprintf('%9.3f\n', a(L))
              else, fprintf('%9.3f\n', imag(SL))
              end
          else, end
  end
end
SLT = SLT/2;
fprintf('   \n'), fprintf('    Total loss                          ')
fprintf('%9.3f', real(SLT)), fprintf('%9.3f\n', imag(SLT))
clear Ik In SL SLT Skn Snk
```

MATLAB PROGRAM FOR REDUCTION OF ADMITTANCE MATRIX

A. REDUCED MATRIX BEFORE FAULT

```
% This function forms the bus admittance matrix including load
% admittances before fault.  The corresponding reduced bus
% admittance matrix is obtained for transient stability study.
%
% Copyright (c) 2010 Fabian I. Izuegbunam

function [Ybus, Ybf] = ybusbf(linedata, yload, nbus1, nbust)
global Pm f H E  Y th ngg

lfybus
for k=1:nbust
Ybus(k,k)=Ybus(k,k)+yload(k);
end
YLL=Ybus(1:nbus1, 1:nbus1);
YGG = Ybus(nbus1+1:nbust, nbus1+1:nbust);
YLG = Ybus(1:nbus1, nbus1+1:nbust);
Ybf=YGG-YLG.'*inv(YLL)*YLG;
```

B. REDUCED MATRIX DURING FAULT

```
% This function forms the bus admittance matrix including load
% admittances during fault.  The corresponding reduced bus
% admittance matrix is obtained for transient stability analysis.
%
% Copyright (c) Fabian I. Izuegbunam
```

```
function Ypf=ybusdf(Ybus, nbus1, nbust, nf)
global Pm f H E  Y th ngg
nbusf=nbust-1;
Ybus(:,nf:nbusf)=Ybus(:,nf+1:nbust);
Ybus(nf:nbusf,:)=Ybus(nf+1:nbust,:);
YLL=Ybus(1:nbus1-1, 1:nbus1-1);
YGG = Ybus(nbus1:nbusf, nbus1:nbusf);
YLG = Ybus(1:nbus1-1, nbus1:nbusf);
Ypf=YGG-YLG.'*inv(YLL)*YLG;
```

C. REDUCED MATRIX AFTER FAULT

```
% This function forms the bus admittance matrix including load
% admittances after removal of faulted line. The corresponding reduced
% bus admittance matrix is obtained for transient stability study.
%
% Copyright (c) 2010 Fabian I. Izuegbunam

function [Yaf]=ybusaf(linedata, yload, nbus1,nbust, nbrt, lrmv);
global Pm f H E  Y th ngg

nl=linedata(:, 1);  nr=linedata(:, 2);
remove = 0;

rtn=1;
while remove ~= 1
  fline= lrmv; %input('Enter the bus to bus Nos. of line to be removed -> ');
  nrmv=length(fline);
  rtn=isempty(fline);
  while (rtn==1 | nrmv~=2)
  fline= lrmv; %input('Enter the bus to bus Nos. of line to be removed -> ');
  rtn=isempty(fline);
  nrmv=length(fline);
  end
  nlf=fline(1); nrf=fline(2);
     for k=1:nbrt
       if nl(k)==nlf & nr(k)==nrf
       remove = 1;
       m=k;
       else, end
    end
    if remove ~= 1
       fprintf('\nThe line to be removed does not exist in the line data. try
again.\n\n')
    end
end
linedat2(1:m-1,:)= linedata(1:m-1,:);
linedat2(m:nbrt-1,:)=linedata(m+1:nbrt,:);

linedat0=linedata;
linedata=linedat2;
lfybus

for k=1:nbust
Ybus(k,k)=Ybus(k,k)+yload(k);
end

YLL=Ybus(1:nbus1, 1:nbus1);
YGG = Ybus(nbus1+1:nbust, nbus1+1:nbust);
YLG = Ybus(1:nbus1, nbus1+1:nbust);
Yaf=YGG-YLG.'*inv(YLL)*YLG;
linedata=linedat0;
```

MATLAB PROGRAM FOR STATE VARIABLE REPRESENTATION OF THE SYSTEM DURING FAULT

```
% State variable representation of the multimachine system
% during fault. (for use with trstab)
% Copyright (c) 2010 Fabian I. Izuegbunam

function xdot = dfpek(t,x)
global Pm f H E  Y th ngg
Pe=zeros(1, ngg);
for ii = 1:ngg
for jj = 1:ngg
Pe(ii) = Pe(ii) + E(ii)*E(jj)*Y(ii, jj)*cos(th(ii, jj)-x(ii)+x(jj));
end, end
for k=1:ngg
xdot(k)=x(k+ngg);
xdot(k+ngg)=(pi*f)/H(k)*(Pm(k)-Pe(k));
end
xdot=xdot';        % use with MATLAB 5 (remove for MATLAB 4)
```

MATLAB PROGRAM FOR STATE VARIABLE REPRESENTATION OF THE SYSTEM AFTER FAULT

```
% State variable representation of the multimachine system
% after fault. (for use with trstab)
%
% Copyright (C) 2010 Fabian I. Izuegbunam

function xdot = afpek(t,x)
global Pm f H E  Y th ngg

Pe=zeros(1, ngg);
for ii = 1:ngg
for jj = 1:ngg
Pe(ii) = Pe(ii) + E(ii)*E(jj)*Y(ii, jj)*cos(th(ii, jj)-x(ii)+x(jj));
end, end
for k=1:ngg
xdot(k)=x(k+ngg);
xdot(k+ngg)=(pi*f)/H(k)*(Pm(k)-Pe(k));
end
xdot=xdot';        % use with MATLAB 5 (remove for MATLAB 4)
```

MATLAB PROGRAM FOR LOADING DATA

```
%This program loads the required data needed for the analysis. It declares
%all necessary variables in the Workspace before further analysis
%Also checks the availability of the required data.
%Copyright (C) 2010 Fabian I. Izuegbunam
clear
% load input data from m.file
fprintf('                                        Transient Stability Analysis of ')
fprintf('\n                                Nigeria Power System: Multimachine
Approach \n')
fprintf('                                    Copyright (c) 2010 Fabian I.
Izuegbunam  \n')
fprintf(' Done At:                                ')
timestamp
% input data file
[dfile,pathname]=uigetfile('*.m','Select Data File');
if pathname == 0
```

```
error(' you must select a valid data file')
else

lfile =length(dfile);
% strip off .m and convert to lower case
dfile = lower(dfile(1:lfile-2));
eval(dfile);
end
if isempty(busdata)
error(' the selected file did not have valid bus data')
end
if isempty(linedata)
    error(' the selected file did not have a valid line data')
end
if isempty(gendata)
error(' the selected file did not have valid machine data')
end
%trstab
```

COHERENCE – BASED DYNAMIC AGGREGATION

A. MATLAB PROGRAM FOR POWER VARIATION (FAULT – ON)

```
% This Power Variation program computes the change in Real power at the
% Generator internal buses when a fault occurs at any point on the network
% It calculates the Real Power at the Pre - Fault state and at the Fault -
% on state. Checks for the variation between the two values. Calculates
% the percentage variation and decomposes the system into Study and
% External System based on this variation.
%
% Copyright (c) 2010 Fabian I. Izuegbunam
resp=0;
   %toc
   while strcmp(resp, 'n')~=1 & strcmp(resp, 'N')~=1 & strcmp(resp, 'y')~=1 &
strcmp(resp, 'Y')~=1
   resp=input('Do you want to check for Power Variation? Enter ''y'' or ''n''
within quotes -> ');
   if strcmp(resp, 'n')~=1 & strcmp(resp, 'N')~=1 & strcmp(resp, 'y')~=1 &
strcmp(resp, 'Y')~=1
   fprintf('\n Incorrect reply, try again \n\n'), end
if resp=='n' | resp=='N', return, else, end
   end
clc

fprintf('\n                                        Power Variation \n')
fprintf('                                  Copyright (c) 2010 Fabian I. Izuegbunam
\n')
fprintf(' Done At:                              ')
 timestamp


tic
global Pm f H E  Y th ngg
f=50;
ngr=gendata(:,1);
ngg=length(gendata(:,1));
for k=1:ngg
zdd(ngr(k))=gendata(k, 2)+j*gendata(k,3);
```

```
H(k)=gendata(k,4);    % new
end
for k=1:ngg
I(k) =conj(S(ngr(k)))/conj(V(ngr(k)));
II(k) = S(ngr(k))/V(ngr(k));           %mine
Ep(k) = V(ngr(k))+zdd(ngr(k))*I(k);   % new
Pm(k)=real(S(ngr(k)));              % new
end
E=abs(Ep); d0=angle(Ep);
Er=real(Ep) ;
Ei=imag(Ep); %mine
Ip=real(I); dp=imag(I);      %mine
Iab = abs(I); dab=angle(I);    %mine
for k=1:ngg
nl(nbr+k) = nbus+k;
nr(nbr+k) = gendata(k, 1);
R(nbr+k)  = real(zdd(ngr(k)));
X(nbr+k)  = imag(zdd(ngr(k)));
Bc(nbr+k)  = 0;
a(nbr+k) = 1.0;
yload(nbus+k)=0;
end
nbr1=nbr; nbus1=nbus;
nbrt=nbr+ngg;
nbust=nbus+ngg;
linedata=[nl, nr, R, X, -j*Bc, a];
[Ybus, Ybf]=ybusbf(linedata, yload, nbus1,nbust);
Ybf;
Ydf=ybusdf(Ybus, nbus1, nbust, nf);
Ydf;

% Calculating currents for Pre - Fault state and Fault  - on State
Epp = Ep.';
Ipre = Ybf*Epp;
Idf  = Ydf*Epp;
Ppre = real(Epp.*conj(Ipre))*basemva;
Pdf = real(Epp.*conj(Idf))*basemva;
PowerVar = Ppre - Pdf;
PercentVar = (PowerVar./Ppre)*100;
fprintf('\n Gathering System Information.............')
fprintf('\n Running Pre - Fault and Fault - on Currents.............')
fprintf('\n Computing Power Variation Parameters.............')
fprintf('\n ------------------------------------------------------------\n')

disp(['     G(i)         Power(prefault)     Power(Fault-on)    PowerVariation
PowerVar(%)'])
for ii = 1:ngg
   fprintf('       %g', ngr(ii)), fprintf('         %8.4f',Ppre(ii)), fprintf('
%8.4f', Pdf(ii)), fprintf('            %8.4f',PowerVar(ii))
    fprintf('        %8.4f \n', PercentVar(ii))
end
fprintf('\n ------------------------------------------------------------\n')

% For Decomposition into Study and Remote areas
fprintf('\n Decomposing System into Study and External Systems.............
')
fprintf('\n Checking Power Variation Parameters.............. ')
fprintf('\n Running Test.............. \n')
fprintf('\n ------------------------------------------------------\n')
for k = 1:ngg
    if PercentVar (k) <= 30
```

```
        fprintf('\n Generator %g',k)
        fprintf(' is in the External System')
     end
end
fprintf('\n ------------------------------------------------------------\n')
fprintf('\n Checking Power Variation Parameters.............. ')
fprintf('\n Running Test.............. \n')
fprintf('\n ------------------------------------------------------------\n')
for k = 1:ngg
    if PercentVar (k) > 30
        fprintf('\n Generator %g',k)
        fprintf(' is in the Study System \n')
        fprintf('-----------------------------------------------------\n')
     end
end
toc
```

B. MATLAB PROGRAM FOR ELECTRICAL PROXIMITY INDEX

```
%This program calculates the proximity index values between generator pairs
% Copyright (c) 2010 Fabian I. Izuegbunam


resp =0;
while strcmp(resp, 'n')~=1 & strcmp(resp, 'N')~=1 & strcmp(resp, 'y')~=1 &
strcmp(resp, 'Y')~=1
   resp=input('Do you want to check for Electricity Proximity? Enter ''y'' or
''n'' within quotes -> ');
   if strcmp(resp, 'n')~=1 & strcmp(resp, 'N')~=1 & strcmp(resp, 'y')~=1 &
strcmp(resp, 'Y')~=1
   fprintf('\n Incorrect reply, try again \n\n'), end
if resp=='n' | resp=='N', return, else, end
end



global Pm f H E  Y th ngg
f=50;
ng = max(gendata(:,1));
ngr=gendata(:,1);
ngg=length(gendata(:,1));
for k=1:ngg
zdd(ngr(k))=gendata(k, 2)+j*gendata(k,3);
H(k)=gendata(k,4);   % new
end
for k=1:ngg
I(k) =conj(S(ngr(k)))/conj(V(ngr(k)));
II(k) = S(ngr(k))/V(ngr(k));          %mine
Ep(k) = V(ngr(k))+zdd(ngr(k))*I(k);  % new
Pm(k)=real(S(ngr(k)));            % new
end
E=abs(Ep); d0=angle(Ep);
Er=real(Ep) ;
Ei=imag(Ep); %mine
Ip=real(I); dp=imag(I);     %mine
Iab = abs(I); dab=angle(I);   %mine
for k=1:ngg
nl(nbr+k) = nbus+k;
nr(nbr+k) = gendata(k, 1);
R(nbr+k)  = real(zdd(ngr(k)));
X(nbr+k)  = imag(zdd(ngr(k)));
Bc(nbr+k)  = 0;
a(nbr+k) = 1.0;
```

```
yload(nbus+k)=0;
end
nbr1=nbr; nbus1=nbus;
nbrt=nbr+ngg;
nbust=nbus+ngg;
linedata=[nl, nr, R, X, -j*Bc, a];
[Ybus, Ybf]=ybusbf(linedata, yload, nbus1,nbust);

Ydf=ybusdf(Ybus, nbus1, nbust, nf);

[Yaf]=ybusaf(linedata, yload, nbus1,nbust, nbrt, lrmv);
clc

fprintf('\n                                    Proximity - INDEX (Post-Fault
Condition) \n')
fprintf('                                    Copyright (c) 2010 Fabian I.
Izuegbunam \n')
fprintf(' Done At:                             ')
 timestamp

 fprintf('\n')
%-----------------------------------------------------------------------
s=input('Enter the Number of Machines in the External Area --> ');
ss=input('Enter the Machine No. of the Generators in the Study System (e.g [9
10]) --> ');

fprintf('\n ')
nn=s;
ns=ss;

bb(1,1)=1.0;
%cc=0.0;
Ya = abs(Yaf);
%c=0.0;
      ccc = sum(Yaf(:,:));
      cb = ccc.';
      if (length(ns)== 1)
      cc = abs(cb - diag(Yaf) - Yaf(:,ns));
      else
          cc = abs(cb - diag(Yaf) - sum(Yaf(:,ns).').');
      end
      B = cc(:,ones(1,ngg));% replicating cc for 10 columns

for ii = 1:ngg
    for jj=1:ngg
        bb(ii,jj)=((nn-1)*abs(Yaf(ii,jj))./B(ii,jj);% \
    end
end

for ii=1:ngg
    for jj=1:ngg
        if(ii==jj)
            bb([ii],[jj])=1.0;
        end
    end
end

 for k=1:ngg
 fprintf('          %g',ngr(k))
 end
 fprintf('\n ')
```

```
disp(bb)
```

C. MATLAB PROGRAM FOR β – INDEX (INERTIA CONDITION)

```
%This program, B - index calculates the B-index(Inertia condition) of an n-
%machine system for coherency identification.This implements the method of
%equal velocity and equal acceleration.
%
%   Copyright (c) 2010 Fabian I. Izuegbunam
resp=0;
   %toc
   while strcmp(resp, 'n')~=1 & strcmp(resp, 'N')~=1 & strcmp(resp, 'y')~=1 &
strcmp(resp, 'Y')~=1
   resp=input('Do you want to evaluate B - Index? Enter ''y'' or ''n'' within
quotes -> ');
   if strcmp(resp, 'n')~=1 & strcmp(resp, 'N')~=1 & strcmp(resp, 'y')~=1 &
strcmp(resp, 'Y')~=1
   fprintf('\n Incorrect reply, try again \n\n'), end
if resp=='n' | resp=='N', return, else, end
   end

   clc
global Pm f H E  Y th ngg ngr
f=50;

fprintf('\n                                    B-INDEX (Inertia Condition) \n')
fprintf('                                  Copyright (c) 2010 Fabian I. Izuegbunam
\n')
fprintf(' Done At:                           ')
 timestamp

% Initializing variables
ngr=gendata(:,1);
ngg=length(gendata(:,1));

H = gendata(:,4);

fprintf('\n Gathering System Information.................')
fprintf('\n Checking Generator Data.................')
fprintf('\n Preparing Index.................')
fprintf('\n ------------------------------------------------------------\n')
fprintf(' The B - Index (Inertia Condition is : ..............)\n')
for ii = 1:ngg
for jj = 1:ngg-1
    b(ii, jj) = abs(H(ii) - H(jj))/max(H(ii),H(jj));
end
end
Bindex= tril(b);
disp(Bindex)
```

D. MATLAB PROGRAM FOR γ – INDEX (DAMPING CONDITION)

```
%This program, Y - index calculates the Y-index(damping condition) of an n-
%machine system for coherency identification.
%
%   Copyright (c) 2010 Fabian I. Izuegbunam

resp=0;
   %toc
```

```
   while strcmp(resp, 'n')~=1 & strcmp(resp, 'N')~=1 & strcmp(resp, 'y')~=1 &
strcmp(resp, 'Y')~=1
   resp=input('Do you want to evaluate Y - Index? Enter ''y'' or ''n'' within
quotes -> ');
   if strcmp(resp, 'n')~=1 & strcmp(resp, 'N')~=1 & strcmp(resp, 'y')~=1 &
strcmp(resp, 'Y')~=1
   fprintf('\n Incorrect reply, try again \n\n'), end
if resp=='n' | resp=='N', return, else, end
   end

global Pm f H E  Y th ngg ngr
f=50;
clc

fprintf('\n                                    Y - INDEX (Damping Condition) \n')
fprintf('                                Copyright (c) 2010 Fabian I. Izuegbunam
\n')
fprintf(' Done At:                              ')
 timestamp

ngr=gendata(:,1);
ngg=length(gendata(:,1));
D = gendata(:,5);
H = gendata(:,4);

fprintf('\n Gathering System Information.................')
fprintf('\n Checking Generator Data.................')
fprintf('\n Preparing Index.................')
fprintf('\n ----------------------------------------------------------\n')

fprintf(' The Y - Index (Damping Condition is : ..............)\n')
%disp(Yindex)
for ii = 1:ngg
for jj = 1:ngg-1
    w(ii, jj) = abs((1/H(ii)*D(ii) -
1/H(jj)*D(jj))/max(1/H(ii)*D(ii),1/H(jj)*D(jj)));
end
end
Yindex= tril(w);
disp(Yindex)
```

E. MATLAB PROGRAM FOR GENERATOR AGGREGATION

```
%This program request for a coherent group of machines and constructs their
%dynamic equivalent.
%Copyright (c) 2010 Fabian I. Izuegbunam

fprintf('\n                                      Dynamic Equivalent Construction
')
fprintf('\n                                    Copyright (c) Fabian I. Izuegbunam
\n')
fprintf(' Done At:                             ')
timestamp
fprintf(' \n')

global Pm f H E  Y th ngg
f=50;
ng = max(gendata(:,1));
ngr=gendata(:,1);
ngg=length(gendata(:,1));
for k=1:ngg
zdd(ngr(k))=gendata(k, 2)+j*gendata(k,3);
H(k)=gendata(k,4);    % new
```

```
end
for k=1:ngg
I(k) =conj(S(ngr(k)))/conj(V(ngr(k)));
II(k) = S(ngr(k))/V(ngr(k));          %mine
Ep(k) = V(ngr(k))+zdd(ngr(k))*I(k);  % new
Pm(k)=real(S(ngr(k)));             % new
end
E=abs(Ep); d0=angle(Ep);
Er=real(Ep) ;
Ei=imag(Ep); %mine
Ip=real(I); dp=imag(I);     %mine
Iab = abs(I); dab=angle(I);   %mine
for k=1:ngg
nl(nbr+k) = nbus+k;
nr(nbr+k) = gendata(k, 1);
R(nbr+k)  = real(zdd(ngr(k)));
X(nbr+k)  = imag(zdd(ngr(k)));
Bc(nbr+k)  = 0;
a(nbr+k) = 1.0;
yload(nbus+k)=0;
end
nbr1=nbr; nbus1=nbus;
nbrt=nbr+ngg;
nbust=nbus+ngg;
linedata=[nl, nr, R, X, -j*Bc, a];
[Ybus, Ybf]=ybusbf(linedata, yload, nbus1,nbust);
Ybf;

% Construction of Dynamic Equivalents

%-----------------------------------------------

  Epp = Ep.';
Ipre = Ybf*Epp;
Eee = conj(Epp).*Ipre;
for k=1:ngg
    Ve(k) = V(k);

end
Veee = Ve.';
Vee = conj(Veee).*Ipre;
%-----------------------------------------------
% solution for the equivalent internal voltage --- Eeq
respfl='y';
vv = input('Enter the coherent group (in brackets i.e [2 3]) -> ');
Esum = sum(Eee(vv));
Isum = sum(Ipre(vv));
Eeq = conj(Esum/Isum);
Eeeq = abs(Eeq);
Eangle = angle(Eeq)*(180/pi);

%-----------------------------------------------------------------
%   solution for the equivalent terminal voltage ----  Veq
Vsum  = sum(Vee(vv));
Veq = conj(Vsum/Isum);
Veeq = abs(Veq);
Vangle = angle(Veq)*(180/pi);

%-------------------------------------------------------------------
% solution for the equivalent transient reactance by paralleling -- X'd
for k = 1:ngg
```

```
Xd(k) = gendata(k,3);
Xed(k) = 1./Xd(k);
end
Xeq = sum(Xed(vv))^(-1);

%-------------------------------------------------------------------------
%   Solution for the Modified Transient Reactance
Xde = abs((Eeq - Veq)/Isum);

%-------------------------------------------------------------------------
% solution for the equivalent inertia constant ----   Heq
Heq = sum(H(vv));

%-------------------------------------------------------------------------
%  solution for the equivalent damping coefficients  ---  Deq
for k = 1:ngg
    D(k) = gendata(k,5);
end
Deq = sum(D(vv));

%-------------------------------------------------------------------------
% Solution for the Equivalent mechanical power input
for k = 1:ngg
    Pe(k) = Pg(k);
end
Peq = sum(Pe(vv));
%-------------------------------------------------------------------------
%  Dislpaying the Equivalent parameters

fprintf('\n Sorting the Parameters of the Coherent Group..... ')
fprintf('\n Constructing Dynamic Equivalents..... \n')
fprintf('\n -------------------------------------------------------------------
\n')
fprintf('The Equivalent Internal Voltage is       = %9.3f \n',  Eeeq)
fprintf('The Equivalent Internal Voltage Angle is = %8.4f \n', Eangle)
fprintf('\n -------------------------------------------------------------------
\n')
fprintf('The Equivalent Terminal Voltage is       = %9.3f \n', Veeq)
fprintf('The Equivalent Terminal Voltage Angle is = %8.4f \n', Vangle)
fprintf('\n -------------------------------------------------------------------
\n')
fprintf('The Equivalent Transient Reactane  X"d is = %8.4f \n' ,     Xeq)
fprintf('The Modified  Transient Reactane  X"de is = %9.3f \n' ,     Xde)
fprintf('\n -------------------------------------------------------------------
\n')
fprintf('The Equivalent Inertia Constant is    = %9.1f \n',    Heq)
fprintf('The Equivalent Damping Coefficient is = %8.4f \n',    Deq)
fprintf('\n-------------------------------------------------------------------
\n')
fprintf('The Equivalent Mechanical Power is    = %9.2f \n',    Peq)
fprintf('\n -------------------------------------------------------------------
\n')

resp=0;
   %toc
   while strcmp(resp, 'n')~=1 & strcmp(resp, 'N')~=1 & strcmp(resp, 'y')~=1 &
strcmp(resp, 'Y')~=1
   resp=input('Do you want to Aggregate another Coherent Group? Enter ''y'' or
''n'' within quotes -> ');
```

```
   if strcmp(resp, 'n')~=1 & strcmp(resp, 'N')~=1 & strcmp(resp, 'y')~=1 &
strcmp(resp, 'Y')~=1
   fprintf('\n Incorrect reply, try again \n\n'), end
if resp=='n' | resp=='N', return, else, end
   end
   Dynagg
```

MATLAB PROGRAM FOR GRAPHICAL USER INTERFACE

```
%This program creates a Graphical User Interface from which other packages
%can be easily used.
%
%Copyright (c) 2010 Fabian I. Izuegbunam

function varargout = tsa(varargin)
% TSA M-file for tsa.fig
%      TSA, by itself, creates a new TSA or raises the existing
%      singleton*.
%
%      H = TSA returns the handle to a new TSA or the handle to
%      the existing singleton*.
%     Copyright (c) 2010 Fabian I. Izuegbunam

gui_Singleton = 1;
gui_State = struct('gui_Name',       mfilename, ...
                   'gui_Singleton',  gui_Singleton, ...
                   'gui_OpeningFcn', @tsa_OpeningFcn, ...
                   'gui_OutputFcn',  @tsa_OutputFcn, ...
                   'gui_LayoutFcn',  [] , ...
                   'gui_Callback',   []);
if nargin && ischar(varargin{1})
    gui_State.gui_Callback = str2func(varargin{1});
end

if nargout
    [varargout{1:nargout}] = gui_mainfcn(gui_State, varargin{:});
else
    gui_mainfcn(gui_State, varargin{:});
end
% End initialization code - DO NOT EDIT
% --- Executes just before tsa is made visible.
function tsa_OpeningFcn(hObject, eventdata, handles, varargin)

handles.output = hObject;

% Update handles structure
guidata(hObject, handles);

% --- Outputs from this function are returned to the command line.
function varargout = tsa_OutputFcn(hObject, eventdata, handles)

varargout{1} = handles.output;


% --- Executes on button press in pushbutton1.
function pushbutton1_Callback(hObject, eventdata, handles)

selection = questdlg(['Close ' get(tsa,'Name') '?'],...
                           ['Close ' get(tsa,'Name') '...'],...
                           'Yes','No','Yes');
        if strcmp(selection,'No')
        else close(handles.figure1);
```

```
        end
            return


% --- Executes during object creation, after setting all properties.
function axes1_CreateFcn(hObject, eventdata, handles)
%
axes(hObject)

imshow('guipic.jpg')
% --- Executes on button press in pushbutton2.
function pushbutton2_Callback(hObject, eventdata, handles)

evalin('base','lfybus')
evalin('base','lfnewton')
evalin('base', 'busout')
evalin('base','lineflow')

% --- Executes on button press in pushbutton3.
function pushbutton3_Callback(hObject, eventdata, handles)

evalin('base','powerVar')
evalin('base','proximity')
evalin('base','B_index')
evalin('base','Y_index')

% --- Executes on button press in pushbutton4.
function pushbutton4_Callback(hObject, eventdata, handles)
% handles    structure with handles and user data (see GUIDATA)
evalin('base','trstab')

% --- Executes on button press in pushbutton5.
function pushbutton5_Callback(hObject, eventdata, handles)

evalin('base','Dynagg')

% --- Executes on button press in pushbutton6.
function pushbutton6_Callback(hObject, eventdata, handles)

evalin('base', 'Datafile');

% --- Executes on button press in pushbutton7.
function pushbutton7_Callback(hObject, eventdata, handles)
clc
```